# UNIVERSITY OF NAPLES "FEDERICO II"

*PhD school of Earth Sciences*

**Doctoral thesis in Sedimentary Geology**

**(XXIV Cycle)**

# THE RECORD OF THE EARLY TOARCIAN AND EARLY APTIAN OCEANIC ANOXIC EVENTS IN THE APENNINIC CARBONATE PLATFORM (SOUTHERN ITALY)


*Supervisor*

**Dr. Mariano Parente**

*Ph.D. student*

**Alberto Trecalli**

*Ph.D. Coordinator*

**Prof. Maria Boni**


**2012**

*Un Oceano di Silenzio scorre lento*
*Senza centro né principio*
*Cosa avrei visto del mondo*
*Senza questa luce che illumina*
*I miei pensieri neri*

Franco Battiato

## *Ringraziamenti*

Il primo dei miei ringraziamenti va al mio Tutor, Dott. Mariano Parente, per avermi dato l'opportunità di svolgere questo dottorato di ricerca su una tematica di enorme interesse scientifico e l'opportunità di partecipare a congressi nazionali e internazionali, durante i quali ho potuto presentare i risultati della mia ricerca e confrontarmi con gli "esperti" del settore.

Ringrazio sia l'attuale che il precedente coordinatore del dottorato di ricerca, rispettivamente la Prof.ssa Maria Boni e il Prof. Stefano Mazzoli, per aver finanziato parzialmente le mie "trasferte" all'estero, con i fondi del dottorato.

Un ringraziamento va al Prof. Filippo Barattolo per avermi sempre concesso l'uso del laboratorio per il taglio delle centinaia di campioni di roccia raccolti durante l'attività di campagna. Ringrazio anche il Dott. Sergio Bravi, per l'assistenza in laboratorio per la preparazione delle sezioni sottili.

Un ringraziamento va anche al Dott. Lucio Tufano, il quale ha sempre mostrato grande disponibilità e celerità nella ricerca di pubblicazioni.

Grazie anche al Dott. Matteo Di Lucia per il suo aiuto "a distanza".

Ringrazio anche la Dott.ssa Tatyana Gabellone. Sì, adesso possiamo chiamarci davvero "Dottori". Co-abitante (cit.) e compagna d'avventura durante questi tre anni. Una delle cose che mi mancherà maggiormente degli otto anni trascorsi a Napoli, saranno le serate vomeresi al "Johnny B. M.". Un grazie anche a Francesco Dati, Ciccio, per la sua interminabile voglia di parlare, che mi è servita come distrazione nei momenti di maggiore stress. Mi mancheranno anche le nostre pizze con il cornicione ripieno.

E un grazie anche al Maestro, Franco Battiato, la cui "dottrina" è stata la mia carica durante la stesura di questa tesi, ma anche "oceano di silenzio" nei momenti di sconforto.

## *Acknowledgements*

I am grateful to Prof. Karl Föllmi for giving me the possibility to spend some periods at his department and to work in the laboratories of the University of Lausanne (CH). I would like to thank as well Dr. Thierry Adatte. They both gave me precious suggestions. Thanks to Dr. Jorge Spangenberg for the isotopic analyses and to all the people who assisted me during the laboratory work.
Thanks to Dr. Ulrike Schulte and Dr. Dieter Buhl who performed the geochemical analyses in Bochum (D).
Finally, thanks to my referee, Prof. Hugh C. Jenkyns of the University of Oxford (UK), for his fast review.

# TABLE OF CONTENTS

# ABSTRACT

About one third of the carbon dioxide released mainly from burning of fossil fuels is absorbed into the oceans where it reacts to form carbonic acid. As a result the pH of the ocean and the amount of carbonate ions decrease in a process called ocean acidification. Detrimental effects on calcifying organisms, which use carbonate minerals to build their protective shells and skeletons, have been documented in the laboratory and in the field. However, due to the spatio-temporal limits of experiments and field observations, the long-term impact on marine ecosystems and the adaptation potential of marine species are best investigated by looking at the geological record of past episodes of ocean acidification.

Episodes of short-term massive injection of $CO_2$ in the atmosphere-ocean system are witnessed by negative carbon isotope events (CIE) recorded by marine carbonates and by marine and continental organic matter. Paroxysmal volcanism and/or clathrates dissociation are generally invoked as the source of isotopically depleted excess $CO_2$. High $pCO_2$ is also held responsible for the dramatic increase of atmospheric and seawater temperature. During the Mesozoic some of these events record also the deposition of large amounts of organic carbon in epicontinental and oceanic basins, witnessing widespread marine anoxia. For this reason they are commonly referred to as Oceanic Anoxic Events (OAEs). The early Toarcian (Posidonienschiefer event, T-OAE, 183 Ma) and early Aptian events (Selli event, OAE1a, 120 Ma) represent two of the most severe and best documented episodes of sudden perturbation of the global carbon cycle and therefore have been chosen as subject of this thesis. There is overwhelming evidence for both the events that geologically rapid injection of $CO_2$ into the ocean-atmosphere system caused abrupt global warming. Ocean acidification has also been proposed for both the events.

Most of what we know about the record of the early Toarcian and early Aptian events has been revealed by the study of relatively deep-water marine sediments, deposited in epicontinental basins and shelves and in oceanic basins. Comparatively much less is known on the response of shallow water carbonate platforms, which represent the other "half" of the ocean, in terms of carbonate production and accumulation.

The Apenninic Carbonate Platform (ACP) grew isolated from major continental landmasses at least since the Early Jurassic. It accumulated more than 4500 m of shallow water carbonates from the Late Triassic to the Late Cretaceous and was able to survive all the Mesozoic OAEs. Its sedimentary archive offer the unique opportunity of investigating the response to $CO_2$-induced perturbations without the obvious drawback of habitat loss due to drowning.

In order to study the response of the ACP to the Late Pliensbachian-Early Toarcian environmental changes, two classical outcrops of platform carbonates of the southern Apennines have been logged and sampled: Mercato San Severino, about 30 km northwest of Salerno, and Monte Sorgenza, about 7 Km east of Formia. Both sections consist of bioclastic limestones of the "Lithiotis member" of the "Palaeodasycladus Limestones Formation" overlain by oolitic limestones of the "Oolitic-oncolitic Limestones Formation".

Paired records of $\delta^{13}C_{carb}$ and $\delta^{13}C_{org}$, total phosphorus content (P) and clay-mineral assemblages have been investigated and integrated with detailed microfacies analysis for both the studied sections. The most prominent features shown by the isotopic records are two sharp negative excursions with an intervening positive excursion. The first negative CIE occurs in the upper part of the "Lithiotis member" and is recorded only by the $\delta^{13}C_{org}$ curves with a shift of about 3-4‰. The second negative CIE starts in the last beds of the "Lithiotis member" and reaches the lowest values at the boundary with the oolitic limestones. This excursion is recorded by both curves but is distinctly larger in the $\delta^{13}C_{org}$

(4-5‰) than in the $\delta^{13}C_{carb}$ curve (2-2.5‰). Chemostratigraphic correlation with the reference section of Peniche allows unprecedented high-resolution dating of the Early Jurassic platform carbonates of the southern Apennines. This correlation is used to explore the response of a resilient carbonate platform to the early Toarcian oceanic anoxic event. The first CIE has been associated to the Pliensbachian-Toarcian boundary event, while the second one to the early Toarcian OAE. In the ACP, the Lithiotis/Palaeodasycladus carbonate factory, so typical of all the Tethyan tropical carbonate platforms during the Pliensbachian, was wiped out at the onset of early Toarcian negative carbon isotope excursion, seemingly marking the definitive extinction of these massive biocalcifiers.

Clay-minerals and P content of the ACP records increased weathering across the Pliensbachian-Toarcian boundary. Many carbonate platforms of the Peri-Tethyan domain responded to the shift of nutrient levels, associated with increased weathering and runoff, by either drowning or shifting to heterotrophic carbonate production. The ACP continued growing in shallow water with no significant shift in the composition of the carbonate factory. This is probably due to the fact that the ACP grew isolated from major continental blocks and seemingly distant from the Early Jurassic upwelling zones. For these reasons nutrient levels seemingly did not cross the threshold of ecological tolerance of the main carbonate producing biota. Moreover, the ACP was situated further from the Jurassic rifting axis than other carbonate platforms, which were progressively drowned during the Early Jurassic. Lower subsidence rate was most probably a significant factor explaining the resilience of the ACP to Early Toarcian palaeoenvironmental perturbations.

The extinction of carbonate platform biocalcifiers is coeval with a biocalcification crisis of calcareous nannoplankton. The coincidence with the negative CIE, interpreted as the result of the massive injection of $CO_2$ into the atmosphere-ocean system, is consistent with a scenario of ocean acidification at the onset of the T-OAE, which likely led to the demise of the Lithiotis/Palaeodasycladus carbonate factory. Clay-minerals and P content show no evidence of enhanced weathering in the ACP across the early Toarcian OAE. Therefore, enhanced nutrient levels were probably not the cause of the demise of the Lithiotis/Palaeodasycladus carbonate factory. This would further support the scenario of ocean acidification.

In the ACP, and in other resilient platforms of the Tethyan ocean, the disappearance of the most prolific biocalcifiers coincide with a shift to chemical precipitation in the form of massive oolitic limestones. Similar to what observed for the Permian-Triassic boundary crisis, chemical precipitation took over on carbonate platforms as soon as ocean alkalinity recovered. The evolution recorded by the ACP across the T-OAE conforms to the expectations of a biogeochemical model for the marine geological signature of ocean acidification. Very prolific biocalcification by massive bivalves and calcareous algae in the "Lithiotis member" represents the pre-event steady state of the model. The abrupt demise of Lithiotis bivalves and *Palaeodasycladus* at the onset of the CIE corresponds to the "dissolution interval". The oolitic limestones represent the "$CaCO_3$ preservation overshoot", marking the recovery of carbonate supersaturation driven by enhanced weathering.

The Early Toarcian record of the southern Apennines could be relevant for research on present and future ocean acidification. The message is that the threat posed by rapid increasing $pCO_2$ could be well beyond the potential of acclimation and evolutionary adaptation of marine biocalcifiers.

For the early Aptian OAE, two Berramian-Aptian sections, cropping out at Monte Raggeto (about 7 km northwest of Caserta) and Monte Tobenna (about 8 km northeast of Salerno) have been logged and sampled. Detailed microfacies analysis and high-resolution carbon isotope analysis have been performed for both the sections. The integration of this

study with the carbon isotope stratigraphy of three Barremian-Aptian successions studied in a previous thesis project, has allowed the proposal of a bio-chemostratigraphic model for the Late Barremian-Aptian interval.

The correlation with the most complete Monte Raggeto section reveals previously undisclosed gaps in the other sections. This highlights the difficulties of applying carbon isotope stratigraphy to inherently incomplete carbonate platform sections. The most significant result of this study is the proposal of chemostratigraphically constrained biostratigraphic criteria for the individuation of the time-equivalent of the Selli event in central and southern Tethyan carbonate platforms. Moreover this study proposes a chemostratigraphically constrained chronostratigraphic calibration of some important biostratigraphic events that are widely used in the Barremian–Aptian biozonations of central and southern Tethyan carbonate platforms.

The interval of decreasing $\delta^{13}C$ values preceding the C3 negative peak, which marks the onset of the Selli event, starts just above the LO of *V. murgensis*. The C4-C6 segments, which correspond in deep-water sections to the interval of black shales deposition, ends just below the first acme of *S. dinarica*. The latter roughly corresponds to the C7 segment of peak $\delta^{13}C$ values. The "Orbitolina level" marks the return the pre-excursion values at the end of the broad positive CIE associated with the OAE1a.

Another valuable result is the definition of a biostratigraphic criterion to spike the Barremian-Aptian boundary. According to the present calibration, the boundary is very closely approximated by the first occurrence of *V. murgensis* and *D. hahounerensis*.

In all the biostratigraphic schemes published so far for the ACP, and other central Tethyan platforms, the chronostratigraphic calibration was anchored to the ages established for selected taxa of orbitolinid foraminifera in the carbonate platform of the northern Tethyan margin. This study proposes the first chronostratigraphic calibration constrained by carbon and strontium isotope stratigraphy. Chemostratigraphy is being successfully applied to Cretaceous carbonate platforms. Its integration with biostratigraphy hold the promise of producing standard biozonations, based on larger foraminifera and calcareous algae, perfectly tied to the chronostratigraphic scale. This would open the possibility of fully exploiting the valuable archive of palaeoenvironmental changes preserved by Cretaceous carbonate platforms.

# RIASSUNTO

Negli ultimi 250 anni i livelli di $CO_2$ in atmosfera sono aumentati di circa il 40%, dai livelli pre-industriali di 280 ppm ai 384 del 2007. Il riscaldamento globale causato dall'aumento della $pCO_2$ nell'atmosfera non è l'unico problema legato all'aumento di questo gas serra. Durante l'ultima decade è emersa una nuova preoccupazione per gli effetti sulla chimica dell'oceano causati dall'assorbimento di $CO_2$. Circa un terzo del carbonio di origine antropica immesso nell'atmosfera viene assorbito dall'oceano, dove causa un aumento del contenuto totale di carbonio inorganico disciolto ed una diminuzione del pH, della concentrazione dello ione carbonato e della saturazione in $CaCO_3$. Questi cambiamenti vengono generalmente indicati come "acidificazione dell'oceano" ed i loro effetti sugli organismi marini e sugli ecosistemi oceanici sono così preoccupanti che l'acidificazione dell'oceano viene indicata come "l'altro problema della $CO_2$". Influenzando direttamente lo stato di saturazione del carbonato di calcio e quindi la capacità da parte degli organismi marini (plancton, coralli, alghe coralline e molti altri invertebrati) di biocalcificare, l'acidificazione dell'oceano porterà ad una diminuzione della diversità ed abbondanza degli organismi calcificatori ed a cambiamenti profondi nella struttura degli ecosistemi marini.

La preoccupazione per il riscaldamento globale e l'acidificazione dell'oceano ha stimolato l'attenzione dei ricercatori verso il record geologico che potrebbe fornire la risposta ad alcune domande fondamentali sugli effetti biotici di una massiccia immissione di $CO_2$ nell'atmosfera e nell'oceano. Il record geologico offre infatti la possibilità di studiare intervalli di tempo in cui l'atmosfera e l'oceano hanno sperimentato livelli di $CO_2$ comparabili o persino superiori a quelli previsti per il futuro. Il principale testimone di perturbazioni del ciclo globale del carbonio è la composizione isotopica del carbonio nel record sedimentario marino e continentale, registrata dai minerali carbonatici precipitati dall'acqua di mare e dalla materia organica. Tale record ha evidenziato la presenza di brusche variazioni dei valori del $\delta^{13}C$ che coincidono con perturbazioni ambientali a grande scala (a volte globale, a volte regionale), come per esempio rapide variazioni climatiche, variazioni della distribuzione dei nutrienti negli oceani ed episodi di estinzione di massa sia sui continenti che negli oceani. L'interpretazione più comunemente accettata é che episodi di rapido riscaldamento globale furono causati da brusche emissioni di $CO_2$ nell'atmosfera a causa di attività vulcanica e/o dissociazione di idrati gassosi di metano. Il rapido riscaldamento globale innescò una cascata di perturbazioni paleoambientali che culminarono in episodi di deposizione su scala globale di sedimenti ricchi di materia organica. Tali episodi sono noti come eventi anossici oceanici (OAEs, *Oceanic Anoxic Events*). Due degli episodi maggiori sono quelli riconosciuti nel Toarciano inferiore (T-OAE, 183 Ma) e nell'Aptiano inferiore (OAE1a, 120 Ma). Essi sono anche l'oggetto di questa tesi di dottorato.

La maggior parte di quello che sappiamo sulla risposta del Sistema Terra e dell'ecosistema oceanico alle perturbazioni del ciclo del carbonio e sugli episodi di acidificazione degli oceani durante il Mesozoico deriva da studi effettuati su sedimenti marini di successioni pelagiche o emipelagiche. Molto meno sappiamo invece dei carbonati di piattaforma, nonostante essi rappresentino l'altra metà del record oceanico, quello di mare basso, dal punto di vista della produzione e dell'accumulo di carbonato. Questa "carenza" di informazioni risulta essere una della maggiori limitazioni quando si vuole investigare il comportamento del nostro pianeta durante queste improvvise perturbazioni ambientali, sia perché i carbonati di piattaforma, in quanto strettamente connessi all'attività biologica, sono particolarmente sensibili alle variazioni ambientali, sia

perché l'accumulo di carbonati nelle scogliere e nelle piattaforme carbonatiche rappresenta una parte importante del ciclo del carbonio.

L'evento dell'Aptiano inferiore è certamente l'evento anossico meglio documentato nelle successioni di piattaforma carbonatica. Dai diversi studi sull'argomento, è stato evidenziato che la crisi e l'annegamento delle prolifiche Piattaforme Urgoniane al margine Nord della Tetide sono state causate probabilmente dalle perturbazioni paleoambientali legate all'aumento brusco di $CO_2$ (aumento dell'input di nutrienti, aumento della temperatura, riduzione della saturazione in $CaCO_3$). Più recentemente l'attenzione si è rivolta alla presenza, a scala da regionale a supraregionale, di facies particolari quali marne ad orbitolinidi appiattiti e/o calcari microbialitici (bindstones a *Lithocodium/Bacinella* e facies associate). Entrambe queste facies sono state interpretate generalmente come la risposta ad un aumento nell'input di nutrienti, con l'alta temperatura e l'alta alcalinità come fattori che concorrevano a favorire l'esplosione di calcificatori microbici. La distribuzione di tali facies nella Piattaforma Carbonatica Appenninica e la loro relazione con l'evento OAE1a sono state oggetto di una precedente tesi di dottorato. Attraverso lo *shift* di facies e della *carbonate factory*, le piattaforme carbonatiche del margine meridionale della Tetide furono generalmente in grado di evitare l'annegamento.

Molto meno investigata è invece la risposta delle piattaforme carbonatiche all'evento del Toarciano inferiore, soprattutto perché episodi di annegamento a grande scala associati alle perturbazioni paleoambientali del Toarciano inferiore, hanno interessato gran parte del dominio giurassico della Tetide. Comunque, ci sono ampie evidenze che molte piattaforme carbonatiche annegarono ben prima dell'inizio del T-OAE o persino prima del limite Pliensbachiano-Toarciano. Una combinazione di diversi fattori (tettonica, eustatismo e deterioramento delle condizioni ambientali) è stata generalmente indicata come causa degli eventi di annegamento o degli *shift* della *carbonate factory*.

La Piattaforma Carbonatica Appenninica (ACP, *Apenninic Carbonate Platform*) si sviluppò dal Triassico superiore al Cretacico superiore, accumulando più di 4500 metri di carbonati di mare basso. A partire dal Giurassico inferiore, crebbe isolata dalle masse continentali. Essa "sopravvisse" a tutti gli eventi anossici del Mesozoico. Il suo archivio sedimentario offre la preziosa opportunità di studiare la risposta dell'ambiente di piattaforma carbonatica alle perturbazioni indotte dall'aumento di $CO_2$, senza l'inconveniente rappresentato dalla perdita dell'habitat a causa dell'annegamento.

La mancanza di *black shales*, la bassa risoluzione stratigrafica della biostratigrafia di mare basso e l'assenza di una precisa calibrazione cronostratigrafica e di precise correlazioni con successione coeve di mare profondo sono generalmente i maggiori problemi legati allo studio degli OAEs in piattaforma carbonatica. Questi problemi possono essere affrontati attraverso l'integrazione di chemostratigrafia e biostratigrafia, un approccio che è stato già utilizzato con successo per l'evento al limite Cenomaniano-Turoniano (OAE2) nella Piattaforma Carbonatica Appenninica.

Lo scopo principale di questa tesi di dottorato è quello di studiare la risposta della ACP agli eventi anossici oceanici del Toarciano inferiore (T-OAE) e dell'Aptiano inferiore (OAE1a).

Al fine di studiare la risposta della ACP ai cambiamenti ambientali che hanno caratterizzato l'intervallo di tempo Pliensbachiano superiore-Toarciano inferiore, sono state campionate e descritte in dettaglio due classiche successioni del Giurassico inferiore dell'Appennino meridionale: Mercato San Severino (circa 30 km a nordovest di Salerno) e Monte Sorgenza (circa 7 km a est di Formia). Entrambe le successioni sono costituite dai calcari bioclastici appartenenti al Membro a Lithiotis della Formazione dei Calcari a Palaeodasycladus, su cui poggiano i calcari oolitici della Formazione dei Carcari oolitici e

oncolitici. Inoltre, la parte inferiore della successione affiorante a Monte Sorgenza, appena sotto al Membro a Lithiotis, è costituito dai calcari della subzona a Orbitopsella. Lo studio sedimentologico e biostratigrafico attraverso l'analisi al microscopio ottico di peels e sezioni sottili, è stato integrato con analisi chimiche e mineralogiche. Per entrambe le successioni è stata analizzata la composizione isotopica del carbonio della componente carbonatica ($\delta^{13}C_{carb}$) e della materia organica ($\delta^{13}C_{org}$), al fine di individuare gli intervalli stratigrafici corrispondenti all'evento associato al limite Pliensbachiano-Toarciano e all'evento anossico oceanico del Toarciano inferiore. La concentrazione totale di fosforo (P) e l'associazione dei minerali argillosi sono stati utilizzati per discriminare il ruolo relativo dell'acidificazione rispetto all'aumento del flusso di nutrienti sulla *carbonate factory* e per confrontare la risposta della ACP con quella delle altre piattaforme carbonatiche tetidee, per le quali l'aumento del flusso dei nutrienti è stato indicato come causa principale della crisi o dell' annegamento.

La caratteristica più evidente delle curve isotopiche del carbonio è rappresentata dalla presenza di due brusche escursioni negative (CIE, *carbon isotope excursion*), separate da un escursione positiva. La prima CIE negativa è in corrispondenza della parte alta del Membro a Lithiotis ed è registrata solamente dalle curve del $\delta^{13}C_{org}$, con uno *shift* di circa 3-4‰. La seconda CIE negativa inizia in corrispondenza degli ultimi strati del Membro a Lithiotis e raggiunge i valori più bassi al passaggio con i calcari oolitici. Questa escursione è registrata da entrambe le curve, ma è più grande nel $\delta^{13}C_{org}$ (4-5‰) che nel $\delta^{13}C_{carb}$ (2-2.5‰). La correlazione chemostratigrafica con la successione di riferimento di Peniche (Bacino Lusitanico, Portogallo), candidata come stratotipo del limite Pliensbachiano-Toarciano, ha permesso una datazione cronostratigrafica con una risoluzione senza precedenti dei carbonati del Giurassico inferiore dell'Apennino meridionale. La prima CIE è stata correlata all'evento del limite Pliensbachiano-Toarciano, mentre la seconda all'evento del Toarciano inferiore.

Nella Piattaforma Carbonatica Appenninica, la *carbonate factory* costituita dai Lithiotis e da *Palaeodasycladus mediterraneus*, tipica di tutte le piattaforme carbonatiche tetidee durante il Pliensbachiano, è stata spazzata via all'*onset* della CIE del Toarciano inferiore, che segna l'estinzione definitiva dei questi biocalcificatori massivi.

I minerali argillosi e la concentrazione totale di fosforo nella ACP registrano un incremento del *weathering* continentale attraverso il limite Pliensbachiano-Toarciano. Molte piattaforme carbonatiche del dominio tetideo reagirono all'aumento di nutrienti, associato all'incremento del *weathering* e del *runoff*, o annegando o attraverso lo *shift* della *carbonate factory* verso una produzione di tipo eterotrofico. Invece la Piattaforma Carbonatica Appenninica continuò a crescere in ambiente di mare basso senza nessuna significante variazione della composizione della *carbonate factory*. Questo è probabilmente dovuto al fatto che la ACP si sviluppò isolata dalle maggiori masse continentali e presumibilmente lontano da zone di *upwelling*. Per queste ragione il livello dei nutrienti non raggiunse mai la soglia di tolleranza ecologica dei principali biota produttori di carbonato. In più, la ACP era situata in aree più lontane dagli assi di *rift* giurassici, rispetto ad altre piattaforme, le quali annegarono progressivamente durante il Giurassico. Il minor tasso di subsidenza fu probabilmente il principale fattore che può spiegare la resistenza o la capacità di recupero che la ACP mostrò verso le perturbazione paleoambientali del Giurassico inferiore.

L'estinzione dei principali biocalcificatori della piattaforma carbonatica è coeva con una crisi di biocalcificazione del nannoplancton calcareo. La coincidenza con la CIE negativa, interpretata come immissione massiva e rapida di $CO_2$ nel sistema oceano-atmosfera., è consistente con uno scenario di acidificazione dell'oceano all'*onset* del T-OAE, che probabilmente portò alla fine della *carbonate factory* costituita da Lithiotis e Palaeodasycladus. I records dei minerali argillosi e del fosforo non mostrano evidenze di

aumento del weathering durante il T-OAE. Perciò, l'incremento del flusso di nutrienti probabilmente non fu un fattore significativo di perturbazione ambientale, almeno per la ACP. Questo supporterebbe ulteriormente l'ipotesi che l'estinzione dei biocalcificatori fu causata da un episodio di acidificazione dell'oceano.

Nella ACP, così come nelle altre piattaforme carbonatiche *"resistenti"*, la scomparsa dei biocalcificatori più prolifici coincide con uno *shift* verso una precipitazione di tipo chimico, sotto forma di calcari oolitici massivi. Similmente a quanto osservato per la crisi al limite Permiano-Triassico, la precipitazione chimica fu stimolata dalla sovrassaturazione immediatamente successiva all' evento di acidificazione dell'oceano. La precipitazione chimica rappresentata dalle ooliti, in assenza di grossi biocalcificatori, potrebbe essere stato l'unico sistema efficace per tamponare l'alta concentrazione degli ioni calcio e bicarbonato nelle acque superficiali, dovuta all'intensificarsi del *weathering* delle masse continentali e/o alla dissoluzione dei carbonati di mare profondo.

L'evoluzione registrata dalla ACP durante l'evento del Toarciano inferiore corrisponde a ciò che è stato previsto da un modello biogeochimico per la firma lasciata nel record marino geologico da un episodio di acidificazione dell'oceano. La prolifica biocalcificazione dovuta ai grossi bivalvi e alle alghe calcaree nel Membro a Lithiotis rappresenta lo *steady state* pre-evento del modello. La brusca fine dei Lithiotis e di Palaeodasycladus all'*onset* della CIE corrisponde al *dissolution interval*. Mentre i calcari oolitici rappresentano il "*$CaCO_3$ preservation overshoot*", marcando il *recovery* della soprassaturazione in carbonato di calcio, guidato dall'aumento del *weathering* continentale.

I risultati di questa parte di tesi, evidenziano che il record del Toarciano inferiore dell'Appennino meridionale potrebbe avere una certa rilevanza per la ricerca sull'acidificazione dell'oceano presente o futura. Il messaggio è che la minaccia rappresentata dal rapido incremento della $pCO_2$ potrebbe ben oltre il potenziale di adattamento evolutivo dei biocalcificatori marini.

Per lo studio dell'evento dell'Aptiano inferiore nella ACP sono state campionate e descritte in dettaglio due classiche successioni del Cretacico inferiore dell'Appennino meridionale: Monte Raggeto (circa 7 km a nordovest di Caserta) e Monte Tobenna (circa 8 a nordest di Salerno). Entrambe le successioni, costituite interamente da calcari appartenenti alla Formazione dei Carcari con Gasteropodi e Requienie, sono state ben studiate nel passato. In particolare a Monte Tobenna affiora il "Livello a Orbitolina", che è considerato un *marker* bio-litostratigrafico dell'Appennino meridionale. Per entrambi le sezioni la chemostratigrafia di alta risoluzione degli isotopi del carbonio ($\delta^{13}C$) e dello stronzio ($^{87}Sr/^{86}Sr$) è stata integrata con un dettagliato studio di analisi di facies. Lo studio di queste due sezioni è stato integrato con la reinterpretazione della chemostratigrafia di tre successioni di età Barremiano-Aptiano, studiate in un precedente lavoro di tesi (Monte Croce, Monte Motola e Monte Coccovello). Lo studio integrato di queste cinque sezioni, distribuite lungo l'asse appenninico dal Lazio meridionale, attraverso la Campania, fino alla Basilicata, ha permesso di proporre uno schema bio-chemostratigrafico per l'intervallo Barremiano superiore-Aptiano per le successioni carbonatiche di mare basso dell'Appennino meridionale.

La correlazione con la più completa sezione affiorante a Monte Raggeto ha evidenziato importanti gap sedimentari presenti nelle altre sezioni, che nella precedente tesi di dottorato non era stato possibile svelare. Questo mette in evidenza le difficoltà nell'applicare la stratigrafia degli isotopi del carbonio a successioni di mare basso che sono caratterizzate, per loro natura, da un record sedimentario incompleto. Il risultato più rilevante di questo studio è la proposta di criteri biostratigrafici, vincolati da una chemostratigrafia di alta risoluzione, per l'individuazione di intervalli stratigrafici

equivalenti al "Livello Selli" nella piattaforme carbonatiche tetidee centrali e meridionali. In più, questo studio propone una calibrazione cronostratigrafica, vincolata chemostratigraficamente, di alcuni importanti eventi biostratigrafici, *first occurrence* (FO) e *last occurrence* (LO) di alcune specie, che sono ampiamente usati nelle biozonazioni del Barremiano-Aptiano delle successioni di piattaforma carbonatica.

L'intervallo stratigrafico corrispondente alla caduta dei valori del $\delta^{13}C$ precedenti al picco negativo C3, che marca l'*onset* dell'evento Selli, inizia appena sopra la LO di *V. murgensis*. Il segmento C4-C6, che nelle sezioni pelagiche corrisponde all'intervallo di deposizione delle *black shales*, finisce appena sotto il primo acme di *S. dinarica*. Quest'ultimo corrisponde approssimativamente al segmento C7 del picco dei valori del $\delta^{13}C$. Il "Livello a Orbitolina" segna il ritorno a valori pre-escursione, alla fine dell'ampia CIE positiva associata all'OAE1a. Un altro importante risultato è la definizione di un criterio biostratigrafico, supportato anche dagli isotopi dello stronzio, per il riconoscimento del limite Barremiano-Aptiano, Secondo questa calibrazione, il limite è molto vicino alla FO di *V. murgensis* e *D. hahounerensis*.

In tutti gli schemi biostratigrafici pubblicati prima di questo lavoro per la Piattaforma Carbonatica Appenninica e per altre piattaforme della Tetide centrale, la calibrazione cronostratigrafica è stata ancorata a età ottenute per orbitolinidi nelle successioni di piattaforma carbonatica del margine settentrionale della Tetide. Invece questo studio propone la prima calibrazione cronostratigrafica vincolata dalla stratigrafia degli isotopi del carbonio e dello stronzio. L'integrazione di chemostratigrafia e cronostratigrafia permette di correlare perfettamente le biozonazioni standard, basate sui macroforaminiferi e sulle alghe calcaree, alla scala cronostratigrafica. Questo può consentire di possibilità di esplorare interamente il prezioso archivio di testimonianze di variazioni paleoambientali, che è preservato nei records sedimentari delle piattaforme carbonatiche del Cretacico.

## Foreword

The present dissertation is divided into 6 chapters. This organization is intended to facilitate future publication. Chapters 3, 4 and 5 will be submitted to peer-reviewed journals as independent papers.

**Chapter 1** is made up of an introduction with a synthesis of the state of the art on anthropogenically induced climate change and ocean acidification and on oceanic anoxic events as episode of $CO_2$-induced perturbations in the geological record. The introduction ends with the motivation and goals of the PhD research project.

**Chapter 2** contains a short introduction to the geology of the Southern Apennines, followed by a synthesis on the stratigraphy of the Apenninic Carbonate Platform.

**Chapter 3** is made up by the first manuscript. We discuss the Late Pliensbachian-Early Toarcian evolution of the Apenninic carbonate platform in the framework of global palaeoenvironmental perturbations recorded in reference sections of European basins. Carbon isotope stratigraphy is used for high resolution correlation.

**Chapter 4** presents a manuscript based on the record of phosphorus and clay-minerals across the Pliensbachian-Toarcian boundary and early Toarcian OAE, with a discussion on the role of enhanced nutrient levels and subsidence rates as key factors of platform drowning.

**Chapter 5** presents a manuscript on the Barremian-Aptian bio-chemostratigraphy of the Apenninic Carbonate Platform, based on two new sections and on a re-interpretation of previously studied sections. The main result is the definition of chemostratigraphically calibrated biostratigraphic criteria for the Barremian-Aptian boundary and for the OAE1a in central Tethyan carbonate platforms.

**Chapter 6** contains the summary of the main results of this thesis and some ideas for future work on the record of Mesozoic OAEs in Tethyan carbonate platforms.

# CHAPTER 1 – INTRODUCTION

## *1.1 Carbon-cycle perturbations: global warming and ocean acidification*

Since the beginning of the industrial revolution atmospheric $CO_2$ level increased by nearly 40%, from preindustrial levels of approximately 280 ppmv to nearly 384 ppmv in 2007 (Solomon et al. 2007). This rate of increase, driven mainly by human fossil fuel combustion and deforestation, is at least an order of magnitude faster than any change which has occurred during the last few million years (Doney and Schimel, 2007).

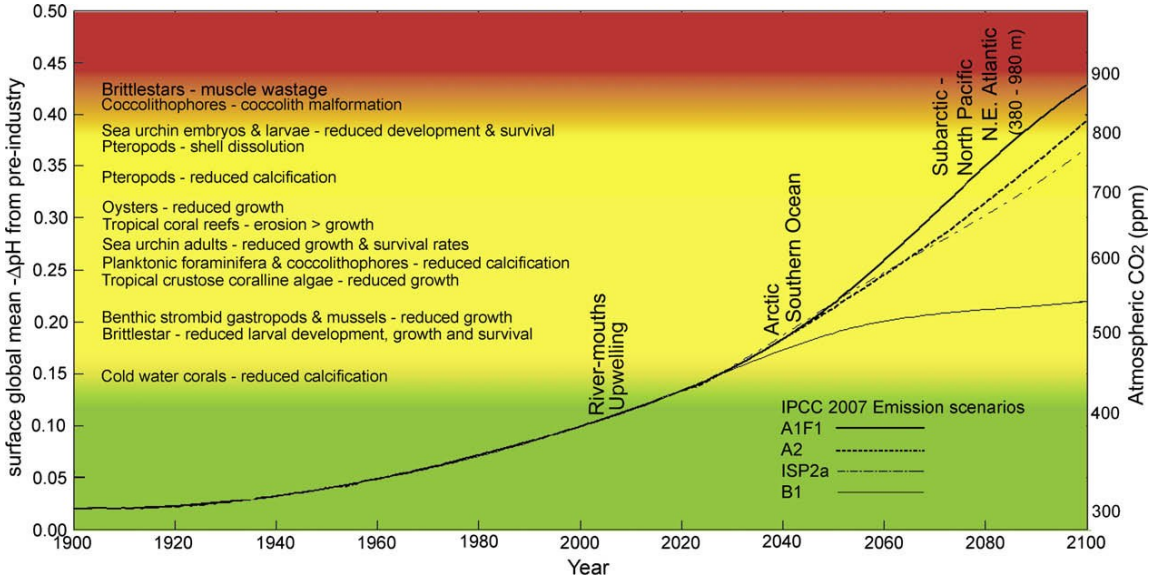


**Figure 1** - Projections for atmospheric $CO_2$ and surface global mean pH difference from pre-industrial to 2100 for different emission scenarios. Experimentally determined biological impacts on the left. On the right, marked above the pH-$CO_2$ curves are the years at which the first localized seasonal occurrence of aragonite undersaturation have been projected to occur for the regions given (Turley et al., 2010).

The current concentration is higher than experienced on Earth for at least the past 800 kyr (Lüthi et al. 2008) and the projected concentration at the end of the century (fig. 1) will be unprecedented during the last 24 Myr (Pearson and Palmer, 2000; Solomon et al., 2007). The oceans have taken up approximately a third of the $CO_2$ produced from fossil fuel burning, cement manufacture and land use changes (Sabine et al., 2004; Sabine and Feely, 2007). Without this oceanic uptake, atmospheric $CO_2$ would be approximately 450 ppmv today, a level of $CO_2$ that would have led to even greater climate change than witnessed today. However, as the ocean's $CO_2$ uptake increases, so its capacity to act as a buffer to atmospheric $CO_2$ levels decreases (Turley et al., 2006). Moreover, ocean $CO_2$ uptake is not completely benign, because the injection of $CO_2$ into the ocean forms carbonic acid in seawater and lowers ambient surface ocean pH (Broecker and Peng, 1982). pH reductions and alterations in fundamental chemical balances are together commonly referred to as ocean acidification. Ocean acidification may be better defined as the change in ocean chemistry driven by the oceanic uptake of chemical inputs to the atmosphere, including just not only carbon, but also nitrogen and sulfur compounds (Guinotte and Fabry, 2008). Because climate change and ocean acidification are both caused, mostly, by increasing atmospheric $CO_2$, acidification is commonly referred to as the "other $CO_2$ problem" (Henderson, 2006; Turley, 2005; Doney et al., 2009).

Being a direct consequence of the excessive addition of $CO_2$ to seawater, ocean acidification is more predictable than temperature and precipitation changes due to rising atmospheric $pCO_2$ (Turley et al., 2010). Since preindustrial times, the average ocean

surface water pH has fallen by approximately 0.1 units, from approximately 8.21 to 8.10 (Royal Society, 2005), and is expected to decrease a further 0.3-0.4 pH units by the end of the century (Caldeira and Wickett, 2003; Orr et al., 2005; Solomon et al., 2007). The rate of this change is cause for serious concern, as many marine organism, particularly those that produce their skeleton by precipitating $CaCO_3$ from seawater, may not be able to adapt quickly enough to survive these fast changes.

A series of chemical reactions is initiated when $CO_2$ is absorbed by seawater. Once dissolved in seawater, this gas reacts with water to form carbonic acid ($H_2CO_3$), which can then dissociate by losing hydrogen ions to form bicarbonate ($HCO_3^-$) and carbonate ($CO_3^{2-}$) ions. The seawater reactions are reversible and near equilibrium (Millero et al. 2002).

$$\mathbf{CO_{2(atmos)} \leftrightarrow CO2_{(aq)} + H_2O \leftrightarrow H_2CO_3 \leftrightarrow H^+ + HCO^-_3 \leftrightarrow 2H^+ + CO_3^{2-}}$$

Adding $CO_2$ to seawater increases aqueous $CO_2$, bicarbonate, and hydrogen ion concentrations; the latter lowers pH because pH = -log10[$H^+$]. The increasing $H^+$ concentration causes a decline of carbonate ion concentration, which leads to a reduction in calcium carbonate saturation state (Ω). The latter may have significant impacts on calcification in a range of ecologically important organisms such as coralline algae, foraminifers, corals, echinoderms, mollusks, bryozoans, coccolithophores and pteropods (Guinotte and Fabry, 2008 and references therein; Rodolfo-Metalpa et al., 2010 and references therein).

Predicting the impacts of ocean acidification on marine calcifiers as a whole is difficult since the major groups calcify via different routes and mechanisms. In fact, as showed in figure 2, the response of the marine organisms to increasing $CO_2$ concentrations has been shown to be variable and complex (Ries et al., 2009).

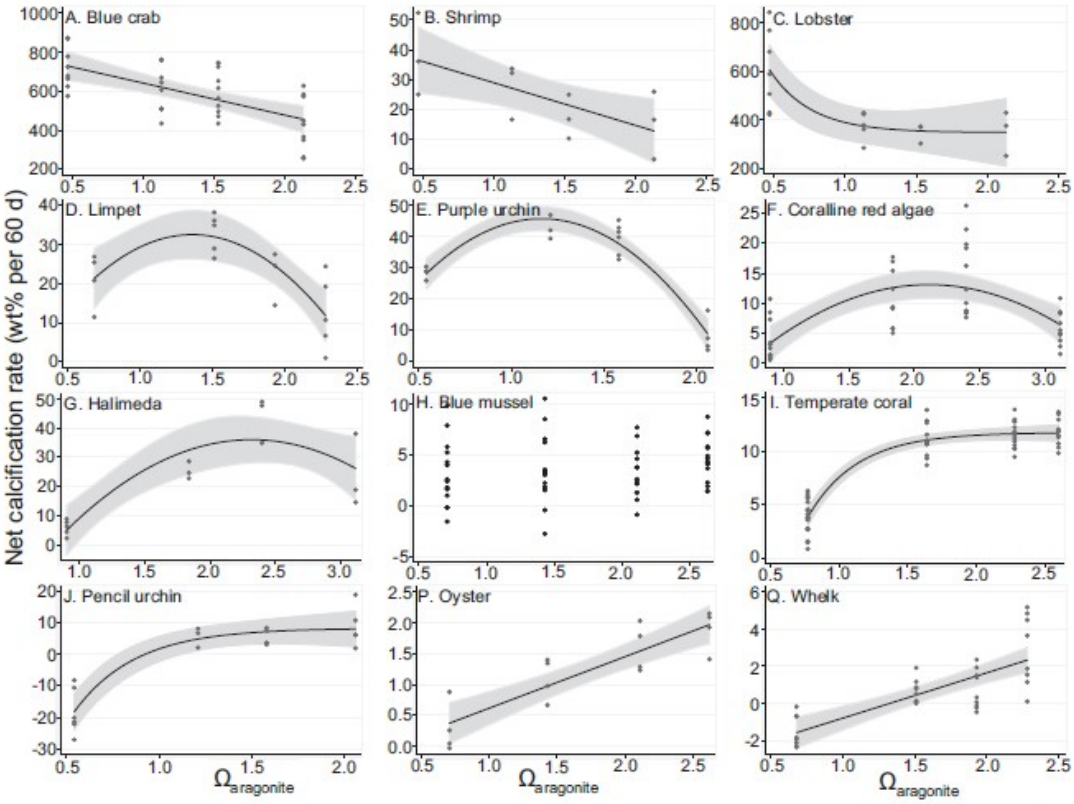


**Figure 2** - The impact of increasing $CO_2$ concentrations on the marine organisms can be variable (Ries et al., 2009).

Calcification is just one process in an organism, which may be impacted by acidification. Other important physiological processes may also adversely affected, such as metabolic processes, photosynthesis or nitrogen fixation (Turley et al., 2010 and references therein).

Scaling up from experimental results and "mesocosm" observations to ecological forecast is problematic because much of the available evidence is based on short-term single species experiments. When the experiments involved more than one species of a phylum, significant differences in sensitivities have been detected. When extrapolating responses to large scale processes such as primary productivity, nitrogen fixation and biodiversity loss, the complexity of the processes limits their predictability (Turley et al., 2010). Moreover, the experiments designed to investigate the physiological reactions to ocean acidification are too short-lived (days to weeks) to take the long-term effects of adaption into account.

In order to overcome these limitations, we have to look at the geological past, which can provide the key to work out what Earth is going towards and better forecast the possible future scenarios. In fact, the sedimentary archive bear witnesses of episodes of "rapid" injection of $CO_2$ to the atmosphere-ocean system, as revealed by rapid carbon isotope excursions (CIEs) recorded by marine carbonates and marine and continental organic matter. Some of these extreme events of global carbon-cycle perturbations involved rapid climatic changes, sudden shifts in the hydrological cycle, changes in the pattern of nutrient distribution in the oceans and episodes of mass extinction on land and in the ocean (Jenkyns, 2003). In some cases there is evidence of a biocalcification crisis affecting calcareous nannoplankton, likely due to ocean acidification episodes (Erba 2004; Mattioli et al., 2009; Erba et al., 2010). Understanding how the Earth System responded to these global perturbations is therefore of particular relevance to the present-day issue of anthropogenically induced climate change and ocean acidification.

The best-documented example of extreme short-lived global warming event from the geological past, is the Paleocene-Eocene Thermal Maximum (PETM), which occurred 55 million years ago. It is thought to be due to a massive injection of isotopically light carbon into the atmosphere-ocean system, caused by the dissociation, release and oxidation of gas hydrates from continental-margin sediments (Jenkyns, 2003; Zachos et al., 2005; Dickens, 2011; McInerney and Wing, 2011 and references therein). According to Röhl et al. (2007) the PETM event may have started in fewer than 1000 kyr with rapid emission of isotopically light carbon that caused severe global warming. As projected anthropogenic carbon inputs within just 300 years is thought to be much faster than the $CO_2$ release during the PETM, the ocean acidification-induced impacts on surface ocean pH and biota will be more severe (Zachos et al., 2005).

### *1.2 Oceanic Anoxic Events*

The Mesozoic Era is punctuated by a number of severe carbon-cycle perturbation events comparable to the PETM, some of which are characterized by widespread marine anoxia, witnessed by deposition of large amounts of organic carbon in epicontinental and oceanic basins. These events, known as Oceanic Anoxic Events, record also dramatic increases of atmospheric and seawater temperature (Jenkyns, 2003, 2010). Schlager and Jenkyns (1976) introduced the concept of OAE for specific time intervals of global anoxia during the middle Cretaceous, after recovery of black shales in the Pacific, Atlantic and Indian Oceans proved coeval with similar lithologies outcropping in the Tethyan domain. Although the number of OAEs recorded in Cretaceous strata has multiplied over time from those initially recognized, only one other definitive example is currently identified from

the rest of the Mesozoic Era, namely the Jurassic event of the early Toarcian (see Jenkyns, 2010 for a recent review). The OAEs of the early Toarcian (Posidonienschiefer event, T-OAE, 183 Ma), early Aptian (Selli event, OAE1a, 120 Ma) and the Cenomanian-Turonian (Bonarelli event, C/T OAE, OAE2, 93 Ma) represent three of the most severe and best documented episodes of sudden perturbation of the global carbon cycle.

The subject of this thesis are the T-OAE and OAE1a, which show several similarities in terms of geochemical sedimentary and biotic records. In both cases the carbon isotope records of marine and continental sections document sharp carbon isotope excursions (CIEs) characterized by a sudden decrease of the $\delta^{13}C$ of both carbonates and organic matter, followed by a more or less pronounced increase.

The excess burial of organic matter, which preferentially removes $^{12}C$ from the ocean-atmosphere system, causing an increase in the $\delta^{13}C$ of the dissolved inorganic carbon (DIC) in the ocean reservoir, is credited as the cause of the positive carbon isotope shift (Scholle and Arthur 1980). Conversely, the release of $^{12}C$ enriched carbon from volcanic degassing (Larson and Erba, 1999; Méhay et al, 2009; Tejada et al., 2009), thermal alteration of organic rich rocks (McElwain et al., 2005; Svensen et al., 2007) or the massive dissociation of methane clathrates (Hesselbo et al. 2000; Jahren et al., 2001; Kemp et al., 2005; McElwain et al. 2005; Gröcke et al., 2009) have been invoked to explain the sharp negative shift recorded at the beginning of the CIEs.

The emplacement of the Ontong-Java large igneous province is thought to be the trigger for the early Aptian oceanic anoxic event (Méhay et al, 2009; Tejada et al., 2009). Large igneous provinces (LIPs) are the most spectacular manifestation of volcanism on Earth. They consist of huge individual basaltic lava flows, with volumes measured in thousands of cubic kilometres, stacked layer upon layer to form vast volcanic plateau. LIPs are consistently associated with mass extinction events and other events of severe perturbation of earth system (Wignall, 2001; Kerr, 2005). The negative CIE associated with the onset of the early Aptian "Selli event" would witness the intense emission of volcanogenic $CO_2$ ($\delta^{13}C$ = ca -7‰) from the Ontong-Java LIP.

The early Toarcian negative CIE is thought to be mostly due to the massive dissociation of methane clathrates (Hesselbo et al. 2000; Kemp et al., 2005), characterized by very low isotopic value ($\delta^{13}C$ = ca -60‰). Methane forms within continental-margin sediments due to bacterial fermentation of organic matter and is stored as crystalline gas hydrates (clathrates) below the sea floor (Dickens, 2011; Kroeger et al., 2011). Dissociation of clathrates in the Early Toarcian, related either to warming of the bottom waters and/or tectonic disruption of the sedimentary pile, led to release of methane gas, much of which transited the water column to be oxidized in the shallow warm levels of the ocean and the atmosphere (Jenkyns, 2003). Furthermore, intrusion of sills from the Karoo-Ferrar LIP either into Gondwana coal deposits or into organic-rich sedimentary rocks (McElwain et al. 2005; Svensen et al. 2007) have been proposed for the early Toarcian event, although the hypothesis has been recently challenged (Gröcke et al., 2009). The global warming associated with $CO_2$ degassing during the emplacement of the Karro-Ferrar LIP, dated as coincident with the T-OAE, may have acted as a trigger of chlatrate dissociation (Pálfy and Smith, 2000).

The fact that a negative carbon isotope excursion (Hesselbo et al., 2007; Suan et al., 2008a; Bodin et al., 2010; Littler et al., 2010) and palaeonvironmental perturbations comparable to the T-OAE occurred across the Pliensbachian-Toarcian boundary (Suan et al., 2008a) indicates that the early Toarcian oceanic anoxic event may be a part of a long-term phase of environmental perturbation and may suggest different paroxysmal episodes of basaltic floods during the Karoo-Ferrar LIP emplacement (Suan et al., 2008b).

Whatever the triggering mechanism, massive $CO_2$ supply to the atmosphere-ocean system caused a cascade of environmental perturbations and geochemical responses,

schematically illustrated by the model proposed by Jenkyns (1999, 2003, 2010) and showed in figure 3. The first effect of the $CO_2$ injection is a global temperature rise, leading to an accelerated hydrological cycle and an increased nutrient flux into the ocean. At the same time increased $CO_2$ concentration in seawater causes ocean acidification: i.e lowering of seawater pH and carbonate saturation ("the other $CO_2$ problem", see the previous paragraph). In case of a volcanogenic event, the global temperature rise may also be responsible of the dissociation of methane gas hydrates from continental-margins, causing a positive feedback loop with further increase of global temperature. Increased nutrient flux into the ocean cause enhanced plankton productivity which may lead to the development of anoxic conditions due to oxygen depletion by organic matter oxidation. At this point there is wide-scale deposition of black-shales, the hallmark of OAEs. $CO_2$ drawdown via increased continental weathering and excess accumulation of organic matter acts as a negative feedback which causes cooling slows down the hydrological cycle and terminates the event.

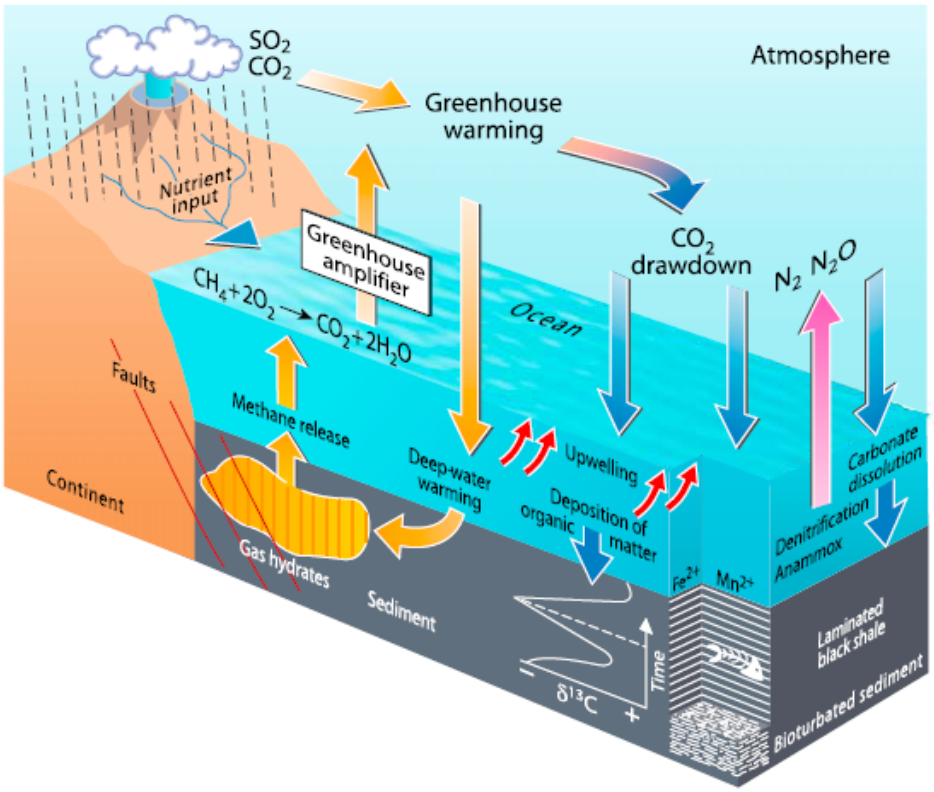


**Figure 3** - Model to illustrate the variety of geochemical processes characteristic of OAEs (Jenkyns, 2010, after Weissert, 2000).

The direct effect of $CO_2$ injection in the atmosphere is a temperature rise, as indicated by geochemical proxies for paleotemperature change, which allowed to associate the OAEs to thermal maxima (Jenkyns, 2010). For example, high resolution oxygen isotope data, $TEX_{86}$ proxy and palynological data suggest a pulse of rapid warming up to 8 °C in the run-up to the early Aptian OAE1a, followed by a cooling trend with fluctuating temperatures during deposition of black shales, which led to $CO_2$ drawdown (Heimhofer et al., 2004; Dumitrescu et al., 2006; Ando et al., 2008).

Oxygen isotope and Mg/Ca ratio of belemnite guards indicate that the T-OAE is coeval with a 6-7 °C warming of seawater (McArthur et al., 2000; Bailey et al., 2003; Rosales et al., 2004; van de Schootbrugge et al., 2005; Gómez et al., 2008). This warming is also observed in fish teeth (Dera et al., 2009b) and brachiopods (Suan et al., 2008a), the

latter indicating also an almost identical warming associated to the Pliensbachian-Toarcian boundary CIE.

Accelerate hydrological cycle and global increase in weathering rates are generally a consequence of temperature rise. As kaolinite forms under intense chemical weathering, indicating high superficial drainage and complete hydrolysis of the source rocks (Chamley, 1989), its abundance through the Mesozoic sediments is used as a proxy of global warming and intensified runoff (Hallam, 1984; Ruffel et al., 2002; Dera et al., 2009a).

A global increase of continental weathering and runoff should also be recorded by the marine isotopic record of $^{87}Sr/^{86}Sr$ and $^{187}Os/^{188}Os$, which are considerably enriched in crustal rocks with respect to the mantle reservoir tapped by hydrothermal fluxes at mid-oceanic ridges (Ravizza and Zachos, 2003). The marine Sr isotope curve, based on the biotic calcite of well preserved belemnites, records a phase of accelerated continental weathering during the T-OAE (Jones et al., 1994; McArthur et al., 2000; Jones and Jenkyns, 2001; Jenkyns et al., 2002, Waltham and Gröcke, 2006). The osmium isotope ratios of Toarcian black shales have been used to infer a dramatic rise of global weathering rates (Cohen et al., 2004), although the signal might be significantly biased by local processes (see discussion in Jenkyns, 2010).

Figure 4 shows that during the early Aptian OAE1a, the general trend of the Sr isotope implies that hydrothermal or other mantle-derived sources of strontium were becoming increasingly important in governing seawater chemistry. In fact, the onset the negative CIE corresponds to a decline in $^{87}Sr/^{86}Sr$ values (Jones and Jenkins, 2001). However, detailed $^{187}Os/^{188}Os$ profiles through the Livello Selli in Italy clearly indicate a pulse of radiogenic osmium to the oceans, suggesting accelerated continental weathering and runoff, interrupting a trend to lower values due to submarine volcanism (Tejada et al., 2009). Increased weathering during the Selli event is also recorded by Ca isotopes of marine carbonates (Blättler et al., 2011) Therefore, isotopic evidence points to increased continental weathering for both the early Toarcian and the early Aptian OAEs. However, for the Selli event the long-term seawater signature was dominated by hydrothermal fluxes associated with submarine volcanism.

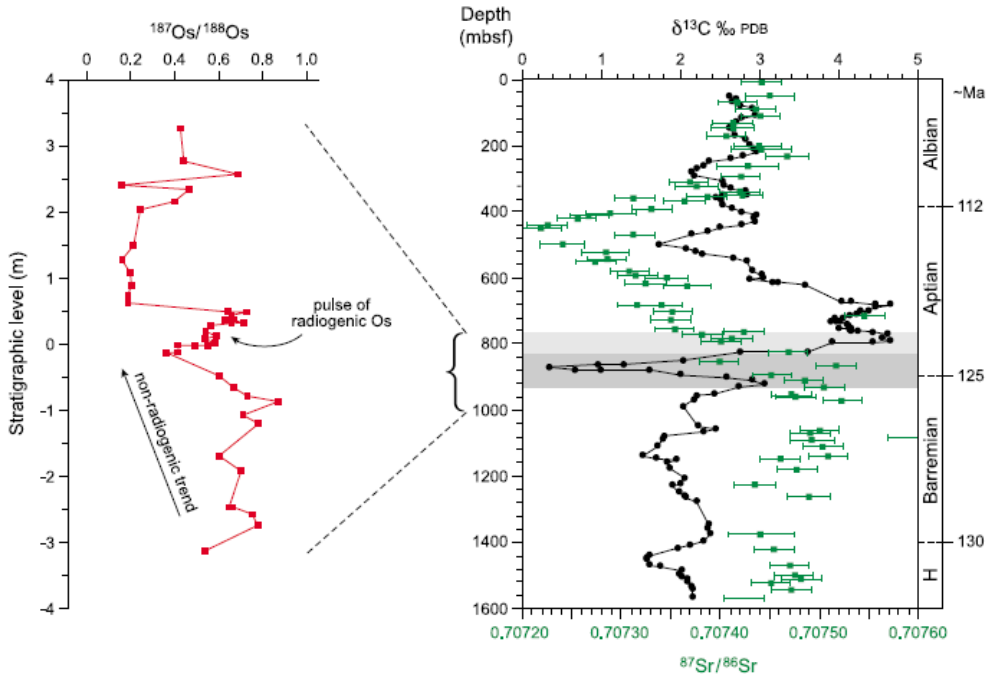


**Figure 4** - Carbon, strontium and osmium profile through early Aptian OAE. Declining $^{87}Sr/^{86}Sr$ values at the onset of the OAE1a suggest increasing relative importance of hydrothermal activity. However, detailed

$^{187}Os/^{188}Os$ profiles through the Livello Selli in Italy clearly indicate a pulse of radiogenic osmium to the oceans, suggesting accelerated continental weathering and runoff (Jenkyns, 2010).

Phosphorus, an essential nutrient for living organism, has been successfully investigated to constrain trophic levels in past oceans (Föllmi, 1995, 1996; van de Shootbrugge et al., 2003; Bodin et al., 2006, 2010; Mort et al., 2007; Godet et al., 2010). Increased nutrient levels are an essential ingredient for OAEs. Two end-member models have been proposed to explain widespread black shale deposition during the Mesozoic OAEs (Pedersen and Calvert, 1990). The stagnant ocean model (STO model) attributes OAEs to depletion of bottom water oxygen as a result of dense vertical ocean stratification; in this case increased preservation of organic matter plays a key role organic-rich sediments accumulation. The expanded oxygen-minimum zone model (OMZ model) proposes the increase of surface ocean productivity as the cause of expansion of the oxygen-minimum layer in the water column. In this model bottom-water anoxia and enhanced preservation of organic matter are not the cause but a positive feedback to enhanced surface productivity.

Besides triggering global warming and enhanced weathering, the massive addition of $CO_2$ to seawater at the onset of OAEs may have caused also ocean acidification. A dramatic drop of pelagic carbonate production by nannoplankton has been recorded both for the Early Toarcian and the early Aptian event (Erba, 2004; Mattioli et al., 2009; Erba et al., 2010).

The hypothesis that high $pCO_2$ was responsible for the nannoplankton biocalcification crisis during the T-OAE has been proposed by Erba (2004), Mattioli et al. (2004) and Tremolada et al. (2005). However, more recently Mattioli et al. (2009) suggested that the combined effects of enhanced runoff and fresh water discharge in the epicontinental basins of the western Tethys was more effective than ocean acidification in producing hostile conditions for calcareous nannoplankton (fig. 5).

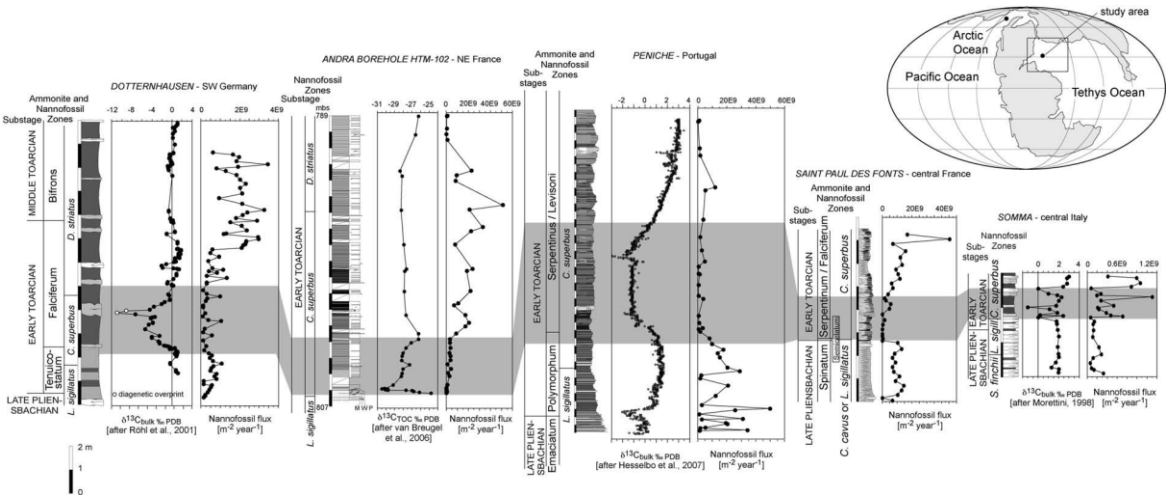


**Figure 5** - Dramatic drop of pelagic carbonate production by nannoplankton during the Early Toarcian (Mattioli et al., 2009).

A biocalcification crisis, the so-called nannoconid crisis, is recorded also at the onset of the early Aptian CIE (Erba, 2004). It has been considered as the response of calcareous nannoplankton to ocean acidification (Erba et al., 2010). However, the hypothesis of ocean acidification is so far not supported by any robust evidence of carbonate dissolution in the deep-sea and of shoaling of the CCD, neither for the Selli event (Gibbs et al., 2011), nor for the T-OAE.

While the Early Aptian event is associated only with a phase of accelerated biotic turnover in the marine plankton (Leckie et al., 2002), a mass extinction event is associated to the T-OAE (Little and Benton, 1995; Harries and Little, 1999; Cecca and Macchioni, 2004;; Wignall et al., 2005; Wignall and Bond, 2008; Dera et al., 2010). Even though the terrestrial biotic record is yet relatively poorly documented, it seems that terrestrial species were also affected (Philipe and Thévenard, 1996).

### *1.3 Motivations and goals*

There is overwhelming evidence for both the T-OAE and the early Aptian OAE1a that geologically rapid injection of $CO_2$ into the ocean-atmosphere system caused abrupt global warming. Ocean acidification has also been proposed for both events. Rates of $CO_2$ injection might have been comparable to current anthropogenic emissions, at least for the T-OAE. Therefore, these two episodes can be used to learn how the earth system and its ecosystems react to a global perturbation of the carbon cycle caused by a $CO_2$ increase.

Most of what we know about the record of the early Toarcian and early Aptian events has been revealed by the study of relatively deep-water marine sediments, deposited in epicontinental basins and shelves and in oceanic basins. Comparatively much less is known on the response of shallow water carbonate platforms, which represent the other "half" of the ocean, in terms of carbonate production and accumulation. This represents a major limitation, not only because carbonate platforms are an important part of the global carbon cycle (Weissert and Erba, 2004) but also because shallow water carbonate sedimentary systems and biota are particularly sensitive to environmental changes (Hallock, 2001) and could therefore tell a complimentary part of the story revealed by their deepwater counterparts.

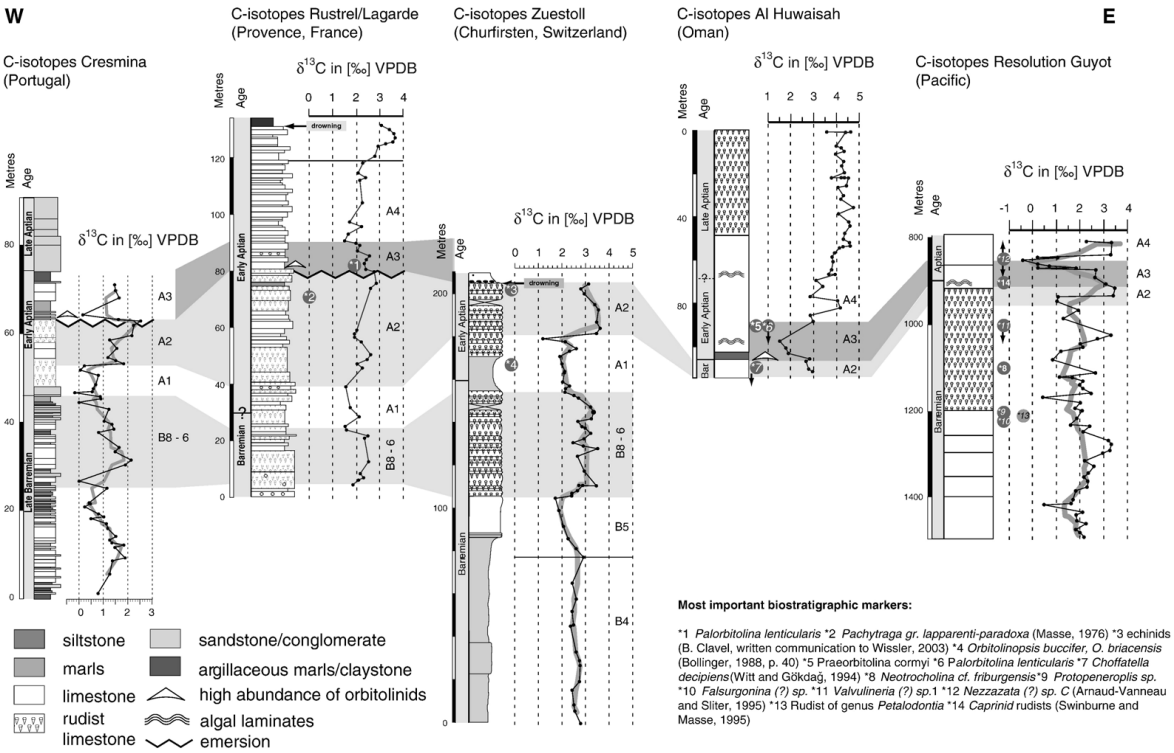


**Figure 6** - Chemostratigraphic correlation of shallow water carbonate successions from the Atlantic, Tethys and Pacific realm (Burla et al. 2008).

The evidence on the response of carbonate platforms to the early Aptian OAE1a has been recently summarized by Burla et al. (2008), who concluded that a supraregional contemporaneous platform "crisis" was probably caused by a combination of surface water acidification and changes in patterns of nutrient inputs to coastal areas, with global warming and rising sea level as additional factors. Regional palaeoenvironmental conditions modulated the type of response and the severity of the platform crisis (fig. 6): while many platforms at the northern margin of the Tethyan ocean were not able to recover and ultimately drowned (Wissler et al., 2003; Föllmi et al., 2006; Huck et al., 2011), southern Tethyan platforms were generally able to escape drowning and reacted with facies and carbonate factory shifts (Immenhauser et al., 2005; Huck et al., 2010).

A widespread episode of carbonate platform drowning is commonly associated with the Early Toarcian paleoenvironmental perturbations (Bassoullet and Baudin, 1994) but there is ample evidence that many Tethyan carbonate platforms drowned well before the onset of T-OAE, either in the Pliensbachian (Marino and Santantonio, 2010; Santantonio and Carminati, 2011 and reference therein) or at the Pliensbachian-Toarcian boundary (Blomeier and Reijmer, 1999; Wilmsen and Neuweiler, 2008; Merino-Tomé et al., 2011). A combination of tectonics, sea-level changes and environmental deterioration is generally invoked as the cause of platform drowning (Cobianchi and Picotti, 2001; Wilmsen and Neuweiler, 2008; Bodin et al., 2010; Merino-Tomé et al., 2011; Léonide et al., 2011) or of a significant carbonate factory shifts (Cobianchi and Picotti, 2001; Woodfine et al., 2008). Woodfine et al. (2008) demonstrated that the Toarcian CIE is preserved in the carbonate isotope records of two resilient Tethyan carbonate platforms, the Trento Carbonate Platform (TCP) and the Apenninic Carbonate Platform (ACP), which reacted to paleoenvironmental perturbations with a shift to more clay-rich facies more or less coinciding with the CIE.

The Apenninic Carbonate Platform grew isolated from major continental landmasses at least since the Early Jurassic (D'Argenio, 1974). It accumulated more than 4500 m of shallow water carbonates from the Late Triassic to the Late Cretaceous and was able to survive all the Mesozoic OAEs. Its sedimentary archive offer the unique opportunity of investigating the response to $CO_2$ induced perturbations without the obvious drawback of habitat loss due to drowning.

Low stratigraphic resolution attained by biostratigraphy (De Castro, 1991; Chiocchini et al., 1994, 2008) and lack of precise correlation with coeval deep-water sequences is generally a major problem in the study of OAEs in carbonate platform sequences. Integration of chemostratigraphy and biostratigraphy has already been used to develop a high-resolution chronostratigraphic framework for the record of the Cenomanian-Turonian boundary OAE2 in the ACP (Parente et al., 2007, 2008).

The main goals of this PhD project are:

1) to study the response of the ACP to the Early Toarcian global perturbations, through the study of two Pliensbachian-Toarcian sequences. Paired carbonate and organic carbon isotope records will be used to pinpoint the stage boundary and the T-OAE. Phosphorus content and clay-minerals will be used to discriminate the relative role of ocean acidification *vs* enhanced nutrient flux on the carbonate factory, and to compare the response of the ACP with that of other carbonate platforms for which increased nutrient levels have been implied as the main cause of crisis or drowning;
2) to study the response of the ACP to the early Aptian OAE, through the integration of the bio-chemostratigraphic work of Di Lucia (PhD thesis, 2009) with the study of two new Barremian-Aptian sections.

## *1.4 References*


Ando A., Kaiho K., Kawahata H. and Kakegawa T. (2008). Timing and magnitude of early Aptian extreme warming: Unraveling primary $\delta^{18}O$ variation in indurated pelagic carbonates at Deep Sea Drilling Project Site 463, central Pacific Ocean. Palaeogeography, Palaeoclimatology, Palaeoecology 260, 463–476.

Bailey T.R., Rosenthal Y., McArthur J.M., van de Schootbrugge B. and Thirlwall M.F. (2003). Paleoceanographic changes of the Late Pliensbachian–Early Toarcian interval: a possible link to the genesis of an Oceanic Anoxic Event. Earth and Planetary Science Letters 212, 307–320.

Bassoullet J.P. and Baudin F. (1994). Le Toarcien inférieur: une période de crise dans les bassins et sur les plates-formes carbonatées de l'Europe du Nord-Ouest et de la Téthys. Geobios, M.S. 17, 645–654.

Blättler C.L., Jenkyns H.C., Reynard L.M. and Henderson G.M. (2011). Significant increases in global weathering during Oceanic Anoxic Events 1a and 2 indicated by calcium isotopes. Earth and Plan. Scie. Lett. 309, 77–88.

Blomeier, D.P.G. and Reijmer J.J.G. (1999). Drowning of a Lower Jurassic Carbonate Platform: Jbel Bou Dahar, High Atlas, Morocco. Facies 41, 81–110.

Bodin S., Godet A., Föllmi K.B., Vermeulen J., Arnaud H., Strasser A., Fiet N. and Adatte T. (2006). The Late Hauterivian Faraoni oceanic anoxic event in the western Tethys: evidence from phosphorus burial rates. Palaeogeography, Palaeoclimatology, Palaeoecology 235, 245–264.

Bodin S., Mattioli E., Fröhlich S., Marshall J.D., Boutib L., Lahsini S. and Redfern J. (2010). Toarcian carbon isotope shifts and nutrient changes from the Northern margin of Gondwana /High Atlas, Marocco, Jurassic): Palaeoenvironmental implications. Palaeogeography, Palaeoclimatology, Palaeoecology 297, 377–390.

Broecker W.S. and Peng, T.-H., (1982). Tracers in the Sea. Lamon-Doherty Geological Observatory, Coumbio University, Palisades, NY. 687 pp.

Burla S., Heimhofer U., Hochuli P.A., Weissert H. and Skelton P. (2008). Changes in sedimentary patterns of coastal and deep-sea successions from the North Atlantic (Portugal) linked to Early Cretaceous environmental change. Palaeogeography, Palaeoclimatology, Palaeoecology 257, 38–57.

Caldeira K. and Wickett M.E. (2003). Anthropogenic carbon and ocean pH. Nature 425, 365.

Cecca F. and Macchioni F. (2004). The two Early Toarcian (Early Jurassic) extinction events in ammonoids. Lethaia 37, 35–56.

Chamley H. (1989). Clay Sedimentology. Springer Verlag, Berlin.

Chiocchini M., Farinacci A., Mancinelli A., Molinari V. and Potetti M. (1994). Biostratigrafia a foraminiferi dasicladali e calpionelle delle successioni carbonatiche mesozoiche dell'Appennino centrale (Italia). In: Mancinelli A. (ed) Biostratigrafia dell'Italia centrale. Studi Geologici Camerti, Volume Speciale, 1994, 9–129.

Chiocchini M., Chiocchini R.A., Didaskalou P. and Potetti M. (2008). Microbiostratigrafia del Triassico superiore, Giurassico e Cretacico in facies di piattaforma carbonatica del Lazio centromeridionale e Abruzzo: revisione finale, Mem. Descr. Carta Geol. d'It., 5–170.

Cobianchi M. and Picotti, V. (2001). Sedimentary and biological response to sea-level and palaeoceanographic changes of a Lower–Middle Jurassic Tethyan platform margin (Southern Alps, Italy). Palaeogeography, Palaeoclimatology, Palaeoecology 169, 219–244.

Cohen A.S., Coe A.L., Harding S.M. and Schwark, L. (2004). Osmium isotope evidence for the regulation of atmospheric $CO_2$ by continental weathering. Geology 32, 157–160.

D'Argenio B. (1974). Le piattaforme carbonatiche periadriatiche: una rassegna di problemi nel quadro geodinamico mesozoico dell'area mediterranea. Memorie della Società Geologica Italiana 13, 137–159.

De Castro P. (1991). Mesozoic in : Barattolo F., De Castro P. and Parente M. (eds) 5th International Symposium on Fossil Algae. Field Trip Guide-Book. Giannani, Napoli, 21–38.

Dera G., Pellenard P., Neige P., Deconinck J.-F., Pucéat E. and Dommergues J.-L. (2009a). Distribution of clay-minerals in Early Jurassic Peritethyan seas: palaeoclimatic significance inferred from multiproxy comparisons. Palaeogeography, Palaeoclimatology, Palaeoecology 271, 39–51.

Dera G., Pucéat E., Pellenard P., Neige P., Delsate D., Joachimski M.M., Reisberg L. and Martinez M. (2009b). Water mass exchange and variations in seawater temperature in the NW Tethys during the Early Jurassic: evidence from neodymium and oxygen isotopes of fish teeth and belemnites. Earth and Planetary Science Letters 286, 198–207.

Dera G., Neige P., Dommergues J.-L., Fara E., Laffont R. and Pellenard P. (2010). High resolution dynamics of Early Jurassic marine extinctions: the case of Pliensbachian-Toarcian ammonites (Cephalopoda). Journal of Geological Society of London 167, 21–33.

Dickens G.R. (2011). Down the Rabbit Hole: toward appropriate discussion of methane release from gas hydrate system during the Paleocene-Eocene thermal maximum and other past hyperthermal events. Clim. Past. 7, 831–846.

Doney S.C., Fabry V.J., Feely R.A. and Kleypas J.A. (2009). Ocean Acidification: The other $CO_2$ problem. Annu. Rev. Marine. Sci. 1, 169–192.

Doney S.C. and Schimel D.S. (2007). Carbon and climate system coupling on timescales from the Precambrian to the Anthropocene. Annu. Rev. Environ. Resour. 32, 31–66.

Dumitrescu M., Brassell S.C., Schouten S., Hopmans E.C and Sinninghe Damsté J. S. (2006). Instability in tropical Pacific sea-surface temperatures during the early Aptian. Geology, 34, 833–836, doi:10.1130/G22882.1.

Erba E. (2004). Calcareous nannofossils and Mesozoic oceanic anoxic events. Mar. Micropaleontol. 52, 85–106.

Erba E., Bottini C., Weissert H.J. and Keller C.E. (2010). Calcareous nannoplankton response to surface-water acidification around Oceanic Anoxic Event 1a. Science 329, 428–432.

Föllmi K.B. (1995). 160 m.y. record of marine sedimentary phosphorus burial: coupling of climate and continental weathering under greenhouse and icehouse conditions. Geology 23, 859–862.

Föllmi K.B. (1996). The phosphorus cycle, phosphogenesis and marine phosphate-rich deposits. Earth-Science Reviews 40, 55–124.

Föllmi K.B., Godet A., Bodin S. and Linder P. (2006). Interactions between environmental change and shallow water carbonate build-up along the northern Tethyan margin and their impact on the early Cretaceous carbon-isotope record. Paleoceanography 21, PA4211.

Gibbs S.J., Robinson S.A., Bown P.R., Jones T.D. and Henderiks J. (2011). Comment on "Calcareous Nannoplankton Response to Surface-Water Acidification Around Oceanic Anoxic Event 1a." Science 332, 175–175.

Godet A., Föllmi K.B., Bodin S., de Kaenel E., Matera V. and Adatte T. (2010). Stratigraphic, sedimentological and palaeoenvironmental constraints on the rise of the Urgonian platform in the western Swiss Jura. Sedimentology 57, 1088–1125.

Gómez J.J., Goy A. and Canales M.L. (2008). Seawater temperature and carbon isotope variations in belemnites linked to mass extinction during the Toarcian (Early Jurassic) in Central and Northern Spain. Comparison with other European sections. Palaeogeography, Palaeoclimatology, Palaeoecololy 258, 28–58.

Gröcke D.R., Rimmer S.M., Yoksoulian L.E., Cairncross B., Tsikos H. and van Hunen, J. (2009). No evidence for thermogenic methane release in coal from the Karoo–Ferrar large igneous province. Earth Planet. Sci. Lett. 277, 204–212.

Guinotte J.M. and Fabry V.J. (2008). Ocean acidification and its potential effects on marine ecosystems. Ann. New York Acad. Sci. 1134, 320–342.

Hallam A. (1984). Continental humid and arid zones during the Jurassic and Cretaceous. Palaeogeography, Palaeoclimatology, Palaeoecology 47, 195–223.

Hallock P. (2001). Coral reefs, carbonate sediment, nutrients, and global change. In: Stanley G.D, editor. Ancient reef ecosystem: their evolution, paleoecology and importance in earth history. New York: Kluwer Academic/Plenum Publishers. p 388-427.

Harries P.J. and Little C.T.S. (1999). The early Toarcian (Early Jurassic) and the Cenomanian–Turonian (Late Cretaceous) mass extinctions: similarities and contrasts. Palaeogeography, Palaeoclimatology, Palaeoecology 154, 39–66.

Heimhofer U., Hochuli P.A., Herrle J.O., Andersen N. and Weissert H. (2004). Absence of major vegetation and palaeoatmospheric $pCO_2$ changes associated with oceanic anoxic event 1a (Early Aptian, SE France). Earth Planet. Sci. Lett. 223, 303–318.

Henderson C. (2006). Ocean acidification: the other $CO_2$ problem. New Scientist. http://environment.newscientist.com/article/mg19125631.200.

Hesselbo S.P., Gröcke D.R., Jenkyns H.C., Bjerrun C.J., Farrimond P., Morgans Bell H.S. and Green O.R. (2000). Massive dissociation of gas hydrate during a Jurassic oceanic anoxic event. Nature 406, 392–395.

Hesselbo S.P., Jenkyns H.C., Duarte L.V. and Oliveira L.C.V. (2007). Carbon-isotope record of the Early Jurassic (Toarcian) Oceanic Anoxic Event from fossil wood and marine carbonate (Lusitanian Basin, Portugal). Earth Planet. Sci. Lett. 253, 455–470.

Huck S., Rameil N., Korbar T., Heimhofer U., Wieczorek T.D. and Immenhauser A. (2010). Latitudinally different responses of Tethyan shoal-water carbonate systems to the Early Aptian oceanic anoxic event (OAE 1a). Sedimentology 57, 1585–1614.

Huck S., Heimhofer U., Rameil N., Bodin S. and Immenhauser A. (2011). Strontium and carbon-isotope chronostratigraphy of Barremian-Aptian shoal-water carbonates: Northern Tethyan platform drowning predates OAE 1a. Earth Planet. Sci. Lett. 304, 547–558.

Immenhauser A., Hillgärtner H. and van Bentum E. (2005). Microbial–foraminiferal episodes in the Early Aptian of the southern Tethyan margin: ecological significance and possible relation to oceanic anoxic event 1a. Sedimentology 52, 77–99.

Jahren A.H., Arens N.C., Sarmiento G., Guerrero J. and Amundson R. (2001). Terrestrial record of methane hydrate dissociation in the Early Cretaceous. Geol. Soc. Am. Bull. 29, 159–162.

Jenkyns H.C. (2003). Evidence for rapid climate change in the Mesozoic-Palaeogene greenhouse world. Philos. Trans. Royal Soc., Ser. A 361, 1885–1916.

Jenkyns H.C. (2010). Geochemistry of oceanic anoxic events,. Geochem. Geophys. Geosyst., 11, Q03004, doi:10.1029/2009GC002788.

Jenkyns H.C., Jones C.E., Gröcke D.R., Hesselbo S.P. and Parkinson D.N. (2002). Chemostratigraphy of the Jurassic system: applications, limitations and implications for palaeoceanography. J. Geol. Soc. 159, 351–378.

Jones C.E. and Jenkyns H.C. (2001). Seawater strontium isotopes, oceanic anoxic events, and seafloor hydrothermal activity in the Jurassic and Cretaceous. Am. J. Sci. 301, 112–149.

Jones C.E., Jenkyns H.C. and Hesselbo S.P. (1994). Strontium isotopes in Early Jurassic seawater. Geochim. Cosmochim. Ac. 58, 1285–1301.

Kemp D.B., Coe A.L., Cohen A.S. and Schwark L. (2005). Astronomical pacing of methane release in the Early Jurassic period. Nature 437, 396–400.

Kerr A.C. (2005). Oceanic LIPs: The kiss of death. Elements 1(5), 289–292.

Kroeger K.F., di Primio R. and Horsfield B. (2011). Atmospheric methane from organic carbon mobilization in sedimentary basins – the sleeping giant? Earth Science Reviews 107, 3–4, 423–442.

Larson R.L. and Erba E. (1999). Onset of the mid-Cretaceous greenhouse in the Barremian-Aptian: Igneous events and the biological, sedimentary, and geochemical responses. Paleoceanography 14, 663–678.

Lekie R.M., Bralower T.J. and Cashman R. (2002). Oceanic anoxic events and plankton evolution: Biotic response to tectonic forcing during the mid-Cretaceous. Paleoceanography vol. 17, no, 3, 10.1029/2001PA000623.

Léonide P., Floquet M., Durlet C., Baudin F. Pittet B. and Lécuyer C. (2011). Drowning of a carbonate platform as a precursor stage of the Early Toarcian global anoxic event (Southern Provence sub-Basin, South-east France). Sedimentology, doi: 10.1111/j.1365-3091.2010.01221.x.

Little C.T.S. and Benton M.J. (1995). Early Jurassic mass extiction: a global long-term event. Geology 23, 495–498.

Littler K., Hesselbo S.P. and Jenkyns H.C. (2010). A carbon-isotope perturbation at the Pliensbachian-Toarcian boundary: evidence from the Lias Group, NE England. Geological Magazine 147, 181–192.

Lüthi D., Le Floch M., Bereiter B., Blunier T. and Barnola J.-M., Siegenthaler U., Raynaud D., Jouzel J., Fisher H., Kawamura K. and Stocker T.F. (2008). High-resolution carbon dioxide concentration record 650,000-800,000 years before present. Nature 453, 379–82.

Mattioli E., Pittet B., Bucefalo Palliani R., Röhl H.-J., Schmid-Röhl A. and Morettini E. (2004). Phytoplankton evidence for timing and correlation of palaeoceanographical changes during the Early Toarcian oceanic anoxic event (Early Jurassic). Journal of Geological Society of London 161, 685–693.

Mattioli E., Pittet B., Petitpierre L. and Mailliot S. (2009). Dramatic decrease of pelagic carbonate production by nannoplankton across the Early Toarcian anoxic event (T-OAE). Global and Planetary Change 65 (3-4), 134–145.

Marino M. and Santantonio M. (2010). Understanding the geological record of carbonate platform drowning across rifted Tethyan margins: Examples from Lower Jurassic of the Apennines and Sicily (Italy). Sedimentary Geology 225, 116–137.

Méhay S., Keller C.E., Bernasconi S.M., Weissert H., Erba E., Bottini C. and Hochuli P.A. (2009). A volcanic $CO_2$ pulse triggered the Cretaceous Oceanic Anoxic Event 1a and a biocalcification crisis. Geology 37, 819–822.

McArthur J.M., Donovan D.T., Thirlwall M.F., Fouke B.W. and Mattey D. (2000). Strontium isotope profile of the early Toarcian (Jurassic) oceanic anoxic event, the duration of ammonite biozones, and belemnite palaeotemperatures. Earth and Planetary Science Letters 179, 269–285.

McElwain J.C., Wade-Murphy J. and Hesselbo S.P. (2005). Changes in carbon dioxide during an oceanic anoxic event linked to intrusion into Gondwana coals. Nature 435, 479–482.

McInerney F.A. and Wing S.L. (2011). The Paleocene-Eocene Thermal Maximum: A perturbation of carbon cycle, climate, and biosphere with implications for the future. Ann. Rev. of Earth and Planet. Scie. 39, 489–516.

Merino-Tomé Ò., Della Porta G., Kenter J.A.M., Verwers K., Harris P.M., Adams E.W., Playton T. and Corrochano D. (2011). Sequence development in an isolated carbonate platform (Lower Jurassic, Djebel Bou Dahar, High Atlas, Marocco): influence of tectonics, eustacy and carbonate production. Sedimentology, doi: 10.1111/j.1365-3091.2011.01232.x.

Millero F.J., Pierrot D., Lee K., Wanninkhof R., Feely R, Sabine C.L., Key R.M. and Takahashi T. (2002). Dissociation constants for carbonic acid determined from field measurements. Deep Sea Research Part I: Oceanogr. Res. Papers 49, 1705–1723.

Mort H.P., Adatte T., Föllmi K.B., Keller G., Steinmann P., Matera V., Berner Z. and Stüben D. (2007). Phosphorus and the roles of productivity and nutrient recycling during oceanic anoxic event 2. Geology 35, 483–486.

Orr J.C., Fabry V.J., Aumont O., Bopp L., Doney S.C., Feely R.A., Gnanadesikan A., Gruber N., Ishida A., Joos F., Key R.M., Lindsay K., Maier-Reimer E., Matear R., Monfray P., Mouchet A., Raymond G., Najjar R.G., Plattner G.-K., Rodgers K.B., Sabine C.L., Sarmiento J.L., Schlitzer R., Slater R.D., Totterdell I.J., Weirig M.-F., Yamanaka Y. and Yool A. (2005). Anthropogenic ocean acidification over the twenty-first century and its impact on calcifying organisms. Nature 437, 681–86.

Pálfy J. and P. L. Smith (2000). Synchrony between Early Jurassic extinction, oceanic anoxic event, and the Karoo-Ferrar flood basalt volcanism. Geology 28, 747–750.

Parente M., Frijia G. and Di Lucia M. (2007). Carbon-isotope stratigraphy of Cenomanian-Turonian platform carbonates from the southern Appennines (Italy): a chemostratigraphic approach to the problem of correlation between shallow water and deep-water successions. Journale of the Geol. Soc., London 164, 609–620.

Parente M., Frijia G., Di Lucia M., Jenkyns H.C., Woodfine R.G. and Baroncini F. (2008). Stepwise extinction of larger foraminifers at the Cenomanian-Turonian boundary: A shallow water perspective on nutrient fluctuations during Oceanic Anoxic Event 2 (Bonarelli Level). Geology v.36, no.9, 715–718.

Pedersen T. F. and Calvert S.E. (1990). Anoxia vs. productivity: What controls the formation of organic-carbon-rich sediments and sedimentary rocks? AAPG Bull. 74, 454–472.

Pearson P.N. and Palmer P.R. (2000). Atmospheric carbon dioxide concentrations over the past 60 million years. Nature 406, 695–699.

Philippe M. and Thévenard F. (1996). Distribution and palaeoecology of the Mesozoic wood genus Xenoxylon: palaeoclimatological implication for the Jurassic of Western Europe. Rev. Palaeobot. Palynology 91, 353–370.

Ravizza G. E. and Zachos J.C. (2003). Records of Cenozoic Ocean Chemistry. In H.D. Holland, K.K. Turekian (eds). Treatise on Geochemistry: The Oceans and Marine Geochemistry, v. 6, Elsevier, p. 551–582.

Ries J., Cohen A. and McCorkle D. (2009). Marine calcifiers exhibit mixed responses to $CO_2$-induced ocean acidification. Geology, 37(12), 1131–1134.

Rodolfo-Metalpa R., Lombardi C., Cocito S., Hall-Spencer J.M. and Gambi M.C. (2010). Effects of ocean acidification and high temperatures on the bryozoan *Myriapora truncata* at natural $CO_2$ vents. Marine Ecology doi:10.1111/j.1439-0485.2009.00354.x.

Röhl U., Westerhold T., Bralower T.J. and Zachos J.C. (2007). On the duration of the Paleocene-Eocene thermal maximum (PETM). Geochem. Geophys. Geosyst. 8, Q12002, doi:10.1029/2007GC001784.

Rosales I., Quesada S. and Robles S. (2004). Paleotemperature variations of Early Jurassic seawater recorded in geochemical trends of belemnites from the Basque–Cantabrian Basin, northern Spain. Palaeogeography, Palaeoclimatology, Palaeoecology 203, 253–275.

Royal Society (2005). Ocean acidification due to increasing atmospheric carbon dioxide. London: The Royal Society, 57 pp.

Ruffell A., McKinley J.M. and Worden R.H. (2002). Comparison of clay-mineral stratigraphy to other proxy palaeoclimate indicators in the Mesozoic of NW Europe. Phil. T. Roy. Soc. A 360, 675–693.

Sabine C.L. and Feely R.A. (2007). The oceanic sink for carbon dioxide. In Greenhouse Gas Sinks, ed. D. Reay, N. Hewitt, J. Grace, K. Smith, pp. 31–49. Oxfordshire: CABI Publishing.

Sabine C.L., Feely R.A., Gruber N., Key R.M., Lee K., Bullister J.L., Wanninkhof R., Wong C.S., Wallace D.W., Tilbrook B., Millero F.J., Peng T.H., Kozyr A., Ono T. and Rios A.F. (2004). The oceanic sink for anthropogenic $CO_2$. Science 305, 367–71.

Santantonio M. and Carminati E. (2011). Jurassic rifting evolution of the Apennines and Southern Alps (Italy): Parallels and differences. GSA Bulletin 123, no. 3-4, 468–484. doi: 10.1130/B30104.1.

Schlanger S.O. and Jenkyns H.C. (1976). Cretaceous oceanic anoxic events:causes and consequences. Geol. Mijnb. 55, 179–184.

Scholle P.A. and Arthur M.A. (1980). Carbonate isotope fluctuations in Cretaceous pelagic limestones: potential stratigraphic and petroleum exploration tool. Bull. Amer. Assoc. Petrol. Geol., 64, 67–87.

Solomon S., Qin D., Manning M., Chen Z., Marquis M., Averyt K., Tignor M. and Miller H.L. (2007). IPCC, 2007: Climate Change 2007: The Physical Science Basis: Contribution of Working Group I to the Fourth Assessment Report of the Intergovernmental Panel on Climate Change. Cambridge University Press, Cambridge, UK and New York, NY, USA.

Suan G., Mattioli E., Pittet B., Mailliot S. and Lécuyer C. (2008a). Evidence for major environmental perturbation prior to and during the Toarcian (Early Jurassic) oceanic anoxic event from the Lusitanian Basin. Paleoceanography 23, PA1202. doi:10.1029/2007PA001459.

Suan G., Pittet B., Bour I., Mattioli E., Duarte L.V. and Mailliot S. (2008b). Duration of the Early Toarcian carbon isotope excursion deduced fromspectral analysis: consequence for its possible causes. Earth Planet. Sci. Lett. 267, 666–679.

Svensen H., Planke S., Chevallier L., Malthe-Sorenssen A., Corfu F. and Jamtveit B. (2007). Hydrothermal venting of greenhouse gases triggering Early Jurassic global warming. Earth and Planetary Science Letters 256, 554–566.

Tejada M.L.G., Suzuki K., Kuroda J., Coccioni R., Mahoney J.J., Ohkouchi N., Sakamoto T. and Tatsumi Y. (2009). Ontong Java Plateau eruption as a trigger for the early Aptian oceanic anoxic event. Geology 37, 855–858.

Tremolada F., van de Schootbrugge B. and Erba E. (2005). Early Jurassic schizosphaerellid crisis in Cantabria, Spain: implications for calcification rates and phytoplankton evolution across the Toarcian oceanic anoxic event. Paleoceanography 20, A201. doi:10.1029/2004PA001120.

Turley C. (2005). The other $CO_2$ problem. openDemocracy. http://www.acamedia.info/sciences/.

Turley C., Blackford J., Widdicombe S., Lowe D., Nightingale P.D. and Rees A.P. (2006). Reviewing the impact of increased atmospheric CO2 on oceanic pH and the marine ecosystem. In: Avoiding Dangerous Climate Change, Schellnhuber, H J., Cramer,W., Nakicenovic, N., Wigley, T. and Yohe, G (Eds), Cambridge University Press, 8, 65–70.

Turley C., Eby M., Ridgwell A.J., Schmidt D.N., Brownlee C., Findlay H.S., Fabry V.J., Feely R.A., Riebesell U. and Gattuso J.-P. (2010). The Societal challenge of ocean acidification. Marine Pollution Bulletin 60, 787–792.

van de Schootbrugge B., Kuhn O., Adatte T., Steinmann P. and Föllmi K.B. (2003). Decoupling of P- and $C_{org}$-burial following Early Cretaceous (Valanginian–Hauterivian) platform drowning along the NW Tethyan margin. Palaeogeography, Palaeoclimatology, Palaeoecology 199, 315–331.

van de Schootbrugge B.,McArthur J.M., Bailey T.R., Rosenthal Y., Wright J.D. and Miller K.G. (2005). Toarcian oceanic anoxic event: an assessment of global causes using belemnite C isotope records. Paleoceanography 20 PA3008, 1–10.

Waltham D. and Gröcke D.R. (2006). Non-uniqueness and interpretation of the seawater $^{87}Sr/^{86}Sr$ curve. Geoch. Et Cosmoch. Acta 70, 384–394.

Weissert H. (2000). Deciphering methane's fingerprint. Nature 406, 356–357.

Weissert H. and Erba E. (2004). Volcanism, $CO_2$ and paleoclimate: a Late Jurassic-Early Cretaceous carbonand oxygen isotope record. J.Geol. Soc. Lond. 161, 695–702.

Wignall, P.B. (2001). Large igneous provinces and mass extinctions. Earth Science Reviews 53, 1–33.

Wignall P.B. and Bond D.P.G. (2008). The end-Triassic and Early Jurassic mass extinction records in the British Isles. Proceedings of the Geologists' Association 119, 73–84.

Wignall P.B., Newton R.J. and Little C.T.S. (2005). The timing of paleoenvironmental change and cause-and-effect relationships during the early Jurassic mass extinction in Europe. Am. J. Sci. 305, 1014–1032.

Wilmsen M. and Neuweiler F. (2008). Biosedimentology of the Early Jurassic postextinction carbonate depositional system, central High Atlas rift basin, Morocco. Sedimentology 55, 773–807.

Wissler L., Funk H. and Weissert H. (2003). Response of Early Cretaceous carbonate platforms to changes in atmospheric carbon dioxide levels. Palaeogeography, Palaeoclimatology, Palaeoecology 200, 187–205.

Woodfine R.G., Jenkyns H.C., Sarti M., Baroncini F. and Violante C. (2008) The response of two Tethyan carbonate platforms to the early Toarcian (Jurassic) oceanic anoxic event: environmental change and differential subsidence. Sedimentology 55, 1011–1028.

Zachos J.C., Röhl U., Schellenberg S.A., Sluijs A. Hodell D.A., Kelly D.C., Thomas E., Nicolo M., Raffi I., Lourens L.J., McCarren H. and Kroon D. (2005). Rapid acidification of the ocean during the Paleocene-Eocene Therminal Maximum. Science 308, 1611–1615.

# CHAPTER 2 – The Southern Apennines and the sedimentary succession of the Apenninic Carbonate Platform

## *2.1 The Southern Apennines fold-and-thrust belt*

The Southern Apennines are a NE verging fold-and-thrust belt (Butler et al., 2004; Mazzoli et al., 2008) that developed during the Neogene at the expense of the Afro-Adriatic continental margin and evolved within the framework of convergent motion between the Afro-Adriatic and European plates since Late Cretaceous times (Dewey et al., 1989; Mazzoli and Helman, 1994; Rosenbaum et al., 2002). The extremely complex geology of the southern Apenninic belt is the product of a polyphasic tectonics, consisting of a collision from the Miocene through the Pliocene, associated in the late stage with transcurrent and extensional faulting (Cello et al., 1982, 2000; Cinque et al., 1993; Oldow et al., 1993).

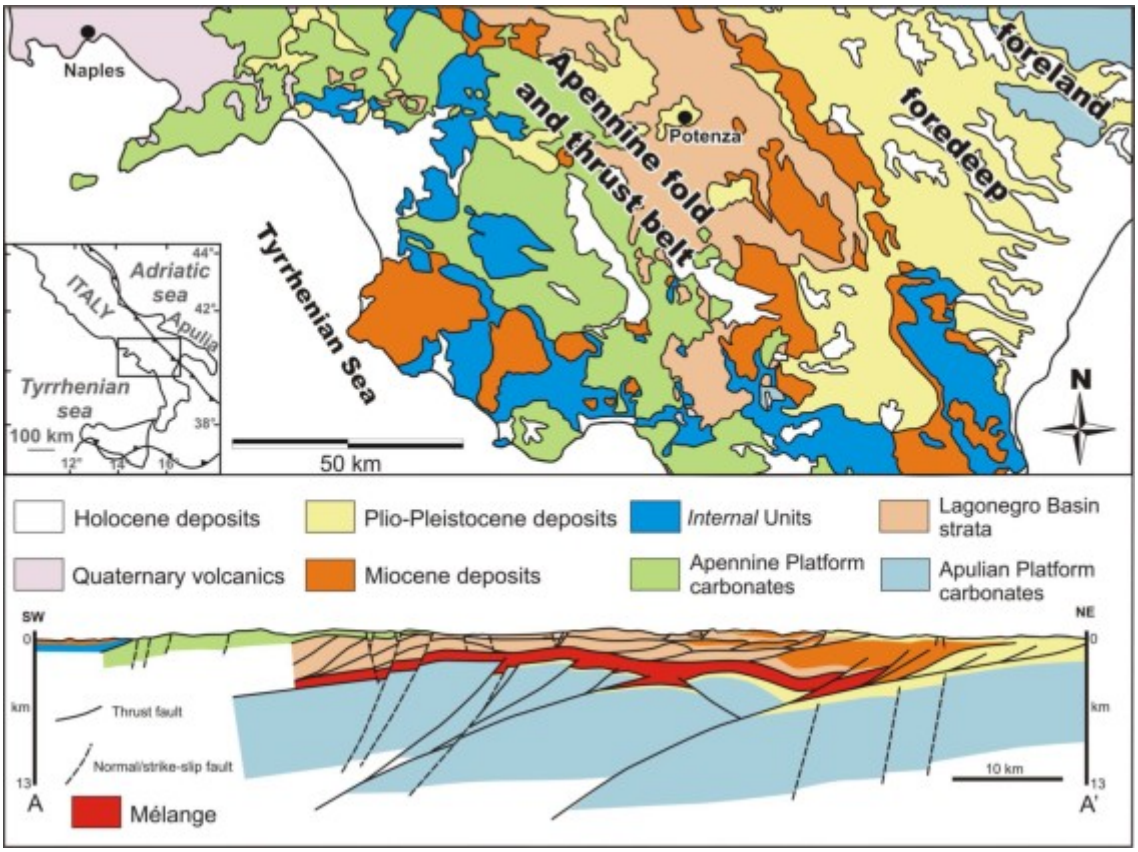


**Figure 1** - Simplified geological scheme of Southern Apennines (Ciarcia et al., 2009).

Except for the remnants of the ophiolite-bearing Liguride Units that occur on top of the thrust pile, outcropping units consist of Mesozoic and Cenozoic rocks derived from the sedimentary cover of the foreland plate. This plate is overlain by an allochthon consisting of both Mesozoic-Palaeogene units, initially deposited on the Adriatic passive margin, and of Miocene flysch units, deposited within the evolving thrust belt. The allochthon includes both the shallow marine carbonates of the Apenninic platform and the deepwater, mixed clastic cherty carbonates of the Lagonegro basin (fig. 1).

Regional criteria indicate that the allochthon has been thrust for a minimum of some 57 km over the buried Apulian platform with the detachment between these two structural units marked by a ‘mèlange zone’ generally several hundreds of metres thick and locally exceeding 1 km (Butler et al., 2004). This mèlange zone dominantly consists of intensely

deformed and overpressured deepwater mudstones and siltstones of Miocene to Early Pliocene age. This unit is interpreted to represent a mixture of Mio-Pliocene foredeep deposits incorporated within the basal decollement zone as the advancing fold and thrust belt overrode its foreland basin.

The interpretation of the subsurface geometry of the fold-and-thrust belt is still not univocal. According to the classical thin-skinned model proposed by Mostardini and Merlini (1986) the basement was not involved in the Apulian compressional structures, which were formed in the hanging walls of low-angle thrusts . A development of this simple thin-skinned interpretation was shown by Casero et al. (1988, 1991), who considered an efficient deep detachment between the Apulian platform and basement within the Burano anhydrites, and assumed that the "mèlange zone" formed a shallow detachment between the Apulian platform and the allochthon. On the other hand, Menardi Noguera and Rea (2000) have shown a mixture of thick- and thin-skinned tectonic styles. In their hypothesis, thrusts on the western end of the line are interpreted as thin-skinned, detaching at the basement sediment cover interface. In contrast, the easternmost compressional structures are related to a transpressive shear zone with a sinistral component that is interpreted to cut the entire crust within the study area and to detach on the Adriatic Moho. Recently, the integration of a large amount of surface geological information with subsurface data gave a big contribution to demonstrate a large-scale complex thin-skinned/thick-skinned thrusting in the shallow part of the Southern Apennines (Shiner et al., 2004; Mazzoli et al., 2001, 2008).

The burial history of the Southern Apennines is constrained by recent studies based on thermal and thermochronological data (Aldega et al., 2003a, 2003b; Corrado et al., 2005; Mazzoli et al., 2006, 2008). These studies highlight that a significant part of the sedimentary rocks exposed in the Southern Apennines experienced substantial tectonic burial (locally in excess of 5 km). This is not true for the Apenninic platform domain whose burial never exceed 2 km.

### *2.2 The Apenninic Carbonate Platform (ACP)*

The shallow water carbonates that are widely exposed in the southern Apennines are the relics of carbonate banks that developed during the Mesozoic on the passive margin of Adria, a promontory of the African Plate (Bosellini, 2002). The different tectonic interpretations of the fold and thrust belt determine different reconstructions of the pre-orogenic paleogeography of the area. The classical restorations of Triassic to Paleogene palaeogeography of the southern Apennines shows that the African (Apulian) passive margin was characterized by carbonate platforms alternating with deep-sea basins (D'Argenio et al., 1975b; Sgrosso, 1988). More simple models suggest the presence of a single Meso-Cenozoic pelagic basin, the Lagonegro Basin, between two carbonate platforms, the Apenninic and Apulian platforms (Mostardini and Merlini, 1986), in accordance with a previous model proposed by Ogniben (1969). Among the several more or less complex reconstructions proposed for the pre-orogenic Meso–Cenozoic paleogeography, the latter is the most widely accepted one, grounded also in subsurface data (Menardi Noguera and Rea, 2000).

The oldest neritic carbonates cropping out in the southern Apennines are Middle Triassic in age and there is ample evidence that shallow water carbonate sedimentation was established over wide areas during the Late Triassic (D'Argenio and Sgrosso, 1974). At least since the Early Jurassic the Apenninic Carbonate Platform grew isolated from major contiental landmasses (D'Argenio, 1974). In the ACP shallow water sedimentation persisted almost to the end of the Cretaceous, when the area underwent a generalized

emersion. It was locally re-established during the Palaeogene (Trentinara Formation; Selli 1962) and the Early Miocene (Roccadaspide–Cerchiara and Cusano Formation; Selli 1957), to be eventually terminated by drowning and siliciclastic sedimentation in the Middle-Late Miocene. The Upper Triassic to Lower Cretaceous carbonates of the ACP are generally referred to flat-topped, tropical carbonate platforms dominated by chloralgal or chlorozoan associations (D'Argenio et al., 1975a) whereas the depositional system of Senonian rudist limestones of the southern Apennines has been interpreted as a ramp-like open shelf dominated by foramol-type assemblages (Carannante et al., 1997).

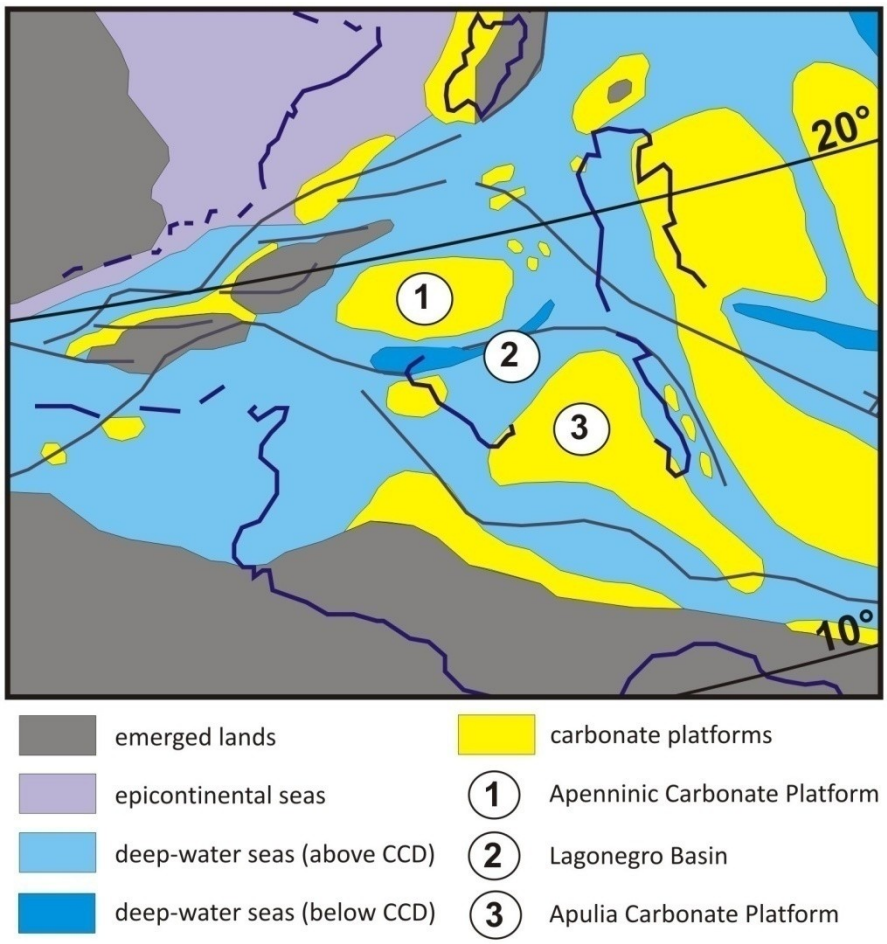


**Figure 2** - Toarcian palaeogeography of the peri-Tethyan domains (redrawn from Bassoullet et al., 1993).

The Apenninic Carbonate Platform (ACP) succession is made of a > 4.5 km-thick pile of shallow water carbonates. The following scheme of the stratigraphic succession of the ACP refers to the recent lithostratigraphic nomenclature adopted by the *Servizio Geologico d'Italia* (Italian geological Survey) for the geological mapping project at scale 1:50.000 (*Progetto CARG*). The Upper Triassic is represented by the "*Dolomia massiva di base"* (lower massive dolomite), followed by the "*Marne con Avicula e Myophoria"* (marls with Avicula and Myophoria) and the "*Dolomia Superiore"* (Upper Dolomite). The Lower Jurassic is represented by the "*Calcari a Palaeodasycladus"* (Palaeodasycladus limestones), while in the Middle and Upper Jurassic there are the "*Calcari oolitici ed oncolitici"* (Oolitic-oncolitic limestone) and the "*Calcari con Cladocoropsis e Clypeina"* (Cladocoropsis and Clypeina limestones). The "*Calcari con requienie e gasteropodi*" (Requienid and gastropod limestones) span from the base of the Lower Cretaceous to the uppermost Cenomanian. The last Mesozoic unit is made by the Upper Cretaceous "*Calcari a radiolitidi"* (Radiolitid limestones). The stratigraphic succession of the ACP in

terminated by the *Formazione di Trentinara* (Trentinara Formation, Eocene) and the *Formazione di Cerchiara* (Cerchiara Formation, Miocene). The siliciclastic deposits of *Formazione di Bifurto* (Bifurto Formation, Miocene) mark the platform drowning.

### *2.3 Location and stratigraphy of the studied sections*

For the study of the early Toarcian OAE two classical outcrops have been selected: Mercato San Severino, about 30 km northwest of Salerno, and Monte Sorgenza, about 7 km northeast of Formia (fig. 3). They have been extensively studied during the second half of the last century (Sartoni and Crescenti, 1962; De Castro, 1962; Chiocchini and Mancinelli, 1977) and have become a reference for the stratigraphy of the Lower Jurassic platform carbonates of the southern Apennines

The Lower Jurassic carbonates of the ACP show a remarkable uniformity of facies all over the southern Apennines. They are included into a single lithostratigraphic unit, defined since the sixties of the last century as the "Calcari a Palaeodasycladus" ("Palaeodasycladus Limestones"). A thickness of about 300 m has been calculated for the "Palaeodasycladus Limestones" in the Lattari Mts and in the Mercato San Severino area (De Castro, 1962). In the classical section of Monte Monaco di Gioia the thickness is about 200 m (Catenacci et al., 1963). The most distinctive fossil is the calcareous alga *Palaeodasycladus mediterraneus (*Barattolo et al., 1994*)*, which often occurs in rock-forming abundance. In the upper part of the "Palaeodasycladus limestones", which has been described as the "Membro a Lithiotis" ("Lithiotis member"), large thick-shelled "Lithiotis" bivalves (Fraser et al., 2004) make spectacular biostromes. Lituolid larger foraminifera (*Orbitopsella* and related taxa; Hottinger, 1967; Septfontaine et al., 1991; Fugagnoli, 2004), are the other typical component of the "Palaeodasycladus limestones". The richest and most diverse larger foraminiferal assemblages, dominated by *Orbitopsella*, occur just below the "Lithiotis member".

The "Palaeodasycladus Limestones" Formation is overlain by the "Calcari oolitici ed oncolitici" (Oolitic-oncolitic limestones) Formation, which is up to 400 m thick and is made in the first part of about 40 m of massive unfossiliferous oolitic limestones. Typically, the change is very sharp and is marked by the disappearance of the "Lithiotis" bivalves and of *Palaeodasycladus mediterraneus*. This biostratigraphic event has been traditionally equated with the Lower-Middle Jurassic boundary but there is evidence that it occurs close to the Pliensbachian-Toarcian boundary (Barattolo and Romano, 2005).

In order to study the early Aptian OAE two well known succession have been chosen: Monte Tobenna, about 8 km northeast of Salerno, and Monte Raggeto, about 7 km northwest of Caserta (fig. 3). Both these sections have been extensively investigated in the past decades for cyclostratigraphic and chemostratigraphic studies (Ferreri et al., 1997; Raspini, 1998; Amodio et al., 2003; D'Argenio et al., 1999, 2004; Wissler et al., 2004). They are made up of limestones belonging to the "Calcari con requienie e gasteropodi" Formation (Requienid and gastropod limestones Fm).

This formation is made up mainly by well-bedded grey limestones with frequent layers crowded by gastropods and requienids. Subordinately, dark thin-bedded limestone, dolomitic limestones and massive to laminated dolostones are present. In the Sala Consilina zone the total thickness of the formation ranges between 400 and 600 m; with similar thickness (500 m) the formation crops out at Monte Terminio. In the lower part of the succession, oolitic and oncolitic limestones are frequent. In the central part dasyclad limestones are alternated with stromatolitic and loferitic limestones and gastropods and requienids limestones. In the upper part, laminated dolostone beds are interbedded to bioclastic limestones with alveolinids.

Monte Tobenna is a classical locality for the "Orbitolina Level" of the southern Apennines (De Castro, 1963; Cherchi et al., 1978). At Monte Tobenna it is composed by two beds. The lower bed is a 150 cm-thick bioturbated marly limestone crowded with flat conical orbitolinids (*Mesorbitolina parva and Mesorbitolina texana*). The argillaceous component decreases upward. The upper bed, which is just 15 cm thick, consists of a packstone crowded with flat conical orbitolinids (*Mesorbitolina parva and Mesorbitolina texana*) and codiacean algae (*Boueina hochstetteri moncharmontiae*). A middle Gargasian age has been proposed for the "Orbitolina Level" (Cherchi et al., 1978).

At Monte Raggeto the "Orbitolina Level" is not present. In the Seventies, Monte Tobenna and Monte Raggeto sections were thought to be originally situated in two different carbonate platforms separated by a wide basin (D'Argenio et al., 1975a; Laubscher and Bernoulli, 1977; Channell et al., 1979). The occurrence or the lack of the "Orbitolina Level" was one of the feature used to distinguish "inner" and "outer" carbonate platform successions. According to the recent interpretations (see previous paragraph), both the section belonged to the single and wide carbonate platform domain.

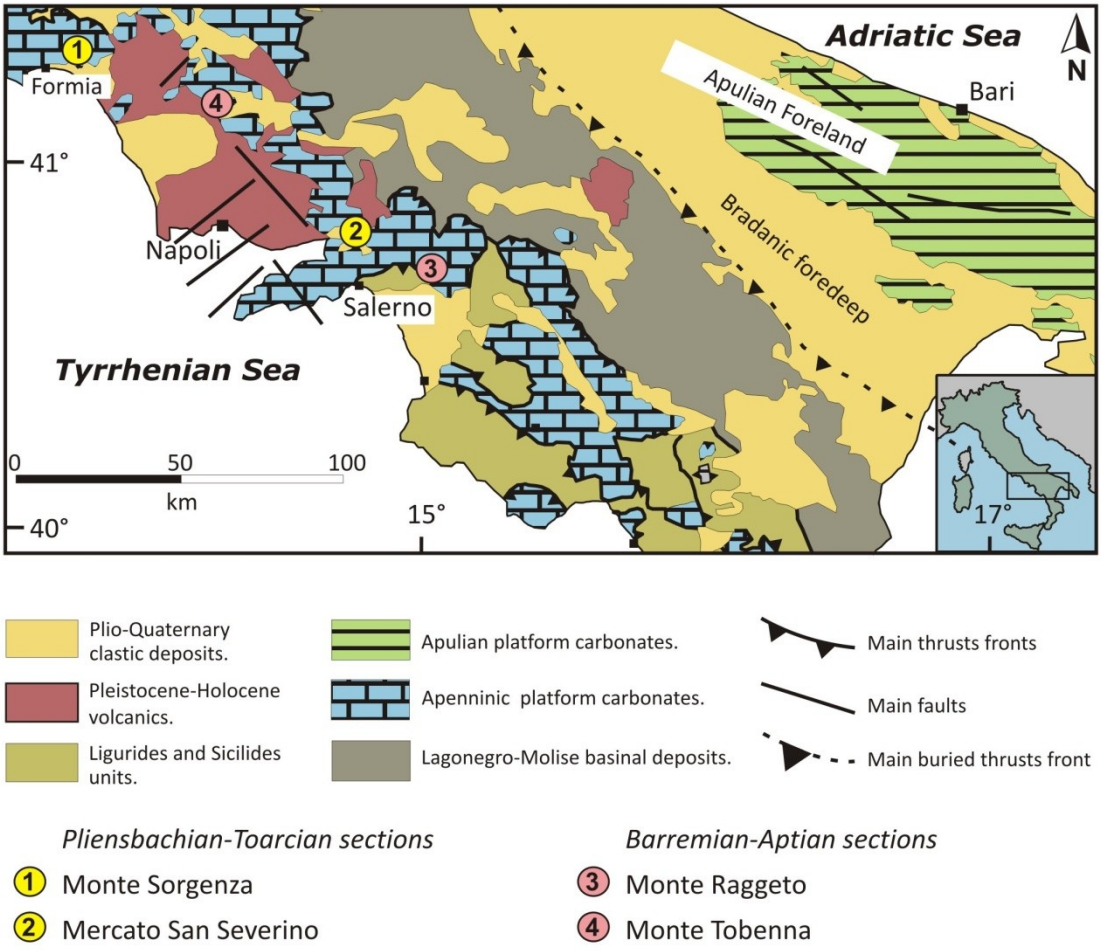


**Figure 3** - Schematic geological map of the central-southern Apennines, with location of the studied sections (modified from Bonardi et al., 1988).

## *2.4 References*


Aldega L., Corrado S., Giampaolo C. and Mazzoli S. (2003a). Studio della mineralogia delle argille per la ricostruzione dei carichi tettonico/sedimentari: esempi dalle Unità Lagonegresi e Liguridi della Lucania sud-occidentale (Appennino Meridionale). Bollettino della Società Geologica Italiana 122, 203–216.

Aldega L., Cello G., Corrado S., Cuadros J., Di Leo P., Giampaolo C., Invernizzi C., Martino C., Mazzoli S., Schiattarella M., Zattin M. and Zuffa G. (2003b). Tectonosedimentary evolution of the Southern Apennines (Italy): Thermal constraints and modelling. Atti Ticinensi di Scienze della Terra, serie speciale, 9, 135–140.

Amodio S., Buonocunto F.P., D'Argenio B., Ferreri V. and Gorla L. (2003). Cyclostratigraphy of Cretaceous shallow water carbonates. Case histories from central and southern Italy. AAPG Search and Discovery Article #90017.

Barattolo F., De Castro P. and Parente M. (1994). Some remark on the genera Palaeodasycladus (PIA, 1920) PIA, 1927 and Eodasycladus CROS & LEMOINE, 1996 ex GRANIER & DELOFFRE, 1993. Green Algae, Dasycladales., Beitr. Paläont. 19, 1–11.

Barattolo F. and Romano R. (2005). Shallow carbonate platform bioevents during the Upper Triassic-Lower Jurassic: an evolutive interpretation. Boll. Soc. Geol. It. 124, 123–142.

Bonardi G., D'Argenio B. and Perrone V. (1988). Carta Geologica dell'Appennino meridionale, SELCA, Firenze.

Bosellini, A. (2002). Dinosaurs "re-write" the geodynamics of the eastern Mediterranean and the paleogeography of the Apulia Platform, Earth Sci. Rev. 59, 211–234.

Butler R.W.H., Mazzoli S., Corrado S., De Donatis M., Di Bucci D., Gambini R., Naso G., Nicolai C., Scrocca D., Shiner P. and Zucconi V. (2004). Applying thickskinned tectonic models to the Apennine thrust belt of Italy; limitations and implications. In: McClay K.R. et al. (ed.) Thrust Tectonics and Hydrocarbon Systems. American Association of Petroleum Geologists, Memoirs, 82, 647–667.

Carannante G., Graziano R., Ruberti D. and Simone L. (1997). Upper Cretaceous temperate-type open shelves from northern (Sardinia) and southern (Apennines-Apulia) Mesozoic Tethyan margins, in: James, N.P. and Clarke, J. (Eds.): Cool-water carbonates,SEPM Spec. P., 56, 309–325.

Casero P., Roure F., Muller C., Moretti I., Sage L. and Vially R. (1988). Evoluzione geodinamica neogenica dell'Appennino meridionale. In: L'Appennino Campano-Lucano nel quadro geologico dell'Italia meridionale. 748 Congresso Società Geologica Italiana, Sorrento, 59–66.

Casero P., Roure F. and Vially R. (1991). Tectonic framework and petroleum potential of the southern Apennines. In: A. M. Spencer (Ed.), Generation, accumulation, and production of Europe's hydrocarbons. Special Publication of the European Association of Petroleum Geoscientists, 1, 381–387.

Catenacci E., De Castro P. and Sgrosso I. (1963). Complessi-guida del Mesozoico calcareo-dolomitico nella zona orientale del Massiccio del Matese. Mem. Soc. Geol. It. 4, pp.20.

Cello G., Guerra I., Tortorici L., Turco E. and Scarpa R. (1982). Geometry of the neotectonic stress field in southern Italy: geological and seismological evidence. Journal of Structural Geology 4, 385–393.

Cello G., Gambini R., Mazzoli S., Read A., Tondi E. and Zucconi V. (2000). Fault zone characteristics and scaling properties of the Val d'Agri Fault System (southern Apennines, Italy). Journal of Geodynamics 29, 293–307.

Channell J.E.T., D'Argenio B. and Horvarth F. (1979). Adria, the African promontory in Mesozoic Mediterranean palaegeography. Earth Science Reviews 15, 213–292.

Cherchi A., De Castro P. and Schroeder R. (1978). Sull'etá dei livelli a Orbitolinidi della Campania e delle Murge Baresi (Italia meridionale). Boll. Soc. Nat., Napoli, 87, 363-385.

Chiocchini M. and Mancinelli A. (1977). Microbiostratigrafia del Mesozoico in facies di piattaforma carbonatica dei Monti Aurunci (Lazio meridionale). Studi Geologici Camerti 3, 109–152.

Ciarcia S., Vitale S., Di Staso A., Iannace A., Mazzoli S. and Torre M. (2009). Stratigraphy and tectonics of an Internal Unit of the southern Apennines: implications for the geodynamic evolution of the peri-Tyrrhenian mountain belt. Terra Nova 21, 88–96.

Cinque A., Patacca E., Scandone P. and Tozzi M. (1993). Quaternary kinematic evolution of the Southern Apennines, relationships between surface geological features and deep lithospheric structures. Annali di Geofisica 36, 249–260.

Corrado S., Aldega L., Di Leo P., Giampaolo C., Invernizzi C., Mazzoli S. and Zattin M. (2005). Thermal maturity of the axial zone of the southern Apennines fold-and-thrust belt (Italy) from multiple organic and inorganic indicators. Terra Nova 17, 56–65.

D'Argenio B. (1974). Le piattaforme carbonatiche periadriatiche: una rassegna di problemi nel quadro geodinamico mesozoico dell'area mediterranea. Memorie della Società Geologica Italiana 13, 137–159.

D'Argenio B., De Castro P., Emiliani C. and Simone L. (1975a). Bahamian and Apenninic limestones of identical lithofacies and age, AAPG Bull., 59, 524–533.

D'Argenio B., Ferreri V., Raspini A., Amodio S. and Buonocunto F.P. (1999). Cyclostratigraphy of a carbonate platform as a tool for high- precision correlation. Tectonophysics. 315, 357–385.

D'Argenio B., Ferreri V., Weissert H., Amodio S., Buonocunto F.P. and Wissler L. (2004). A multidisciplinary approach to global correlation and geochronology: the Cretaceous shallow water

carbonates of southern Apennines, Italy, in: D'Argenio, B., Fischer, A.G., Premoli Silva I., Weissert, H. and Ferreri, V. (Eds.): Cyclostratigraphy: Approaches and Case Histories, SEPM Spec. P., 81, 103–122.

D'Argenio B., Pescatore T. and Scandone P. (1975b). Structural pattern of the Campania-Lucania Appennines. In Structural model of Italy – Maps and explanatory notes (eds Ogniben L., Parotto M. and Praturlon A.). Consiglio Nazionale delle Ricerche, Quaderni de La Ricerca Scientifica, 90, 313–327.

D'Argenio B. and Sgrosso I. (1974). Le piattaforme carbonatiche sudappenniniche. Ist. di Geologia e Geofisica dell'Università di Napoli. Pub. n. 52

De Castro P. (1962). Il Giura-Lias dei Monti Lattari e dei rilievi ad Ovest della Valle dell'Irno e della Piana di Montoro. Boll. Soc. Natur. Napoli 71, 21–52.

De Castro P. (1963). Nuove osservazioni sul livello ad Orbitoline in Campania, Boll. Soc. Nat. Napoli, 71, 103–135..

Dewey J.F., Helman M.L., Turco E., Hutton D.H.W. and Knott S.D. (1989). Kinematics of the western Mediterranean. In: Coward M.P., Dietrich D. and Park R.G. (eds), Alpine Tectonics: Geological Society of London Special Publication, 45, 265–283.

Ferreri V., Weissert H. D'Argenio B. and Buonocunto F.P. (1997). Carbon-isotope stratigraphy: a tool for basin to carbonate platform correlation. Terra Nova 9,. 57–61.

Fraser N., Bottjer D. and Fischer A. (2004). Dissecting "Lithiotis" bivalves: Implications for the Early Jurassic reef eclipse. PALAIOS 19, 51–67.

Fugagnoli A. (2004). Trophic regimes of benthic foraminiferal assemblages in Lower Jurassic shallow water carbonates from northeastern Italy (Calcari Grigi, Trento Platform, Venetian Prealps). Palaeogeography, Palaeoclimatology, Palaeoecology 205, 111–130.

Hottinger L. (1967). Foraminifeères imperforés du mésozoique marocain. Note Mem. Serv. Geol. Maroc. 209, 61–168.

Laubscher H.P. and Bernoulli D. (1977). Mediterranean and Tethys. In: Nairn, A.E.M., Kanes, W.H., and Stehli, F.G., eds., The Ocean Basins and Margins: London, Plenum Press, vol. 4, 1–28.

Mazzoli S., Aldega L., Corrado S., Invernizzi C. and Zattin M. (2006). Pliocene-Quaternary thrusting, syn-orogenic extension and tectonic exhumation in the southern Apennines (Italy): Insights from the Monte Alpi area, in Mazzoli, S., and Butler, R.W.H., eds., Styles of continental contraction. Geological Society of America Special Paper, 414, 55–77.

Mazzoli S., Barkham S., Cello G., Gambini R., Mottioni L., Shiner P. and Tondi E. (2001). Reconstruction of continental margin architecture deformed by the contraction of the Lagonegro Basin, Southern apennines, Italy. Journal of Geological Society of London, 158, 309–319.

Mazzoli S., D'Errico M., Aldega L., Corrado S., Invernizzi P., Shiner P. and Zattin M. (2008). Tectonic burial and "young" (<10 Ma) exhumation in the southern Apennines fold-and-thrust belt (Italy). Geology 36, 243–246.

Mazzoli S. and Helman M. (1994). Neogene patterns of relative motion for Africa-Europe: Some implications for recent central Mediterranean tectonics: Geologische Rundschau 83, 464–468.

Menardi Noguera A. and Rea G. (2000). Deep structure of the Campanian-Lucanian Arc (southern Apennines). Tectonophysics 324, 239–265.

Mostardini F. and Merlini S. (1986). Appennino centro-meridionale. Sezioni geologiche e proposta di modella strutturale. Memorie della Società Geologica Italiana 35, 177–-202.

Ogniben L. (1969). Schema introduttivo alla geologia del confine calabro-lucano. Mem.Soc. Geol. Ital. 8, 453–763.

Oldow J.S., D'Argenio B., Ferranti L., Pappone G., Marsella E. and Sacchi M. (1993). Large-scale longitudinal extension in the Southern Apennines contractional belt, Italy. Geology 21, 1123–1126.

Raspini A. (1998). Microfacies analysis of shallow water carbonates and evidence of hierarchically organized cycles. Aptian of Monte Tobenna, southern Apennines, Italy. Cretaceous Research 19, 197–223.

Rosenbaum G., Lister G.S. and Duboz C. (2002). Relative motions of Africa, Iberia and Europe during Alpine orogeny: Tectonophysics, 359, 117–129.

Sartoni S. and Crescenti U. (1962). Ricerche biostratigrafiche sul Mesozoico dell'Appennino meridionale. Giorn. Geol., s. II, 29, 153–302.

Selli R. (1957). Sulla trasgressione del Miocene nell'Italia meridionale. Giornale di Geologia, 2, 1–54.

Selli R. (1962). Il Paleogene nel quadro della geologia dell'Italia meridionale. Mem. Soc. Geol. Ital., 3.

Septfontaine M., Arnaud-Vanneau A., Bassoullet J.P., Gusic I., Ramalho M. and Velic I. (1991). Les foraminiféres imperforés des plates-formes carbonatées jurassiques état des connaissances et perspectives d'avenir. Bull. Soc. Vaud. Sci. Nat. 80 (3), 255–277.

Sgrosso I. (1988). Nuovi elementi per un più articolato modello paleogeografico nell'Appennino centro meridionale. Mem. Soc. Geol. Ital. 41, 225–242.

Shiner P., Beccacini A. and Mazzoli S. (2004). Thin-skinned versus thick-skinned structural models for Apulian carbonate reservoirs: Constraints from the Val D'Agri Fields. Marine and Petroleum Geology, 21, 805–827.

Wissler L., Weissert H., Buonocunto F.P., Ferreri V. and D'Argenio B. (2004). Calibration of the Early Cretaceous time scale: a combined chemostratigraphic and cyclostratigraphic approach to the Barremian-Aptian interval Campania Apennines and southern Alps (Italy). In. D'Argenio, B. et al. (eds), Cyclostratigraphy, approaches and case histories, SEPM Spec. Publ. 81, 123–134.

# CHAPTER 3 – Carbonate platform evidence of ocean acidification at the onset of the early Toarcian oceanic anoxic event

## *3.1 Introduction*

About one third of the carbon dioxide released mainly from burning of fossil fuels is absorbed into the oceans where it reacts to form carbonic acid. As a result the pH of the ocean and the amount of carbonate ions decrease in a process called ocean acidification (Doney et al., 2009)

Detrimental effects on calcifying organisms, which use carbonate minerals to build their protective shells and skeletons, have been documented in the laboratory (Fabry et al., 2008) and in the field (Halls-Spencer et al., 2008). However, due to the spatio-temporal limits of experiments and field observations, the long-term impact on marine ecosystems and the adaptation potential of marine species are best investigated by looking at the geological record of past episodes of ocean acidification (IPCC workshop, 2011).

Episodes of short-term massive injection of $CO_2$ in the atmosphere-ocean system are witnessed by negative carbon isotope events (CIE) recorded by marine carbonates and by marine and continental organic matter (Jenkyns, 2010). Paroxysmal volcanism and/or clathrates dissociation are generally invoked as the source of isotopically depleted excess $CO_2$. Several episodes have been investigated; the one which occurred about 55 Ma, known as the Paleocene-Eocene thermal maximum (PETM), is certainly the best studied. Ocean acidification during the PETM is witnessed by carbonate dissolution in deep-water sections, implying shallowing of the CCD (Zachos et al., 2005). No evidence has been documented of severe reduction of $CaCO_3$ saturation in the shallow ocean. Carbonate platforms were able to continue growing (Robinson, 2010), but a change from coral-dominated to larger foraminifera-dominated platforms has been documented (Scheibner and Speijer, 2008). In the open ocean no major extinction nor a major bias in extinction or diversification towards less calcifying planktic species have been documented (Gibbs et al., 2006).

Another episode of severe perturbation of the ocean-atmosphere system, which bears some analogies with the PETM (Cohen et al., 2007) occurred in the early Toarcian (Early Jurassic, about 183 Ma). The geological record of this event is characterized by abrupt global warming, widespread coeval deposition of organic-rich sediments and a major extinction in marine invertebrates (Jenkyns and Clayton, 1986; Jenkyns, 2003, 2010; Wignall et al., 2005; Cohen et al., 2007; Suan et al., 2008a). The early Toarcian CIE is possibly the largest in the whole Phanerozoic (Hesselbo and , 2011) and is associated with a biocalcification crisis of calcareous nannoplankton (Erba, 2004; Mattioli et al., 2009). The global nature of the CIE has been questioned on the basis of its absence in the record of well preserved belemnites (van de Schootbrugge et al., 2005; McArthur et al., 2008) but its presence in the record of marine sediments and marine and continental organic matter across a variety of facies and palaeogeographic settings indicates that the event was really a global perturbation of the carbon cycle (Hesselbo et al., 2007; Suan et al., 2008a; Al-Suwaidi et al., 2010; Hesselbo and , 2011). Several candidates have been discussed as the source of rapid $CO_2$ injection into the atmosphere-ocean system, which triggered the cascade of palaeoenvironmental changes recorded during the T-OAE. The most cited ones are dissociation of methane hydrates and thermogenic methane release from coal associated with intrusions of the Karoo-Ferrar large igneous province (Hesselbo et al., 2000; McElwain et al., 2005; Beerling and Bretnall, 2007; Svensen et al., 2007; Suan et al., 2008b; Gröcke et al., 2009).

Very little is known of the response of carbonate platforms and shallow benthic calcifiers to the early Toarcian event. Many Tethyan platforms drowned during the Pliensbachian as the result of extensional tectonics linked to the opening of the western Tethyan ocean (Bernoulli and Jenkyns, 1974; Manatschal and Bernoulli, 1999; Santantonio and Carminati, 2011). For those platforms that continued growing, the terminal drowning is seen as the combined effect of tectonics, accelerated sea-level rise and palaeoenvironmental deterioration close to Pliensbachian-Toarcian boundary (Bassoulet and Baudin, 1994; Blomeier and Reijmer, 1999; Wilmsen and Neuweiler, 2008; Léonide et al., 2011; Merino-Tomé et al., 2011).

But drowning was not the fate of all Tethyan platforms. Some resilient platforms continued growing in shallow water across the Pliensbachian-Toarcian boundary and the T-OAE (Trento Platform, Cobianchi and Picotti, 2001; Woodfine et al., 2008; Apenninic Platform, Woodfine et al., 2008; Adriatic-Dinaric Platform, Vlahović et al., 2005; Pelagonian platform, Scherreiks et al., 2009). The Apenninic Carbonate Platform (ACP) of southern Italy, which grew at tropical latitudes in the central Tethys, preserves a continuous record of shallow water carbonate sedimentation across the early Toarcian event (Woodfine et al., 2008). It offers the unique possibility of studying the response of shallow water carbonate platforms and benthic calcifiers to an episode of massive release of $CO_2$ into the ocean-atmosphere system.

In this paper we present evidence of a dramatic shift of carbonate production mode from massive biocalcification to chemical precipitation across the early Toarcian event in the ACP. We discuss the local *vs* supraregional significance of this shift and propose a scenario envisaging abrupt decline of carbonate saturation forced by $CO_2$ release during the negative wing of the early Toarcian CIE, followed by a calcification overshoot driven by the recovery of ocean alkalinity.

### *3.2 Geological setting*

The ACP is made of a 5 km-thick pile of shallow water carbonates that were deposited during the Mesozoic at the southern margin of the Tethyan Ocean (Bosellini, 2004). With the Neogene deformation of the passive continental margin of the Adria promontory, the ACP was incorporated into the southern Apenninic thrust and fold belt. The oldest neritic carbonates cropping out in the southern Apennines are Middle Triassic in age. Shallow water carbonate sedimentation was established over wide areas during the Late Triassic and persisted almost to the end of the Cretaceous. Since the Early Jurassic the ACP developed as an epi-oceanic platform bordered by deep basins (fig. 1). Upper Triassic to Lower Cretaceous formations have been referred to a flat-topped tropical platform dominated by chloralgal and chlorozoan associations (D'Argenio et al., 1975), whereas the depositional system of the Upper Cretaceous rudist limestones has been interpreted as a ramp-like open shelf dominated by foramol-type assemblages (Carannante et al., 1997).

The Lower Jurassic carbonates of the ACP show a remarkable uniformity of facies all over the southern Apennines. They are included into a single lithostratigraphic unit, defined since the sixties of the last century as the "Calcari a Palaeodasycladus" ("Palaeodasycladus Limestones"). In the classical section of Monte Monaco di Gioia the "Palaeodasycladus limestones are about 200 m thick and consists mainly of well bedded peritidal carbonates. The most distinctive fossil is the calcareous alga *Palaeodasycladus mediterraneus (*Barattolo et al., 1994*)*, which often occurs in rock-forming abundance. In the upper part of the "Palaeodasycladus limestones", which has been described as the "Membro a Lithiotis" ("Lithiotis member") large thick-shelled "Lithiotis" bivalves (Fraser et al., 2004) make spectacular biostromes. Lituolid larger foraminifera (*Orbitopsella* and

related taxa; Hottinger, 1967; Septfontaine et al., 1991; Fugagnoli, 2004), are the other typical component of the "Palaeodasycladus limestones". The richest and most diverse larger foraminiferal assemblages, dominated by *Orbitopsella*, occur just below the "Lithiotis member".

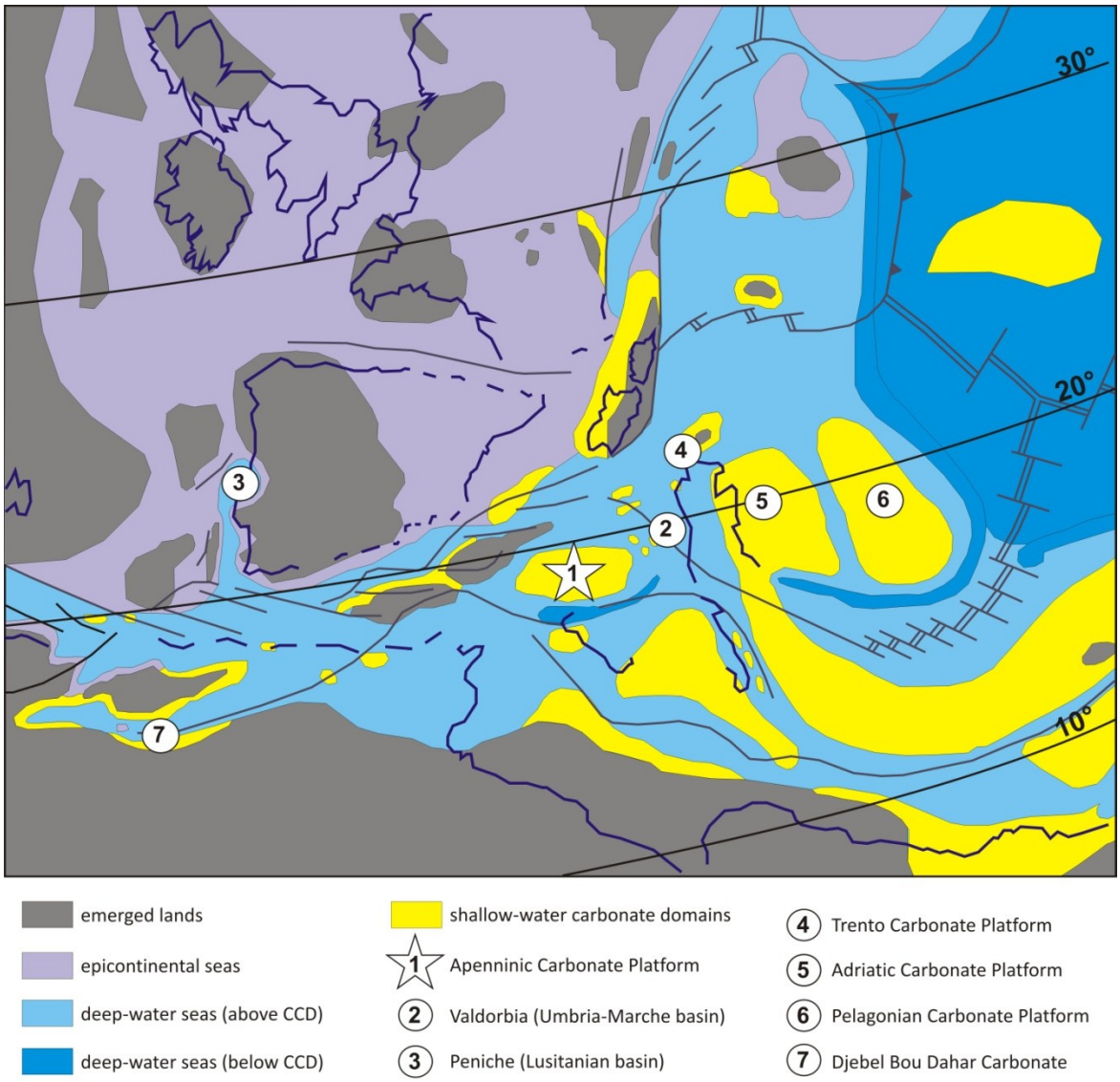


**Figure 1** - Toarcian palaeogeography of the peri-Tethyan domains (redrawn from Bassoullet et al., 1993) with position of key areas cited in the text.

The "Palaeodasycladus Limestones" Formation is overlain by the "Calcari oolitici ed oncolitici" (Oolitic-oncolitic limestones) Formation, which is up to 400 m thick and is made in the first part of about 40 m of massive unfossiliferous oolitic limestones. Typically, the change is very sharp and is marked by the disappearance of the "Lithiotis" bivalves and of *Palaeodasycladus mediterraneus*. This biostratigraphic event has been traditionally equated with the Lower-Middle Jurassic boundary but there is evidence that it occurs close to the Pliensbachian-Toarcian boundary (Barattolo and Romano, 2005).

For this study we selected two classical outcrops which have been extensively studied during the second half of the last century (Sartoni and Crescenti, 1962; De Castro, 1962; Chiocchini and Mancinelli, 1977) and have become a reference for the stratigraphy of Lower Jurassic platform carbonates of the southern Apennines: Mercato San Severino, about 30 km northwest of Salerno, and Monte Sorgenza, about 7 Km northeast of Formia.

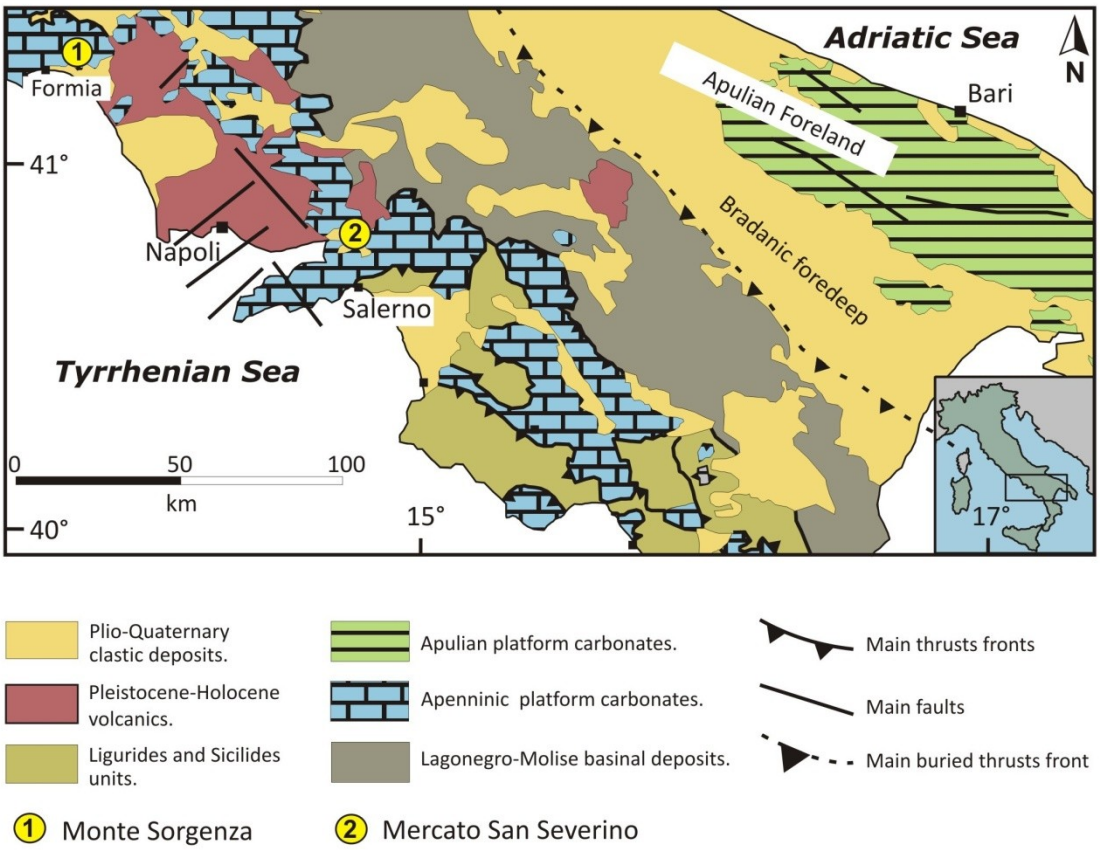


**Figure 2** - Schematic geological map of the southern Apennines (redrawn from Bonardi et al., 1988) with location of the studied sections

## *3.3 Materials and methods*

### *3.3.1 Sedimentology and biostratigraphy*

Two shallow water carbonate successions have been selected for this study: Mercato San Severino (north of Salerno, Campania) and Monte Sorgenza (east of Formia, Lazio).

The studied sections have been logged in the field at decimetre to meter scale, depending on the outcrop quality, and sampled with an average resolution of about one sample per meter. A higher resolution was adopted for the transition inteval between the "Palaeodasycladus limestones" and the "Oolitic limestones". The preliminary field description of textural components, sedimentary structures and fossil content was subsequently integrated with the sedimentological and micropalaeontological study of 100 thin sections and 293 acetate peels under the optical microscope.

### *3.3.2 Carbon isotopes*

*Carbonate component*

Two hundreds and ninety-three samples were analysed for the carbon isotope ratio of the carbonate component ($\delta^{13}C_{carb}$). We used mudstones as a first choice and the micritic matrix of wackestones and floatstones as a second choice. About 2 mg of powder was obtained from each sample by micro-drilling a polished slab under a binocular microscope with a 0.5 mm or 0.8 mm Tungsten bit. The analyses were performed at the Isotopen-labor of the Institut für Geologie, Mineralogie und Geophysik at the Ruhr University (Bochum, Germany). Approximately 0.5 mg of sample powder was heated for 18 hrs at 105 °C.

Samples were reacted online by individual acidic ($H_3PO_4$) addition with a Finnigan Gas Bench II. Stable isotope ratios were measured with a Finnigan Delta S mass spectrometer. The results are reported in ‰ in the conventional δ notation with reference to the Vienna Pee Dee Belemnite (VPDB) standard. The precision (1σ) monitored by repeated analyses of international and laboratory standards, is ±0.09‰ for carbon and ±0.13‰ for oxygen isotopes. Replicate measurements show reproducibility in the range of ±0.1‰ for $\delta^{13}C$ and ±0.2‰ for $\delta^{18}O$.

*Organic matter component*

Ninety-four samples were analysed for the carbon isotope ratio of the bulk organic matter ($\delta^{13}C_{org}$).

Samples were crushed in a mortar and subsequently de-carbonated by HCl 10% (1.25 N) leaching during 20 min. Dissolution of the samples was promoted by ultrasonic disaggregation (3 minutes per sample). The insoluble residue was washed and centrifuged until a neutral suspension was obtained (pH 7–8). After drying in a oven at temperature lower than 80°C, the de-carbonated residue was collected for $\delta^{13}C$ analysis of the organic matter component. The carbon isotope composition was determined at the Stable Isotopes Laboratory of the University of Lausanne (UNIL) by flash combustion on a Carlo Erba 1108 elemental analyzer (EA) connected to a Thermo Fisher Scientific Delta V (Bremen, Germany) isotope ratio mass spectrometer (IRMS) that was operated in the continuous helium flow mode via a Conflo III split interface (EA-IRMS). An aliquot of the sample was wrapped in a tin capsule and combustion was done in an $O_2$ atmosphere in a quartz reactor at 1020°C packed with $Cr_2O_3$ and $(Co_3O_4)Ag$ to form $CO_2$, $N_2$, $NO_x$ and $H_2O$. The gases were then passed through a reduction reactor containing elemental copper and copper oxide at 640°C to remove excess of $O_2$ and to reduce the non-stoichiometric nitrous products ($NO_x$) to $N_2$. Water was subsequently removed by anhydrous $Mg(ClO_4)_2$. $N_2$ and $CO_2$ were then separated in a gas chromatograph fitted with a packed column (Pora-PLOT Q, 5 m length, 1/4 inch i.d.) at 70°C, and analyzed for their isotopic composition on the IRMS. Pure $CO_2$ gases were inserted in the He carrier flow as pulses of standard gases. The results are reported in ‰ in the conventional δ notation with reference to the Vienna Pee Dee Belemnite (VPDB) standard. The calibration and assessment of the reproducibility and accuracy of the isotopic analysis based on replicate analyses of laboratory standard materials (glycine, urea and pyridine) were better than 0.1‰ (1σ). The accuracy of the analyses was checked periodically by analyses of the international reference materials USGS-24 graphite, IAEA-PEF1 polyethylene foil and NBS-22 oil.

## *3.4. Results*

### *3.4.1 Facies and stratigraphy*

*Mercato San Severino*

The studied succession is beautifully exposed in a quarry west of Mercato San Severino (40°46'53"N, 14°43'45"E). It includes the "Lithiotis member" of the "Palaeodasycladus Limestones" (0–126.1 m) and the lower part of the "Oolitic-oncolitic Limestones" (126.1–164 m) (fig. 3).

The "Lithiotis member" consists mainly of meter-thick "Lithiotis" biostromes, alternating with coarse peloidal-intraclastic grainstones and rudstones with abundant remains of *Palaeodasycladus mediterraneus*. Other lithofacies occurring in this interval are fine-grained peloidal packstones-grainstones with gastropods and small benthic

foraminifers (mainly valvulinids) and mudstone-wackestone with rare *Palaeodasycladus*, small thin-shelled gastropods and ostracods.

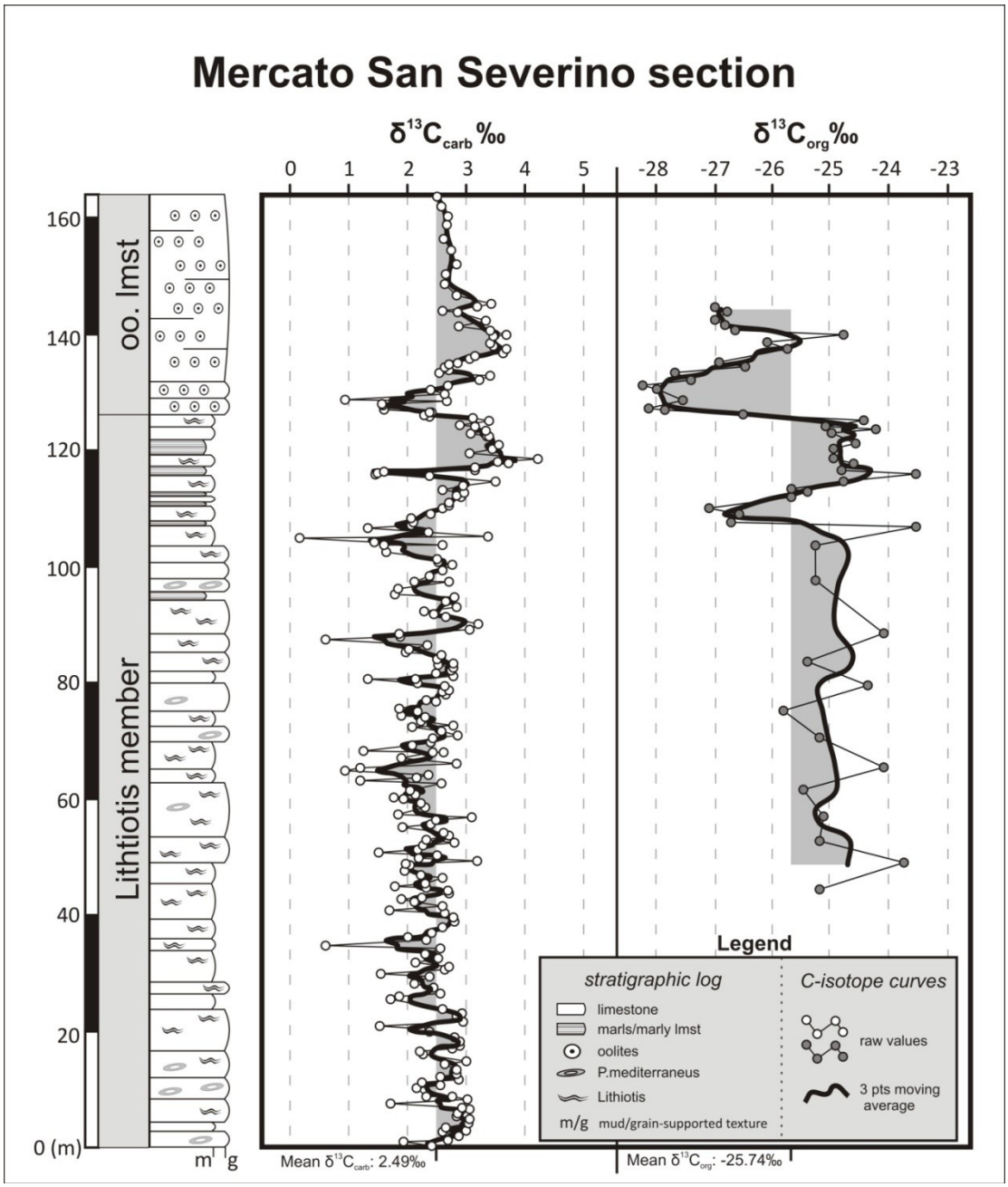


**Figure 3** - Lithology and carbon isotope stratigraphy of the Mercato San Severino section.

Millimetre- to cm-thick discontinuous green marls cap some beds and permeates downward, filling a complex network of irregular cavities. The thickest marly levels contain nodules of mudstones with ostracods and thin-shelled gastropods. These marly caps, which mark periods of ephemeral platform emersion, are not distributed evenly in the section. A first cluster of thicker and more closely spaced nodular marly levels occurs at 79–88 m. A second cluster occurs between 116 and 120 m. In this uppermost part of the Lithiotis member, the Lithiotis biostromes become thinner, more discontinuous and less frequent. Moreover, grain-supported lithofacies are replaced by mud-rich facies consisting of mudstones with ostracods and thin-shelled gastropods and mudstones-wackestones with benthic foraminifers and *Palaeodasycladus mediterraneus*. The first bed of oolitic grainstone is at 126.1 m. It is followed by a 15 cm-thick Lithiotis floatstone with dull

whitish to pink subangular stout fragments of bivalve shells. At the top of this bed the Lithiotis shells are truncated by a sharp surface overlain by a massive 130 cm-thick bed of oolitic grainstone. The next bed is made of oolitic limestone with a few pinkish abraded fragments of bivalve shells with a thin oolitic coating. From there to the top, the section is made exclusively of massive unfossiliferous oolitic grainstones.

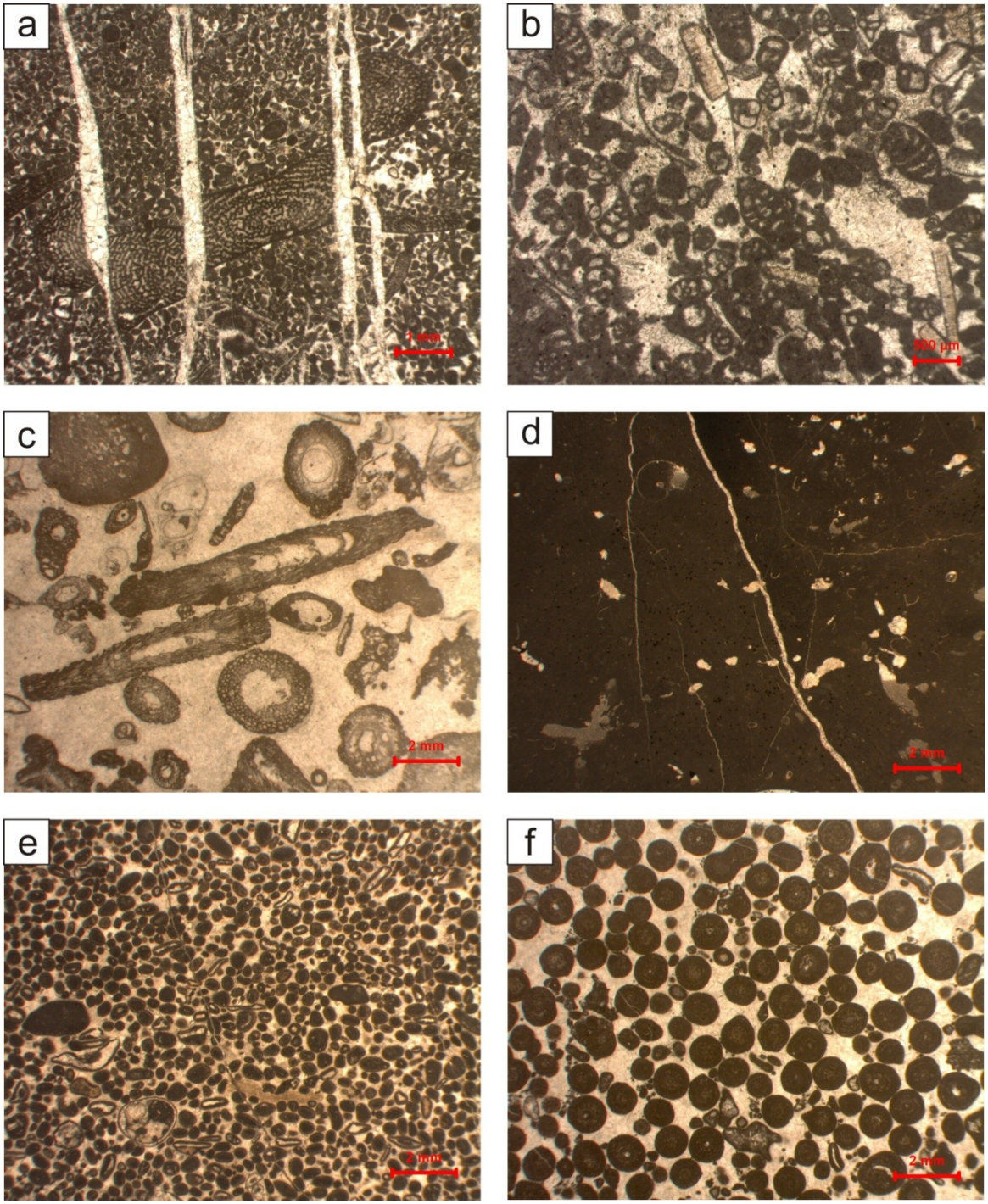


**Figure 4** - a: peloidal/foraminiferal grainstone with *Orbitopsella* (Monte Sorgenza); b: peloidal/bioclastic grainstone with small benthic foraminifers and shell fragments (Monte Sorgenza); c: algal/oncoidal rudstone with *Palaeodasycladus* (Mercato San Severino); d: mudstone with ostracods and thin-shelled gastropods (Mercato San Severino); e: peloidal/bioclastic grainstone with shell fragments and surficial ooids (Monte Sorgenza); f: oolitic grainstone (Mercato San Severino).

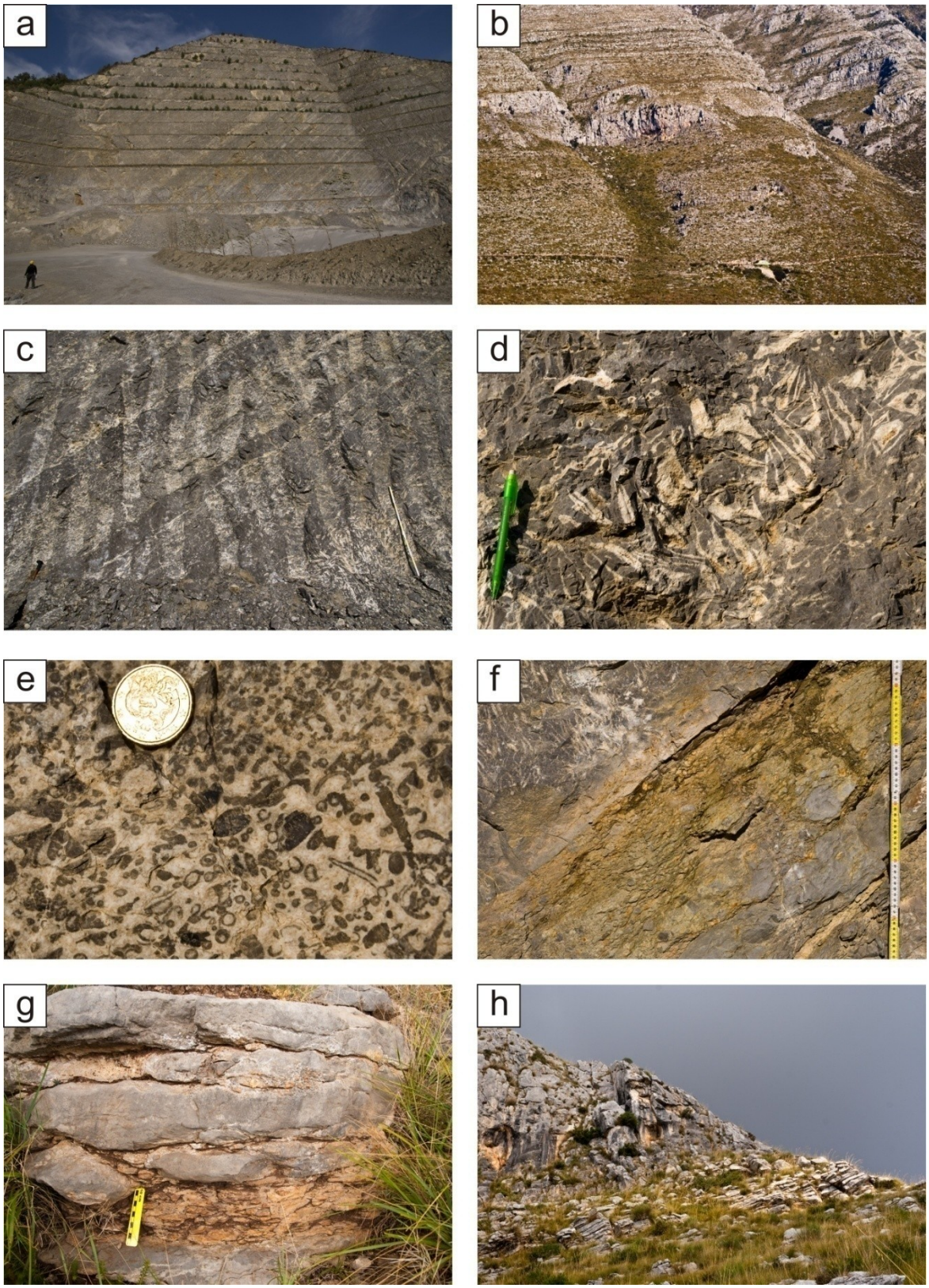


**Figure 5** - a: The Maiellaro quarry at Mercato San Severino; b: Monte Sorgenza, view from Castellonorato (south); c: m-thick Lithiotis biostromes (Mercato San Severino); d: Lithiotis bivalves preserved in life position (Mercato San Severino); e: *Palaeodasycladus* rudstone; f: dm-thick marly level with nodules of limestone (Mercato San Severino); g: marls and nodular limestones (Monte Sorgenza); h: transition interval between the Lithiotis member and the massive oolitic limestones (Monte Sorgenza).

*Monte Sorgenza*

This 164 m-thick section (fig. 6), has been logged on the southern slope of Monte Sorgenza (41°17'39"N, 13°40'57"E) and coincides with the first part of the section studied by Woodfine et al. (2008). Stratigraphy and facies are basically the same as in the Mercato San Severino quarry but the base of the Monte Sorgenza section is slightly older, as it includes in the lower part the "Orbitopsella limestones" (0–39 m). The latter consist mainly of oncoidal-peloidal grainstones to rudstones with abundant *Palaeodasycladus* and lituolid larger foraminifers, alternating with wackestones with *Orbitopsella* and other lituolids.

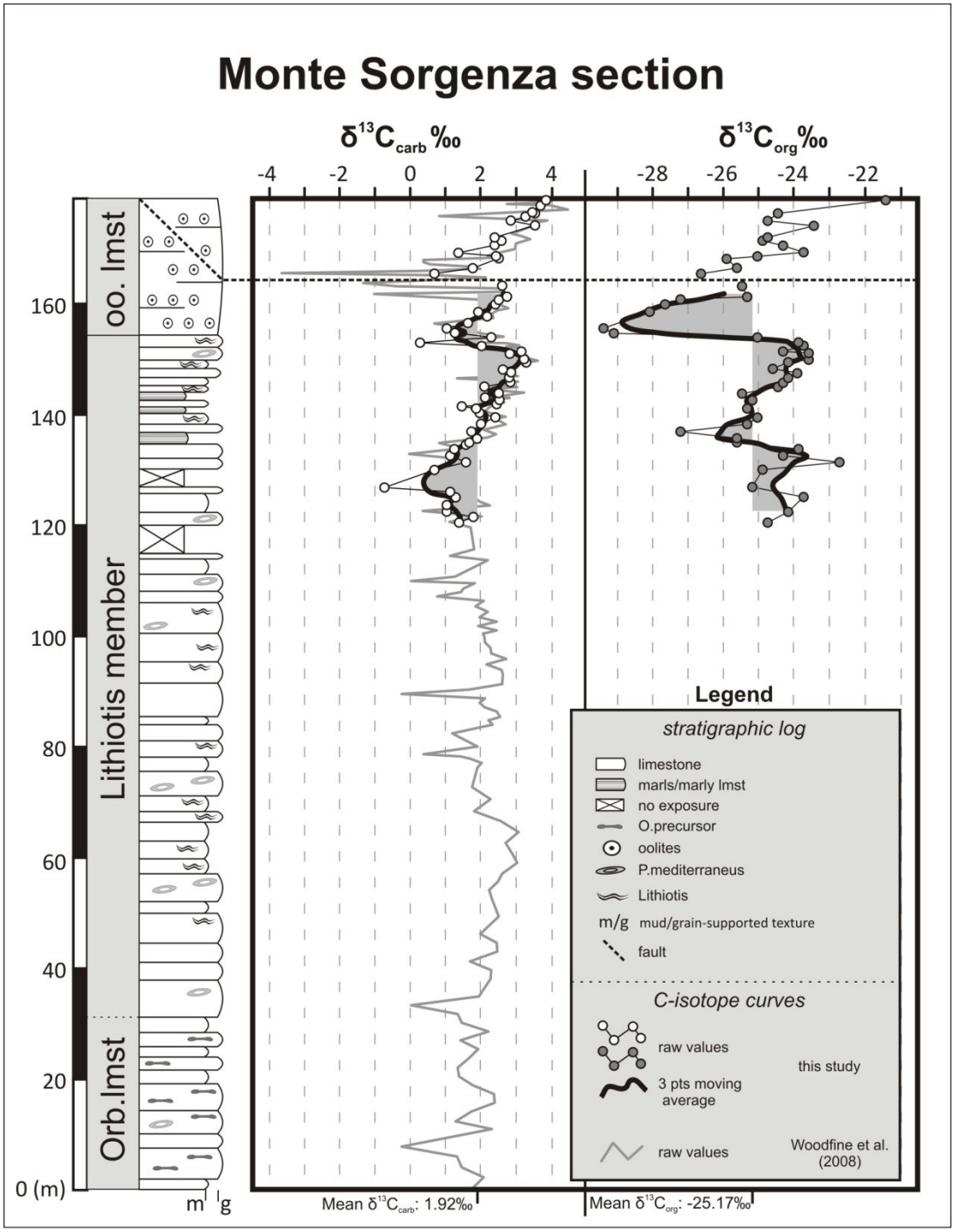


**Figure 6** - Lithology and carbon isotope stratigraphy of the Monte Sorgenza section. The first part of the $\delta^{13}C_{carb}$ curve is taken from Woodfine et al. (2008).

The first Lithiotis biostrome is at about 54 m from the base of the section. Compared with its equivalent in the Mercato San Severino quarry, the Lithiotis member at Monte Sorgenza is characterized by a reduced frequency and thickness of Lithiotis biostromes. The most recurrent facies are wackestone-packstones with *P. mediterraneus* and coarse peloidal-intraclastic packstones-grainstones with *P. mediterraneous*, gastropods, and benthic foraminifers. As in the other section, subaerial exposure surfaces are marked by mm- to cm- thick nodular marly caps. A first cluster of thicker (up to 20 cm) and closely spaced marls occurs between 60 and 70 m. Between 115 and 130 m there is a poorly exposed interval which corresponds to the gentler and more densely vegetated segment of the slope. This interval seemingly corresponds to a second cluster of marly levels. A third cluster of nodular marls occurs between 138 and 143 m. As at Mercato San Severino, the uppermost part of the Lithiotis member is marked by the decreased frequency and thickness of the Lithiotis biostromes and by a shift to more muddy facies. The oolitic limestones starts at 154 m. Their lower part is very massive and makes a steep cliff about 10 m high. The uppermost part of the section is disturbed by a small normal fault (see also fig.5 of Woodfine et al., 2008).

### *3.4.2 Carbon isotope stratigraphy*

*Mercato San Severino*

From 0 to 106.7 m $\delta^{13}C_{carb}$ values oscillate wildly between +1 and +3‰, with a few outliers below 1‰. The moving average curve shows a slight decreasing trend superimposed on the high-frequency fluctuations, which are defined only by a single or a few data points. From 106.7 m $\delta^{13}C_{carb}$ values start to climb and reach a peak of +4.22‰ at 118.6 m from the base of the section, in the uppermost part of the Lithiotis member. Then, there is a decreasing trend that becomes very steep from 125.2 m, just below the base of the "Oolitic Limestones", and leads to a minimum value of +1.57‰ at 128 m. In the last part of the curve, $\delta^{13}C_{carb}$ values rise again, reaching a maximum of about 3.7‰ at 140 m, and then declines gradually toward values <3‰ at the end of the section.

The carbon isotopic ratio of total organic carbon ($\delta^{13}C_{org}$) is available only between 44.1 and 144.7 m. Between 44.1 and 106.7 m $\delta^{13}C_{org}$ values fluctuates between -25.85 and -23.54‰ (-25.74 ± 1.28‰). Then there is a very sharp negative excursion, reaching a minimum of -27.1‰ at 110 m and recovering at pre-excursion values of -23.5‰ at 115.9 m. After a small plateau, defined by values fluctuating between -25.1 and -24.2‰, there is a second very sharp negative shift (about 4‰) starting at 125.2 m and reaching a minimum of -28.2‰ at 131.2 m from the base of the section. As for $\delta^{13}C_{carb}$, the last part of the $\delta^{13}C_{org}$ curve is occupied by a positive excursion, with a peak of -24.8‰ at 140 m followed by a decrease to values around -27‰.

*Monte Sorgenza*

In figure 6 we have plotted the $\delta^{13}C_{carb}$ data of Woodfine et al. (2008) plus our new $\delta^{13}C_{carb}$ and $\delta^{13}C_{org}$ data for the upper part of the section.

In the Orbitopsella limestones $\delta^{13}C_{carb}$ values oscillates mainly between +1.3 and +2.4‰, with a few outliers to more negative values. A positive trend starts at the base of the Lithiotis member leading to a positive peak of about +3‰ at 64.4 m from the base of the section. From there to about 93 m $\delta^{13}C_{carb}$ values fluctuate around +2‰. Then there is a shift to about +3‰, followed by a decreasing trend ending with a minimum of about +0.5‰ at 130 m from the base of the section.

Between 130 and 151 m, in the uppermost part of the Lithiotis member, our data show a regular positive trend, leading from values of about +1‰ to values > +3‰. This

positive trend is truncated by a sharp negative excursion, of about 3‰. The minimum value of +0.3‰ is reached at 153 m. In the first beds of the oolitic limestones $\delta^{13}C_{carb}$ values are still low at about +1‰, then they start rising, reaching a relative maximum of +2.7‰ at 161.2 m. Beyond this level the section is disturbed by a small fault.

The carbon isotopic ratio of total organic carbon ($\delta^{13}C_{org}$) is available only starting from 120 m from the base of the section. Up to 130 m $\delta^{13}C_{org}$ values fluctuates mainly between -24 and -25‰. Then there is a sharp negative shift, reaching a minimum of -27.3‰ at 136.8 m, followed by a rising trend leading to a peak of -23.9‰ at 153 m from the base of the section, in the last beds of the Lithiotis member. Then there is second sharp negative shift, reaching a minimum of -29.1‰ in the first beds of the "Oolitic Limestones". Then values start rising again, reaching a -25.3‰ at 161.2 m from the base, where the section is interrupted by the fault.

## *3.5 Discussion*

### *3.5.1 The inadequacy of carbonate platform biostratigraphy*

The Early Jurassic evolution of the Apenninic carbonate platform, as recorded in the two studied sections, can be roughly divided into four phases. During phase 1, recorded only in the lowermost part of the Monte Sorgenza section (0–39 m), the carbonate factory is dominated by calcareous green algae (*P. mediterraneus*) and lituolid larger foraminifers (*Orbitopsella* assemblage). In phase 2 (39–138 m at Monte Sorgenza; 0–116 m at Mercato San Severino) the most prolific carbonate producers are *P. mediterraneus* and the thick-shelled bivalves of the *Lithiotis* group. *Orbitopsella* disappears at the base of this interval but some smaller and less complex lituolids (i.e *Amijella amiji* and *Lituosepta compressa*) are still present, albeit never dominant. In the third phase (138–154.7 m at Monte Sorgenza; 116–126.2 m at Mercato San Severino) Lithiotis bivalves and *P. mediterraneus* are still present but they are not dominant any more. At the same time there is a shift from grainy bioclastic to muddy facies and a significant increase in the thickness and frequency of marly interlayers. The fourth phase is marked by the disappearance of Lithiotis bivalves and calcareous algae as the carbonate factory shifts to chemical precipitation with massive oolitic limestones.

What is the relation between this evolution and the phases of rapid climate change and perturbations of the global carbon cycle recorded by the reference sections of epicontinental European basins (Jenkyns and Clayton, 1986; Hesselbo et al., 2000; Kemp et al., 2005; Hesselbo et al., 2007; Suan et al., 2008a, 2010; Hermoso et al., 2009; Littler et al., 2010)? Unfortunately biostratigraphic resolution and chronostratigraphic calibration in the Apenninic Carbonate Platform are not adequate to address this question.

The disappearance of *P. mediterraneus* and of the Lithiotis bivalves in the Apenninic carbonate platform has been traditionally equated with the Lower-Middle Jurassic boundary (De Castro, 1991; Chiocchini et al., 1994). However, there is evidence that both these events occurred close to the Pliensbachian-Toarcian boundary (Bassoulet et al., 1997; Fraser et al., 2004). The Upper Triassic-Lower Jurassic biostratigraphy of central and southern Tethyan carbonate platforms has been recently reviewed by Barattolo and Romano (2005). Also this paper equates the disappearance of *P. mediterraneus* with the Pliensbachian-Toarcian boundary, but supporting evidence is unclear, since no ammonite has been found in close relation to this bioevent. In conclusion, at the present state of knowledge, in the southern Apenninic carbonate platform it is not possible to constrain by biostratigraphy neither the position of the Pliensbachian-Toarcian boundary nor of the interval corresponding to the early Toarcian OAE. Since both these time-intervals are known to be characterized by prominent CIEs (Hesselbo et al., 2007; Suan et al., 2008a;

Littler et al., 2010), carbon isotope stratigraphy seems to be the most adequate dating and correlation tool.

### *3.5.2 Reliability of the carbonate isotope record of ancient platform carbonates*

During the last twenty years many papers have documented that the prominent CIEs recorded by the oceanic $\delta^{13}C$ record of deep-sea sediments during the Mesozoic OAEs and other episodes of global perturbation of the carbon cycle can be faithfully recorded also in platform carbonates (Ferreri et al., 1997; Grötsch et al., 1998; Wissler et al., 2004; Immenhauser et al., 2005; Parente et al., 2007, 2008; Woodfine et al., 2008; Huck et al., 2010, 2011). On the other hand, it is widely known that the $\delta^{13}C$ records of carbonate platforms can depart significantly from the open ocean record for several reasons. True open ocean conditions may not have been present at these locations, a phenomenon often referred to as seawater ageing on platform top (Immenhauser et al., 2008, and references therein). Vital or mineralogical effects may produce carbonate components with different $\delta^{13}C$ values. It has been shown that in modern carbonate platforms the range of $\delta^{13}C$ values shown by different grains is larger than the amplitude of most CIEs recorded by ancient deep-sea carbonates (Swart et al., 2009).

After deposition the carbon isotope record of platform carbonates can be considerably altered by diagenesis, especially by interaction with meteoric fluids (Allan and Matthews, 1982; Lohmann, 1988).

Any of the potential biases listed above can make very problematic the interpretation of the carbon isotope record of platform carbonates. Therefore, for this study we relied on paired records of $\delta^{13}C_{carb}$ and $\delta^{13}C_{org}$. It is generally accepted that CIEs that are recorded by both the carbonate and the organic component in a sedimentary sequence indicate a real change in the carbon isotope ratio of the dissolved inorganic carbon pool (DIC) of the environment (Margaritz et al., 1986; Gale, 1993; Underwood et al., 1997; Jarvis et al., 2006).

The most prominent features shown by our records are two sharp negative excursions with an intervening positive excursion. The first negative CIE occurs in the upper part of the Lithiotis member and is recorded only by the $\delta^{13}C_{org}$ curves with a shift of about 3-4‰. The second negative CIE starts in the last beds of the "Lithiotis member" and reaches the lowest values at the boundary with the "Oolitic limestones". This excursion is recorded by both curves but is distinctly larger in the $\delta^{13}C_{org}$ (4-5‰) than in the $\delta^{13}C_{carb}$ curve (2-2.5‰).

The covariation of $\delta^{13}C_{carb}$ and $\delta^{13}C_{org}$ makes a strong argument in favour of the primary origin of the second negative CIE. The main argument backing this assumption is that the potential biases acting on the inorganic and organic component of marine carbonate sediments are different and not expected to act synchronously. In particular the carbon isotope ratio of organic matter is considered to be much more resilient to early diagenetic modification by meteoric fluids, the most common bias plaguing the $\delta^{13}C_{carb}$ record of platform carbonates. On the other hand, changes in the composition of organic matter, the greatest potential source of bias for the $\delta^{13}C$ record of bulk organic matter (Hayes et al., 1990; Hayes, 1993), are not expected to affect also the inorganic component of sediments.

The view that covariation of the isotopic signal recorded by inorganic and organic components of marine sediments implies a primary "oceanic" signal has been recently challenged by Oehlert et al. (2011). According to their data, the $\delta^{13}C_{org}$ of recent sediments of the Great Bahama Bank (GBB) is substantially heavier than that of organic matter produced in pelagic environments, especially on the shallow interior of the bank. Towards the platform margins the $\delta^{13}C_{org}$ values become more depleted. This spatial pattern

correlates with grain-size distribution. On the other hand, the carbon isotope ratio of the inorganic component of bank top sediments is relatively homogeneous for all the facies. As a result, there is no significant correlation between the $\delta^{13}C_{org}$ and $\delta^{13}C_{carb}$ values with the exception of mud-dominated facies (fig. 7), where there is a positive correlation between the two fractions.

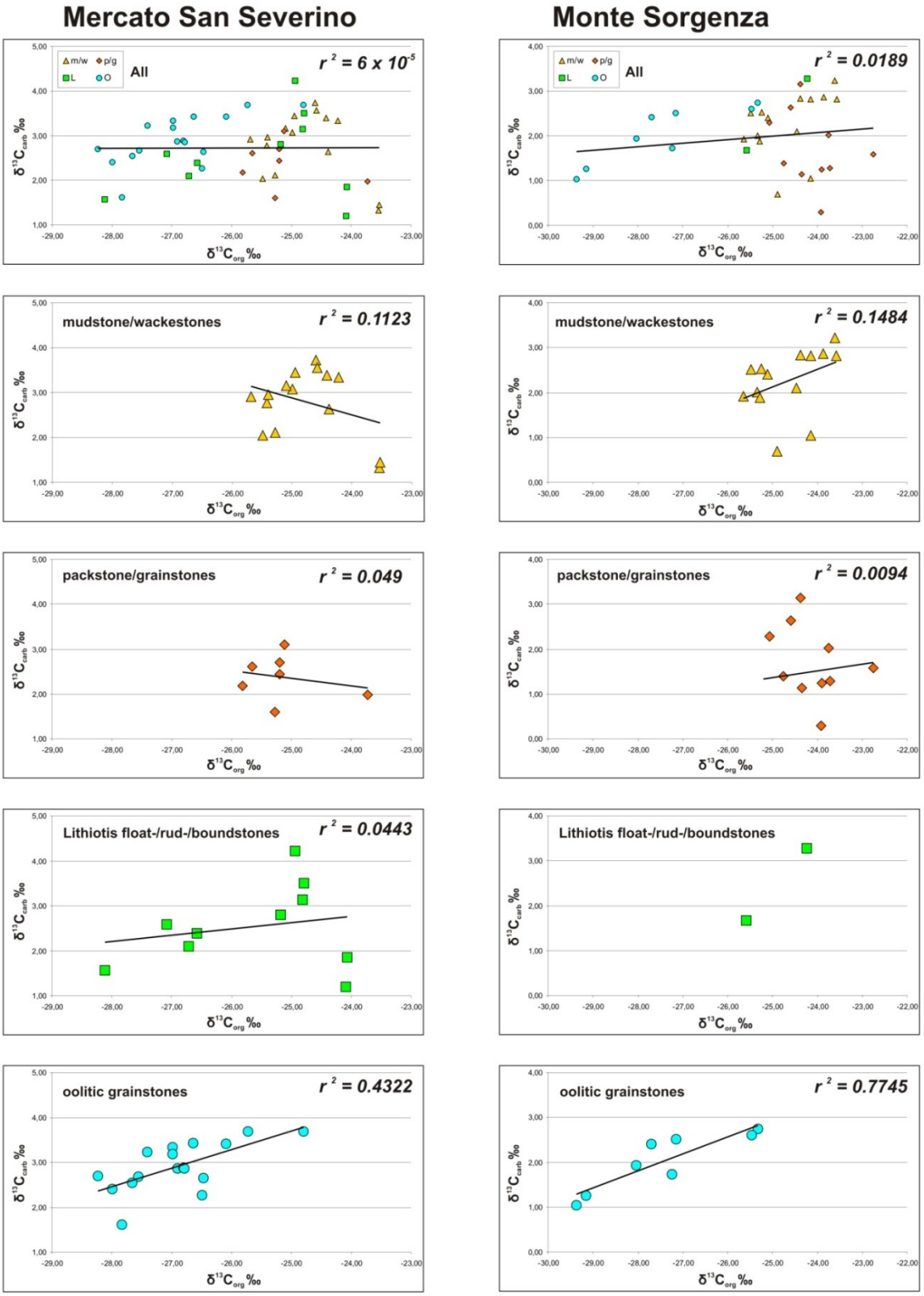


**Figure 7** - Crossplots of the $\delta^{13}C$ of the organic and carbonate component.

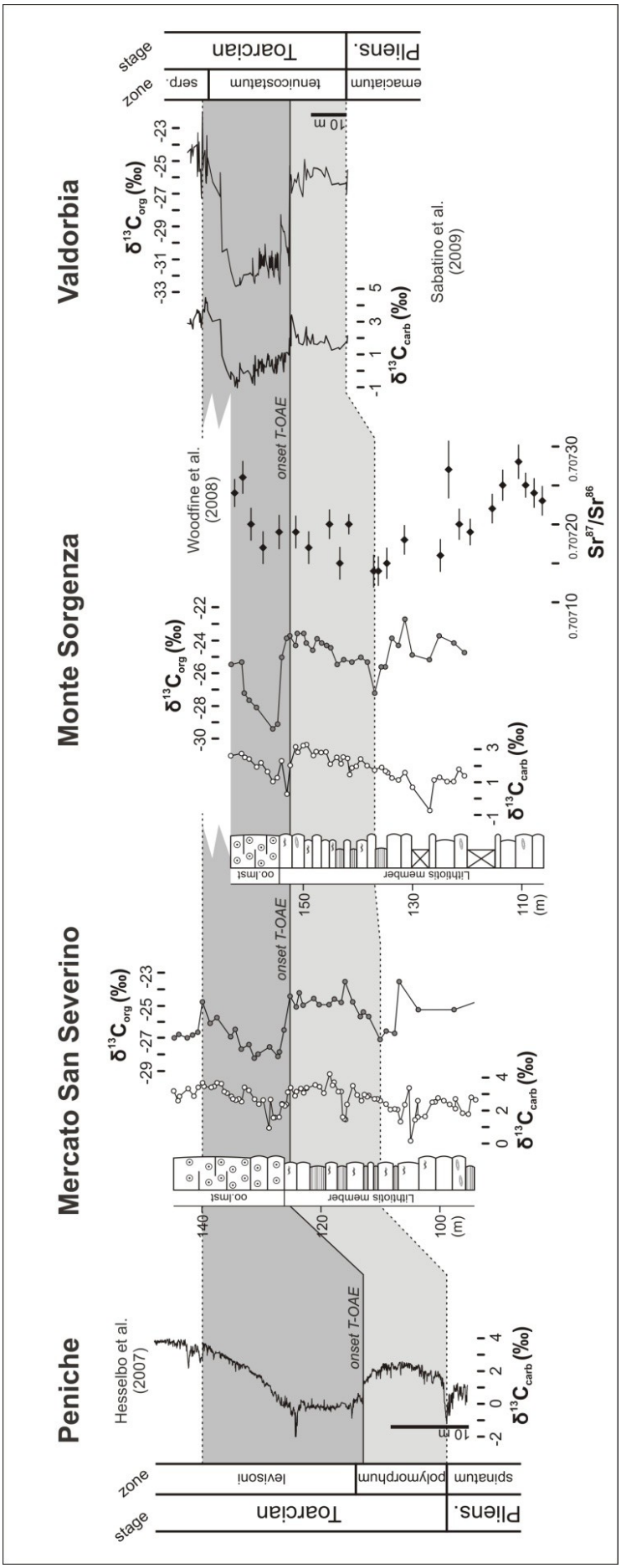
Peniche
Mercato San Severino
Monte Sorgenza
Valdorbia
stage
zone
Pliens.
Toarcian
spinatum
polymorphum
levisoni
emaciatum
tenuicostatum
serp.
Hesselbo et al. (2007)
Woodfine et al. (2008)
Sabatino et al. (2009)
onset T-OAE
Lithiotis member
oo.limst
δ13Corg (‰)
δ13Ccarb (‰)
Sr87/Sr86
(m)
10 m

**Figure 8 (previous page)** - Chemostratigraphic correlation of the platform carbonate sections of the southern Apennines with the reference section of Peniche (Lusitanian basin, Portugal, Hesselbo et al., 2007) and with the Valdorbia section (Umbria-Marche Basin; Sabatino et al., 2009). The strontium isotope stratigraphy of Monte Sorgenza is from Woodfine et al. (2008).

Our dataset is not comparable to the GBB one, inasmuch as it is not made of samples of exactly the same age: i.e. it incorporates the effects of secular changes of the carbonate platform DIC isotopic composition. Anyway, what we found is that correlation between $\delta^{13}C_{org}$ and $\delta^{13}C_{carb}$ is very low if we pool all the samples. When we consider the single lithofacies, correlation is high for oolitic limestones, moderate for mudstone-wackestone, poor for packstone-grainstone and Lithiotis-rich facies.

The close association of the second negative CIE with the prominent change from mud-rich facies to oolitic grainstones also merits evaluation. Actually, the excursion straddles this facies boundary. Very low values are reached already in the last beds of the mud-rich interval of the Lithiotis member and persist in the first beds of the oolitic limestones. Then, there is a recovery to higher values, comparable to pre-excursion ones, within the oolitic limestones. Therefore, there is no strict relation between facies and carbon isotope ratios, which could call for a control by local sedimentary processes. This further supports the hypothesis that the negative CIE at the boundary between the Lithiotis member and the oolitic limestones, records a change in the isotopic composition of the oceanic DIC.

The interpretation of the first negative CIE is more problematic, because it is recorded only by $\delta^{13}C_{org}$. Assuming that it represents a real feature, its absence in the carbon isotope record of carbonate could be due to diagenetic overprint. It is worth noticing that the interval where the negative CIE is measured in $\delta^{13}C_{org}$, is largely made of grainy facies (packstone-grainstone with *P. mediterraneus*) and Lithiotis-rich limestones. In both sections these lithofacies are characterized by the lowest correlation between $\delta^{13}C_{org}$ and $\delta^{13}C_{carb}$, which could be an indication that their $\delta^{13}C_{carb}$ is largely controlled by carbonate diagenesis.

The alternative explanation is that this negative CIE is not recorded by the carbonate component because it is due to a change in the composition of the organic matter and not to a change in the isotopic composition of the oceanic DIC.

### *3.5.3 Correlation with reference $\delta^{13}C$ curves*

In figure 8 we propose a correlation between the carbon isotope curves of the ACP and the reference section of Peniche (Lusitanian Basin, Hesselbo et al., 2007; Suan et al, 2008a), a GSSP candidate for the basal Toarcian. We added also the Valdorbia section (Umbria-Marche Basin, Sabatino et al., 2009), which refers to a basin that was only a few tens of km north of the ACP in the Early Jurassic (fig. 1).

We tentatively correlate the first negative CIE of our curves with the Pliensbachian-Toarcian boundary excursion and the second negative CIE with the T-OAE excursion. This correlation is compatible with the low resolution biostratigraphy of the APC if an age close to the Pliensbachian-Toarcian boundary is accepted for the extinction of *P. mediterraneus* (Bassoulet, 1997; Barattolo and Romano, 2005) and for the demise of Lithiotis bivalves (Fraser et al., 2004). The correlation is also supported by the strontium isotope stratigraphy of Woodfine et al. (2008), showing that the lowest Sr isotope values, seemingly corresponding to the Pliensbachian-Toarcian boundary (McArthur et al., 2000), occurs at the level of the first CIE.

From fig. 6 it is evident that the second negative CIE of our Monte Sorgenza carbon isotope profile is not the -6‰ excursion within the oolitic limestones that Woodfine et al. (2008) interpreted as the T-OAE excursion. The latter occurs very close to a fault zone and

its very depleted $\delta^{13}C_{carb}$ values (down to -3‰) are probably associated with diagenetic calcite precipitated by fluids circulating in the fault damage zone. This is supported by three arguments: 1) this excursion is much attenuated in our samples that were taken along the same sampling path but at a slightly larger distance from the fault surface; 2) very negative $\delta^{18}O$ and very positive $^{87}Sr/^{86}Sr$ values (see fig. 5 in Woodfine et al., 2008) across this segment of the curve suggest the influx of diagenetic fluids; 3) the Woodfine et al. (2008) $\delta^{13}C_{carb}$ negative excursion corresponds in our $\delta^{13}C_{org}$ record to a minor shift (about 1.5‰); this would be at odds with all the other records of the T-OAE showing a much larger excursion in $\delta^{13}C_{org}$ than in $\delta^{13}C_{carb}$ (Cohen et al., 2007).

From fig. 8 it is evident that the second negative CIE of our Monte Sorgenza carbon isotope profile is not the -6‰ excursion within the oolitic limestones that Woodfine et al. (2008) interpreted as the T-OAE excursion. The latter occurs very close to a fault zone and its very depleted $\delta^{13}C_{carb}$ values (down to -3‰) are probably associated with diagenetic calcite precipitated by fluids circulating in the fault damage zone. This is supported by three arguments: 1) this excursion is much attenuated in our samples that were taken along the same sampling path but at a slightly larger distance from the fault surface; 2) very negative $\delta^{18}O$ and very positive $^{87}Sr/^{86}Sr$ values (see fig. 5 in Woodfine et al., 2008) across this segment of the curve suggest the influx of diagenetic fluids; 3) the Woodfine et al. (2008) $\delta^{13}C_{carb}$ negative excursion corresponds in our $\delta^{13}C_{org}$ record to a minor shift (about 1.5‰); this would be at odds with all the other records of the T-OAE showing a much larger excursion in $\delta^{13}C_{org}$ than in $\delta^{13}C_{carb}$ (Cohen et al., 2007).

Our interpretation of carbon isotope stratigraphy of the ACP produces a better correlation with the Trento platform by equating the base of the "Oolitic limestones" of southern Appennines with the base of the upper Tenno Formation, which marks the appearance of oolitic limestones on wide sectors of the Trento platform, close to the boundary between the *tenuicostatum* and the *serpentinum* ammonite zones (Cobianchi and Picotti, 2001).

The T-OAE $\delta^{13}C_{org}$ excursion is distinctly smaller in the ACP than at Hawsker Bottoms (Kemp et al., 2005) and Valdorbia (Sabatino et al., 2009) (-5‰ *vs* -7‰ and -6.5‰, respectively). This could be due to the presence of a gap in the carbonate platform sections, corresponding to the time interval when the lowest values were reached in deep-water sections. The presence of a gap is also supported by the very sharp profile of the excursion in the ACP, lacking the distinct steps, which are a very significant feature of this isotopic event (Hesselbo and , 2011). Moreover the plateau of depleted isotopic values, observed for instance at Peniche and Valdorbia (fig. 8), is very reduced in our sections. Two alternative estimates, both based on cyclostratigraphy, have been proposed for the duration of the Early Toarcian CIE. According to the precession-based astronomical time scale of Kemp et al. (2005), the interval of more negative values takes 120 kyr. According to the eccentricity-based time scale of Suan et al. (2008b) and Sabatino et al. (2009), the same interval takes about 400 kyr. Since at least part of this interval is represented in our sections, the two alternative time-scales constrain the maximum duration of the gap in the Apenninic Carbonate Platform to < 120 kyr or to < 400 kyr.

### *3.5.4 The late Pliensbachian-early Toarcian evolution of the Apenninic Carbonate Platform in the time-frame set by the carbon-isotope correlation*

Chemostratigraphic correlation with the well-dated reference section of Peniche sets the stage for discussing the evolution of the ACP in the framework of Late Pliensbachian-Early Toarcian palaeoenvironmental perturbations.

During the Pliensbachian the ACP was a very healthy carbonate platform in the supersaturated shallow waters of the tropical Tethys. Like many carbonate platforms in

that latitudinal belt, it was dominated by very productive aragonitic biocalcifiers: the massive bivalves of the Lithiotis group (Fraser et al., 2004) and the calcareous alga *Palaeodasycladus mediterraneus* (Flügel, 1991; Barattolo, 1991; Barattolo et al., 1993).

In the earliest Toarcian (i.e. between the first and second negative CIEs) the contribution of Lithiotis bivalves and *Palaeodasycladus* to the carbonate factory decreases. Lithiotis biostromes become thinner and less recurrent, and there is a shift to mud-dominated facies. The occurrence of multiple subaerial exposure surfaces, marked by marls with nodules of restricted marine to paralic mudstones-wackestones, indicates that in both sections a sequence boundary zone (*sensu* Strasser et al., 2000) is present at this stratigraphic level. The Pliensbachian-Toarcian boundary interval is known as a time of severe palaeoenvironmental perturbations and rapid climatic changes (Suan et al., 2010) and is also associated with the onset of the Toarcian mass-extinction event (Wignall et al., 2005). This is also the time of carbonate platform crisis and drowning on both sides of the Tethyan Ocean (Bassoulet and Baudin, 1994; Cobianchi and Picotti, 2001; Léonide et al., 2011). Climate-forced increased delivery of nutrients to coastal areas, coupled to rapid sea-level changes, is envisaged as the main cause of platform crisis (Cobianchi and Picotti, 2001; Wilmsen and Neuweiller, 2008; Bodin et al., 2010; Merino-Tomé et al., 2011).

The thick marly interlayers close to the Pliensbachian-Toarcian boundary in the ACP record increased weathering under a warm-humid climate (see also Woodfine et al., 2008). However, the ACP continued growing in shallow water, with Lithiotis bivalves and *Palaeodasycladus* still making a significant contribution when fully marine facies are present. Therefore, in this resilient carbonate platform there is no significant biotic change at the Pliensbachian-Toarcian boundary.

A drastic change occurs, indeed, in the Early Toarcian, at the level of the T-OAE isotopic excursion. Lithiotis bivalves and the green alga *P. mediterraneus*, the most productive biocalcifiers of Pliensbachian tropical carbonate platforms, disappear and the carbonate factory switches from a biogenic to a chemical mode with the massive occurrence of unfossiliferous oolitic limestones.

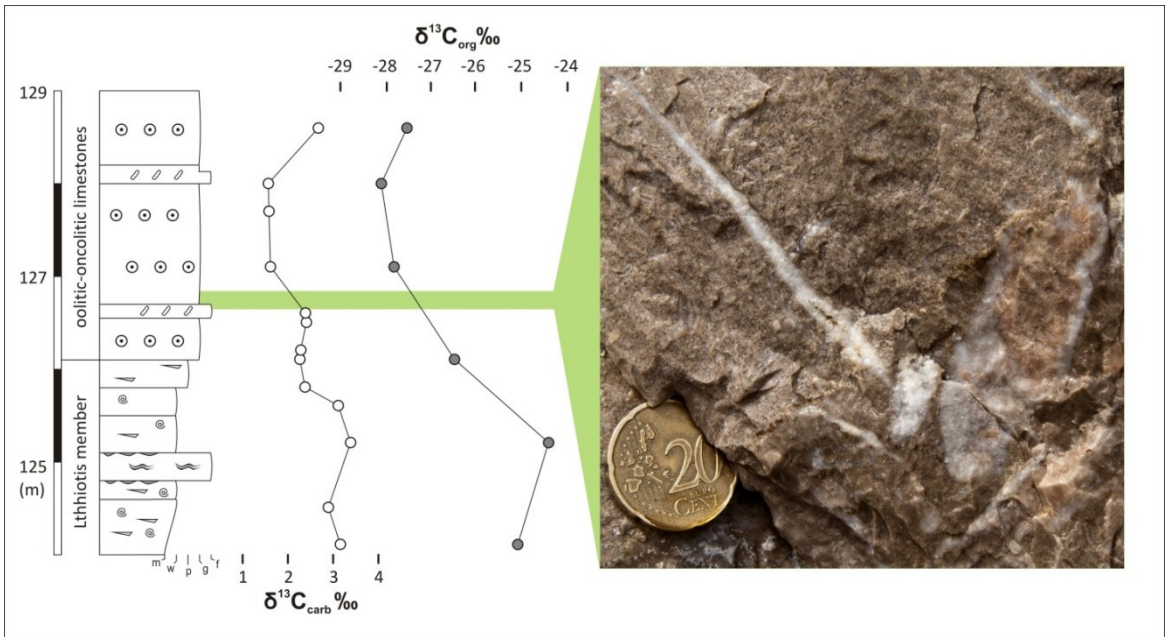


**Figure 9** - Close-up of the boundary between the "Lithiotis member" and the "Oolitic Limestones" in the Mercato San Severino section.

A close-up of the boundary between the "Lithiotis member" and the "Oolitic Limestones" in the Mercato San Severino section (fig. 9) shows that a first bed of oolitic grainstones records a -2‰ shift of $\delta^{13}C_{org}$ values. This is followed by a thin bed of Lithiotis floatstone truncated by an erosional surface. The next bed marks the definitive switch to massive oolitic limestones and records a further -1.8 shift in $\delta^{13}C_{org}$. As explained above, the shape of the $\delta^{13}C_{org}$ curve suggests the occurrence of a gap whose maximum duration is estimated to between less than 120 kyr and less than 400 kyr (see above). The best candidate for a gap is the erosional surface truncating the last bed of Lithiotis floatstone and overlain by oolitic grainstone (fig. 9). As there is no evidence of emersion or meteoric diagenesis, we interpret it as a submarine hardground. Of course, a polyphase history would be expected for this surface, especially if the long estimate of the gap duration is accepted.

### *3.5.5 Disentangling local from global factors*

The late Pliensbachian-early Toarcian evolution described above for the ACP is not a local pattern.

The large bivalves of the Lithiotis group were the most prolific carbonate producers of many Tethyan carbonate platforms during the Pliensbachian (Broglio-Loriga and Neri, 1976; Fraser et al., 2004). The green alga *P. mediterraneus* is also a very typical component, often in rock-forming abundance, in Early Jurassic shallow water limestones (Flügel, 1991; Barattolo, 1991).

In many Tethyan carbonate platforms the demise of the Lithiotis/Palaeodasycladus carbonate factory coincides with platform drowning, in some cases heralded by the backstepping of platform margin facies on inner lagoonal facies. Diachronous drowning across the Tethyan realm was controlled by synsedimentary block-faulting related to the opening of the Jurassic Tethys (Bernoulli and Jenkyns, 1974; Manatschal and Bernoulli, 1999; Santantonio and Carminati, 2011). A widespread platform drowning event occurred in the middle Carixian *ibex* zone in the Western Tethys (Marino and Santantonio, 2010). Among the few platforms that survived this drowning event, the carbonate banks of the High Atlas (Morocco) were terminated by diachronous drowning close to Pliensbachian-Toarcian boundary. The terminal drowning was seemingly caused by a combination of tectonically enhanced rapid sea-level rise and paleoenvironmental disturbance associated with increased nutrient levels (Wilmsen and Neuweiler, 2008; Merino-Tomé et al., 2011).

If we look at the resilient platforms that survived even this drowning event at the Pliensbachian-Toarcian boundary, it seems that the shift from a biotic carbonate factory, dominated by Lithiotis bivalves and *P. mediterraneus*, to a chemical carbonate factory, dominated by oolites, is a common pattern. In the Trento Carbonate Platform, the Lithiotis/Palaeodasycladus carbonate factory is well developed in the Rotzo member of the Calcari Grigi Formation. In the western sector of the platform, the Rotzo member is overlain by platform margin oolitic grainstones already in the latest Pliensbachian (close to the *margaritatus-spinatum* boundary, Cobianchi and Picotti, 2001). But more to the east, in the Altopiano di Folgaria, the Lithiotis/Paleodasycladus limestones of the Rotzo member continue in the early Toarcian, when they are sharply overlain by the oolitic limestones of the San Vigilio Oolite Formation, which at this time covers the whole platform (Masetti et al., 1998). The base of the San Vigilio Oolite is poorly dated but in the adjacent Lombardian basin the ooids of the San Vigilio Oolite appear in the late Early Toarcian *serpentinum* zone (Picotti and Cobianchi, 1996).

Also in the Pelagonian Carbonate Platform (NE Evvoia, Greece) Lithiotis limestones are abruptly overlain by oolitic limestones (Scherreiks et al., 2009) at a level that, within the uncertainty of poor biostratigraphic dating, could be coeval with the shift observed in the ACP.

In the Adriatic Carbonate Platform, Lithiotis limestones are very common in inner platform sectors during the Pliensbachian. In the Early Toarcian dark heavily bioturbated limestones ("spotty limestones"), were deposited in the NW part of the platform (Slovenia, central and W Croatia and W Bosnia), while the rest of the platform was characterised by oolitic limestones (Vlahović et al., 2005; Čadjenović et al., 2008).

The record of all these resilient platforms confirms that, on a supraregional to global scale, the final demise of the Lithiotis/Palaeodasycladus carbonate factory occurred close to the Pliensbachian-Toarcian boundary and most probably in the early Toarcian. An early Toarcian extinction of Lithiotis bivalves is also documented out of the western Tethys, in south America and Oman (Fraser et al., 2004) and in Tibet (Newton et al., 2011). Within the limits of biostratigraphic dating, this is fully compatible with our hypothesis, supported in the ACP by carbon isotope stratigraphy, that the final demise is coeval with the onset of the early Toarcian CIE. Also the pattern of a sharp change from a biotic carbonate factory, dominated by bivalves and calcareous algae, to a chemical carbonate factory, with widespread deposition of oolitic limestones, seems to be a common feature of Tethyan platforms.

### *3.5.6 What caused the demise of the Lithiotis/Palaeodasycladus carbonate factory?*

A dramatic decrease in pelagic carbonate production by nannoplankton and a reduction in the size of some species have been documented across the T-OAE (Erba, 2004; Mattioli et al., 2004, 2008, 2009; Tremolada et al., 2005). Acidification of surface waters, driven by a rapid increase of $pCO_2$, has been invoked to explain this biocalcification crisis (Mattioli et al., 2004; Erba, 2004; Tremolada et al., 2005). However, according to Mattioli et al. (2009), other causes played a major role in the nannoplankton crisis, like enhanced runoff and freshwater discharge with ensuing increase in nutrient levels and decrease of salinity in surface waters of western Tethys epicontinental basins.

A decrease in carbonate saturation of surface waters would have been detrimental also for the prolific biocalcifiers of carbonate platform environments. Recent research on ocean acidification, based mainly on single species laboratory manipulations and on mesocosm experiments, demonstrates that calcifying organisms can be threatened by the decrease of pH and surface water carbonate saturation forced by the rapid increase of $pCO_2$ (Royal Society, 2005; Fabry et al., 2008; Doney et al., 2009).

Lithiotis bivalves, the most typical carbonate producing biota of Pliensbachian carbonate platforms, were aberrant pterioid bivalves which constructed bioherms in nearshore tropical environments (Fraser et al., 2004). They are actually a group of five genera that shared the same shell microstructure, an outer layer of calcitic prisms with middle and inner nacreous layers (Accorsi Benini and Broglio Loriga, 1982; Broglio Loriga and Posenato, 1996), but had different morphologies and habitats. In particular two genera, *Lithiotis* and *Cochlearites*, have been interpreted as possible mixotrophs, building bioherms in oligotrophic environments, while *Lithioperna* seemingly inhabited a niche similar to that of modern oyster reefs (Fraser et al., 2004).

Under the assumption that Jurassic Lithiotis bivalves shared the same physiology and calcification mechanisms of extant bivalves, the data on gregarious bivalves like mussels and oysters are particularly relevant to evaluate the possible response of Lithiotis to ocean acidification. Laboratory manipulations have shown that the calcification rates of the edible mussel (*Mytilus edulis*) and of the Pacific oyster (*Crassostrea gigas*) decline linearly with increasing $pCO_2$ (Gazeau et al., 2007). Early developmental stages of these bivalves are particularly affected. The growth of the planktonic larvae of *Mytilus edulis* is significantly affected by a decrease of pH (Gazeau et al., 2010) and increased sea-water $pCO_2$ has detrimental effects on the early development of *Crassostrea gigas* (Kurihara et al., 2008, Gazeau et al., 2011). The combined effect of decreasing hatching rates and

reduced shell growth could lead to a significant decline of the settlement success of mussels and other shellfishes (Gazeau et al., 2010; Talmage and Gobler, 2010).

Along with Lithiotis bivalves, the other prolific biocalcifier of the Pliensbachian tropical carbonate factory was the dasycladalean alga *Palaeodasycladus mediterraneus* (Barattolo et al, 1993). Dasycladalean algae are a major group of benthic marine chlorophytes with a rich and diverse fossil record. Maximum diversity was attained during the Permian–Mid Triassic, Late Jurassic–Early Cretaceous, and Paleocene–Eocene (Aguirre and Riding, 2005). Dasyclad species diversity has declined since the Paleocene, and currently is at its lowest level since the Jurassic with only 38 species in 10 genera (Berger and Kaever, 1992; Berger, 2006). In modern carbonate platforms the role of Dasycladales as prolific carbonate producers has been taken by Bryopsidales like *Halimeda* (Hillis, 2001; Granier, in press). All extant dasycladaleans are aragonitic, and, with a few exceptions (Simmons et al., 1991), this was the mineralogy of the group throughout its history (Berger and Kaever, 1992). Calcification in extant Dasycladales is mainly extracellular. In particular, aragonite crystals precipitate in the mucilage within the intercellular space (Flajs, 1977). There are no specific studies on the effects of ocean acidification on dasyclads. However, many data exist on *Halimeda*. These data are particularly relevant because *Halimeda* is characterized by the same type of extracellular calcification as extant dasycladales (Borowitzka and Larkum, 1976a). It has been recently demonstrated that calcification of *H. discoidea* is directly coupled to the local pH, thus it is to be expected that acidification of seawater will decrease the calcification (De Beer and Larkum, 2001). The detrimental effect of a pH decrease on *Halimeda* calcification, already reported by Borowitzka and Larkum (1976b), has been recently confirmed by Sinutok et al. (2011). Direct manipulation of $pCO_2$ produced a net calcification increase in *H. incrassata* relative to the control under intermediate $pCO_2$ levels (605 and 903 ppm), followed by a decline at the highest $pCO_2$ level (2856 ppm) (Ries et al., 2009). A decrease in diversity, abundance, percentage cover and reproductive capacity has also been documented for *Halimeda*, and other calcareous algae, in natural environments exposed to elevated $CO_2$ levels (Porzio et al., 2011).

Assuming that the mechanism and energetic cost of calcification was the same as in their modern counterparts (i.e. shellfishes and *Halimeda*), Lithiotis bivalves and the dasycladalean alga *P. mediterraneus* were seemingly vulnerable to ocean acidification. Their abrupt disappearance at the onset of the negative CIE associated with the T-OAE suggests a common causal link. The massive injection of isotopically depleted $CO_2$, which is generally invoked to explain the negative CIE (Hesselbo et al, 2000; McElwain et al., 2005; Kemp et al., 2005; Beerling and Bretnall, 2007; Cohen et al., 2007), could have caused also a decrease in surface water carbonate saturation. Even if for the T-OAE there is no positive proof of a significant shoaling of the CCD, like that documented for the PETM, the crisis of calcareous nannoplankton has been taken as evidence of ocean acidification (Erba, 2004; Mattioli et al., 2004; Tremolada et al., 2005). On this basis we put forward the hypothesis that the demise of the Lithiotis/Palaeodasycladus carbonate factory of Pliensbachian tropical carbonate platforms was caused by a short-term drop in carbonate saturation. The rapid sea-water temperature rise at the onset of the T-OAE (McArthur et al. 2000; Bailey et al. 2003; Rosales et al. 2004; van de Schootbrugge et al. 2005; Suan et al., 2008a) may have played an additional role. To this regard it is worth mentioning that synergistic detrimental effects of elevated temperature and $CO_2$ concentration on calcification have been documented both for shellfishes (Lannig et al., 2010) and *Halimeda* (Sinutok et al., 2011). As to increased nutrient input, another feature of the T-OAE (Cohen et al., 2004; Suan et al., 2008; Dera et al., 2009), it is difficult to envisage how it could have acted on isolated carbonate platforms, like the ACP (fig. 1). Even at a time of increased weathering driven by global warming, palaeogeographic and

palaeoceanographic conditions would have probably assured the existence of "oligotrophic refugia". Moreover, even if there is no consensus about the trophic requirements of Lithiotis bivalves, at least some of them were probably adapted to mesotrophic conditions (Fraser et al., 2004).

The hypothesis of demise of the Lithiotis/Paleodasycladus carbonate factory by ocean acidification is not at odds with the hypothesis that Lithiotis bivalves were adapted to high $pCO_2$ (Fraser et al., 2004). High $CO_2$ concentration and long-term increase of $pCO_2$ do not promote acidification because the ocean is buffered on time scales longer than 10s of kyr (Kump et al., 2009). On these time-scales carbonate saturation can be maintained high and decoupled from pH as long as a balance is kept between sources (weathering) and sinks of alkalinity ($CaCO_3$ burial in shallow and deep-water). Only events of geologically `rapid' (<10 kyr) $CO_2$ release will overwhelm the alkalinity buffer and produce a coupled decline in both pH and carbonate saturation (Kump et al., 2009; Ridgwell and Schmidt, 2010).

Estimates of the duration of the first two stages of the early Toarcian CIE, i.e. the negative shift and the interval of persistent low isotopic values (C1 and C2 intervals of Suan et al., 2008b), ranges from ca 200 kyr to ca 600 kyr, based on cyclostratigraphy (Kemp et al., 2005; Suan et al., 2008b; Sabatino et al., 2009). Alternative estimates imply very different rates of $CO_2$ release, which are the most significant constrain on the possible cause of the isotopic excursion, together with estimates of the size of the light carbon reservoir. Under the hypothesis that the whole CIE lasted ca. 200 kyr, each of the three abrupt $\delta^{13}C_{org}$ steps making the negative wing of the excursion would take ca. 2 kyr (Kemp et al., 2005) or even less (Cohen et al., 2007). Given the magnitude of the excursion, this timescale implies a rate of $CO_2$ release that would be rapid enough to overwhelm the buffering capacity of ocean alkalinity and cause a significant drop of seawater carbonate saturation also in the shallow tropics. In the alternative estimate of Suan et al. (2008b), the whole negative shift takes ca. 150 kyr but each of the abrupt steps may have lasted less than 20 kyr. Considering that the buffering capacity of the Early Jurassic ocean could have been less efficient than that of the modern ocean, owing to a different partition of carbonates between shallow and deep water (Zeebe and Westbroek, 2003; Ridgwell, 2005; Ridgwell and Zeebe, 2005), also with this longer timescale the rate of $CO_2$ release could be rapid enough for a scenario of ocean acidification.

Caldeira and Wickett (2003) calculated that oxidation of 5000 Gt carbon over time scales of <100 kyr would produce a decrease in surface ocean pH by >0.7 units and deep-ocean pH by 0.4 units, corresponding to a fivefold reduction in carbonate ion concentration. Estimates of the mass of light carbon necessary to produce the magnitude of the $\delta^{13}C$ excursion observed at the T-OAE range from >6000 to >9000 Gt of biogenic $CH_4$ (Beerling and Bretnall, 2007). Therefore, both the estimated rate and mass of carbon release during the T-OAE are adequate for a scenario of ocean acidification.

### *3.5.7 Oolitic limestones as the carbonate overshoot following ocean acidification*

The studied sections record a shift from biogenic carbonate production (Lithiotis/Palaedasycladus limestones) to chemical carbonate precipitation ("Oolitic Limestones"), coinciding with the onset of the early Toarcian CIE. This shift appears very abrupt (fig. 5), but we cannot exclude that a more gradual change occurred over the time interval that in our sections seemingly correspond to a gap. In any case the widespread occurrence of oolitic limestones following the demise of the Lithiotis/Palaedodasycladus carbonate factory is a common feature in many resilient platforms of the Tethyan ocean.

Ooids are a common component of tropical shallow water carbonate sediments. They are the result of direct physico-chemical carbonate precipitation. Conditions necessary for the occurrence of ooids are: (1) water supersaturated with respect to

aragonite or high Mg-calcite; (2) a source of nuclei; and (3) a means of agitation. Modern distribution of oolitic sands, and notably their abundance in the Bahamas and rarity in the Pacific atolls, indicates that elevated carbonate supersaturation, favored by high pH and high alkalinity, is the essential factor limiting the global distribution of oolitic sands today (Rankey and Reeder, 2009). The same factors may have ruled the uneven distribution of ooids in the Phanerozoic record (Sandberg, 1985; Opdyke and Wilkinson, 1990). Seawater supersaturation might also have been a controlling factor for the short-term "exclusive" occurrence of oolites after biocalcification crisis. A case in point is the Permian-Triassic crisis, which records the abrupt transition from skeletal to microbial and oolitic facies in carbonate platforms across the global tropics, coeval with a biotic crisis and a large carbon cycle perturbation (Payne et al., 2007, 2010).

A biogeochemical model has been recently proposed for the marine geological signature of an ocean acidification event caused by rapid injection of large amounts of $CO_2$ into the ocean/atmosphere system (Kump et al., 2009). According to this model, on short time scales (kyr to 10s of kyr), the effects of ocean acidification should dominate the record, with dissolution of seafloor carbonates and a biocalcification crisis in surface waters. On longer timescales (>10s kyr) the global warming resulting form enhanced $pCO_2$ promotes enhanced rock weathering and neutralization of the $CO_2$ and hence enhanced burial of $CaCO_3$. In figure 10 we try to apply this model to the record of shallow water carbonate sedimentation during the T-OAE witnessed by the ACP.

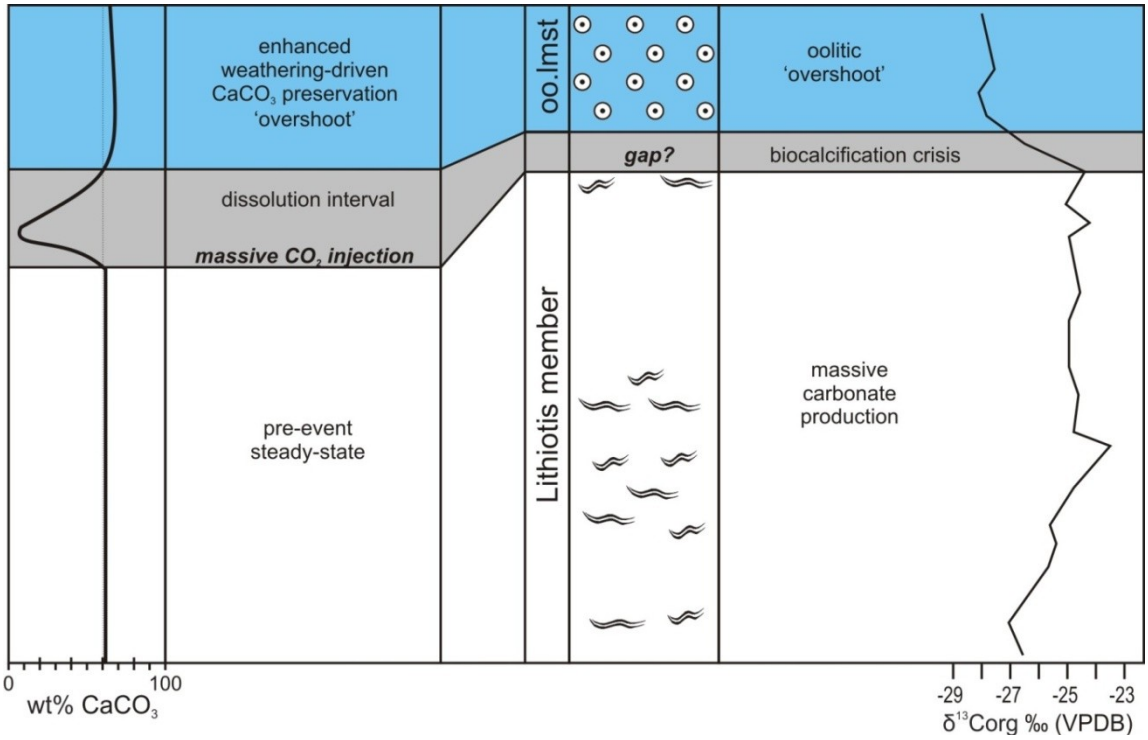


**Figure 10** - A comparison between the Late Pliensbachian-Early Toarcian evolution of the Apenninic Carbonate Platform and the expectations of a biogeochemical model of ocean acidification (Kump et al., 2009).

In the first interval of our sections, large bivalves of the Lithiotis group and the green alga *P. mediterraneus* proliferated under very favourable environmental conditions. This "healthy" carbonate factory would correspond to the pre-event steady-state of the model.

The demise of the Lithiotis/Palaeodasycladus carbonate factory coincides with the onset of the negative CIE associated with the T-OAE event. The adverse effects of decreasing pH and carbonate saturation have been proved in the lab and in the field for modern bivalves and calcareous green algae (see discussion above). Moreover, at the same

time a biocalcification crisis is documented by calcareous nannoplankton in the pelagic domain (Erba, 2004; Mattioli et al., 2009). On these grounds we surmise that the demise of shallow water biocalcifiers at the onset of the T-OAE records an episode of ocean acidification, corresponding to the "dissolution interval" of the Kump et al. (2009) model.

The widespread occurrence of oolitic limestones after the demise of the Lithiotis bivalves and *P. mediterraneus* seems to represent more than a "normal" facies shift. In the absence of massive biocalcifiers, chemical precipitation, assisted or not by microbial activity, could have been the only effective way to buffer the increasing alkalinity of the shallow water ocean, forced by enhanced continental weathering and/or dissolution of deep-water carbonates. Deposition on a wide scale of oolitic limestones would represent the "overshoot" in the $CaCO_3$ preservation of the Kump et al. (2009) model. The fact that oolitic limestones are so frequent and dominant for the whole Toarcian-Aalenian interval, suggests that a new steady state at higher saturation levels was reached and that chemical precipitation prevailed until a new stock of massive tropical biocalcifiers evolved, some million years after the early Toarcian mass extinction event.

### *3.6 Conclusions*

Chemostratigraphic correlation with the reference section of Peniche (Hesselbo et al., 2007; Suan et al., 2008b) allows unprecedented high-resolution dating of the Early Jurassic platform carbonates of the southern Apennines. This correlation is used to explore the response of a resilient carbonate platform to the early Toarcian oceanic anoxic event.

In the Apenninic Carbonate Platform, the Lithiotis/Palaeodasycladus carbonate factory, so typical of all the Tethyan tropical carbonate platforms during the Pliensbachian, was wiped out at the onset of early Toarcian negative carbon isotope excursion, seemingly marking the definitive extinction of these massive biocalcifiers. Drowning of other Tethyan platforms during the Pliensbachian or at the Pliensbachian-Toarcian boundary, was a local to regional process, controlled by the interplay of tectonic subsidence, sea level changes and palaeoenvironmental disturbance (Merino-Tomé et al., 2011). In the ACP, and in other resilient platforms, the disappearance of biocalcifiers coincide with a shift to chemical precipitation in the form of massive oolitic limestones.

The extinction of carbonate platform biocalcifiers is coeval with a biocalcification crisis of calcareous nannoplankton (Erba, 2004). The coincidence with the negative CIE, interpreted as the result of the massive injection of $CO_2$ into the atmosphere-ocean system, is consistent with a scenario of ocean acidification at the onset of the T-OAE. Laboratory manipulations and observations on naturally perturbed ecosystems suggest that shellfishes (a possible analogue of Lithiotis bivalves) and the green calcareous alga *Halimeda* (sharing the same mineralogy and probably also the same calcification mechanism of the Early Jurassic dasyclad *Palaeodasycladus mediterraneus*) are adversely affected by decreasing pH and carbonate saturation.

We surmise that the demise of the Lithiotis/Palaeodasycladus carbonate factory was caused by ocean acidification at the onset of the early Toarcian anoxic event.

Massive oolitic limestones occur on top of the Lithiotis/Palaeodasycladus limestones in the Apenninic Carbonate Platform of southern Italy and in other resilient platforms of the Tethyan ocean. Similar to what observed for the Permian-Triassic boundary crisis, chemical precipitation took over on carbonate platforms as soon as ocean alkalinity recovered.

The evolution recorded by the Apenninic Carbonate Platform across the T-OAE conforms to the expectations of a biogeochemical model for the marine geological signature of ocean acidification (Kump et al., 2009).

Very prolific biocalcification by massive bivalves and calcareous algae in the Lithiotis member represents the pre-event steady state of the model. The abrupt demise of Lithiotis bivalves and *Palaeodasycladus* at the onset of the CIE corresponds to the "dissolution interval". The oolitic limestones represent the "$CaCO_3$ preservation overshoot", marking the recovery of carbonate supersaturation driven by enhanced weathering.

The Early Toarcian record of the southern Apennines could be relevant for research on present and future ocean acidification. The message is that the threat posed by rapid increasing $pCO_2$ could be well beyond the potential of acclimation and evolutionary adaptation of marine biocalcifiers.

## *3.7 References*


Accorsi Benini C. and Broglio Loriga C. (1977). Lithiotis Gumbel 1871 e Cochlearites Reis 1903, 1° revisione morfologica e tassonomica. Bollettino della Società Paleontologica Italiana 16, 15–60.

Aguirre J. and Riding R. (2005). Dasycladalean algal biodiversity compared with global variations in temperature and sea level over the past 350 Myr. Palaios 20, 581–588.

Allan J.R. and Matthews R.K. (1982). Isotope signature associated with early meteoric diagenesis. Sedimentology 29, 797–897.

Al-Suwaidi A.H., Angelozzi G.N., Baudin F., Damborenea S.E., Hesselbo S.P., Jenkyns H.C., Manceñido M.O. and Riccardi A.C. (2010). First record of the Early Toarcian Oceanic Anoxic Event from the Southern Hemisphere, Neuquén Basin, Argentina. Journal of the Geol. Society 176, 633-636.

Barattolo F. (1991). Mesozoic and Cenozoic marine benthic calcareous algae with particular regard to Mesozoic dasycladaleans. In Riding R. ed., Calcareous Algae and Stromatolites. Springer-Verlag, Berlin, p. 504–540.

Barattolo F., De Castro P. and Parente M. (1994). Some remark on the genera Palaeodasycladus (PIA, 1920) PIA, 1927 and Eodasycladus CROS & LEMOINE, 1996 ex GRANIER & DELOFFRE, 1993. Green Algae, Dasycladales., Beitr. Paläont. 19, 1–11.

Barattolo F. and Romano R. (2005). Shallow carbonate platform bioevents during the Upper Triassic-Lower Jurassic: an evolutive interpretation. Boll. Soc. Geol. It. 124, 123-142.

Bassoullet J.P. (1997). Algues dasycladales. Distribution des principales espèces. In: Biostratigraphie du Jurassique ouest-Européen et Méditerranéen (Coord. E. Cariou and P. Hantzpergue). Mém. Centres Rech. Explo.-Prod. Elf Aquitaine 17, 339–341.

Bassoullet J.P. and Baudin F. (1994). Le Toarcien inférieur: une période de crise dans les bassins et sur les plates-formes carbonatées de l'Europe du Nord-Ouest et de la Téthys. Geobios, M.S. 17, 645–654.

Bassoullet J.-P., Elmi S., Poisson A., Cecca F., Belion Y., Guiraud R. and Baudin F. (1993). Mid Toarcian, in Atlas Tethys Paleoenvironmental Maps, edited by J. Dercourt et al., pp. 63 – 80, Becip-Franlab, Rueil-Malmaison, France.

Bailey T.R., Rosenthal Y., McArthur J.M., van de Schootbrugge B. and Thirlwall M.F. (2003). Paleoceanographic changes of the Late Pliensbachian–Early Toarcian interval: a possible link to the genesis of an Oceanic Anoxic Event. Earth Planet. Sci. Lett. 212, 307–320.

Beerling D.J. and Brentnall S.J. (2007). Numerical evaluation of mechanisms driving Early Jurassic changes in global carbon cycling. Geology 35, 247–250.

Berger S. and Kaever M. J. (1992). Dasycladales. An illustrated monograph of a fascinating algal order. Georg Thieme Verlag, 247 p.

Berger S. (2006). Photo-Atlas of living Dasycladales. Carnets de Géologie, Book/Livre 2006/02 (CG2006_BOOK_02), 348 p.

Bernoulli D. and Jenkyns H. (1974). Alpine, Mediterranean, and Central Atlantic Mesozoic facies in relation to the early evolution of the Tethys. In: Dott, R. H., Shaves, R. H. (Eds.), Modern and Ancient Geosynclinal Sedimentation, SEPM Spec. Publ. 19, 129–157.

Blomeier D.P.G. and Reijmer J.J.G. (1999). Drowning of a Lower Jurassic Carbonate Platform: Jbel Bou Dahar, High Atlas, Morocco. Facies 41, 81–110.

Bonardi G., D'Argenio B. and Perrone V. (1988). Carta Geologica dell'Appennino meridionale, SELCA, Firenze.

Borowitzka M.A. and Larkum A.W.D. (1976a). Calcification in the green algae Halimeda. I. An ultrastructure study of thallus development. Journal of Phycology 13, 6–16.

Borowitzka M.A. and Larkum A.W.D. (1976b). Calcification in the green algae Halimeda. III. The sources of inorganic carbon for photosynthesis and calcification and a model of the mechanism of calcification. Journal of Experimental Botany 27, 879– 893.

Bosellini A. (2004). The western passive margin of Adria and its carbonate platforms. In V. Crescenti, S. D'Offizi, S. Merlino, L. Sacchi, Editors , Geology of Italy, special volume of the Italian Geological Society for the IGC 32 Florence-2004, pp. 79–92.

Broglio Loriga C. and Neri C. (1976). Aspetti paleobiologici e pa- leogeografici della facies a ''Lithiotis'' (Giurese Inferiore): Rivista Italiana di Paleontologia e Stratigrafia, v. 82, 651–706.

Broglio Loriga C. and Posenato R. (1996). Adaptive strategies of Lower Jurassic and Eocene multivincular bivalves: *in* Cherchi, A., ed., Autecology of Selected Fossil Organisms: Achievements and Problems: Bollettino della Società Paleontologica Italiana, Volume Speciale no. 3, 45–61.

Čadjenović D., Kilibarda Z. and Radulović N. (2008). Late Triassic to Late Jurassic evolution of the Adriatic Carbonate Platform and Budva Basin, Southern Montenegro. Sedimentary Geology 204, 1–17.

Caldeira K. and Wickett M.E. (2003). Anthropogenic carbon and ocean pH. Nature 425, 365.

Carannante G., Graziano R., Ruberti D. and Simone L. (1997). Upper Cretaceous temperate-type open shelves from northern (Sardinia) and southern (Apennines-Apulia) Mesozoic Tethyan margins, in: James, N.P. and Clarke, J. (Eds.): Cool-water carbonates,SEPM Spec. P. 56, 309–325.

Chiocchini M., Farinacci A., Mancinelli A., Molinari V. and Potetti M. (1994). Biostratigrafia a foraminiferi dasicladali e calpionelle delle successioni carbonatiche mesozoiche dell'Appennino centrale (Italia). In: Mancinelli A. (ed) Biostratigrafia dell'Italia centrale. Studi Geologici Camerti, Volume Speciale, 1994, 9–129.

Chiocchini M. and Mancinelli A. (1977). Microbiostratigrafia del Mesozoico in facies di piattaforma carbonatica dei Monti Aurunci (Lazio meridionale). Studi Geologici Camerti 3, 109–152.

Cobianchi M. and Picotti V. (2001). Sedimentary and biological response to sea-level and palaeoceanographic changes of a Lower–Middle Jurassic Tethyan platform margin (Southern Alps, Italy). Palaeogeography, Palaeoclimatology, Palaeoecology 169, 219–244.

Cohen A.S., Coe A.L., Harding S.M. and Schwark, L. (2004). Osmium isotope evidence for the regulation of atmospheric $CO_2$ by continental weathering. Geology 32, 157–160.

Cohen A.S., Coe A.L. and Kemp D.B. (2007). The Late Palaeocene Early Eocene and Toarcian (Early Jurassic) carbon isotope excursions: a comparison of their time scales, associated environmental changes, causes and consequences. Journal of the Geological Society 164, 1093–1108.

D'Argenio B., De Castro P., Emiliani C. and Simone L. (1975). Bahamian and Apenninic limestones of identical lithofacies and age. AAPG Bull. 59, 524–533.

De Beer D. and Larkum A. (2001). Photosynthesis and calcification in the calcifying algae Halimeda discoidea studied with microsensors. Plant Cell Environ 24, 1209–1217.

De Castro P. (1962). Il Giura-Lias dei Monti Lattari e dei rilievi ad Ovest della Valle dell'Irno e della Piana di Montoro. Boll. Soc. Natur. Napoli 71, 21–52.

De Castro P. (1991). Mesozoic in : Barattolo F., De Castro P. and Parente M. (eds) 5th International Symposium on Fossil Algae. Field Trip Guide-Book. Giannani, Napoli, 21–38.

Dera G., Pellenard P., Neige P., Deconinck J.-F., Pucéat E. and Dommergues J.-L. (2009). Distribution of clay-minerals in Early Jurassic Peritethyan seas: palaeoclimatic significance inferred from multiproxy comparisons. Palaeogeography, Palaeoclimatology, Palaeoecology 271, 39–51.

Doney S.C., Fabry V.J., Feely R.A. and Kleypas J.A. (2009). Ocean Acidification: The other $CO_2$ problem. Annu. Rev. Marine. Sci. 1, 169–192.

Erba E. (2004). Calcareous nannofossils and Mesozoic oceanic anoxic events. Mar. Micropaleontol. 52, 85–106.

Fabry V.J., Seibel B.A., Feely R.A. and Orr J.C. (2008). Impacts of ocean acidification on marine fauna and ecosystem processes. Ices J Mar Sci 65, 414–432.

Ferreri V., Weissert H., D'Argenio B. and Buonocunto F.P. (1997). Carbon isotope stratigraphy: a tool for basin to carbonate platform correlation. Terra Nova 9, 57–61.

Flajs G. (1977). Skeletal structures of some calcifying algae. In Flügel E. (ed), Fossil algae. Springer-Verlag, 225–231.

Flügel, E. (1991). Triassic and Jurassic marine calcareous algae: a critical review. In Riding, R., ed., Calcareous Algae and Stromatolites, Springer-Verlag, Berlin, 481–503.

Fraser N., Bottjer D. and Fischer A. (2004). Dissecting "Lithiotis" bivalves: Implications for the Early Jurassic reef eclipse. PALAIOS 19, 51–67.

Fugagnoli A. (2004). Trophic regimes of benthic foraminiferal assemblages in Lower Jurassic shallow water carbonates from northeastern Italy (Calcari Grigi, Trento Platform, Venetian Prealps). Palaeogeography, Palaeoclimatology, Palaeoecology 205, 111–130.

Gale A. (1993). Chemostratigraphy vs biostratigraphy: data from around the Cenomanian–Turonian boundary. J. Geol. Soc. London 150, 29–33.

Gazeau F., Gattuso J.-P., Greaves M., Elderfield H., Peene J., Heip C.H.R. and Middelburg J.J. (2011). Effect of carbonate chemistry alteration on the early embryonic development of the Pacific Oyster (Crassostrea gigas). PLoS ONE 6, e23010.

Gazeau F., Gattuso J.-P., Dawber C., Pronker A.E., Peene F., Heip C.H.R. and Middelburg J.J. (2010). Effect of ocean acidification on the early life stages of the blue mussel Mytilus edulis. Biogeosciences 7, 2051–2060.

Gazeau F., Quiblier C., Jansen J.M., Gattuso J.-P., Middelburg J.J. and Heip C.H.R. (2007). Impact of elevated $CO_2$ on shellfish calcification. Geophys. Res. Lett. 34, L07603, doi:10.1029/2006GL028554.

Gibbs S.J., Bown P.R., Sessa J.A., Bralower T.J. and Wilson P.A. (2006). Nannoplankton extinction and origination across the Paleocene-Eocene Thermal Maximum. Science 314, 1770–1773.

Granier B. (in press). The contribution of calcareous green algae to the production of limestones: a review. Geodiversitas 34 (1).

Gröcke D.R., Rimmer S.M., Yoksoulian L.E., Cairncross B., Tsikos H. and van Hunen, J. (2009). No evidence for thermogenic methane release in coal from the Karoo–Ferrar large igneous province. Earth Planet. Sci. Lett. 277, 204–212.

Grötsch J., Billing I. and Vahrenkamp V. (1998). Carbon-isotope stratigraphy in shallow water carbonates: implications for Cretaceous black-shale deposition. Sedimentology 45, 623–634.

Hall-Spencer J.M., Rodolfo-Metalpa R., Martin S., Ransome E., Fine M., Turner S.M., Rowley S.J., Tedesco D. and Buia M.-C. (2008). Volcanic carbon dioxide vents show ecosystem effects of ocean acidification. Nature 454, 96–99.

Hayes J.M. (1993). Factors controlling C-13 contents of sedimentary organic-compounds – principles and evidence. Mar. Geol. 113, 111–125.

Hayes J.M., Freeman K.H., Popp B.N. and Hoham C.H. (1990). Compound-specific isotopic analyses – a novel tool for reconstruction of ancient biogeochemical processes. Org. Geochem. 16, 1115–1128.

Hermoso M., Le Callonnec L., Minoletti F., Renard M. and Hesselbo S.P. (2009). Expression of the Early Toarcian negative carbon-isotope excursion in separated carbonate microfractions (Jurassic, Paris Basin). Earth and Planetary Science Letters 277, 194–203.

Hesselbo S.P., Gröcke D.R., Jenkyns H.C., Bjerrun C.J., Farrimond P., Morgans Bell H.S. and Green O.R. (2000). Massive dissociation of gas hydrate during a Jurassic oceanic anoxic event. Nature 406, 392–395.

Hesselbo S.P. and Pieńkowski G. (2011). Stepwise atmospheric carbon-isotope excursion during the Toarcian Oceanic Anoxic Event (Early Jurassic, Polish Basin). Earth and Planetary Science Letters 301, 365–372.

Hesselbo S.P., Jenkyns H.C., Duarte L.V. and Oliveira L.C.V. (2007). Carbon-isotope record of the Early Jurassic (Toarcian) Oceanic Anoxic Event from fossil wood and marine carbonate (Lusitanian Basin, Portugal). Earth Planet. Sci. Lett. 253, 455–470.

Hillis L. (2001). The calcareous reef alga Halimeda (Chlorophyta, Byropsidales): a cretaceous genus that diversified in the Cenozoic. Palaeogeography.

Hottinger L. (1967). Foraminifeères imperforés du mésozoique marocain. Note Mem. Serv. Geol. Maroc. 209, 61–168.

Huck S., Heimhofer U., Rameil N., Bodin S. and Immenhauser A. (2011). Strontium and carbon-isotope chronostratigraphy of Barremian-Aptian shoal-water carbonates: Northern Tethyan platform drowning predates OAE 1a. Earth Planet. Sci. Lett. 304, 547–558.

Huck S., Rameil N., Korbar T., Heimhofer U., Wieczorek T.D. and Immenhauser A. (2010). Latitudinally different responses of Tethyan shoal-water carbonate systems to the Early Aptian oceanic anoxic event (OAE 1a). Sedimentology 57, 1585–1614.

Immenhauser A., Hillgärtner H. and van Bentum E. (2005). Microbial–foraminiferal episodes in the Early Aptian of the southern Tethyan margin: ecological significance and possible relation to oceanic anoxic event 1a. Sedimentology 52, 77–99.

Immenhauser A., Holmden C. and Patterson W.P. (2008). Interpreting the Carbon-Isotope Record of Ancient Shallow Epeiric Seas: Lessons from the Recent, in: Pratt, B.R. and Holmden, C., (Eds.): Dynamics of Epeiric Seas: Geological Association of Canada Special Publication 48, 135–174.

IPCC 2011. Workshop on Impacts of Ocean Acidification on Marine Biology and Ecosystems. ipcc-wg2.gov at http://www.ipcc-wg2.gov/meetings/workshops/index.html#OA

Jarvis I., Gale A.S., Jenkyns H.C. and Pearce M.A. (2006). Secular variation in Late Cretaceous carbon isotopes: a new $\delta^{13}C$ carbonate reference curve for the Cenomanian–Campanian (99.6–70.6 Ma). Geol. Mag. 143, 561–608.

Jenkyns H.C. (2003). Evidence for rapid climate change in the Mesozoic-Palaeogene greenhouse world. Philos. Trans. Royal Soc., Ser. A 361, 1885–1916.

Jenkyns H.C. (2010). Geochemistry of oceanic anoxic events,. Geochem. Geophys. Geosyst., 11, Q03004, doi:10.1029/2009GC002788.

Jenkyns H.C. and Clayton C.J. (1986). Black shales and carbon isotopes from the Tethyan Lower Jurassic. Sedimentology,33, 87–106.
Kemp D.B., Coe A.L., Cohen A.S. and Schwark L. (2005). Astronomical pacing of methane release in the Early Jurassic period. Nature 437, 396–400.
Kump L.R., Bralower T.J. and Ridgwell A. (2009). Ocean Acidification in Deep Time. Oceanography 22, 94–107.
Kurihara H. (2008). Effects of $CO_2$-driven ocean acidification on the early developmental stages of invertebrates. Mar. Ecol. Prog. Ser. 373, 275–284.
Lannig G., Eilers S., Pörtner H.O., Sokolova I.M. and Bock C. (2010). Impact of ocean acidification on energy metabolism of oyster, Crassostrea gigas – Changes in metabolic pathways and thermal response. Marine Drugs 8, 2318–2339.
Léonide P., Floquet M., Durlet C., Baudin F. Pittet B. and Lécuyer C. (2011). Drowning of a carbonate platform as a precursor stage of the Early Toarcian global anoxic event (Southern Provence sub-Basin, South-east France). Sedimentology, doi: 10.1111/j.1365-3091.2010.01221.x.
Littler K., Hesselbo S.P. and Jenkyns H.C. (2010). A carbon-isotope perturbation at the Pliensbachian-Toarcian boundary: evidence from the Lias Group, NE England. Geological Magazine 147, 181–192.
Lohmann K.C. (1988). Geochemical patterns of meteoric diagenetic systems and their application to studies of paleokarst. In: James, N.P. & Choquette, P.W. (eds) Paleokarst. Springer, Berlin, 58–80.
Manatschal G., and Bernoulli D. (1999). Architecture and tectonic evolution of non-volcanic margins: Present- day Galicia and ancient Adria.Tectonics 18, 1099–1199, doi: 10.1029/1999TC900041.
Margaritz M., Holser W.T. and Kirschvink J.L. (1986). Carbon-isotope events across the Precambrian/Cambrian boundary on the Siberian Platform. Nature, 320, 258–259.
Marino M. and Santantonio M. (2010). Understanding the geological record of carbonate platform drowning across rifted Tethyan margins: Examples from Lower Jurassic of the Apennines and Sicily (Italy). Sedimentary Geology 225, 116–137.
Masetti D., Claps M., Giacometti A, Lodi P. and Pignatti P. (1998). I Calcari Grigi della piattaforma di Trento (Lias inferiore e medio, Prealpi venete): Atti Ticinensi di Scienze della Terra 40, 139–183.
Mattioli E., Pittet B., Bucefalo Palliani R., Röhl H.-J., Schmid-Röhl A. and Morettini E. (2004). Phytoplankton evidence for timing and correlation of palaeoceanographical changes during the Early Toarcian oceanic anoxic event (Early Jurassic). Journal of Geological Society of London 161, 685–693.
Mattioli E., Pittet B., Petitpierre L. and Mailliot S. (2009). Dramatic decrease of pelagic carbonate production by nannoplankton across the Early Toarcian anoxic event (T-OAE). Global and Planetary Change 65 (3-4), 134–145.
Mattioli E., Pittet B., Suan, G. and Mailliot S. (2008). Calcareous nannoplankton changes across the early Toarcian oceanic anoxic event in the western Tethys. Paleoceanography 23, PA3208, doi:10.1029/2007PA001435.
McArthur J.M., Donovan D.T., Thirlwall M.F., Fouke B.W. and Mattey D. (2000). Strontium isotope profile of the early Toarcian (Jurassic) oceanic anoxic event, the duration of ammonite biozones, and belemnite palaeotemperatures. Earth and Planetary Science Letters 179, 269–285.
McArthur J.M., Algeo T.J., van de Schootbrugge B., Li Q. and Howarth R.J. (2008). Basinal restriction, black shales, Re-Os dating, and the Early Toarcian (Jurassic) oceanic anoxic event. Paleoceanography 23, PA4217, doi:10.1029/2008PA001607.
McElwain J.C., Wade-Murphy J. and Hesselbo S.P. (2005). Changes in carbon dioxide during an oceanic anoxic event linked to intrusion into Gondwana coals. Nature 435, 479–482.
Merino-Tomé Ò., Della Porta G., Kenter J.A.M., Verwers K., Harris P.M., Adams E.W., Playton T. and Corrochano D. (2011). Sequence development in an isolated carbonate platform (Lower Jurassic, Djebel Bou Dahar, High Atlas, Marocco): influence of tectonics, eustacy and carbonate production. Sedimentology, doi: 10.1111/j.1365-3091.2011.01232.x.
Newton R.J., Reeves E.P., Kafousia N., Wignall P.B., Bottrell S.H. and Sha J.-G. (2011). Low marine sulfate concentrations and the isolation of the European epicontinental sea during the Early Jurassic. Geololy 39, 7–10.
Oehlert A.M., Lamb-Wozniak K.A., Devlin Q.B., Mackenzie G.J., Reijmer J.J.G. and Swart P.K. (2011). The stable carbon isotopic composition of organic material in platform derived sediments: implications for reconstructing the global carbon cycle. Sedimentology, doi:10.1111/j.1365-3091.2011.01273.x.
Opdyke B. and Wilkinson B. (1990). Paleolatitude distribution of Phanerozoic marine ooids and cements. Palaeogeography, Palaeoclimatology, Palaeoecology 78, 135–148.
Parente M., Frijia G. and Di Lucia M. (2007). Carbon-isotope stratigraphy of Cenomanian-Turonian platform carbonates from the southern Appennines (Italy): a chemostratigraphic approach to the problem of

correlation between shallow water and deep-water successions. Journale of the Geol. Soc., London 164, 609–620.
Parente M., Frijia G., Di Lucia M., Jenkyns H.C., Woodfine R.G. and Baroncini F. (2008). Stepwise extinction of larger foraminifers at the Cenomanian-Turonian boundary: A shallow water perspective on nutrient fluctuations during Oceanic Anoxic Event 2 (Bonarelli Level). Geology v.36, no.9, 715–718.
Payne J.L., Turchyn A.V., Paytan A., DePaolo D.J., Lehrmann D.J., Yu M. and Wei J. (2010). Calcium isotope constraints on the end-Permian mass extinction. Proceedings of the National Academy of Sciences 107, 8543–8548.
Payne J.L., Lehrmann D.J., Follett D., Seibel M., Kump L.R., Riccardi A., Altiner D., Sano H. and Wei J. (2007). Erosional truncation of uppermost Permian shallow-marine carbonates and implications for Permian-Triassic boundary events. Geological Society of America Bulletin 119, 771–784.
Picotti V. and Cobianchi M. (1996). Jurassic periplatform sequences of the eastern Lombardian Basin (Southern Alps). The deep-sea record of the tectonic evolution, growth and demise history of a carbonate platform. Memorie di Scienze Geologiche 48, 171–219.
Porzio L., Buia M.-C. and Hall-Spencer J.M. (2011). Effects of ocean acidification on macroalgal communities. Journal of Experimental Marine Biology and Ecology 1–10, doi:10.1016/j.jembe.2011.02.011.
Rankey E.C. and Reeder S.L. (2009). Holocene ooids of Aitutaki Atoll, Cook Islands, South Pacific. Geology 37, 971–974.
Ridgwell A. (2005). A Mid Mesozoic Revolution in the regulation of ocean chemistry. Marine Geology 217, 339–357.
Ridgwell A. and Schmidt D.N. (2010). Past constraints on the vulnerability of marine calcifiers to massive carbon dioxide release. Nature Geoscience 3, 1–5.
Ridgwell A. and Zeebe R. (2005). The role of the global carbonate cycle in the regulation and evolution of the Earth system. Earth and Planetary Science Letters 234, 299–315.
Ries J., Cohen A. and McCorkle D. (2009). Marine calcifiers exhibit mixed responses to $CO_2$-induced ocean acidification. Geology, 37(12), 1131–1134.
Robinson S.A. (2010). Shallow water carbonate record of the Paleocene-Eocene Thermal Maximum from a Pacific Ocean guyot. Geology 39, 51–54.
Rosales I., Quesada S. and Robles S. (2004). Paleotemperature variations of Early Jurassic seawater recorded in geochemical trends of belemnites from the Basque–Cantabrian Basin, northern Spain. Palaeogeography, Palaeoclimatology, Palaeoecology 203, 253–275.
Royal Society (2005). Ocean acidification due to increasing atmospheric carbon dioxide. London: The Royal Society, 57 pp.
Sabatino N., Neri R., Bellanca A., Jenkyns H.C., Baudin F., Parisi G. and Masetti D. (2009). Carbon-isotope records of the Early Jurassic (Toarcian) oceanic anoxic event from the Valdorbia (Umbria-Marche Apennines) and Monte Mangart (Julian Alps) sections: palaeoceanographic and stratigraphic implications. Sedimentology 56, 1307–1328.
Sandberg P.A. (1985). Nonskeletal aragonite and $pCO_2$ in the Phanerozoic and Proterozoic. American Geophysical Union Monograph 32, 585–594.
Santantonio M. and Carminati E. (2011). Jurassic rifting evolution of the Apennines and Southern Alps (Italy): Parallels and differences. GSA Bulletin 123, no. 3-4, 468–484. doi: 10.1130/B30104.1.
Sartoni S. and Crescenti U. (1962). Ricerche biostratigrafiche sul Mesozoico dell'Appennino meridionale. Giorn. Geol., s. II, 29, 153–302.
Scheibner C. and Speijer R.P. (2008). Late Paleocene–early Eocene Tethyan carbonate platform evolution — A response to long- and short-term paleoclimatic change. Earth Science Reviews 90, 71–102.
Scherreiks R., Bosence D., BouDagher-Fadel M., Meléndez G. and Baumgartner P.O. (2009). Evolution of the Pelagonian carbonate platform complex and the adjacent oceanic realm in response to plate tectonic forcing (Late Triassic and Jurassic), Evvoia, Greece. Int. J. Earth Sci. (Geol. Rundsch.) 99, 1317–1334.
Septfontaine M., Arnaud-Vanneau A., Bassoullet J.P., Gusic I., Ramalho M. and Velic I. (1991). Les foraminiféres imperforés des plates-formes carbonatées jurassiques état des connaissances et perspectives d'avenir. Bull. Soc. Vaud. Sci. Nat. 80 (3), 255–277.
Simmons M.D., Emery D. and Pickard N.A.H. (1991). Hensonella dinarica (RADOICIC), an originally calcitic Early Cretaceous Dasycladacean alga. Palaeontology 34, 955–961.
Sinutok S., Hill R., Doblin M.A., Wuhrer R. and Ralph P.J. (2011). Warmer more acidic conditions cause decreased productivity and calcification in subtropical coral reef sediment-dwelling calcifiers. Limnol. Oceangr. 56, 1200–1212.
Strasser A., Hillgärtner H., Hug W. and Pittet B. (2000). Third-order depositional sequences resulting from Milankovitch cycles. Terra Nova 12, 303–311.

Suan G., Mattioli E., Pittet B., Mailliot S. and Lécuyer C. (2008a). Evidence for major environmental perturbation prior to and during the Toarcian (Early Jurassic) oceanic anoxic event from the Lusitanian Basin. Paleoceanography 23, PA1202. doi:10.1029/2007PA001459.

Suan G., Pittet B., Bour I., Mattioli E., Duarte L.V. and Mailliot S. (2008b). Duration of the Early Toarcian carbon isotope excursion deduced fromspectral analysis: consequence for its possible causes. Earth Planet. Sci. Lett. 267, 666–679.

-Marx B., Duarte L.V., Philippe M., Reggiani L., and Martineau F. (2010). Secular environmental precursors to Early Toarcian (Jurassic) extreme climate changes. Earth and Planetary Science Letters 290, 448–458.

Svensen H., Planke S., Chevallier L., Malthe-Sorenssen A., Corfu F. and Jamtveit B. (2007). Hydrothermal venting of greenhouse gases triggering Early Jurassic global warming. Earth and Planetary Science Letters 256, 554–566.

Swart P.K., Reijmer J.J.G and Otto R. (2009). A re-evaluation of facies on Great Bahama Bank II: variations in the δ13C, δ18O and mineralogy of surface sediments. Int. Assoc. Sedimentol. Spec.Publ. 41, 1–14.

Talmage S.C. and Gobler C.J. (2010). Effects of past, present, and future ocean carbon dioxide concentrations on the growth and survival of larval shellfish. Proceedings of the National Academy of Sciences 107, 17246–17251.

Tremolada F., van de Schootbrugge B. and Erba E. (2005). Early Jurassic schizosphaerellid crisis in Cantabria, Spain: implications for calcification rates and phytoplankton evolution across the Toarcian oceanic anoxic event. Paleoceanography 20, A201. doi:10.1029/2004PA001120.

Underwood C.J., Crowley S.F., Marshall J.D. and Brenchley P.J. (1997). High-resolution carbon isotope stratigraphy of the basal Silurian Stratotype (Dob's Linn, Scotland) and its global correlation. J. Geol. Soc. London, 154, 709–718.

van de Schootbrugge B.,McArthur J.M., Bailey T.R., Rosenthal Y., Wright J.D. and Miller K.G. (2005). Toarcian oceanic anoxic event: an assessment of global causes using belemnite C isotope records. Paleoceanography 20 PA3008, 1–10.

Vlahović I., Tišljar J., Velić I. and Matičec D. (2005). Evolution of the Adriatic Carbonate Platform: Palaeogeography, main events and depositional dynamics. Palaeogeography, Palaeoclimatology, Palaeoecology 220, 333–360.

Wignall P.B., Newton R.J. and Little C.T.S. (2005). The timing of paleoenvironmental change and cause-and-effect relationships during the early Jurassic mass extinction in Europe. Am. J. Sci. 305, 1014–1032.

Wilmsen M. and Neuweiler F. (2008). Biosedimentology of the Early Jurassic postextinction carbonate depositional system, central High Atlas rift basin, Morocco. Sedimentology 55, 773–807.

Wissler L., Weissert H., Buonocunto F.P., Ferreri V. and D'Argenio B. (2004). Calibration of the Early Cretaceous time scale: a combined chemostratigraphic and cyclostratigraphic approach to the Barremian-Aptian interval Campania Apennines and southern Alps (Italy). In. D'Argenio, B. et al. (eds), Cyclostratigraphy, approaches and case histories, SEPM Spec. Publ. 81, 123–134.

Woodfine R.G., Jenkyns H.C., Sarti M., Baroncini F. and Violante C. (2008) The response of two Tethyan carbonate platforms to the early Toarcian (Jurassic) oceanic anoxic event: environmental change and differential subsidence. Sedimentology 55, 1011–1028.

Zachos J.C., Röhl U., Schellenberg S.A., Sluijs A. Hodell D.A., Kelly D.C., Thomas E., Nicolo M., Raffi I., Lourens L.J., McCarren H. and Kroon D. (2005). Rapid acidification of the ocean during the Paleocene-Eocene Therminal Maximum. Science 308, 1611–1615.

Zeebe R.E. and Westbroek P. (2003). A simple model for the $CaCO_3$ saturation state of the ocean: the bStrangelove,Q the bNeritan,Q and the bCretanQ Ocean. Geochem. Geophys. Geosyst. 4, doi:10.1029/2003GC000538.

# CHAPTER 4 – Clay-mineral assemblages and phosphorus content in upper Pliensbachian to lower Toarcian sediments of the Apenninic Carbonate Platform: isolated carbonate platforms are not threatened by increased continental weathering?

## *4.1 Introduction*

The Late Pliensbachian-Early Toarcian was a time of important climatic changes with a long term rise in seawater temperature punctuated by cold and hot snaps (Dera et al., 2009b; Suan et al., 2008a, 2010; Dera et al., 2011). Across the same time interval, the sedimentary archive contains evidence of two severe perturbations of the global carbon cycle, witnessed by prominent carbon isotope excursions (CIE) in marine carbonates and continental and marine organic matter. The first one occurred at the Pliensbachian-Toarcian boundary (Hesselbo et al., 2007; Suan et al., 2008a; Littler et al., 2010). The second one starts at the end of the *tenuicostatum* ammonite zone and continues into the *exaratum* subzone (Jenkins and Clayton, 1997; Hesselbo et al., 2000, 2007; Röhl et al., 2001; van Breugel et al., 2006).

The latter CIE is associated with an episode of widespread deposition of organic-rich sediments known as the early Toarcian oceanic anoxic event (T-OAE; 183 Ma; Jenkyns, 1988), one of the most important global events in the Mesozoic Era. The global nature of the Early Toarcian event has been challenged because the corresponding CIE is not recorded by the biotic calcite of belemnite guards from England, Germany and Spain (van de Schootbrugge et al., 2005; McArthur et al., 2008; Gomez et al., 2008). This prompted the revival of models explaining the CIE by local (intrabasinal) paleoceanographic processes (the so-called Küspert effect; Küspert, 1982). However, these models are not able to explain why the perturbation involved also the atmospheric reservoir, as demonstrated by the record of fossil wood (Hesselbo et al., 2000, 2007). Moreover, the discovery of the CIE in deep-water successions of Argentina and Japan confirms the truly global nature of the T-OAE carbon cycle perturbation (Al-Suwaidi et al., 2010; Gröcke et al., 2011).

The early Toarcian CIE is thought to be due to massive input of isotopically light carbon, sourced either from the massive dissociation of methane hydrates (Hesselbo et al., 2000; Kemp et al., 2005) or from the generation of thermogenic methane associated with the Karoo-Ferrar large igneous province (LIP) (McElwain et al., 2005; Svensen et al., 2007).

Geochemical and isotopic data from belemnite guards, brachiopods and fish teeth indicate that the T-OAE was coeval with a 6-7 °C very rapid warming of seawater (McArthur et al., 2000; Bailey et al., 2003; Rosales et al., 2004; van de Schootbrugge et al., 2005; Gomez et al., 2008; Suan et al., 2008a; Dera et al., 2009b). This hot snap would have forced a global enhanced continental weathering, for which there is isotopic evidence from the record of $^{187}Os/^{188}Os$ and $^{87}Sr/^{86}Sr$ (Cohen et al., 2004) and mineralogical and geochemical evidence from clay-minerals and phosphorus (P) content of marine sediments (Dera et al., 2009a; Bodin et al., 2010). Fuelling of primary productivity by increased delivery of nutrients to coastal areas was the main cause of black shale deposition for the T-OAE, as for the other Mesozoic OAEs (Jenkyns, 2003).

The T-OAE is also associated with a mass extinction event, resulting in a dramatic decline of biotic diversity in marine ecosystems (Little and Benton, 1995; Harries and Little, 1999; Cecca and Macchioni, 2004; Wignall et al., 2005; Wignall and Bond, 2008; Dera et al., 2010). Even though the terrestrial biotic record is yet relatively poorly

documented, it seems that terrestrial species were also affected (Philipe and Thévenard, 1996).

The Pliensbachian-Toarcian boundary interval has received comparatively less attention than the T-OAE, but there is overwhelming evidence that it was a time of important climatic change and faunal turnover. Actually, the Early Toarcian mass-extinction event started at the Pliensbachian-Toarcian boundary (Little and Benton, 1995; Harries and Little, 1999; Wignall et al., 2005; Wignall and Bond, 2008) and oxygen isotope data from brachiopods indicate that a marked warming, comparable to the one reported for the T-OAE, occurred also across the Pliensbachian-Toarcian boundary (Suan et al., 2008a, 2010). That dramatic palaeoenvironmental perturbations started well before the onset of the T-OAE is also confirmed by the occurrence of a prominent CIE, first recorded at Peniche (Portugal, Hesselbo et al., 2007; Suan et al., 2008a) and subsequently also in Yorkshire (UK, Littler et al., 2010) and in the High Atlas (Morocco, Bodin et al., 2010). As suggested by Bodin et al. (2010), the absence of the negative shift at the Pliensbachian-Toarcian boundary in some Northern European successions could be due to a hiatus or to strong condensation (Morard et al., 2003; Wignall and Bond, 2008; Mailliot et al., 2009).

Even if black shales are not so widespread as for the T-OAE, the Pliensbachian-Toarcian boundary in the British Isles is marked by the occurrence of a pyrite-rich, black shale interval (Wignall and Bond, 2008), indicating that anoxic conditions developed at least locally.

A widespread episode of carbonate platform drowning is commonly associated with the Early Toarcian paleoenvironmental perturbations (Bassoullet and Baudin, 1994) but there is ample evidence that many Tethyan carbonate platforms drowned well before the onset of T-OAE, either in the Pliensbachian (Marino and Santantonio, 2010; Santantonio and Carminati, 2011 and references therein) or at the Pliensbachian-Toarcian boundary (Blomeier and Reijmer, 1999; Wilmsen and Neuweiler, 2008; Merino-Tomé et al., 2011). A combination of tectonics, eustatic sea-level changes and environmental deterioration is generally invoked as the cause of platform drowning (Wilmsen and Neuweiler, 2008; Bodin et al., 2010; Merino-Tomé et al., 2011; Léonide et al., 2011) or of platform crisis and significant carbonate factory shifts (Cobianchi and Picotti, 2001; Woodfine et al., 2008).

The Trento Carbonate Platform of northeastern Italy (Cobianchi and Picotti, 2001; Woodfine et al., 2008) and the Apenninic Carbonate Platform (ACP) of southern Italy continued growing in shallow water during the Toarcian. According to Woodfine et al. (2008), at Monte Sorgenza, a classical section for the Jurassic platform carbonates of the ACP (Chiocchini et al., 1994), clay-rich facies, indicative of reduced platform growth, occur close to the Pliensbachian-Toarcian boundary. During the T-OAE shallow water oolitic sediments were deposited: no significant facies change is recorded at the level of the negative CIE. The reconstruction of Woodfine et al. (2008) has been recently challenged (chapter 3). Their carbon isotope stratigraphy of two sections of the ACP (including Monte Sorgenza) shows two subsequent negative CIEs. The first one is recorded in the upper part of the Lithiotis member and closely precedes an interval with frequent cm to dm-thick marly interlayers, seemingly corresponding to the clay-rich interval of Woodfine et al. (2008). This excursion is interpreted as the expression in the ACP of the Pliensbachian-Toarcian boundary CIE (chapter 3). The second, more prominent negative CIE, interpreted as the early Toarcian negative CIE, occurs at the top of the Lithiotis member, while the massive Oolitic limestones record a recover to more positive $\delta^{13}C$ values. The very prominent negative excursion of Woodfine et al. (2008), occurring within the oolitic limestones at Monte Sorgenza, is seemingly caused by circulation of diagenetic fluids along a fault (chapter 3). These data indicate that in the ACP the demise of the most

prolific biocalcifiers of early Jurassic Tethyan carbonate platforms, i.e. the Lithiotis bivalves and the calcareous alga *Palaeodasycladus mediterraneus*, coincided with the T-OAE negative CIE, while the "clay-rich" interval is associated with a cluster of subaerial exposure surfaces in a sequence boundary zone (chapter 3).

The main aim of this paper is to further investigate the response of the ACP to Late Pliensbachian–Early Toarcian paleoenvironmental perturbations. We produce the first record of P content and of clay-mineral assemblages for a late Pliensbachian-Early Toarcian carbonate platform. Phosphorus is the main biolimiting nutrient on geologic time scales (Tyrrell, 1999), and clay-minerals are a useful proxy of climate-induced changes in weathering intensity (Singer, 1984; Chamley, 1989). We use this original dataset, in conjunction with the carbon isotope stratigraphy of chapter 3, to compare the evolution of the ACP with that of other carbonate platforms for which increased nutrient levels have been implied as the main cause of crisis or drowning.

### *4.2 Geological setting*

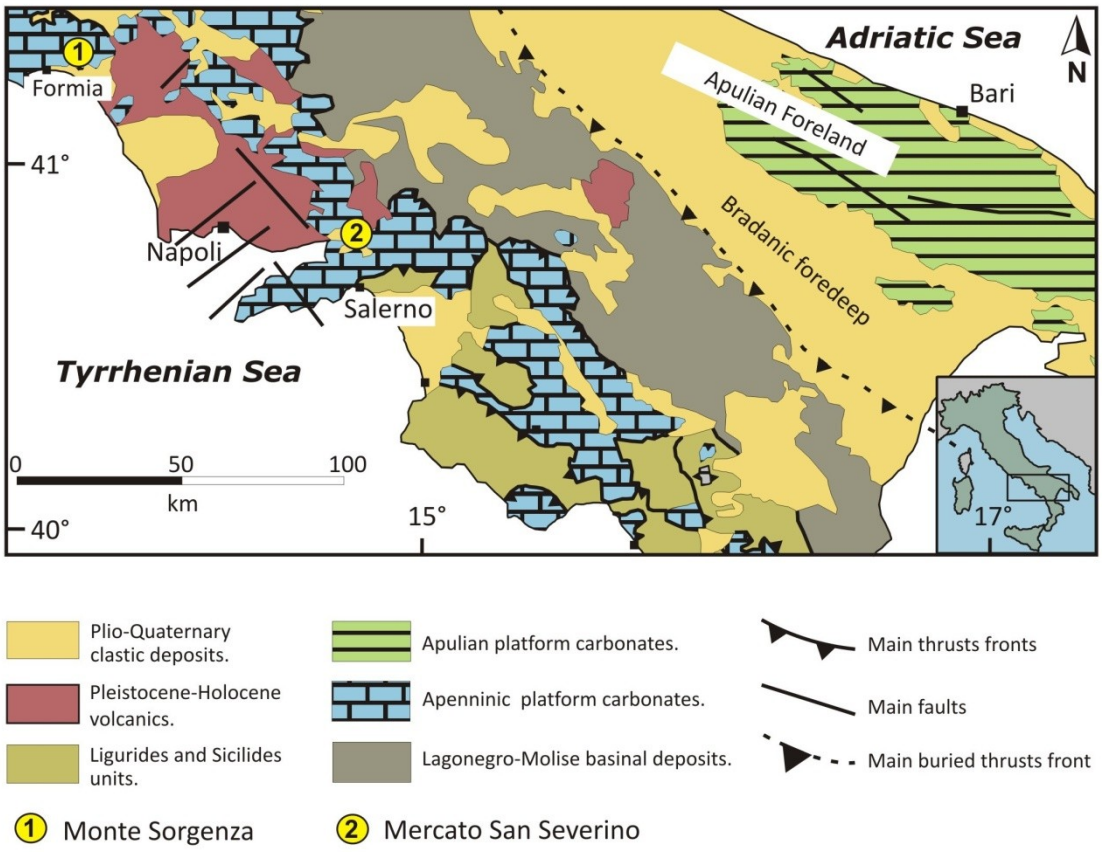


**Figure 1** - Schematic geological map of the southern Apennines (redrawn from Bonardi et al., 1988) with location of the studied sections.

The southern Apennine chain is a NE verging fold-and-thrust belt (Butler et al., 2004; Mazzoli et al., 2008) that developed during the Neogene at the expense of the Afro-Adriatic continental margin and evolved within the framework of convergent motion between the Afro-Adriatic and European plates since Late Cretaceous times (Dewey et al., 1989; Mazzoli and Helman, 1994; Rosenbaum et al., 2002). Except for the remnants of the ophiolite-bearing Liguride Units that occur on top of the thrust pile, outcropping units consist of Mesozoic and Cenozoic rocks derived from the sedimentary cover of the

foreland plate. These include carbonate platform and pelagic basin successions, locally covered by Neogene foredeep and/or thrust-top basin sediments. The Apulian promontory represents the orogenic foreland (Mazzoli et al., 2008).

Among the several more or less complex reconstructions proposed for the pre-orogenic Meso–Cenozoic paleogeography of the southern Apennines, the most widely accepted one, grounded also in subsurface data, envisages two carbonate platforms, the Apenninic Carbonate Platform (ACP) and the Apulian Carbonate Platform, separated by a deep basin, the Lagonegro Basin (Menardi Noguera and Rea, 2000 and references therein). The oldest neritic carbonates cropping out in the southern Apennines are Middle Triassic in age and there is ample evidence that shallow water carbonate sedimentation was established over wide areas during the Late Triassic (D'Argenio and Sgrosso, 1974). In the ACP shallow water sedimentation persisted almost to the end of the Cretaceous, when the area underwent a generalized emersion. It was locally re-established during the Palaeogene (Trentinara Formation; Selli, 1962) and the Early Miocene (Roccadaspide–Cerchiara and Cusano Formation; Selli, 1957), to be eventually terminated by drowning and siliciclastic sedimentation in the Middle-Late Miocene.

The Upper Triassic to Lower Cretaceous carbonates of the ACP are generally referred to flat-topped, tropical carbonate platforms dominated by chloralgal or chlorozoan associations (D'Argenio et al., 1975) whereas the depositional system of Senonian rudist limestones of the southern Apennines has been interpreted as a ramp-like open shelf dominated by foramol-type assemblages (Carannante et al., 1997).

### *4.3 Materials and methods*

All the analyses were carried out at the Institute of Geology and Paleontology of the University of Lausanne, Switzerland. The composition of clay-mineral assemblages of 70 samples, 63 limestones and 7 calcareous marls, of the Mercato San Severino section and 25 samples of limestones of the Monte Sorgenza was analysed with X-ray diffraction (Scintag XRD 2000 Diffractometer; Thermo-ARL, Ecublens, Switzerland), based on methods developed by Kübler (1987) and Adatte et al. (1996). Samples were crushed in a mortar and subsequently de-carbonated by HCl 10% (1.25 N) leaching during 20 min. Dissolution of the samples was promoted by ultrasonic disaggregation (3 minutes per sample). The insoluble residue was washed and centrifuged until a neutral suspension was obtained (pH 7-8). Two granulometric fractions (<2 μm and 2–16 μm) were separated using the Stokes law. The selected fraction was pipetted and deposited on a glass plate. A first analysis was performed after air-drying at temperature room and a second one after saturation of the sample with ethylen-glycol, in order to identify swelling minerals. The intensity of the peaks of the identified minerals was measured for a semi-quantitative estimate of the proportion of clay-minerals, which is therefore given in relative percent without correction factors, because of the small error margin (<5%).

Total phosphorus analyses were performed on 115 limestone samples, 72 from Mercato San Severino and 43 from Monte Sorgenza. After crushing in a mortar, about 100 mg of powder per sample were mixed with 1 ml of $MgNO_3$ and left to dry in an oven at 45 °C for 2 h. The samples were then heated in a furnace at 550 °C for 2 h. After cooling, 10 ml of 1 N HCl was added and the solution was subjected to constant shaking for 14 h. The solutions were filtered through a 63 μm filter, diluted ten times and analysed using the ascorbic acid method of Eaton et al. (1995). For this process, the solution was mixed with ammonium molybdate and potassium antimonyl tartrate, which in an acid medium react with orthophosphate to form phosphomolybdic acid. This acid was reduced with ascorbic acid to give an intense blue colour to the solution. The intensity of the blue colour,

determined with a photospectrometer (Perkin Elmer UV/Vis Photospectrometer Lambda 10; Perkin Elmer, Waltham, MA, USA) gives the concentration of $PO_4$ in mg/l by calibration with standard solutions of known concentration. Individual samples were measured three times and precision was better than 5%. Replicate analyses of samples have a precision better than 10%.

## *4.4 Results*

### *4.4.1 Lithology and Stratigraphy*

The Mercato San Severino section is exposed in a quarry near the village of Mercato San Severino, 30 km northwest of Salerno (40°46'53"N, 14°43'45"E) (fig. 1). For this study we have analyzed a 99.8m thick succession including the upper part of the "Lithiotis member" of the "Palaeodasycladus Limestones" (0–82.1 m) and the lower part of the "Oolitic-oncolitic Limestones" (82.1–100 m) (fig. 2).

The "Lithiotis member" consists mainly of meter-thick "Lithiotis" biostromes, alternating with coarse peloidal-intraclastic grainstones and rudstones with abundant remains of *Palaeodasycladus mediterraneus*. Other lithofacies occurring in this interval are fine-grained peloidal packstones-grainstones with gastropods and small benthic foraminifers (mainly valvulinids) and mudstone-wackestone with rare *Palaeodasycladus*, small thin-shelled gastropods and ostracods. Millimetre- to cm-thick discontinuous green marls cap some beds and permeates downward, filling a complex network of irregular cavities. The thickest marly levels contain nodules of mudstones with ostracods and thin-shelled gastropods. These marly caps, which mark periods of ephemeral platform emersion, are not distributed evenly in the section. A first cluster of thicker and more closely spaced nodular marly levels occurs at 37–46 m. A second cluster occurs between 74 and 78 m. In this uppermost part of the Lithiotis member, the Lithiotis biostromes become thinner, more discontinuous and less frequent. Moreover, grain-supported lithofacies are replaced by mud-rich facies consisting of mudstones with ostracods and thin-shelled gastropods and mudstones-wackestones with benthic foraminifers and *P. mediterraneus*. The first bed of oolitic grainstone is at 82.1m from the base of the section. It is followed by a 15 cm-thick Lithiotis floatstone with dull whitish to pink subangular stout fragments of bivalve shells. At the top of this bed the Lithiotis shells are truncated by a sharp surface overlain by oolitic grainstone. The next bed is made of oolitic limestone with a few pinkish abraded fragments of bivalve shells with a thin oolitic coating. From there to the top, the section is made exclusively of massive unfossiliferous oolitic grainstones.

The Monte Sorgenza section has been logged on the southern slope of Monte Sorgenza, about 7 km northeast of Formia (41°17'39"N, 13°40'57"E) (fig. 1). Stratigraphy and facies are basically the same as in the Mercato San Severino quarry but the Lithiotis member at Mt Sorgenza is characterized by a reduced frequency and thickness of Lithiotis biostromes (fig. 2). The most recurrent facies are wackestone-packstones with *P. mediterraneus* and coarse peloidal-intraclastic packstones-grainstones with gastropods, *P. mediterraneous* and benthic foraminifers. As in the other section, subaerial exposure surfaces are marked by mm- to cm- thick nodular marly caps. Between 24 and 39 m there is a poorly exposed interval which corresponds to the gentler and more densely vegetated segment of the slope. This interval seemingly corresponds to a cluster of marly levels. A second cluster of nodular marls occurs between 47 and 52 m. As at Mercato San Severino, the uppermost part of the Lithiotis member is marked by the decreased frequency and thickness of the Lithiotis biostromes and by a shift to more muddy facies. The oolitic

limestones start at 63.5 m. Their lower part is very massive and makes a steep cliff about 10 m high. The top of the section is truncated by a small normal fault.

The last occurrence of *P. mediterraneus* at top of the Lithiotis member is the most significant biostratigraphic event to constrain the age of these sections. In the biostratigraphic schemes of the southern Apennines it has been traditionally equated with the Lower-Middle Jurassic boundary (De Castro, 1991, Chiocchini et al., 1994), but there is evidence that it occurs close to the Pliensbachian-Toarcian boundary (Bassoulet, 1997; Barattolo and Romano, 2005).

The carbon isotope stratigraphy of the Mercato San Severino and Monte Sorgenza sections has been recently presented (chapter 3). Two subsequent negative shifts have been recognized in the $\delta^{13}C_{org}$ curves. The first shift, of about -4‰, occurs in the upper part of the Lithiotis member. The second shift, of about -5‰, coincides with the boundary between the "Lithiotis member" and the "Oolitic limestones". The first negative shift has been equated with the Pliensbachian-Toarcian boundary CIE and the second has been correlated with the negative wing of the T-OAE CIE (chapter 3). Based on chemostratigraphic correlation with the well-dated reference section of Peniche, a chronostratigraphic calibration has been developed for the two studied sections.

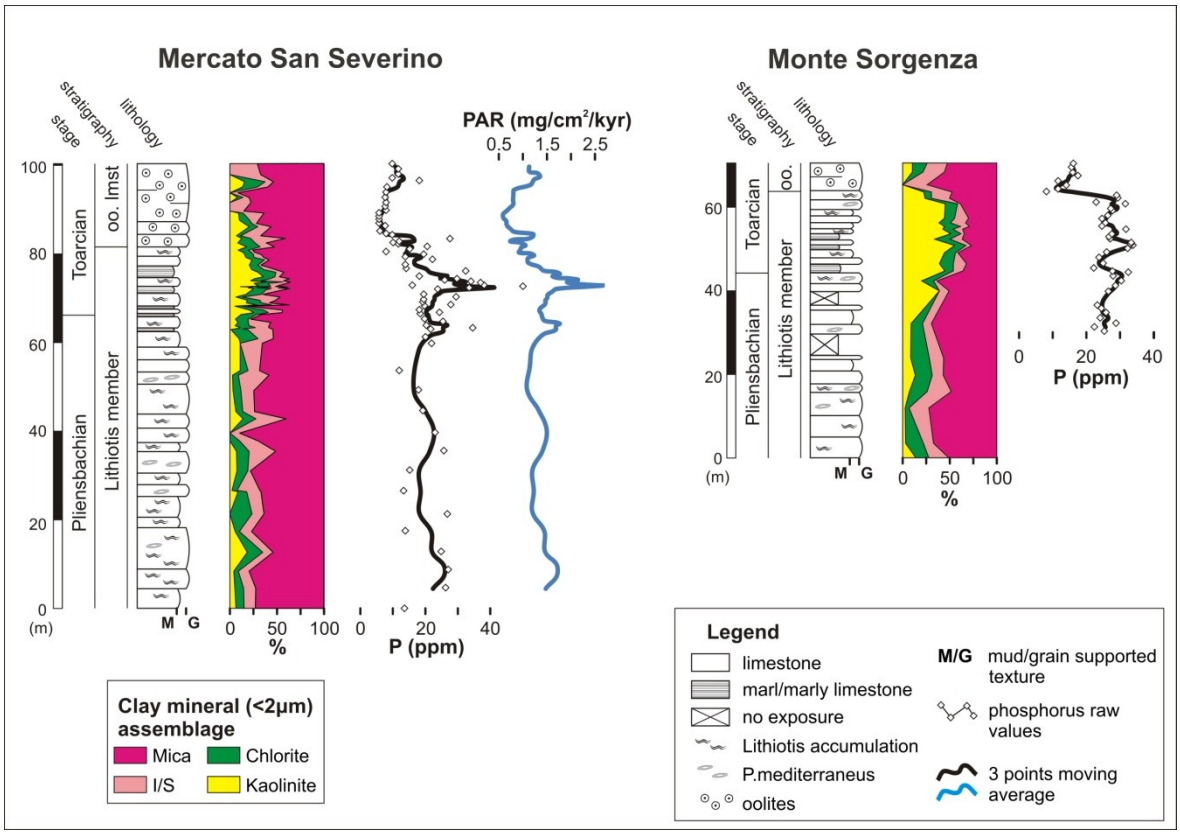


**Figure 2** - Stratigraphy, lithology, clay-mineral assemblages and P content of the Mercato San Severino and Monte Sorgenza sections.

### *4.4.2 Composition of clay-mineral assemblages*

The clay-mineral assemblages of the Mercato San Severino section are relatively homogeneous and consist of kaolinite, chlorite, mica (illite) and illite-smectite mixed layers (I/S). Mica is the most abundant clay-mineral along the whole section (36–89%, average = 59±13%). Chlorite shows the lowest abundance (0–23%, average = 11±6%), with no significant trend. I/S and kaolinite show similar relative proportions (3–40%, average = 16±9% and 0–39% average = 13±10%, respectively), but opposite trends (fig. 2).

In the lower part of the Lithiotis member (0-66.4 m), I/S is generally more abundant than kaolinite, whose relative abundance stays below 19%. This pattern is reversed in the uppermost part of the Lithiotis member (66.4-81.1 m) where kaolinite becomes more abundant than I/S, reaching a maximum of 39% at 75.3 m from the base of the section. Kaolinite proportions return low (<9%) at the top of the Lithiotis member. In the Oolitic Limestones I/S is generally more abundant than kaolinite but there are two minor peaks of kaolinite abundance at 87.3 m (21%) and 97.4 m (16%).

The Monte Sorgenza section is very similar to the Mercato San Severino section in terms of composition of the clay-mineral assemblages (fig. 2). The only remarkable difference is the distinctly higher abundance of kaolinite (0–55%, average = 27±18%) which substitutes illite/mica as the most abundant clay-mineral in the interval between 44.5 and 60.6 m. Apart from this short interval, illite is the dominant clay-mineral (27–74%, average = 48±14%). As at Mercato San Severino, Chlorite shows the lowest abundance (0–19%, average = 12±5%), while I/S shows a slightly lower proportion (2–26%, average = 14±7%). Relative trends of abundance between I/S and kaolinite are broadly comparable to those observed at Mercato San Severino. In the first part of the section (0–32 m) I/S is generally more abundant than kaolinite. The relative increase in kaolinite starts earlier at Monte Sorgenza, where, according to our chemostratigraphic correlation, kaolinite becomes more abundant than I/S already in the upper part of the *spinatum* ammonite zone (fig. 2). A broad plateau of kaolinite enrichment, with percentages fluctuating between 34 and 55%, coincides with the uppermost part of the Lithiotis member (44.5–60.6 m). Then the proportion of kaolinite decreases sharply in the last beds of the Lithiotis member, reaching minimum values at the base of the Oolitic limestones. In the uppermost part of the section the kaolinite percentage rises again but it remains less abundant than I/S.

#### *4.4.3 Total Phosphorus content*

Total phosphorus (P) concentrations are very low across the whole Mercato San Severino section section, ranging from 6 to 50 ppm (average = 18±9 ppm). The P-curve can be divided into three segments (fig. 2). In the first segment (0–53.4 m) values fluctuate between 12 and 27 ppm (average 21±6 ppm). The smoothed curve shows a slightly decreasing trend. The second segment (53.4–82.1 m), corresponding to the uppermost part of the Lithiotis member, is occupied by a broad positive excursion, with superimposed high frequency fluctuations. A positive peak of 50 ppm is reached at 72 m and then the values decrease to a minimum of 10 ppm. The last segment of the curve (82.1–99.8 m), corresponding to the Oolitic limestones, after a kick to 28 ppm, shows very low P concentrations (6–12 ppm, average = 10±5 ppm), with a single positive kick to 18 ppm. A slight rising trend is highlighted by the smoothed curve.

Phosphorus data are available only for the upper part of the Monte Sorgenza section. Total P concentrations are very low (8–34 ppm, average = 25±6 ppm). The P-curve can be divided into two segments (fig. 2). In the lower segment (30.1–63.5 m), corresponding to the upper part of the Lithiotis member, values fluctuate between 22 and 34 ppm (average = 28±3 ppm). The second segment (63.5-70.3 m) corresponds to the Oolitic Limestones. At its base there is a sharp decrease in P concentration, down to 8 ppm, followed by a gradual recovery toward slightly higher values at the top of the section (16 ppm).

## *4.5 Discussion*

### *4.5.1 Diagenetic and authigenic biases with regards to the palaeoclimatic interpretation of clay-mineral assemblages*

Clay-minerals in ancient marine sediments can be a useful indicator of palaeoclimatic conditions, provided that their composition is inherited from continental landmasses and has not been significantly altered by sediment reworking, authigenesis and diagenesis (Thiry, 2000). Therefore, the role of any of these potential biases must be carefully evaluated before inferring a palaeoclimatic signal from the clay-mineral assemblages data of the studied sections.

Illite is the most abundant clay-mineral in both studied sections. This clay-mineral is formed during the initial stage of continental weathering (Weaver, 1989) and a crystallinity index is usually intepreted as due to minimum hydrolysation under either cold or dry conditions (Singer, 1988). However, illite and I/S mixed layers also derive from illitization, the progressive conversion of smectite to illite during burial diagenesis (Hower et al., 1976; Weaver, 1989).

Burial depth and $T_{max}$ values are usually suitable indices of the intensity of the illitization process, assuming that significant illitization of smectite starts when burial depth reaches about 2000 m and/or when $T_{max}$ reaches 430/440 °C (Burtner and Warner, 1986; Chamley, 1989). Burial data from independent thermal indicators for the Miocene terrigenous sediments resting unconformably on the top of ACP successions suggest minimal influence by tectonic loading (Corrado et al., 2005) as the thickness of the tectonic loading did not exceed 1-1.5 km (Aldega et al., 2003). A minimum non-decompacted, thickness of about 1-1.5 km carbonate strata separates the Lower Jurassic sediments from the top of the whole ACP succession. $T_{max}$ data for the Cretaceous of the ACP range between 429 and 448 °C (Frijia et al., 2005). On the basis of these considerations, the complete lack of a pure smectitic phase in the studied sections is not unexpected.

Apart from burial diagenesis, there is evidence that early illitization at low temperatures can occur in shallow marine alkaline environments submitted to wetting and drying cycles, under a hot and seasonally humid climate (Deconinck et al., 1998), or by K-enriched brines formed by evaporation in marginal marine environments (Sandler et al., 2006).

Therefore, the illite and I/S contained in the clay-mineral assemblages of the studied sections could be at least partly due to illitization of former smectite, whose formation in continental environments is controlled by the weathering of soil under warm, semi-arid climates, with seasonal wet and dry regimes (Singer, 1984; Chamley, 1989).

Chlorite, as illite, forms during the initial stage of continental weathering (Weaver, 1989) and under cold and dry climate conditions. However, the occurrence of chlorite can be also related to burial diagenesis and particularly to the reactions between dioctaedral clay-mineral (kaolinite and mica) and carbonates (Hutcheon et al., 1980; Hillier, 1993). Therefore, most, if not all, of the chlorite in our sections could be due to diagenetic transformation, at the expense of the other clay phases.

Kaolinite is the result of intense chemical weathering under humid subtropical and tropical climates and indicates intense hydrolysis of the source rocks in areas with a high superficial drainage (Hallam, 1984; Chamley, 1989). During burial diagenesis kaolinite can be transformed into illite and/or chlorite (Hurst and Irwin, 1982; Larson et al., 1996). Significant burial diagenetic overprint in our successions is implied by data on the burial history of the ACP (Aldega et al., 2003; Corrado et al., 2005; Mazzoli et al., 2008). However, kaolinite is relatively more resistant to illitization than smectite (Lanson et al., 2002). Moreover, while burial diagenesis can produce a progressive decrease of kaolinite

abundance with depth (e.g. Hurst and Irwin, 1982; Lanson et al., 1996), it cannot produce reversible trends as those observed in the two studied sections (fig. 2).

On the other hand, meteoric water circulation during early diagenesis may remove alkali elements in solution, leading to the development of authigenic kaolinite (Dera et al., 2009a). In heterogeneous successions, zones of authigenic kaolinite enrichment should coincide with more porous and permeable lithologies, favouring diagenetic fluid circulation. The opposite pattern is observed in the studied sections, where the maximum abundance of kaolinite is found in the upper part of the Lithiotis member, which is dominated by mud-rich facies, by comparison with both overlying and underlying intervals, which are dominated by grain-supported facies. In conclusion, we assume that absolute proportions of kaolinite might have been slightly enhanced by authigenesis or diminished by burial diagenesis, but the initial signal of kaolinite variations through time has not been significantly distorted. The primary nature of the kaolinite signal is also supported also by the parallel trends observed in both sections and by the consistency of the total P signal (fig. 2). The slightly lower kaolinite abundance at Monte Sorgenza could be explained by a lower abundance in the source area or by a greater distance from the source. Because of their larger size, kaolinite particles are deposited generally closer to the landmass, unlikely smectite particles, which are deposited further from the source (Gibbs, 1977). Moreover, kaolinite has a high capacity to flocculate (Ruffell et al., 2002). A pattern of selective enrichment of kaolinite in more proximal areas has been observed in Valanginian-Hauterivian carbonate platform successions in the Swiss Jura (Adatte and Rumley, 1989), for the middle Jurassic succession of the Western Swiss Jura (Bolle et al., 1996) and for platform-to-basin transects in the Lower Cretaceous of the northern Tethyan margin between France and Switzerland (Godet et al., 2008) and in the Upper Cretaceous of the Basque-Cantabrian Basin (Jiménez-Berrocoso et al., 2008).

#### *4.5.2 The source of detrital clay-minerals in the platform carbonates of the ACP*

While the Cretaceous carbonate platforms of the northern Tethyan margin were attached to the European continetal block, the ACP grew as an isolated platform, separated by relatively deep basins from all the landmasses, at least since the Early Jurassic (D'Argenio, 1974) (fig. 3). This rules out any direct riverine supply from continental areas as the source of the terrigenous material in the carbonate sediments. The high potential of the eolian transport as a source of terrigenous material to shallow water carbonate banks far away from landmasses is hardly questionable, as demonstrated for instance by evidence of present-day long-range transport of African mineral dust to soils of western Atlantic islands (e.g. Prospero et al., 2001; Muhs et al., 2007).

The open debate on the origin of the "terra rossa", kaolinite-rich red clays associated with karst carbonates (see Merino and Banerjee, 2008, for a recent review), can provide significant ideas for the interpretation of the source of the clay-minerals in our successions. After comparing the insoluble residue left by dissolving limestones of the Apulian Carbonate Platform to the "terra rossa" occurring above the limestones, Moresi and Mongelli (1988) proposed a residual origin for Apulian "terra rossa". More recent studies (Durn et al., 1999; Durn, 2003) suggest that the main component of "terra rossa" is detrital, from eolian dust, while the residual component is subordinate. In order to produce a significant amount of terrigenous residue from carbonate platform dissolution, relative long-time or frequent emersion phases are clearly required. For the latest Pliensbachian-Early Toarcian there are indeed geological evidences that reveal the existence of small emergent areas in the Lazio-Abruzzo sector (central Italy) of the ACP (Colacicchi, 1967; 1987). This is also confirmed by the occurrence of levels with fossil plants in the "Palaeodasycladus limestones" of Abruzzo (Praturlon, 1968), probably coeval to the more famous Venetian flora of the Rotzo Member of the Calcari Grigi Formation (e.g. De Zigno,

1868; Wesley, 1956, 1958). On the basis of geochemical and mineralogical data, Ortega-Huertas et al. (1993) proposed that paleosols, developed by karstification and pedogenetic processes on emerged islands in the Lazio-Abruzzo sector of the ACP, were the source of terrigenous input into the Umbria-Marche basinal sediments.

We surmise that paleosols, developed on emerged sectors of the ACP, were the main source also of the clay-minerals in the carbonate sediments of the studied sections. The lower content of kaolinite in the Early Toarcian Umbria-Marche basinal sections (generally <8%, with a peak of 17%; Ortega-Huertas et al., 1993), compared with the platform carbonates of the ACP (maximum percentages of 34-55%), conforms to the pattern of selective enrichment of kaolinite in more proximal areas along a platform-to-basin transect (Godet et al., 2008).

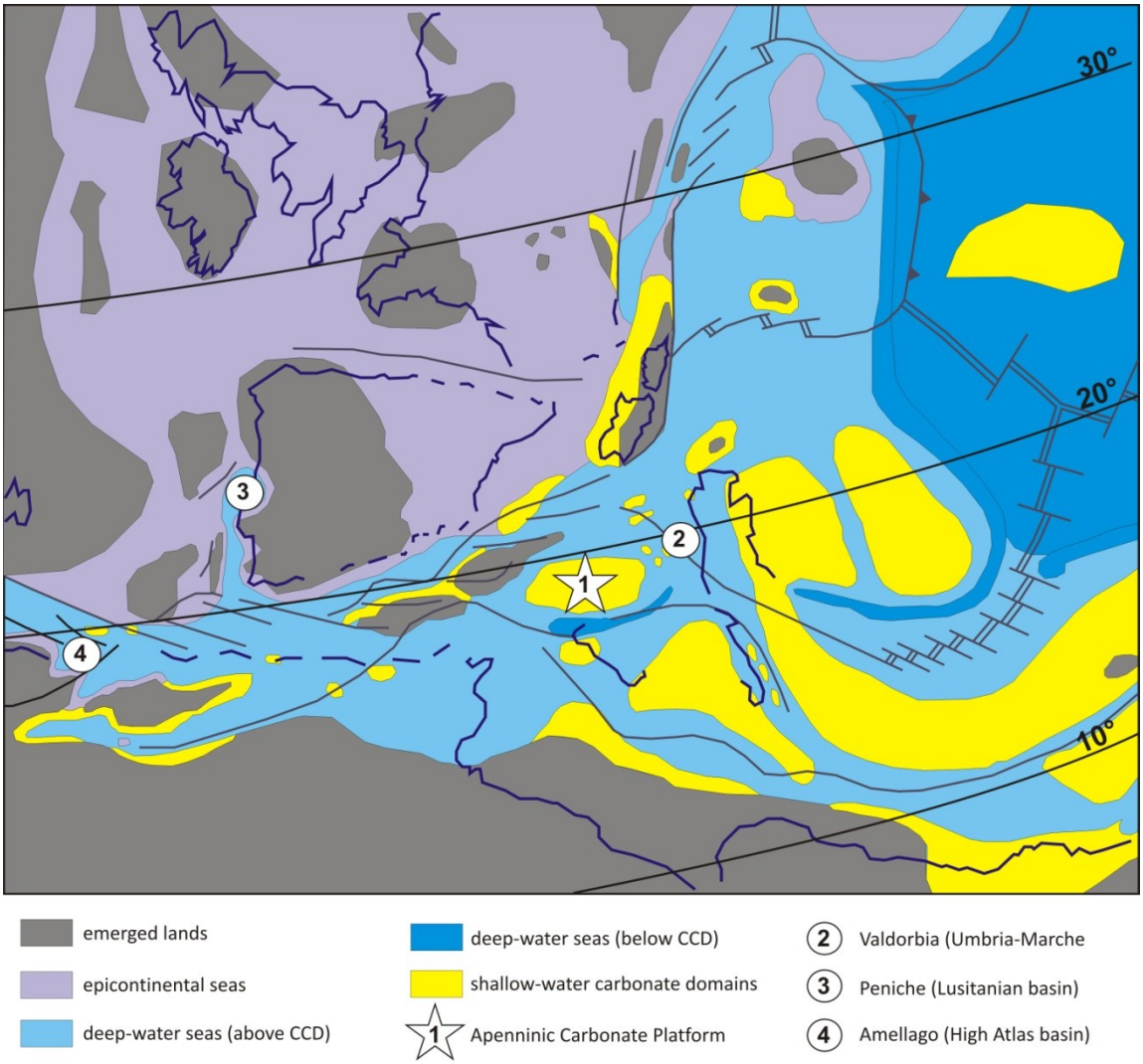


**Figure 3** - Toarcian palaeogeography of the peri-Tethyan domains (redrawn from Bassoullet et al., 1993) with position of key localities cited in the text.

### *4.5.3 Clay-minerals in the Early Jurassic of the Peritethyan seas*

The distribution of clay-minerals in the Early Jurassic Peryitethyan seas has been recently reviewed by Dera et al. (2009a), who focused particularly on changes trough time of kaolinite abundance. According to these authors there were two major phases of kaolinite enrichments in marine sediments of northern Tethys: during the Pliensbachian *davoei* zone and during the Early and Middle Toarcian. Peaks of kaolinite abundance coincide with short term (1 Myr) periods of warming, as evidenced by the $\delta^{18}O$ and Mg/Ca

proxies in belemnites, and with high gradient rising segments of the marine $^{87}Sr/^{86}Sr$ curve, used a proxy of continental weathering. According to the Dera et al. (2009a) database, the kaolinite signal is limited to Northern Tethyan basins, at latitudes between 30° and 45°N, implying wet conditions similar to those observed at present in tropical regions. By contrast the stable low abundance of kaolinite between 25° and 20°N, in the eastern and western Mediterranean domains, is taken as evidence of a drier climatic belt.

The evolution of kaolinite abundance in the Apenninic Carbonate Platform seems to be partly in contrast with the conclusions drawn by Dera et al. (2009a). The clay-mineral assemblages of the studied sections are characterized by a general predominance of illite (up to 89%), pointing to a semi-arid to seasonally contrasted climate for most of the Late Pliensbachian-Early Toarcian, in agreement with the latitudinal distribution of clay-minerals summarized by Dera et al. (2009a). However, both our sections record a distinct increase in kaolinite abundance in the Early Toarcian *polymorphum* zone (corresponding to the boreal *tenuicostatum* zone), suggesting a shift to more humid and warm climate (fig. 4). This phase of kaolinite enrichment, starting at the Pliensbachian-Toarcian boundary in the Mercato San Severino section and in the latest Pliensbachian at Monte Sorgenza, ends in the uppermost part of the *polymorphum* zone, in correspondence of the onset of the early Toarcian negative CIE. Therefore kaolinite enrichment in southern Apennines would closely correspond to the global warming phase associated with the Pliensbachian-Toarcian boundary event (Suan et al., 2008a) (fig. 4). The dataset of Dera et al. (2009a) shows no evidence of kaolinite enrichment at the transition from the Late Pliensbachian *spinatum* to the Early Toarcian *polymorphum* zone in the central Mediterranean domains. However, the only entries in the database are from early Toarcian sediments of the Umbria-Marche basin (Ortega-Huertas et al., 1993; Monaco et al., 1994) and Lombardian basin (Deconinck and Bernoulli, 1991). There are no data for the late Pliensbachian. Therefore the apparent mismatch could be actually due to undersampling of the central mediterranean area in the Dera et al. (2009a) database.

An overprint of sea-level fluctuations on the climatic signal recorded by the ACP cannot be ruled out. For instance, Ortega-Huertas et al. (1993) interpret the increase of kaolinite abundance towards the top of their sections as due to a regressive trend from the Early Toarcian to the Middle and Late Toarcian, making the studied sites more proximal to the source area. Similarly the kaolinite abundance in ACP sections could be also bear a eustatic signal. In fact, the enrichment phase occurs in correspondence of a sea-level fall reported just above the Pliensbachian-Toarcian boundary stage, while the following trend of decreasing abundance could parallel the Early Toarcian transgression (Hallam, 2001) (fig. 4).

#### *4.5.4 Phosphorus concentration as a proxy of nutrient levels*

Phosphorus represents an essential nutrient for living organisms and is the main biolimiting factor on a geological time scale (Tyrrell, 1999). The flux of dissolved and particulate P into the ocean is mainly controlled by the rate of continental weathering, erosion, runoff and atmospheric transport (Föllmi, 1996; Compton et al., 2000). P is transferred into the sediments via accumulation of organic matter, absorption of P on clay-minerals and Fe- and Mn- hydroxides, direct precipitation of dissolved inorganic P, possibly due to microbial activity. The efficiency of P storage in the sedimentary reservoir depends on redox conditions. P accumulation is favoured under oxic conditions while P recycling is favoured in oxygen-depleted bottom waters (Ingall and Jahnke, 1994; van Cappellen and Ingall, 1996; Colman and Holland, 2000; Emeis et al., 2000). This process may result in a positive feedback mechanism between water-column anoxia, enhanced benthic P regeneration and increased marine productivity (Ingall and Jahnke, 1994, 1997; van Cappellen and Ingall, 1996; Colman and Holland, 2000).

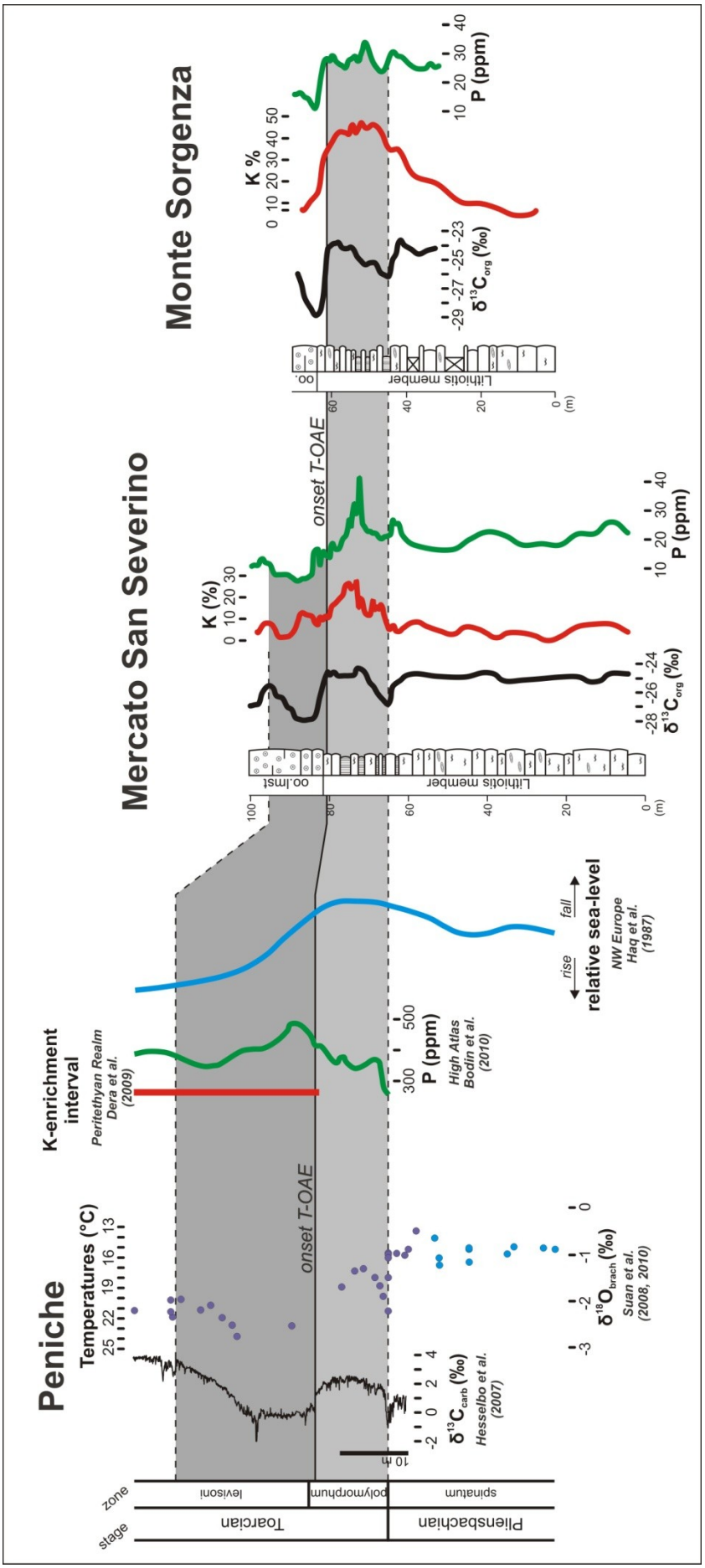
Monte Sorgenza
Mercato San Severino
Peniche
stage
zone
Pliensbachian
Toarcian
spinatum
polymorphum
levisoni
onset T-OAE
Lithiotis member
oo.lmst
oo.
(m)
K %
K (%)
P (ppm)
δ13Corg (‰)
δ13Ccarb (‰)
δ18Obrach (‰)
Temperatures (°C)
K-enrichment interval
Peritethyan Realm
Dera et al. (2009)
High Atlas
Bodin et al. (2010)
relative sea-level
NW Europe
Haq et al. (1987)
rise
fall
Hesselbo et al. (2007)
Suan et al. (2008, 2010)
10 h

**Figure 4 (previous page)** - A comparison of clay-minerals and phosphorus changes in the Apenninic carbonate platform with the record of P content in the Amellago section (High-Atlas, Morocco; Bodin et al., 2010) and of kaolinite abundance in the Peritethyan seas (Dera et al., 2009a). The sealevel curve is from Haq et al. (1987) seawater temperature is from Suan et al. (2008a; 2010).

The amount of P in the sediments is therefore mainly controlled by three factors: the rate of delivery from the continents, the degree of bottom-water oxygenation, and the sediment accumulation rate. By knowing the sediment accumulation rate it is possible to estimate the P accumulation rate (PAR). Changes through time of PAR in ancient marine sediments have been successfully used to constrain nutrient levels in past oceans (Föllmi, 1995, 1996; van de Schootbrugge et al., 2003; Bodin et al., 2006, 2010; Mort et al., 2007; Godet et al., 2010) and to investigate palaeoclimatic and palaeoceanographic processes regulating the P cycle.

### *4.5.5 Phosphorus concentration in the Late Pliensbachian-Early Toarcian of the Apenninic Carbonate Platform*

In order to convert the values of P concentration measured in our sections into meaningful P accumulation rates, a high-resolution age-model is requested. A chronostratigraphic calibration of our sections has been obtained through carbon isotope stratigraphy by chemostratigraphic correlation to the well-dated reference section of Peniche (chapter 3). We used four tie points of this correlation (namely the negative peak of the Pliensbachian-Toarcian CIE, the onset of the T-OAE negative CIE, the onset and the end of its positive wing), the cyclostratigraphic framework of Suan et al. (2008b) and the assumption of constant accumulation rate for each lithological interval, to estimate the PAR at Mercato San Severino (see additional material for further details). We obtained a range of values of 0.05-0.33 mg/cm$^2$/kyr (0.13 ± 0.05). The same procedure cannot be applied at Monte Sorgenza where the positive wing of the T-OAE CIE is truncated by a fault. No major differences are observed between the shape and trends of the PAR and P concentration curves (fig. 2). Therefore, also because of the overlying simplistic assumption of constant sediment accumulation rate, we decided to use the P concentration curves to discuss nutrient level changes in the ACP.

Total P concentration exhibits very low values in both studied sections. As riverine P from the continents, in particulate and dissolved forms, is rapidly consumed by primary producers in coastal areas and transferred to deep water or to the sedimentary record, P concentrations are near zero in most surface waters (Filippelli, 2008). Therefore is not surprising to find such low values in the sedimentary record of the ACP, which grew isolated from large continental blocks at least since the Early Jurassic (D'Argenio, 1974). Moreover, although we are aware that a comparison should be done between PAR values, we remark that similar low P concentrations have been recently reported for the healthy photozoan carbonate factory of the Late Barremian Lower Schrattenkalk member (around 8 ppm) and the Early Aptian Upper Schrattenkalk member (15 ppm) in the Helvetic Alps (Stein et al., 2011).

Total P concentration curves show broadly comparable trends in the two studied sections (fig. 2). The most significant features are the positive excursion in the uppermost part of the Lithiotis member (corresponding to the *polymorphum* ammonite zone) and the very low P concentrations measured in the last beds of the Lithiotis member and especially in the lowermost part of the "Oolitic limestones". The positive excursion has a sharp peak of 50 ppm at 72 m from the base in the Mercato San Severino section while it is flatter at Monte Sorgenza, where the maximum value is 34 ppm. Moreover, at Monte Sorgenza there is a sharp decrease in P concentrations (from 29 to 8 ppm), coinciding exactly with the T-OAE $\delta^{13}C$ negative shift, while at Mercato San Severino there is a more gradual decrease.

An increase in phosphorus concentrations, such as the one occurring in the uppermost part of the Lithiotis member, could be the result of reduced sedimentation rate. However, there is no sedimentological evidence of condensation in our sections and the positive excursion is present also in the PAR curves (fig. 2). Therefore, we can exclude that it is an artifact of changing sediment accumulation rates. Since there is no evidence of a change from dysoxic to oxic conditions, which would favor P accumulation, we conclude that the rise of concentration in the uppermost part of the Lithiotis member is due to enhanced delivery of P from adjacent emerged areas. The parallel increase in kaolinite abundance (fig. 2) suggests that both proxies are recording the same process, i.e. a phase of increased continental weathering in the *polymorphum* zone. This interpretation is further supported by the record of the Amellago section in the High Atlas (Morocco) (fig. 4), roughly at the same latitude of the southern Apennines (fig. 3), which shows a rapid increase in P content associated with the Pliensbachian-Toarcian boundary event (Bodin et al., 2010). The second marked increase in the P content which at Amellago is associated with the T-OAE $\delta^{13}C$ negative shift (Bodin et al., 2010) is not observed in the southern Apennines, which exhibits in the same time interval a more or less sharp decrease in P concentration. One possible explanation is that local processes bias this specific interval of the P curve in the ACP sections. For instance, the very low P concentration in the "Oolitic Limestones" could be controlled by the removal of fine-grained matrix, seemingly bearing most of the P, under high energy. However there are at least three elements that falsify this hypothesis: 1) our dataset show no systematic co-variation between texture and P content (table 1) at Mercato San Severino a gradual decrease in P concentration starts already in the Lithiotis member, where some samples have P concentrations as low as those measured at the base of the "Oolitic limestones" (fig. 2; 3) a significant increase of P concentration is observed within the "Oolitic Limestones", in the uppermost part of the studied sections (fig. 2).

| **Mercato S.S.** | **n** | **Range (ppm)** | **Average (ppm)** | **st. dev.(ppm)** |
|---|---|---|---|---|
| *m/w* | 25 | 8–50 | 23 | 9 |
| *p/g* | 10 | 12–26 | 19 | 5 |
| *Lithiotis f/r/b* | 15 | 8–37 | 23 | 6 |
| *Oolitic g* | 22 | 6–28 | 10 | 4 |
| **Mt Sorgenza** | | | | |
| *m/w* | 18 | 22–34 | 29 | 4 |
| *p/g* | 15 | 8–31 | 25 | 5 |
| *Lithiotis f/r/b* | 2 | 28–28 | | |
| *Oolitic g* | 8 | 11–25 | 16 | 4 |

**Table 1 -** Phosphorus content.

Another possibility is that most, if not all, of the T-OAE positive excursion of total P concentration recorded at Amellago (Bodin et al., 2010) is lost in a gap at the boundary between the Lithiotis member and the "Oolitic limestones", whose presence in our sections is supported by the lack of the distinctive steps in the negative wing of the CIE and by a less extended plateau of depleted $\delta^{13}C$ values (chapter 3).

### *4.5.6 Climate, sea-level, nutrients and carbonate platform evolution*

According to Suan et al. (2008a, 2010) the main cause of Early Toarcian palaeoenvironmental perturbations was a twofold increase in nutrient levels associated with two pulses of temperature rise, seemingly triggered by volcanogenic $CO_2$. The first phase is associated with the Pliensbachian-Toarcian boundary CIE. Increased nutrient

levels have been first invoked on the basis of a decrease in the abundance and size of *Schizosphaerella* in hemipelagic successions of Portugal, Italy and Switzerland (Picotti and Cobianchi, 1996; Erba, 2004; Suan et al., 2008a). Increased continental weathering and runoff, forced by a change from semiarid to humid climate, are documented in the High Atlas by a rapid increase of P content in hemipelagic successions (Bodin et al., 2010) and by an increased input of terrigenous material in proximal areas (Wilmsen and Neuweiler, 2008). Increased nutrient levels have been invoked as the main cause of carbonate platform drowning close to the Pliensbachian-Toarcian boundary in the High Atlas (Blomeier and Reijmer, 1999; Wilmsen and Neuweiler, 2008; Bodin et al., 2010), with regional tectonics and sea-level changes playing perhaps an equally important role (Lachkar et al., 2009; Merino-Tomé et al., 2011). This phase of carbonate platform drowning has been recorded also in other Tethyan localities (Bassoullet and Baudin, 1994, Cobianchi and Picotti, 2001). The increase in kaolinite abundance and P concentration, documented in this paper, witnesses that the signal of increased weathering and enhanced nutrient level is also recorded in the Apenninic Carbonate Platform of southern Italy. However, this platform was able to continue growing in shallow water.

Carbonate platforms, and especially those dominated by photozoan carbonate factories, should be particularly vulnerable to increased nutrient levels, since they are adapted to oligotrophic conditions (Hallock and Schlager, 1986; Mutti and Hallock, 2003). Vecsei (2003) proposed a sea-water $PO_4^{3-}$ concentration of 30 ppm as a threshold for oligotrophic conditions in the present oceans. As the composition of the carbonate factory of the ACP, and seemingly its growth potential, were not significantly affected by the increase in nutrient levels, we suppose that the "phosphorus threshold" was not reached. In fact, the large bivalves of the Lithiotis group and the green calcareous alga *P. mediterraneus* are still the dominant carbonate producers also in the interval characterized by the highest P concentration and by the highest relative abundance of kaolinite.

The reduction in thickness and frequency of Lithiotis biostromes and the shift from grainy to mud-dominated facies, could be simply the result of a regressive trend (chapter 3).

A widespread episode of carbonate platform drowning is commonly associated with the Early Toarcian paleoenvironmental perturbations (Bassoullet and Baudin, 1994) but there is ample evidence that many Tethyan carbonate platforms drowned well before the onset of the T-OAE. Increased nutrient levels have been invoked as the main cause of carbonate platform drowning close to the Pliensbachian-Toarcian boundary in the High Atlas (Blomeier and Reijmer, 1999; Wilmsen and Neuweiler, 2008; Bodin et al., 2010). Regional tectonics and sea-level changes probably played an important role (Lachkar et al., 2009; Merino-Tomé et al., 2011). Eodiagenetic ferroan calcite cements below hardground surfaces in carbonate platform successions from Southern Provence sub-Basin (France) have been recently interpreted as episodic eutrophication events at the Pliensbachian-Toarcian transition (Léonide et al., 2011). Final drowning of the carbonate platform occurred before the onset of T-OAE, due to a combination of palaeonvironmental deterioration, sea-level change and block faulting (Léonide et al., 2007, 2011).

Further evidences of enhanced nutrient levels come from the Trento Carbonate Platform (TCP) of the Southern Alps, which continued growing in shallow water during the Toarcian. The western sectors of the TCP (the Venetian carbonate platform of Cobianchi and Picotti, 2001), show a progressive shift from a photozoan to an heterozoan carbonate factory across the Pliensbachian-Toarcian boundary, followed by a shift to a prevalently non-skeletal carbonate factory in the Early Bajocian and eventually by drowning in the Aalenian. A gradual increase of trophic resources, forced by the interplay of climate and sea-level changes, is proposed as the main cause of these shifts (Cobianchi and Picotti, 2001). The appearance of spiculitic cherts close to the Pliensbachian-Toarcian

boundary has been interpreted as a sign of increased nutrient levels by Woodfine et al., (2008). A shift to clay-rich cherty facies, at the level of the T-OAE negative CIE, indicates a relative deepening under stressful eutrophic conditions, with rising seawater temperature possibly playing an additional role (Woodfine et al., 2008). In spite of this deepening event, the western sector of the TCP survived the T-OAE to be eventually drowned in the Aalenian.

The Early Jurassic evolution of the Trento platform was clearly controlled by tectonics (Winterer and Bosellini, 1981; Santantonio and Carminati, 2011). Block faulting and consequent rapid subsidence have been generally assumed to be predominant factors in the disintegration and drowning episodes of Jurassic Tethyan carbonate platform (Bernoulli and Jenkyns, 1974). Woodfine et al. (2008) suggested that the lower subsidence rate (half of that estimated for the Trento Carbonate Platform), may have saved the ACP from drowning.

The importance of the subsidence rate as a key variable, in addition to climatic and environmental changes, in controlling the fate of carbonate platforms is more evident by comparing the evolution of the ACP to the other Italian carbonate platforms that grew during the Early Jurassic at about the same latitude (i.e. in the same climatic belt) and in the same palegeographic conditions (i.e. isolated from large continental blocks). The Panormide Carbonate Platform (Sicily, Italy), separated from the ACP by a deep basin, shows evidence of rapid subsidence from the Early to the Late Pliensbachian, drowning definitely well before the Pliensbachian-Toarcian boundary (Marino and Santantonio, 2010 and references therein).

The Calcare Massiccio Formation of central Italy shows that close to the Hettangian-Sinemurian boundary continued extension fragmented this sector of the wide carbonate platform, leading to the formation of intrabasinal highs bounded by steep marine escarpments. In the early Pliensbachian (middle Carixian, *ibex* zone), benthic carbonate production ceased also on all intrabasinal highs (Santantonio and Carminati, 2011 and references therein).

More to the south, in the Campanian-Lucanian sector of the ACP, shallow intra-platform basins formed during the Late Triassic as a result of extensional tectonics and persisted during the Jurassic. However, all these small basins were eventually filled by the progradation of platform margin facies during the Middle Jurassic (Iannace and Zamparelli, 2002; Iannace et al., 2005). In agreement with Woodfine et al. (2008), we believe that the different fate of the southern Apennine sector of the ACP is more easily explained in terms of lower subsidence rates than of different palaeoenvironmental conditions.

### *4.6 Conclusions*

Clay-minerals and P content of the Apenninic Carbonate Platform record increased weathering across the Pliensbachian-Toarcian boundary. Many carbonate platforms of the Peri-Tethyan domain responded to the shift of nutrient levels, associated with increased weathering and runoff, by either drowning or shifting to heterotrophic carbonate production. The ACP continued growing in shallow water with no significant shift in the composition of the carbonate factory. This is probably due to the fact that the ACP grew isolated from major continental blocks and distant from the Early Jurassic upwelling zones. For these reasons nutrient levels did apparently not cross the threshold of ecological tolerance of the main carbonate producing biota.

Moreover, the Apenninic Carbonate Platform was situated further from the Jurassic rifting axis than other carbonate platforms, which were progressively drowned during the

Early Jurassic. Lower subsidence rate was most probably a significant factor explaining the resilience of the ACP to Early Toarcian palaeoenvironmental perturbations.

Across the early Toarcian OAE, clay-minerals and P content show no evidence of enhanced weathering in the ACP. Therefore, enhanced nutrient levels were probably not the cause of the demise of the Lithiotis/Palaeodasycladus carbonate factory. Massive biocalcifiers were wiped out by shallow water ocean acidification caused by the massive release of $CO_2$ at the onset of the early Toarcian CIE, with the shift to the chemical carbonate factory of the "Oolitic limestones" witnessing the ensuing overshoot of seawater carbonate saturation (chapter 3).

## *4.7 References*


Adatte, T. and Rumley G. (1989). Sedimentology and mineralogy of the Valanginian and Hauterivian in the stratotypic region (Jura mountains, Switzerland). In: Wiedmann, J. (Ed.), Cretaceous of the Western Tethys: proceedings of the 3rd International Cretaceous Symposium, Tübingen 1987. E. Schweizerbart'sche Verlagsbuchhandlung, Stuttgart, pp. 329–351.

Adatte T., Stinnesbeck W. and Keller, G. (1996). Lithostratigraphic and mineralogic correlations of near K/T boundary sediments in northeastern Mexico: Implications for origin and nature of deposition. In: Ryder, G., Fastovsky, D., Gartner, S. (Eds.), The Cretaceous-Tertiary Event and Other Catastrophes in Earth History. Geological Society of America Special Paper 307, 211–226.

Aldega L., Corrado S., Giampaolo C. and Mazzoli, S. (2003). Studio della mineralogia delle argille per la ricostruzione dei carichi tettonico/sedimentari: esempi dalle Unità Lagonegresi e Liguridi della Lucania sud-occidentale (Appennino Meridionale). Bollettino della Società Geologica Italiana 122, 203–216.

Al-Suwaidi A.H., Angelozzi G.N., Baudin F., Damborenea S.E., Hesselbo S.P., Jenkyns H.C., Manceñido M.O. and Riccardi A.C. (2010). First record of the Early Toarcian Oceanic Anoxic Event from the Southern Hemisphere, Neuquén Basin, Argentina. Journal of the Geol. Society 176, 633–636.

Bailey T.R., Rosenthal Y., McArthur J.M., van de Schootbrugge B. and Thirlwall M.F. (2003). Paleoceanographic changes of the Late Pliensbachian–Early Toarcian interval: a possible link to the genesis of an Oceanic Anoxic Event. Earth and Planetary Science Letters 212, 307–320.

Barattolo F. and Romano R. (2005). Shallow carbonate platform bioevents during the Upper Triassic-Lower Jurassic: an evolutive interpretation. Boll. Soc. Geol. It. 124, 123–142.

Bassoullet, J.P. (1997) Algues dasycladales. Distribution des principales espèces. In: Biostratigraphie du Jurassique ouest-Européen et Méditerranéen (Coord. E. Cariou and P. Hantzpergue), Mém. Centres Rech. Explo.-Prod. Elf Aquitaine, 17, 339–341.

Bassoullet J.P. and Baudin F. (1994). Le Toarcien inférieur: une période de crise dans les bassins et sur les plates-formes carbonatées de l'Europe du Nord-Ouest et de la Téthys. Geobios, M.S. 17, 645–654.

Bassoullet J.-P., Elmi S., Poisson A., Cecca F., Belion Y., Guiraud R. and Baudin F. (1993). Mid Toarcian, in Atlas Tethys Paleoenvironmental Maps, edited by J. Dercourt et al., pp. 63 – 80, Becip-Franlab, Rueil-Malmaison, France.

Bernoulli D. and Jenkyns H. (1974). Alpine, Mediterranean, and Central Atlantic Mesozoic facies in relation to the early evolution of the Tethys. In: Dott, R. H., Shaves, R. H. (Eds.), Modern and Ancient Geosynclinal Sedimentation, SEPM Spec. Publ. 19, 129–157.

Blomeier D.P.G. and Reijmer J.J.G. (1999). Drowning of a Lower Jurassic Carbonate Platform: Jbel Bou Dahar, High Atlas, Morocco. Facies 41, 81–110.

Bodin S., Godet A., Föllmi K.B., Vermeulen J., Arnaud H., Strasser A., Fiet N. and Adatte T. (2006). The Late Hauterivian Faraoni oceanic anoxic event in the western Tethys: evidence from phosphorus burial rates. Palaeogeography, Palaeoclimatology, Palaeoecology 235, 245–264.

Bodin S., Mattioli E., Fröhlich S., Marshall J.D., Boutib L., Lahsini S. and Redfern J. (2010). Toarcian carbon isotope shifts and nutrient changes from the Northern margin of Gondwana /High Atlas, Marocco, Jurassic): Palaeoenvironmental implications. Palaeogeography, Palaeoclimatology, Palaeoecology 297, 377–390.

Bolle M.-P., Adatte T., Mangold C. and Remane J. (1996). Microfaciès, minéralogie, stratigraphie du Dogger de la région du Furcil (NE). Bulletin de la Sociéte neuchâteloise des Sciences Naturelles 119, 123–144.

Bonardi G., D'Argenio B. and Perrone V. (1988). Carta Geologica dell'Appennino meridionale, SELCA, Firenze.

Burtner R.L. and Warner M.A. (1986). Relationship between illite/smectite diagenesis and hydrocarbon generation in Lower Cretaceous Mowry and Skull Creek Shales of the northern Rocky Mountain area. Clays and Clay-minerals 34, 390–402.

Butler R.W.H., Mazzoli S., Corrado S., De Donatis M., Di Bucci D., Gambini R., Naso G., Nicolai C., Scrocca D., Shiner P. and Zucconi V. (2004). Applying thickskinned tectonic models to the Apennine thrust belt of Italy; limitations and implications. In: McClay K.R. et al. (ed.) Thrust Tectonics and Hydrocarbon Systems. American Association of Petroleum Geologists, Memoirs, 82, 647–667.

Carannante G., Graziano R., Ruberti D. and Simone L. (1997). Upper Cretaceous temperate-type open shelves from northern (Sardinia) and southern (Apennines-Apulia) Mesozoic Tethyan margins, in: James, N.P. and Clarke, J. (Eds.): Cool-water carbonates,SEPM Spec. P. 56, 309–325.

Cecca F. and Macchioni F. (2004). The two Early Toarcian (Early Jurassic) extinction events in ammonoids. Lethaia 37, 35–56.

Chamley H. (1989). Clay Sedimentology. Springer Verlag, Berlin.

Chiocchini M., Farinacci A., Mancinelli A., Molinari V. and Potetti M. (1994). Biostratigrafia a foraminiferi dasicladali e calpionelle delle successioni carbonatiche mesozoiche dell'Appennino centrale (Italia). In: Mancinelli A. (ed) Biostratigrafia dell'Italia centrale. Studi Geologici Camerti, Volume Speciale, 1994, 9–129..

Cobianchi M. and Picotti, V. (2001). Sedimentary and biological response to sea-level and palaeoceanographic changes of a Lower–Middle Jurassic Tethyan platform margin (Southern Alps, Italy). Palaeogeography, Palaeoclimatology, Palaeoecology 169, 219–244.

Colacicchi R. (1967). Geologia della Marigica orientale. Geol. Romana 6, 189–316.

Colacicchi R. (1987). Sedimentation on a carbonate platform as controlled by sea level changes and tectonic movement. Mem. Soc. Geol. Ital. 40, 199–208.

Colman A.S. and Holland H.D. (2000). The global diagenetic flux of phosphorus from marine sediments to the oceans; redox sensitivity and the control of atmospheric oxygen levels. In: Glenn, C.R., Prévôt-Lucas, L., Lucas, J. (Eds.), Marine Authigenesis; From Global to Microbial, SEPM Special Publication, vol. 66, pp. 53–75.

Cohen A.S., Coe A.L., Harding S.M. and Schwark, L. (2004). Osmium isotope evidence for the regulation of atmospheric $CO_2$ by continental weathering. Geology 32, 157–160.

Compton J., Mallinson D., Glenn C.R., Filippelli G.M., Föllmi K.B., Shields G., and Zanin Y. (2000). Variations in the global phosphorus cycle. In: Glenn, C.R., Prévôt-Lucas, L., Lucas, J. (Eds.), Marine Authigenesis; From Global to Microbial, SEPM Special Publication, vol. 66, pp. 21–33.

Corrado S., Aldega L., Di Leo P., Giampaolo C., Invernizzi C., Mazzoli S. and Zattin M. (2005). Thermal maturity of the axial zone of the southern Apennines fold-and-thrust-belt (Italy) from multiple organic and inorganic indicators. Terra Nova 17, 56–65.

D'Argenio B. and Sgrosso I. (1974) - Le piattaforme carbonatiche sudappenniniche. In: Istituto di Geologia e Geofisica dell'Università di Napoli, Pubblicazione, n.s., 51.

D'Argenio B., De Castro P., Emiliani C. and Simone L. (1975). Bahamian and Apenninic limestones of identical lithofacies and age, AAPG Bull. 59, 524–533.

De Castro P. (1991). Mesozoic in : Barattolo F., De Castro P. and Parente M. (eds) 5th International Symposium on Fossil Algae. Field Trip Guide-Book. Giannani, Napoli, 21–38.

Deconinck J.-F. and Bernoulli D. (1991). Clay-mineral assemblages of Mesozoic pelagic and flysch sediments of the Lombardian Basin (Southern Alps): implications for palaeotectonics, palaeoclimate and diagenesis. Geol. Rundsch. 80, 1–17.

Deconinck J.F., Strasser A. and Debrant P. (1988). Formation of illitic minerals at surface temperatures in Purbeckian sediments (Lower Berriasian, Swiss and French Jura). Clay-minerals 23, 91–103.

Dera G., Pellenard P., Neige P., Deconinck J.-F., Pucéat E. and Dommergues J.-L. (2009a). Distribution of clay-minerals in Early Jurassic Peritethyan seas: palaeoclimatic significance inferred from multiproxy comparisons. Palaeogeography, Palaeoclimatology, Palaeoecology 271, 39–51.

Dera G., Pucéat E., Pellenard P., Neige P., Delsate D., Joachimski M.M., Reisberg L. and Martinez M. (2009b). Water mass exchange and variations in seawater temperature in the NW Tethys during the Early Jurassic: evidence from neodymium and oxygen isotopes of fish teeth and belemnites. Earth and Planetary Science Letters 286, 198–207.

Dera G., Neige P., Dommergues J.-L., Fara E., Laffont R. and Pellenard P. (2010). High resolution dynamics of Early Jurassic marine extinctions: the case of Pliensbachian-Toarcian ammonites (Cephalopoda). Journal of Geological Society of London 167, 21–33.

Dera G., Brigaud B., Monna F., Laffont R., Pucéat E., Deconinck J-.F., Pellenard P., Joachimski M.M. and Durlet C. (2011). Climatic ups and downs in a disturbed Jurassic world. Geology v.39 no.3, 215-218.

Dewey J.F., Helman M.L., Turco E., Hutton D.H.W., and Knott S.D. (1989). Kinematics of the western Mediterranean. In M. P. Coward, D. Dietrich & Park R.G. (Eds.), Alpine Tectonics, 45, 265–283. Special Publication,Geological Society of London.

De Zigno A. (1868). Descrizione di alcune Cicadacee fossili rinvenute nell'oolite delle Alpi Venete. Atti R. Ist. Ven. Sc. Lett. Arti, s.3, vol. 13, pp. 1213-1227, 1 pl., Venezia.
Durn G. (2003). Terra rossa in the Mediterranean region: parent materials, composition and origin. Geologia Croatica 56/1, 83-100.
Durn G., Ottner F. and Slovenec D. (1999). Mineralogical and geochimical indicators of the polygenetic nature of terra rossa in Istria, Croazia. Geoderma 91, 125-150.
Eaton A.D., Clesceri L.S. and Greenberg A.E. (1995). Standard methods for the examination of water and wastewater, 19th edition. American Public Health Association, New York.
Emeis K.-C., Struck U., Leipe T., Pollehne F., Kunzendorf H. and Christiansen C. (2000). Changes in the C, N, P burial rates in some Baltic Sea sediments over the last 150 years – relevance to P regeneration rates and the phosphorus cycle. Marine Geology 167, 43–59.
Erba E. (2004). Calcareous nannofossils and Mesozoic oceanic anoxic events. Mar. Micropaleontol. 52, 85–106.
Filippelli G.M. (2008). The Global Phosphorus Cycle: Past, Present, and Future. Elements 4, 89–95.
Föllmi K.B. (1995). 160 m.y. record of marine sedimentary phosphorus burial: coupling of climate and continental weathering under greenhouse and icehouse conditions. Geology 23, 859–862.
Föllmi, K.B., 1996. The phosphorus cycle, phosphogenesis and marine phosphate-rich deposits. Earth-Science Reviews 40, 55–124.
Frijia G., Parente M. and Iannace A. (2005). Thermal maturity of the Southern Apenninic Platform Unit (southern Italy): Constraints from rock-eval pyrolysis Tmax data. Atti Ticinensi di Scienze della Terra, S.S. 10, 95–98.
Gibbs R. J. (1977). Clay-mineral segregation in the marine environment. Journal of Sedimentary Petrology 47, 237–243.
Godet A., Bodin S., Adatte T. and Föllmi K.B. (2008). Platform-induced clay-mineral fractionation along a northern Tethyan basin-platform transect: implications for the interpretation of Early Cretaceous climate change (Late Hauterivian-Early Aptian). Cretaceous Res. 29, 830–847.
Godet A., Föllmi K.B., Bodin S., de Kaenel E., Matera V. and Adatte T. (2010). Stratigraphic, sedimentological and palaeoenvironmental constraints on the rise of the Urgonian platform in the western Swiss Jura. Sedimentology 57, 1088–1125.
Gómez J.J., Goy A. and Canales M.L. (2008). Seawater temperature and carbon isotope variations in belemnites linked to mass extinction during the Toarcian (Early Jurassic) in Central and Northern Spain. Comparison with other European sections. Palaeogeography, Palaeoclimatology, Palaeoecololy 258, 28–58.
Gröcke, D.R., Hori R.S., Trabucho-Alexandre J., Kemp D.B. and Schwark (2011). Solid Earth Discussions, v. 3, issue 1, 385–410.
Hallam A. (1984). Continental humid and arid zones during the Jurassic and Cretaceous. Palaeogeography, Palaeoclimatology, Palaeoecology 47, 195–223.
Hallam A. (2001). A review of the broad pattern of Jurassic sealevel changes and their possible causes in the light of current knowledge. Palaeogeogr. Palaeoclimatol. Palaeoecol. 167, 23–37.
Hallock P. and Schlager W. (1986). Nutrient excess and the demise of coral reefs and carbonate platforms. Palaios 1, 389–398.
Haq B.U., Hardenbol J. and Vail P.R. (1987). Chronology of fluctuating sea levels since the Triassic. Science 235, 1156–1167.
Harries P.J. and Little C.T.S. (1999). The early Toarcian (Early Jurassic) and the Cenomanian–Turonian (Late Cretaceous) mass extinctions: similarities and contrasts. Palaeogeography, Palaeoclimatology, Palaeoecology 154, 39–66.
Hesselbo S.P., Gröcke D.R., Jenkyns H.C., Bjerrun C.J., Farrimond P., Morgans Bell H.S. and Green O.R. (2000). Massive dissociation of gas hydrate during a Jurassic oceanic anoxic event. Nature 406, 392–395.
Hesselbo S.P., Jenkyns H.C., Duarte L.V. and Oliveira L.C.V. (2007). Carbon-isotope record of the Early Jurassic (Toarcian) Oceanic Anoxic Event from fossil wood and marine carbonate (Lusitanian Basin, Portugal). Earth Planet. Sci. Lett. 253, 455–470.
Hillier S. (1993). Origin, diagenesis, and mineralogy of chlorite minerals in Devonian lacustrine mudrocks, Orcadian Basin, Scotland. Clays and Clay-minerals 41, 240–259.
Hower J., Eslinger E.V., Hower M.E. and Perry E.A. (1976). The mechanism of burial metamorphism of argillaceous sediment: 1. Mineralogical and chemical evidence Geol. Soc. Amer. Bull. 87, 725–737.
Hutcheon I., Oldershaw A. and Ghent D. (1980). Diagenesis of Cretaceous sandstones of the Kootenay Formation at Elk Valley (southeastern British Columbia) and Mt. Allan (southwestern Alberta). Geochimica et Cosmochimica Acta 44, 1425–1435.
Hurst A. and Irwin H. (1982). Geological modelling of clay diagenesis in sandstone. Clay-minerals 17, 5–22.

Iannace A. and Zamparelli V. (2002). Upper Triassic platform margin biofacies and the paleogeography of Southern Apennines. Palaeogeogr., Palaeoclimat., Palaeoecol. 179, 1–18.
Iannace A., Parente M. and Zamparelli V. (2005). The Upper Triassic platform margin facies of Southern Apennines and their Jurassic fate: state of the art. Boll. Soc.Geol. It. 124, 203–214.
Ingall E.D. and Jahnke R. (1994). Evidence for enhanced phosphorus regeneration from marine sediments overlain by oxygen depleted waters. Geochimica et Cosmochimica Acta 58 (11), 2571–2575.
Ingall E.D. and Jahnke R. (1997). Influence of water-column anoxia on the elemental fractionation of carbon and phosphorus during sediment diagenesis. Marine Geology 139, 219– 229.
Jenkyns H.C. (1988). The Early Toarcian (Jurassic) Anoxic Event: stratigraphy, sedimentary, and geochemical evidence. American Journal of Science 288, 101–151.
Jenkyns H.C. (2003). Evidence for rapid climate change in the Mesozoic-Palaeogene greenhouse world. Philos. Trans. Royal Soc., Ser. A 361, 1885–1916.
Jenkyns H.C. and Clayton C.J. (1997). Lower Jurassic epicontinental carbonates and mudstones from England and Wales: chemostratigraphic signals and the early Toarcian anoxic event. Sedimentology 44, 687–706.
Jiménez-Berrocoso A., Zuluaga M. C. and Elorza J. (2008). Diagenesis, palaeoclimate and tectono-sedimentary influences on clay-mineralogy and stable isopotes from Upper Cretaceous marine successions of the Basque-Cantabrian Basin (N Spain). Cretaceus Research 29, 386–404.
Kemp D.B., Coe A.L., Cohen A.S. and Schwark L. (2005). Astronomical pacing of methane release in the Early Jurassic period. Nature 437, 396–400.
Kübler B. (1987). Cristallinité de l'illite: méthodes normalisées de préparation, méthode normalisée de mesure, méthode automatique normalisée de mesure. Cahiers de l'Institut de Géologie, Université de Neuchâtel, Suisse Série ADX n° 2.
Küspert W. (1982). In: Einsele, S., Seilacher, A. (Eds.), Environmental change during oil shale deposition as deduced from stable isotope ratios.: Cyclic and event stratification. Springer-Verlag, Berlin, pp. 482–501.
Lachkar N., Guiraud M., El Harfi A., Dommergues J.-L., Dera G. and Durlet C. (2009). Early Jurassic normal faulting in a carbonate extensional basin: characterization of tectonically driven platform drowning (High Atlas rift, Morocco). J. Geol. Soc. London 166, 413–430.
Lanson B., Beaufort D., Berger G., Baradat J. and Lacharpagne J.C. (1996). Illitization of diagenetic kaolinite-to-dickite conversion series: late-stage diagenesis of the Lower Permian Rotliegend sandstone Reservoir, offshore of the Netherlands. Journal of Sedimentary Research 66, 501–518.
Lanson B., Beaufort D., Berger G., Bauer A., Cassagnabère A. and Meunier A. (2002). Authigenic kaolin and illitic minerals during burial diagenesis of sandstones: a review. Clay Miner. 37, 1–22.
Léonide, P. et al. Drowning of a carbonate platform as a precursor stage of the Early Toarcian global anoxic event (Southern Provence sub-Basin, South-east France). Sedimentology (2011) doi:10.1111/j.1365-3091.2010.01221.x
Léonide P., Floquet M., Durlet C., Baudin F. Pittet B. and Lécuyer C. (2011). Drowning of a carbonate platform as a precursor stage of the Early Toarcian global anoxic event (Southern Provence sub-Basin, South-east France). Sedimentology, doi: 10.1111/j.1365-3091.2010.01221.x.
Little C.T.S. and Benton M.J. (1995). Early Jurassic mass extiction: a global long-term event. Geology 23, 495–498.
Littler K., Hesselbo S.P. and Jenkyns H.C. (2010). A carbon-isotope perturbation at the Pliensbachian-Toarcian boundary: evidence from the Lias Group, NE England. Geological Magazine 147, 181–192.
Mailliot S., Mattioli E., Bartolini A., Baudin F., Pittet B. and Guex J. (2009). Late Pliensbachian–Early Toarcian (Early Jurassic) environmental changes in an epicontinental basin of NW Europe (Causses area, central France): a micropaleontological and geochemical approach. Palaeogeography, Palaeoclimatology, Palaeoecology 273, 346–364.
Marino M. and Santantonio M. (2010). Understanding the geological record of carbonate platform drowning across rifted Tethyan margins: Examples from Lower Jurassic of the Apennines and Sicily (Italy). Sedimentary Geology 225, 116–137.
Mazzoli S. and Helman M. (1994). Neogene patterns of relative plate motion for Africa-Europe: some implications for recent central Mediterranean tectonics. GeologischeRundschau, 83, 464–468.
Mazzoli S., D'Errico M., Aldega L., Corrado S., Invernizzi C., Shiner P. and Zattin M. (2008). Tectonic burial and "young" (<10 Ma) exhumation in the southern Apennines fold-and-thrust belt (Italy). Geology 36, 243–246.
McArthur J.M., Donovan D.T., Thirlwall M.F., Fouke B.W. and Mattey D. (2000). Strontium isotope profile of the early Toarcian (Jurassic) oceanic anoxic event, the duration of ammonite biozones, and belemnite palaeotemperatures. Earth and Planetary Science Letters 179, 269–285.
McArthur J.M., Cohen A.S., Coe A.L., Kemp D.B., Bailey R.J. and Smith D.G. (2008). Discussion on the Late Palaeocene–Early Eocene and Toarcian (Early Jurassic) carbon isotope excursions: a comparison

of their time scales, associated environmental changes, causes and consequences. Journal, Vol. 164, 2007, 1093–1108. Journal of the Geological Society of London 165, 875–880.
McElwain J.C., Wade-Murphy J. and Hesselbo S.P. (2005). Changes in carbon dioxide during an oceanic anoxic event linked to intrusion into Gondwana coals. Nature 435, 479–482.
Menardi Noguera A. and Rea G. (2000). Deep structure of the Campanian-Lucanian Arc (southern Apennines). Tectonophysics 324, 239–265.
Merino E. and Banerjee A. (2008). Terra rossa genesis, implication for karst, and eolian dust: a geodynamic thread. The Journal of Geology 116, 62–75. The University of Chicago.
Merino-Tomé Ò., Della Porta G., Kenter J.A.M., Verwers K., Harris P.M., Adams E.W., Playton T. and Corrochano D. (2011). Sequence development in an isolated carbonate platform (Lower Jurassic, Djebel Bou Dahar, High Atlas, Marocco): influence of tectonics, eustacy and carbonate production. Sedimentology, doi: 10.1111/j.1365-3091.2011.01232.x.
Monaco P., Nocchi M., Ortega-Huertas M., Palomo I., Martinez F. and Chiavini G. (1994). Depositional trends in the Valdorbia Section (Central Italy) during the Early Jurassic, as revealed by micropaleontology, sedimentology and geochemistry. Eclogae geol. Helv. 87, 157–223.
Morard A., Guex J., Bartolini A., Morettini E. and De Wever P. (2003). A new scenario for the Domerian–Toarcian transition. Bulletin de la Société Géologique de France 174,351–356.
Moresi M. and Mongelli G. (1988). The relation between the terra rossa and the carbonate-free residue of the underlying limestones and dolostones in Apulia, Italy. Clay-minerals 23, 439–446.
Mort H.P., Adatte T., Föllmi K.B., Keller G., Steinmann P., Matera V., Berner Z. and Stüben D. (2007). Phosphorus and the roles of productivity and nutrient recycling during oceanic anoxic event 2. Geology 35, 483–486.
Muhs D.R., Budahn J., Prospero J. M. and Carey S.N. (2007). Geochemical evidence for African dust inputs to soils of western Atlantic islands: Barbados, the Bahamas and Florida. J. Geophys. Res. 112:F02009, doi:10.1029/2005JF000445.
Mutti M. and Hallock P. (2003). Carbonate systems along nutrient and temperature gradients: some sedimentological and geochemical constraints. International Journal of Earth Sciences (Geologische Rundschau) 92, 465–475.
Ortega-Huertas M., Monaco P. and Palomo I. (1993). First data on clay-mineral assemblages and geochemical characteristics of Toarcian sedimentation in the Umbria–Marche Basin (Central Italy). Clay Miner. 28, 297–310.
Philippe M. and Thévenard F. (1996). Distribution and palaeoecology of the Mesozoic wood genus Xenoxylon: palaeoclimatological implication for the Jurassic of Western Europe. Rev. Palaeobot. Palynology 91, 353–370.
Picotti V. and Cobianchi M. (1996). Jurassic periplatform sequences of the eastern Lombardian Basin (Southern Alps). The deep-sea record of the tectonic evolution, growth and demise history of a carbonate platform. Memorie di Scienze Geologiche 48, 171–219.
Praturlon A. (1968). Cycadophyta and Coniferophyta from the Lias of M. Palombo (Marsica, Central Apennines). Geol. Romana 7, 1–26.
Prospero J. M., Olmez, I., and Ames M. (2001). Al and Fe in PM 2.5 and PM 10 suspended particles in south-central Florida: impact of long-range transport of African mineral dust. Water Air Soil Pollut. 125, 291–317.
Röhl H.-J., Schmid-Röhl A., Oschmann W., Frimmel A. and Schwark L. (2001). The Posidonia Shale (Lower Toarcian) of SW-Germany: an oxygen-depleted ecosystem controlled by sea level and palaeoclimate. Palaeogeography, Palaeoclimatology, Palaeoecology 165, 27–52.
Rosales I., Quesada S. and Robles S. (2004). Paleotemperature variations of Early Jurassic seawater recorded in geochemical trends of belemnites from the Basque–Cantabrian Basin, northern Spain. Palaeogeography, Palaeoclimatology, Palaeoecology 203, 253–275.
Rosenbaum G., Lister G.S. and Duboz. (2002). Relative motions of Africa, Iberia and Europe during Alpine orogeny: Tectonophysics 359, 117–129.
Ruffell A., McKinley J.M. and Worden R.H. (2002). Comparison of clay-mineral stratigraphy to other proxy palaeoclimate indicators in the Mesozoic of NW Europe. Phil. T. Roy. Soc. A 360, 675–693.
Santantonio M. and Carminati E. (2011). Jurassic rifting evolution of the Apennines and Southern Alps (Italy): Parallels and differences. GSA Bulletin 123, no. 3-4, 468–484. doi: 10.1130/B30104.1.
Sandler A. and Harlavan Y. (2006). Early diagenetic illitization of illite-smectite in Cretaceous sediments (Israel): evidence from K-Ar dating. Clay-minerals 41, 637–658.
Selli R. (1957). Sulla trasgressione del Miocene nell'Italia meridionale. Giornale di Geologia 2, 1–54.
Selli R. (1962). Il Paleogene nel quadro della geologia dell'Italia meridionale. Mem. Soc. Geol. Ital. 3, 737–789.
Singer A. (1984). The paleoclimatic interpretation of clay-minerals in sediments—a review. Earth-Sci. Rev. 21, 251–293.

Singer A. (1988). Illite in aridic soils, desert dusts and desert loess. Sediment. Geol. 59, 251–259.
Stein M., Arnaud-Vanneau A., Adatte T., Freitmann D., Spangenberg J.E. and Föllmi K.B. (2011). Palaeoenvironmental and palaeoecological change on the northern Tethyan carbonate platform during the Late Barremian to earliest Aptian. Sedimentology, doi: 10.1111/j.1365-3091.2011.01286.x.
Suan G., Mattioli E., Pittet B., Mailliot S. and Lécuyer C. (2008a). Evidence for major environmental perturbation prior to and during the Toarcian (Early Jurassic) oceanic anoxic event from the Lusitanian Basin. Paleoceanography 23, PA1202. doi:10.1029/2007PA001459.
Suan G., Pittet B., Bour I., Mattioli E., Duarte L.V. and Mailliot S. (2008b). Duration of the Early Toarcian carbon isotope excursion deduced fromspectral analysis: consequence for its possible causes. Earth Planet. Sci. Lett. 267, 666–679.
-Marx B., Duarte L.V., Philippe M., Reggiani L., and Martineau F. (2010). Secular environmental precursors to Early Toarcian (Jurassic) extreme climate changes. Earth and Planetary Science Letters 290, 448–458.
Svensen H., Planke S., Chevallier L., Malthe-Sorenssen A., Corfu F. and Jamtveit B. (2007). Hydrothermal venting of greenhouse gases triggering Early Jurassic global warming. Earth and Planetary Science Letters 256, 554–566.
Thiry M. (2000). Palaeoclimatic interpretation of clay-minerals in marine deposits: an outlook from the continental origin. Earth-Sci. Rev. 49, 201–221.
Tyrrell T. (1999). The relative influences of nitrogen and phosphorus on oceanic primary production. Nature 400, 525–531.
van Breugel Y., Baas M., Schouten S., Mattioli E. and Damste J.S.S. (2006). Isorenieratane record in black shales from the Paris Basin, France: constraints on recycling of respired $CO_2$ as a mechanism for negative carbon isotope shifts during the Toarcian oceanic anoxic event. Paleoceanography 21, PA4220.
van Cappellen P. and Ingall E.D. (1996). Redox stabilization of the atmosphere and oceans by phosphorus-limited marine productivity. Science 271, 493–496.
van de Schootbrugge B., Kuhn O., Adatte T., Steinmann P. and Föllmi K.B. (2003). Decoupling of P- and $C_{org}$-burial following Early Cretaceous (Valanginian–Hauterivian) platform drowning along the NW Tethyan margin. Palaeogeography, Palaeoclimatology, Palaeoecology 199, 315–331.
van de Schootbrugge B., McArthur J.M., Bailey T.R., Rosenthal Y., Wright J.D. and Miller K.G. (2005). Toarcian oceanic anoxic event: an assessment of global causes using belemnite C isotope records. Paleoceanography 20 PA3008, 1–10.
Vecsei A. (2003). Nutrient control on the global occurrence of isolated carbonate banks. Int. J. Earth Sci. (Geol. Rundsch.) 92, 476–481.
Weaver C.E. (1989). Clays, Muds, and Shales. Developments in Sedimentology, 44, Elsevier Science Publishers B. V., Amsterdam, 819 pp.
Wesley A. (1956). Contributions to the knowledge of the flora of the Grey Limestones of Veneto: part. I. Mem. Ist. Geol. Min. Univ. Padova, vol. 19 (1955-56). Padova.
Wesley A. (1958). Contributions to the knowledge of the flora of the Grey Limestones of Veneto: part. II. Mem. Ist. Geol. Min. Univ. Padova, vol. 21 (1959-60). Padova.
Wignall P.B. and Bond D.P.G. (2008). The end-Triassic and Early Jurassic mass extinction records in the British Isles. Proceedings of the Geologists' Association 119, 73–84.
Wignall P.B., Newton R.J. and Little C.T.S. (2005). The timing of paleoenvironmental change and cause-and-effect relationships during the early Jurassic mass extinction in Europe. Am. J. Sci. 305, 1014–1032.
Wilmsen M. and Neuweiler F. (2008). Biosedimentology of the Early Jurassic postextinction carbonate depositional system, central High Atlas rift basin, Morocco. Sedimentology 55, 773–807.
Winterer E.L. and Bosellini A. (1981). Subsidence and sedimentation on Jurassic passive continental margin, southern Alps, Italy: American Association of Petroleum Geologists (AAPG) Bulletin, 65, 394–421.
Woodfine R.G., Jenkyns H.C., Sarti M., Baroncini F. and Violante C. (2008) The response of two Tethyan carbonate platforms to the early Toarcian (Jurassic) oceanic anoxic event: environmental change and differential subsidence. Sedimentology 55, 1011–1028.

# CHAPTER 5 - BIO-CHEMOSTRATIGRAPHY OF THE BARREMIAN−APTIAN SHALLOW WATER CARBONATES OF THE SOUTHERN APENNINES: PINPOINTING THE OAE1a IN A TETHYAN CARBONATE PLATFORM

## *5.1 Introduction*

The Early Aptian oceanic anoxic event 1a (OAE1a), also known as the Selli event, was a time of severe perturbation of the global carbon cycle. The most popular scenario holds that intense volcanism, associated with the emplacement of the Ontong-Java large igneous province, forced the rapid increase of atmospheric $pCO_2$ which triggered a cascade of palaeoenvironmental changes (Larson and Erba, 1999; Méhay et al. 2009; Tejada et al. 2009). The deposition on a global scale of organic-rich marine sediments, the demise of the northern Tethyan carbonate platform and a biocalcification crisis recorded by calcareous nannoplankton, are among the most significant testimonies left in the geological record (Arthur et al., 1990; Wissler et al., 2003; Weissert and Erba, 2004; Erba et al., 2010).

Most of what we known about the response of the Earth System to the perturbations associated with the Selli event comes from the vast amount of data recovered during the last decades from hemipelagic and pelagic sedimentary successions deposited in epicontinental and oceanic basins. Much less is known of the response of tropical carbonate platforms, which potentially contain a very valuable archive of environmental change (Hallock, 2001; Strasser et al., 2011).

While the long-lived Urgonian platform was drowned shortly before the onset of the OAE1a (Wissler et al., 2003; Föllmi et al., 2006; Huck et al., 2011), some carbonate platforms in the central and southern Tethys were able to continue growing in shallow water. These resilient platforms preserve the record of palaeoecologic disturbance of tropical neritic ecosystems (Immenhauser et al., 2005; Huck et al., 2010). In order to unlock this archive, the first step is to bracketing the segments corresponding to OAEs, but this is not a trivial task in shallow water carbonate successions. Black shales are notably absent in carbonate platforms and also the occurrence of dysoxic facies can be misleading, because it is more often the result of locally restricted circulation than of global ocean anoxia (Davey and Jenkyns, 1999). Biostratigraphy may not always offer a complete solution either. The onset of the OAE1a has been dated to the lower part of the *Deshayesites deshayesi* ammonite zone (Föllmi et al., 2007). However, ammonites are very rarely found in shallow water carbonate platforms and there is at present no precise calibration of shallow water biostratigraphic schemes with the ammonite standard zonation and with the geological time scale. A recent review has highlighted how low biostratigraphic resolution and lack of precise chronostratigraphic calibration hinders a full appraisal of the response of carbonate platforms to climate and ocean chemistry changes during the Aptian (Skelton and Gili, 2011).

Biozonations of central and southern Tethyan Early Cretaceous carbonate platforms are based on benthic foraminifers and calcareous algae (De Castro, 1991; Simmons, 1994; Husinec and Sokač, 2006; Velić, 2007; Chiocchini et al, 2008). Resolution is rather low (3 biozones over 18 Myr, adopting the Geological Time Scale of Gradstein et al., 2004; hereinafter GTS2004) but can be considerably improved with orbitolinid foraminifers (fig. 1).

The chronostratigraphic scale tied to these shallow water biostratigraphic schemes conveys the impression that long-distance precise correlation between different carbonate platforms, as well as correlation with coeval deep-water facies, can be easily attained. However, a more in-depth appraisal of the papers on the biostratigraphy of Tethyan

carbonate platforms reveals that the chronostratigraphic calibration of the biozones is admittedly tentative (De Castro, 1991; Chiocchini et al., 2008) or entirely based on the age of orbitolinid foraminifera as established in the Urgonian Platforms of the Northern Tethyan margin (Bachmann and Hirsch, 2006; Velić, 2007).

In the absence of black shales and of a reliable biostratigraphic criterion, the identification of segments corresponding to the Selli event in the resilient carbonate platforms of the central and southern Tethys is generally based on carbon isotope stratigraphy. However, the pristine carbon isotope signal of the open ocean can be modified by local palaeoceanographic processes and later overprinted to a considerable extent by diagenesis (see Immenhauser et al., 2008, for a recent review). As a result, many published carbon isotope profiles of Lower Cretaceous shallow water carbonate successions are markedly different from, and very difficult to correlate with, basinal reference curves (D'Argenio et al., 2004; Huck et al., 2010; Tešović et al., 2011). Carbon isotope stratigraphy has been already applied to several Barremian–Aptian carbonate successions of the Apenninic Carbonate Platform (ACP) of Southern Italy (Ferreri et al., 1997; D'Argenio et al., 2004; Wissler et al., 2004; Di Lucia and Parente, 2008; Di Lucia, 2009).

The first attempt to use carbon isotope stratigraphy for correlation with well dated basinal sections and for bracketing the interval corresponding to the OAE1a, was made by Ferreri et al. (1997). A higher resolution $\delta^{13}C$ curve for the same section investigated by Ferreri et al. (1997), Mt. Raggeto, was produced by Wissler et al. (2004). Both these papers incorporate a high resolution cyclostratigraphic framework, but provide very few biostratigraphic data.

In this paper we present the re-interpretation of the carbon isotope stratigraphy of three Barremian–Aptian successions formerly studied by Di Lucia and Parente (2008) and Di Lucia (2009) and new biostratigraphic and chemostratigraphic data on two key sections formerly studied by Wissler et al. (2004) and D'Argenio et al. (2004): Mt. Raggeto and Mt. Tobenna. In particular, the correlation with the most complete Mt. Raggeto section reveals previously undisclosed gaps in the other sections. This highlights the difficulties of applying carbon isotope stratigraphy to inherently incomplete carbonate platform sections.

The most significant result of our study is the proposal of chemostratigraphically constrained biostratigraphic criteria for the individuation of the time-equivalent of the Selli event and of the Barremian–Aptian boundary in central and southern Tethyan carbonate platforms. Moreover we propose a chronostratigraphic calibration of some important biostratigraphic events that are widely used in the Barremian–Aptian biozonations of central and southern Tethyan carbonate platforms.

## *5.2 Geological setting*

The shallow water carbonates that are widely exposed in southern Italy (fig. 2) are the relics of carbonate banks that developed during the Mesozoic on the passive margin of Adria, a promontory of the African Plate (Bosellini, 2002). Starting from the Middle Triassic, the continental rifting individuated two wide platforms, the Apenninic Carbonate Platform and the Apulian Carbonate Platform, separated by a deep basin (the Lagonegro Basin). Shallow water carbonate sedimentation persisted almost to the end of the Cretaceous, when the platforms emerged, and was locally re-established during the Palaeogene and the Early Miocene to be eventually terminated by drowning and siliciclastic deep-water deposits. The total thickness of the Mesozoic succession of the Apenninic Carbonate Platform can be estimated to about 4-5 Km with about 1-1.2 Km pertaining to the Cretaceous (Sartoni and Crescenti, 1962; D'Argenio and Alvarez, 1980;

Frijia et al., 2005). The Upper Triassic to Lower Cretaceous limestones and dolomites are generally referred to flat-topped, Bahamian-type tropical carbonate platforms, dominated by chloralgal and chlorozoan associations (D'Argenio et al., 1975) whereas the depositional system of the Upper Cretaceous rudist limestones has been interpreted as a ramp-like open shelf, dominated by foramol-type assemblages (Carannante et al., 1997).

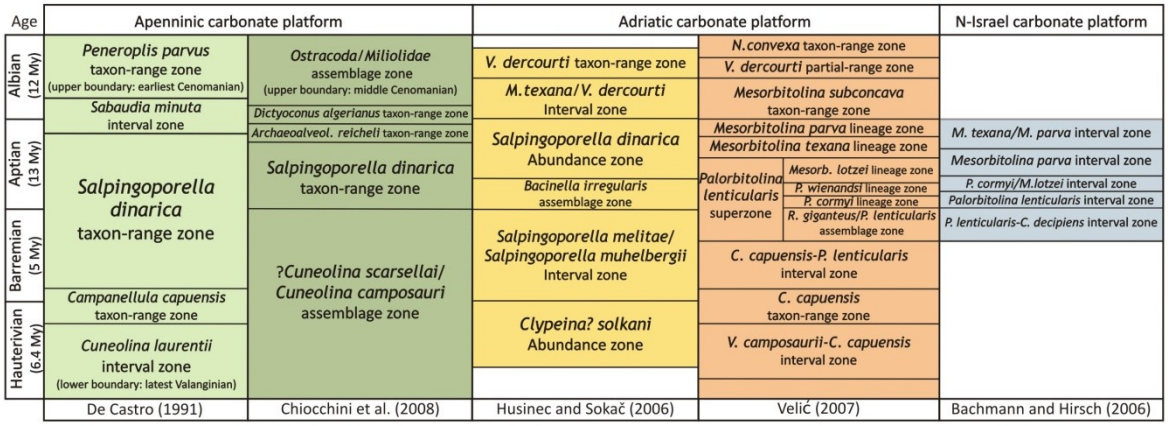


**Figure 1** - Barremian-Aptian biostratigraphy of central-southern Tethyan carbonate platforms. These schemes suffer of low resolution and poorly constrained chronostratigraphic calibration.

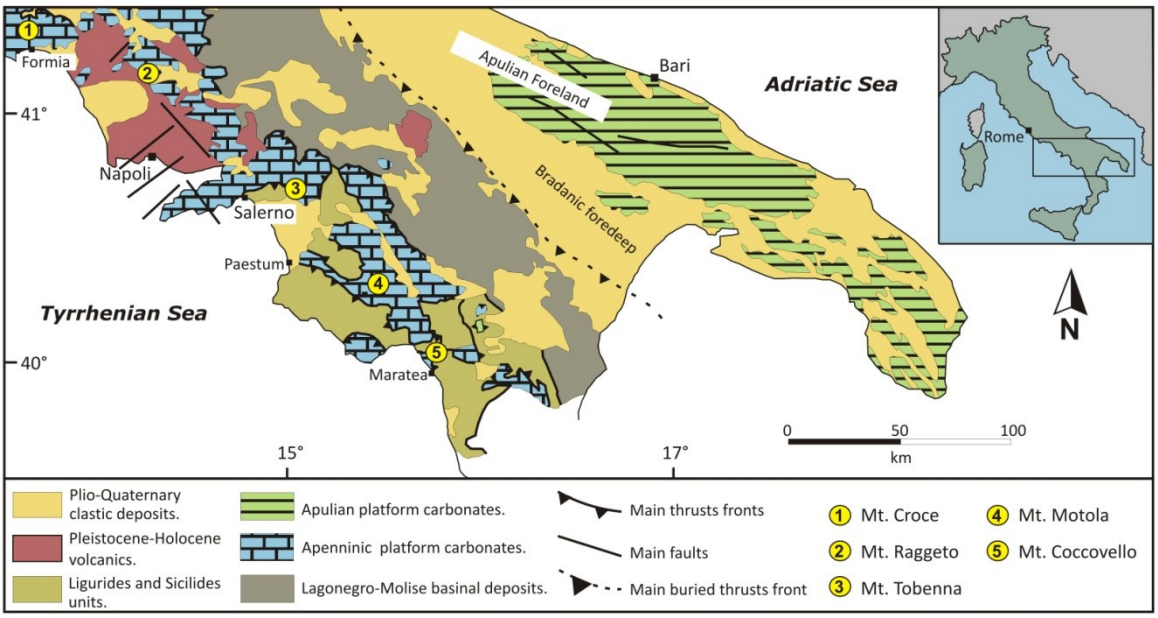


**Figure 2** - Schematic geological map of the central-southern Apennines, with location of the studied sections (modified from Bonardi et al., 1988).

## *5.3 Materials and Methods*

### *5.3.1 Sedimentology and biostratigraphy*

Five shallow water carbonate successions have been selected for this study: Mt. Croce (north of Formia, Lazio), Mt. Raggeto (northwest of Caserta, Campania), Mt. Tobenna (east of Salerno, Campania), Mt. Motola (south of Salerno, Campania) and Mt. Coccovello (north of Maratea, Basilicata) (fig. 2). The studied sections were logged in the field at decimetre to meter scale, depending on the outcrop quality, and sampled with an average resolution of about one sample per meter. The preliminary field description of

textural components, sedimentary structures and fossil content was subsequently integrated with the sedimentological and micropalaeontological study of about 520 double-polished thin sections.

### *5.3.2 Carbon and oxygen isotopes*

Six hundred samples were analysed for the $^{13}C/^{12}C$ and $^{18}O/^{16}O$ ratios. We used mudstones as a first choice and the micritic matrix of wackestones and floatstones as a second choice. About 2 mg of powder was obtained from each sample by micro-drilling a polished slab under a binocular microscope with a 0.5 mm or 0.8 mm Tungsten bit. The analyses were performed at the Isotopen-labor of the Institut für Geologie, Mineralogie und Geophysik at the Ruhr University (Bochum, Germany). Approximately 0.5 mg of sample powder was heated for 18 hrs at 105 °C. Samples were reacted online by individual acidic ($H_3PO_4$) addition with a Finnigan Gas Bench II. Stable isotope ratios were measured with a Finnigan Delta S mass spectrometer. The results are reported in ‰ in the conventional δ notation with reference to the Vienna Pee Dee Belemnite (VPDB) standard. The precision (1σ) monitored by repeated analyses of international and laboratory standards, is ±0.09‰ for carbon and ±0.13‰ for oxygen isotopes. Replicate measurements show reproducibility in the range of ±0.1‰ for $\delta^{13}C$ and ±0.2‰ for $\delta^{18}O$.

A three-points moving average smoothing has been applied to the $\delta^{13}C$ and $\delta^{18}O$ profiles in order to filter out high frequency (meter scale) fluctuations and to facilitate visual correlation between the studied successions and the reference curves.

### *5.3.3 Strontium isotopes*

Thirteen fragments of requienid shells from four different stratigraphic levels, plus the micritic matrix of the same levels were analysed for the $^{87}Sr/^{86}Sr$ isotope ratio. The best preserved shells were selected in the field using as first guidance colour preservation (yellowish to dark brown or dark grey) and preliminary analysis of shell microstructure with the hand lens. The samples were then passed through a complete procedure of diagenetic screening, involving standard petrography (optical microscopy, cathodoluminescence and SEM) and analysis of minor and trace element concentration (see Frijia and Parente, 2008, for a full description of the screening procedure and for analytical details). The numerical ages of the samples were derived from the look-up table of McArthur et al. (2001, version 4: 08/04), which is tied to the GTS2004. Minimum and maximum ages were obtained by combining the statistical uncertainty (2 s. e.) of the mean values of the Sr-isotope ratios of the samples with the uncertainty of the seawater curve.

## *5.4 Results*

### *5.4.1 Lithostratigraphy, lithofacies associations and palaeoenvironmental interpretation*

From a lithostratigraphic point of view, the five studied sections belong entirely to the “Calcari con Requienie e Gasteropodi” Formation (Requienid and Gastropod limestones Formation). Eight Lithofacies Associations (LA) (tab. 1) have been identified on the basis of texture, components (with special emphasis on fossil assemblages) and sedimentary structures. The main skeletal components are mollusks (gastropods, ostreids and requienid rudists), benthic foraminifers and green algae, with additional contribution from microbial nodules and crusts. Non-skeletal grains are mainly represented by peloids and intraclasts. The nomenclature of the LA conforms to that adopted by previous Authors for the Lower Cretaceous carbonates of the Apenninic Carbonate Platform and of other carbonate platforms of the central-southern Tethyan domain (Raspini, 2001; Pittet et al. 2002; Hillgärtner et al. 2003; D´Argenio et al. 2004; Bachmann and Hirsch, 2006).

Table 1 - Lithofacies description and palaeoenvironmental interpretation

| Lithofacies associations (LA) | Texture | Skeletal and non-skeletal components | Sedimentary and diagenetic features | Environmental interpretation |
|---|---|---|---|---|
| Chara-Ostracodal limestones (LA 1) | Mudstone/ Wackestone | Thin shelled ostracods (**a**), characean oogonia (c) and stems (r), small and thin shelled gastropods (r). | Dissolution cavities with vadose silt and/or sparry calcite infilling. | Ephemeral supratidal ponds |
| Fenestral and/or Microbialitic limestones (LA 2) | Mudstone/ Wackestone | Ostracods (**c**), small miliolids (**c**), thin-shelled gastropods (r), Thaumatoporella (r). | Fenestrae, birdseyes, dissolution cavities (with vadose silt, sparry calcite or marly infilling), mud-cracks and black pebbles. | Tidal flat and/or very restricted lagoon |
| Mili-Ostr-Algal limestones (LA 3) | Mudstone/ Wackestone | Ostracods (**a**), small miliolids (**a**), green algae (**c**), thin-shelled gastropods (**r**), textularids (**c**). | Dissolution cavities with vadose silt and/or sparry calcite infilling. | Intertidal to shallow subtidal protected lagoon |
| *S. dinarica* limestones (LA 4) | Wackestone/Packstone | *S. dinarica* (va), cuneolinids (r), nezzazzatids (r), ostracods (r), peloids (r). | *S. dinarica* sometimes crushed and isoriented parallel to bedding. | Shallow subtidal protected lagoon |
| Bio-Peloidal limestones (LA 5) | Packstone/ Grainstone | Benthic forams and green algae (**a**), molluskan shell fragments and ostracods (r). Peloids and intraclasts (a), ooids, oncoids and aggregate grains (r). | Parallel lamination (**r**), gradation (r). | Shallow subtidal sand bars |
| For-Algal limestones (LA 6) | Wackestone/Packstone | Benthic forams (**a**), green algae (**c**), ostracods (**r**), molluskan and echinoid shell fragments (**c**), Lithocodium/Bacinella nodules (c to a) and faecal pellets (r). | Bioturbation. | Subtidal open lagoon |
| Molluskan limestones (LA 7) | Floatstone | Requienid and/or gastropods (**a**). Matrix of bio-peloidal-intraclastic wackestone/packstone/ grainstone, with benthic forams (c), green algae (c), Lithocodium/Bacinella (r) and faecal pellets (r). | Bioturbation, Bioerosion of molluskan shells. | Subtidal open lagoon |
| Palorbitolina limestones and Orbitolinid/codiaceans marls and limestones (LA 8) | Mudstone/ Wackestone | Orbitolinids (*P. lenticularis*) (**c** to **a**), miliolids and textularids (**c**), Lithocodium/Bacinella nodules (**c**), molluskan and echinoid shell fragments (**c**), sponge spicules (**a**), oncoids, intraclasts and peloids (**r**). | Bioturbation, stylonodular structures. | Deep open lagoon |
| | Packstone | Orbitolinids (**va**) (*Mesorbitolina. parva*, *M. texana*) and codiaceans (va) (*B. hochstetteri moncharmontiae*), dasycladaceans (r), textularids (r) and echinoid shell fragments (c), micritic intraclasts (c). | Bioturbation,micritization of orbitolinid shells, stylonodular structures. | |

**va** = very abundant; **a** = abundant; **c** = common; **r** = rare

The described lithofacies represent a full range of sub-environments, from supratidal marsh with ponds, to tidal flat to subtidal restricted to open lagoon (fig. 3). A synoptic description of LA is given in table 1. All the studied successions can be generally referred to an inner platform setting. The Mt. Raggeto and the Mt. Croce sections show more open marine facies, organized mainly in subtidal and, subordinately, in peritidal metric cycles. More restricted environments occur at Mt. Tobenna, Mt. Motola and Mt. Coccovello, where peritidal cycles dominate the successions and subaerial exposure surfaces are more prominent and frequent.

Greenish marly levels are a very typical feature of the Mt. Tobenna section (see also Raspini, 1998, 2011). They occur as mm-thick partings between calcareous beds or as cm to dm-thick laterally discontinuous levels. The thickest levels often contain nodules of mudstones-wackestones with charophytes and ostracods (LA1). These marly levels document phases of subaerial exposure of the platform top. In all the other sections mm-thick recessive marly partings are often observed while the thickest marly levels seemingly correspond to poorly exposed intervals covered by grass and shrubs.

### *5.4.2 Biostratigraphy*

The following species of benthic foraminifers and calcareous algae have been used in this paper for the biostratigraphic subdivision and correlation of the studied successions (figs. 4, 5)

- *Praechrysalidina infracretacea* LUPERTO SINNI, 1979
- *Salpingoporella dinarica* RADOIČIĆ, 1959
- *Palorbitolina lenticularis* (BLUMENBACH, 1805)
- *Voloshinoides murgensis* LUPERTO SINNI & MASSE, 1993
- *Debarina hahounerensis* FOURCADE, RAOULT & VILA, 1972
- *Mesorbitolina parva* (DOUGLASS, 1960)
- *Mesorbitolina texana* (ROEMER, 1849)
- *Archaeoalveolina reicheli* (DE CASTRO, 1966)
- *Cuneolina parva* HENSON, 1948

The first and last occurrences (FO and LO) of these species are the basis of the most widely used biostratigraphic schemes for the central and southern Tethyan domain and their homotaxial order has been documented from the Apenninic, to the Adriatic-Dinaric to the Gavrovo-Tripolitza to the north African and Middle East carbonate Platforms (Chiocchini et al. 1994, 2008; Simmons, 1994; Husinec and Sokač, 2006; Velić, 2007; Tešovic et al. 2011).

For the correlation of the studied successions we relied in particular on the following biostratigraphic markers that can be easily recognized also in the field:

(1) The "*Archaeoalveolina reicheli* level", represented by few meters of wackestone-packstones with abundant *A. reicheli*.

(2) The "*Orbitolina* level", a 40 to 170 cm-thick composite bed consisting of marls and marly limestones full of flat low-conical orbitolinids (*M. parva* and *M. texana*). The top 15-20 cm are typically made of packstones/grainstones with orbitolinids and codiacean green algae (*Boueina hochstetteri moncharmontiae* DE CASTRO, 1978) (fig. 6, 7a). In the Mt. Coccovello section there are several cm-thick levels of marls with orbitolinids within a 6 m-thick interval of poor exposure. This interval terminates with a 15 cm thick bed of packstones with orbitolinids and codiacean algae.

(3) The *Salpingoporella dinarica* acmes, represented by two distinct m-thick intervals of packstones crowded with *S. dinarica,* occurring respectively a few meters below and above the "Orbitolina level" (fig. 7b).

(4) The Palorbitolina limestones, represented by 10-20 m of wackestones with *P. lenticularis*, ostreids, *Lithocodium*/*Bacinella* nodules and sponge spicules.

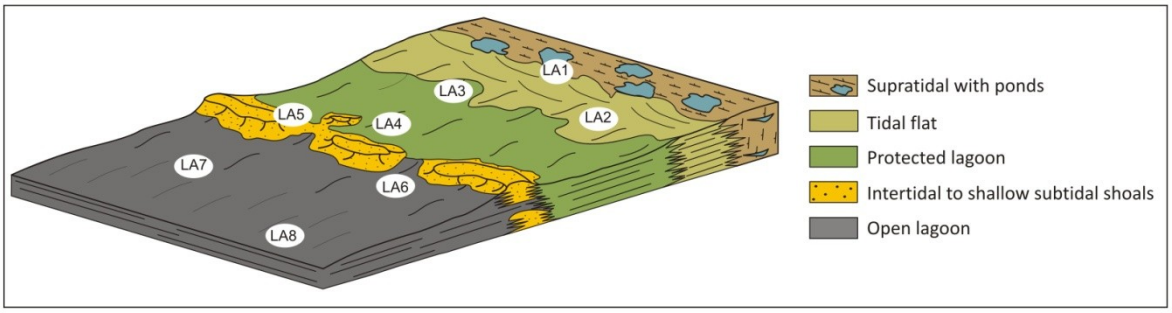


**Figure 3** - Schematic depositional model with facies distribution.

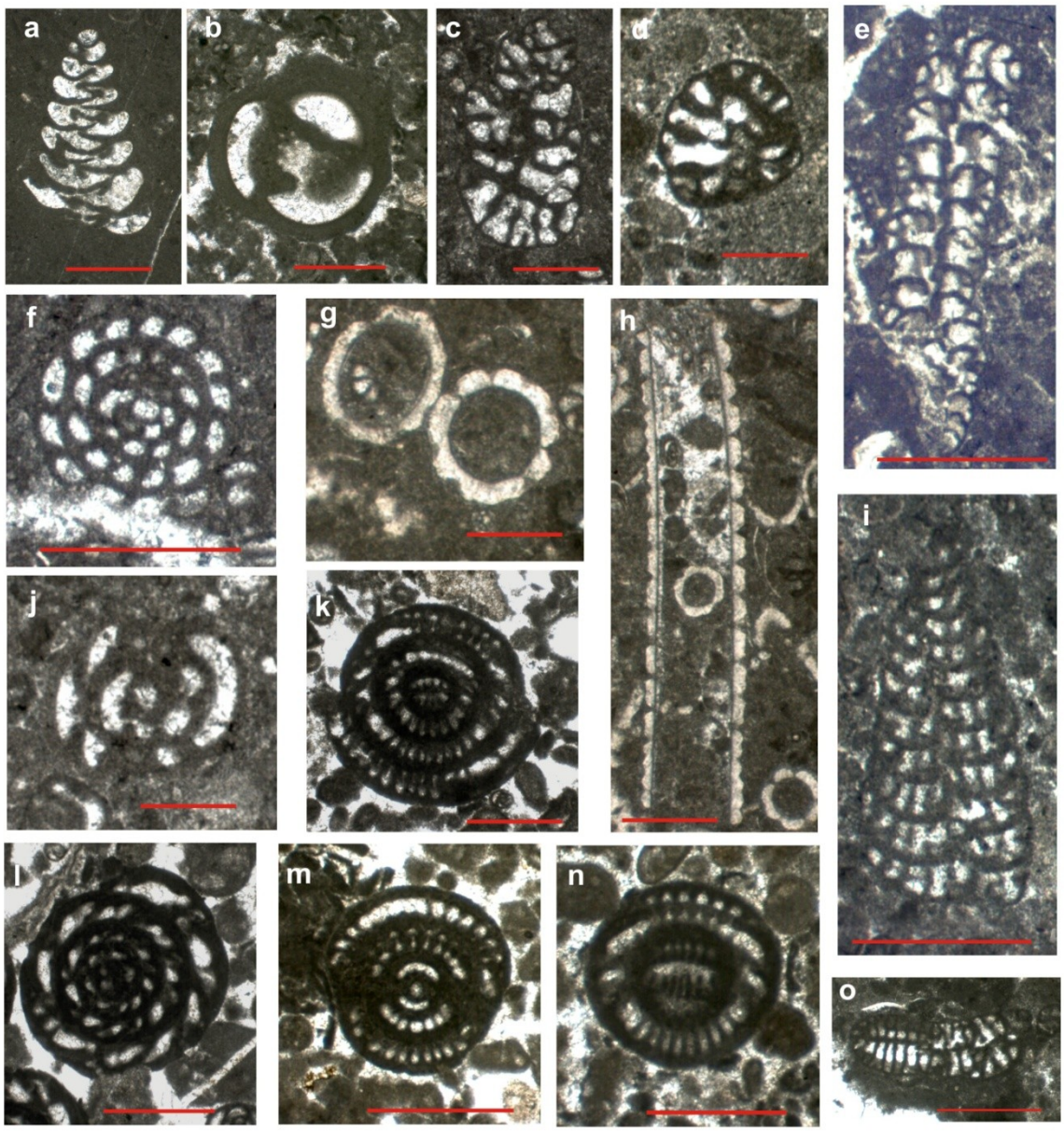

**Figure 4 (previous page)** - a: *Praechrysalidina infracretacea*, axial section (Mt. Croce, sample CR 70.5); b: *Praechrysalidina infracretacea*, transversal section (Mt. Croce, CR 55.4); c: *Voloshinoides murgensis*, sub-axial section (Mt. Coccovello, CO 1.8); d: *Voloshinoides murgensis*, sub-transversal section (Mt. Motola, MO 89.7); e: *Cuneolina parva*, axial section (Mt. Motola, MO 137.7); f: *Debarina hahounerensis*, equatorial section (Mt. Coccovello, CV 79.2a); g: *Salpingoporella dinarica*, transversal section (Mt. Motola, MO 103.8); h: *Salpingoporella dinarica*, axial section (Mt. Motola, MO 103.8); i: *Cuneolina parva*, axial section (Mt. Motola, MO 137.7); j: *Debarina hahounerensis*, sub-axial section (Mt. Coccovello, CV 79.2a); k: *Archaeoalveolina reicheli*, sub-axial section (Mt. Coccovello, CO 30.2); l: *Archaeoalveolina reicheli*, equatorial section (Mt. Coccovello, CO 30.2); m: *Archaeoalveolina reicheli*, axial section (Mt. Coccovello, CO 30.2); n: *Archaeoalveolina reicheli*, tangential section (Mt. Coccovello, CO 30.2); o: *Cuneolina parva*, sub-transversal section (Mt. Motola, MO 137.7). Scale bar is 500 microns for all photographs.

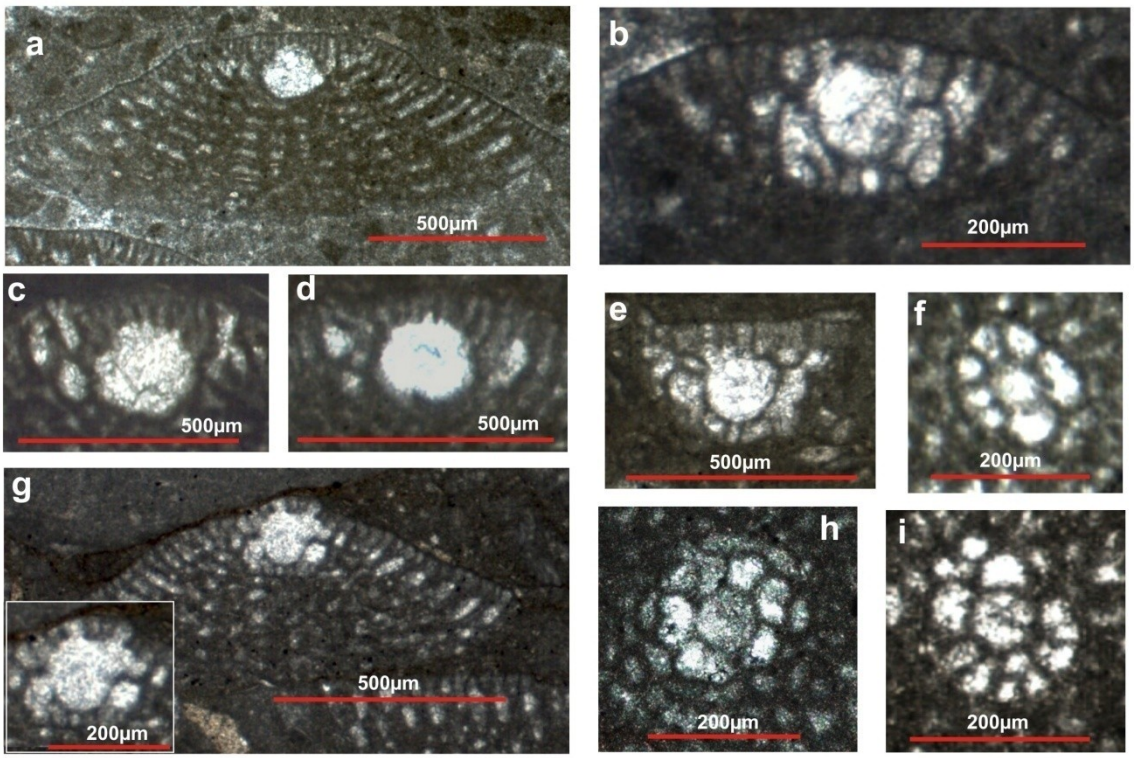


**Figure 5** - a: *Palorbitolina lenticularis*, axial section through the embryonic apparatus (Mt. Coccovello, sample CV 71.7); b: *Mesorbitolina texana*, axial section through the embryonic apparatus; c-d: *Palorbitolina lenticularis*, axial section through the embryonic apparatus (Mt. Coccovello, CV 65.4a); e: *Mesorbitolina texana*, axial section through the embryonic apparatus (Mt. Coccovello, CV 77.9a); f: *Mesorbitolina texana*, subtransversal section of the embryonic apparatus, slightly oblique through the subembryonic zone (Mt. Coccovello, CV 77.9a); g: *Mesorbitolina parva*, axial section through the embryonic apparatus, with detail of the embryonic apparatus (Mt. Coccovello, CV 77.9a); h: *Mesorbitolina parva*, transversal section through the embryonic apparatus (Mt. Tobenna, TB 8.3); i: *Mesorbitolina parva*, subtransversal section of the embryonic apparatus, oblique through the subembryonic zone (Mt. Coccovello, CV 77.9a).

### *5.4.3 Stratigraphy of the studied sections*

*Mt. Croce*

This succession was logged on the southern side of Mt. Croce in the Aurunci Mountains, about 17 Km northwest of Formia (41°23'55"N, 13°31'45"E) (fig. 2). It is 146.2 m thick and has been divided into four intervals (A-D) on the basis of major changes in LA at the decametre scale (fig. 8).

Interval A (0–45 m) shows a regular alternation of fenestral, mili-ostr-algal and bio-peloidal limestones arranged in metric shallowing-upward (SU) cycles.

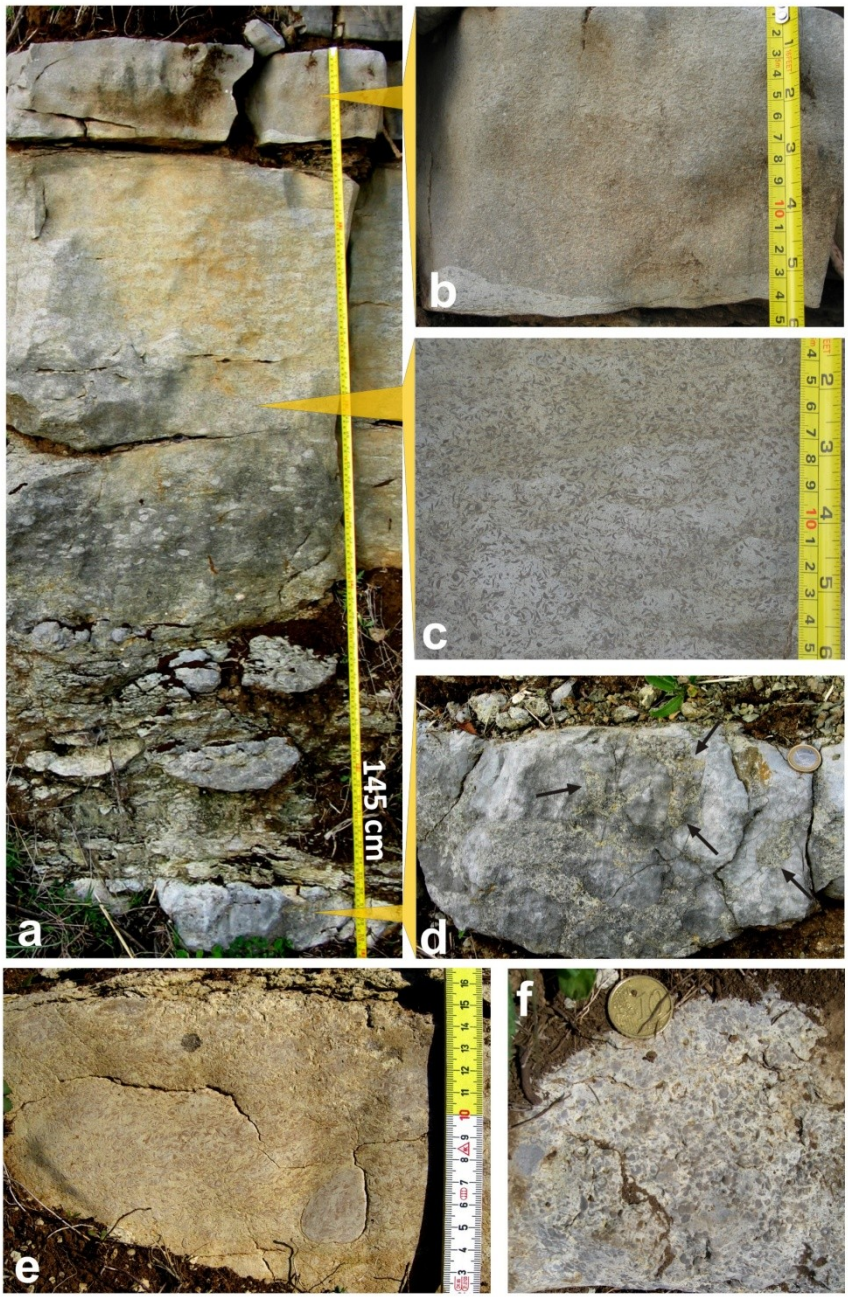


**Figure 6** - The "Orbitolina level" at Mt. Tobenna (a) is made by a nodular marly basal interval followed by a marly limestone crowded with flat low-conical orbitolinids (c). At the top there is a bed of orbitolinid-codiacean packstone/grainstone (b). The underlying bed (d) is penetrated by a network of dissolution cavities filled by orbitolinid marly-packstone (see arrows); e: orbitolinid marly-packstone at Mt. Croce; f: orbitolinid marly-packstone at Mt. Coccovello.

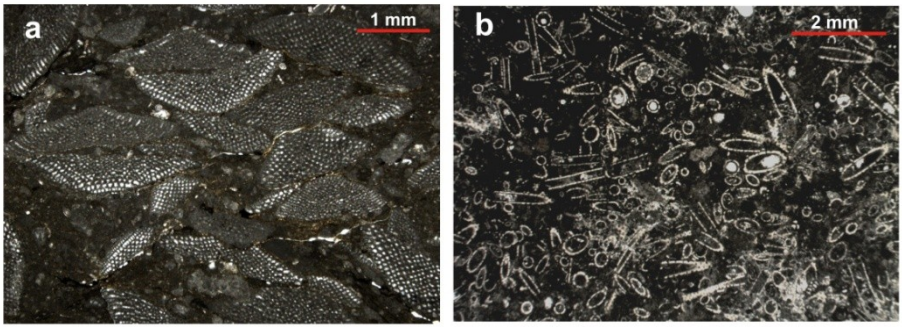


**Figure 7** - a: orbitolinid marly-packstone at Mt. Tobenna, microfacies (sample TB 8.3); b: *Salpingoporella dinarica* acme at Mt. Motola, microfacies (sample MO 103.8).

In the first 20 m intertidal and supratidal facies prevail and subaerial exposure surfaces are well developed at the top of some SU cycles. The thickness of subtidal facies increases in the second half of this interval, marking the onset of a transgressive trend.

The lower part of Interval B (45–60 m) consists mainly of "Palorbitolina limestones", with a few levels of requienid-gastropod floatstone and of for-algal wackestone-packstone. *Lithocodium/Bacinella* bindstones occur as dm-thick intercalations from 53.6 to 59.0 m. The upper part (60−75 m) is mainly made of for-algal wackestones/packstones alternating with a few levels of bio-peloidal packstone-grainstone. *Salpingoporella dinarica* wackestones-packstone are present at the top. Interval B terminates with a very prominent surface of subaerial exposure marked by a lens of nodular marly limestones made of rounded micritic clasts in a yellowish to greenish marly matrix.

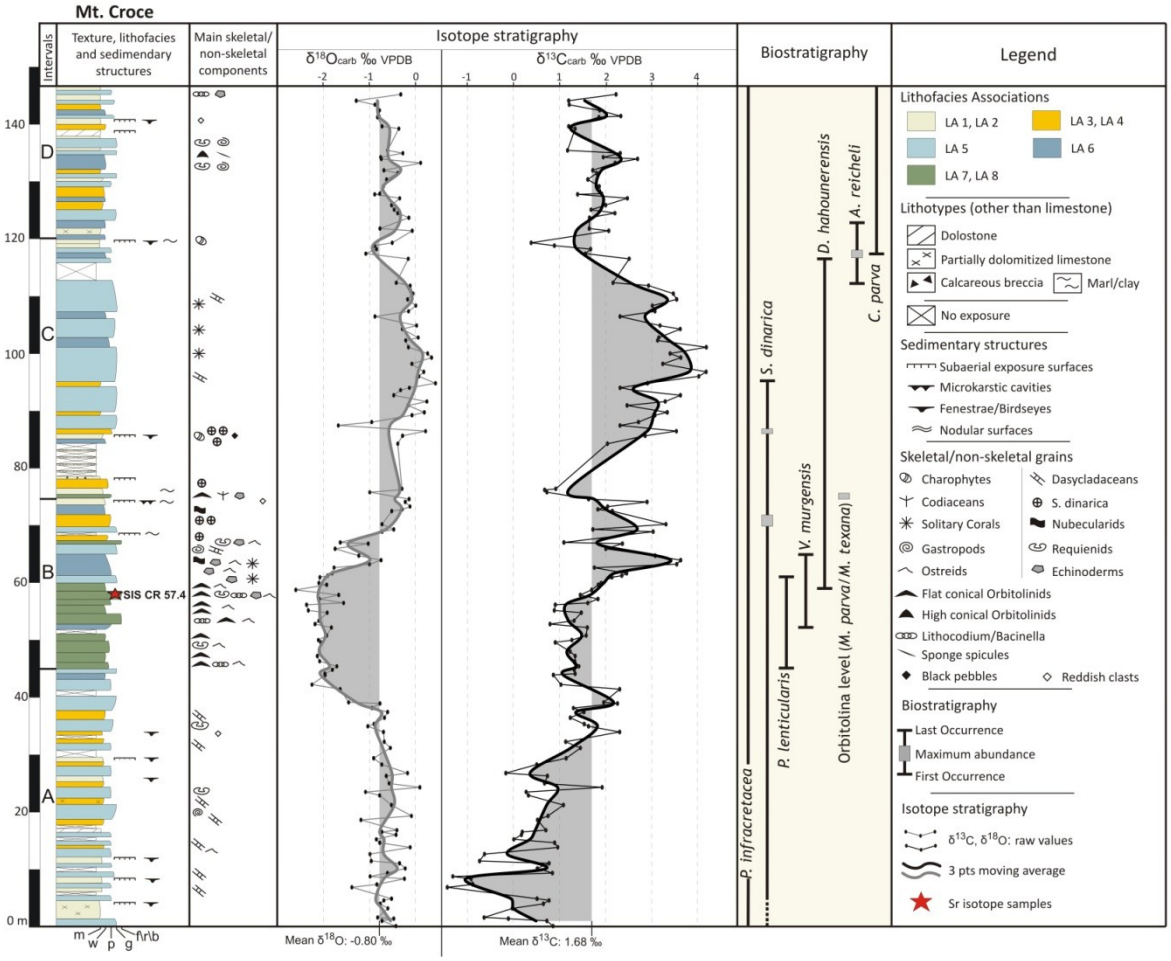


**Figure 8** - Mt. Croce section: lithological–sedimentological log, isotope stratigraphy and biostratigraphy. The thick curves represent the 3-point moving averages of O- (grey) and C-isotope ratios (black).

Interval C (75−120 m) starts with the "Orbitolina level", consisting of about 40 cm of marly limestones crowded with flat low-conical orbitolinids and codiaceans. The "Orbitolina level" is overlain by a few meters of fenestral mudstones and *S. dinarica* wackestones. From 79 to 84 m the quality of the outcrop is very poor. A few cm-thick beds of green marls are discontinuously exposed under a dense vegetation cover. The first beds after this covered interval consist of dm-thick levels of *S. dinarica* packstones. From about 87 to 112 m there are m-thick amalgamated beds of bio-peloidal packstone-grainstone, separated by thin levels of mili-ostr-algal mudstone-wackestone and for-algal wackestone. Interval C ends with dm-thick beds of bio-peloidal packstone-grainstone and

for-algal wackestone-packstone, overlain by microbial/fenestral mudstones and chara-ostracodal mudstones-wackestones.

Interval D (120−146.2 m) consists of a regular alternation of dm-thick beds of mili-ostracodal mudstone-wackestone, for-algal wackestone and bio-peloidal packstone-grainstone. A few beds of partially dolomitized fenestral mudstone occur at the top of the interval.

The following biostratigraphic events have been recognized in the Mt. Croce section (fig. 8):

−*P. infracretacea* occurs from the base to the top of the section.

−The FO of *S. dinarica* is at 4.6 m; the first acme is found at 69.8−79.8 m; the second acme is at 86.8−87.8 m; the LO is at 95.4 m.

−The range of *P. lenticularis* spans from 45.0 to 60.2 m.

−The FO of *V. murgensis* is at 52.4 m; the LO at 65 m.

−*D. hahounerensis* occurs from 59 to 118 m.

−The "Orbitolina level" is found at 75.9−76.3 m. The first 20 cm contain exclusively *Mesorbitolina parva* and *M. texana*. The upper part contains also *B. hochstetteri moncharmontiae*.

−The FO of *A. reicheli* is at 112.3 m but the species becomes abundant from 117.9 to 118.8 m (*A. reicheli* level), in concomitance with the FO of *C. parva*.

*Mt. Raggeto*

The Lower Cretaceous shallow water carbonates of Mt. Raggeto (7 km northwest of Caserta, 41°09'14"N, 14°14'51"E, fig. 2) have been extensively studied during the last 20 years (D'Argenio et al., 1993, 1999a, 2004; Ferreri et al., 1997; Buonocunto, 1998; Amodio et al., 2003; Wissler et al., 2004). We logged a 97 m-thick section, starting about 30 m below the thin bedded limestones identified by Wissler et al. (2004) as the equivalent of the Selli level. Based on lithofacies associations, we subdivided our section into three intervals (A-C) (fig. 9).

Interval A (0–39.3 m) starts with a few meters of bio-peloidal packstones with nubecularids, followed by for-algal wackestones with *Lithocodium/Bacinella* nodules and bioturbated wackestones with *Palorbitolina*. Dolomite-filled Thalassinoides burrows make a tridimensional network that is well visible on weathered surfaces. After a 9 m thick interval of no exposure, the log continues in an abandoned quarry. At the base of the quarry wall there is a 7.5m-thick dolomitized interval, made of massive dolomites and thinly bedded dolomitized mudstones-wackestones. It corresponds roughly to the superbundle "14" of Wissler et al. (2004) that, according to Amodio et al. (2003), consists mainly of *Palorbitolina* wackestone-packstones. Even if dolomitized limestones are not reported in the Wissler et al. (2004) log, their presence is confirmed by the abrupt shift of about 2‰ in the $\delta^{18}O$ at this level (see fig. 3 of Wissler et al., 2004). This dolomitized interval is followed by about 6 meters of well bedded bio-peloidal packstones with nubecularids and for-algal wackestones-packstones with *Lithocodium/Bacinella* nodules, alternating with floatstones with requienids and ostreids.

The last part of the interval A is characterized by poorly exposed thin beds of bio-peloidal packstone with nubecularids, alternating with ostracodal mudstones-wackestones.

Interval B (39.3–75 m) is mainly made of algal wackestones-packstones rich of *S. dinarica,* with a few beds of requienid floatstones and of bio-peloidal packstones. *Lithocodium*/*Bacinella* nodules are particularly abundant between 45.5 and 53 m from the base of the section, associated with requienid floatstones. In the upper part of this interval, between 62 and 69 m from the base of the section, some beds of chara-ostracodal mudstones mark a regressive trend culminating with a cluster of nodular marly levels.

Interval C (75–97.3m) is mainly made of bio-peloidal packstones-grainstones. At the base they alternate with some beds of ostreid-requienid floatstones while in the uppermost part (from 87 to 97.3 m from the base of the section) there are some intercalations of mili-ostracodal mudstone-wackestones. The section ends with a few beds of foraminiferal wackestones with primitive forms of *A. reicheli* and nodules of *Lithocodium/Bacinella*.

The following biostratigraphic events were recognized in the Mt. Raggeto section (fig. 9):

–*P. infracretacea* is present from the base to the top of the section.

–*S. dinarica* occurs from the base of the section to 82.5m; a first interval of maximum abundance occurs between 43 to 53 m from the base of the section; the second acme is between 70 and 73 m.

–*P. lenticularis* has been found from 6 to 24 m from the base of the section.

–*D. hahounerensis* occurs from 39.8 m to the top of the section.

–The FO of *A. reicheli* and *C. parva* is at 76.3 m.

*Mt. Tobenna*

This section is 48.5 m thick (fig. 10) and was logged on the southern slope of Monte Tobenna in the Picentini Mountains, about 8 km northeast of Salerno(fig. 2). This is a classical locality for the Orbitolina level of southern Apennines (De Castro, 1963; Cherchi et al., 1978). The lower half of the section (from 0 to 24m) is exposed in an abandoned quarry(40°42.01"N, 14°51'43"E) and has been the object of many papers dealing mainly with cyclostratigraphy (Raspini, 1998, 2011; D'Argenio et al., 1999b, 2004). Our section continues on the mountain slope above the edge of the quarry.

On the basis of the LA trends, the section can be clearly divided into two intervals (A and B). In interval A (0–24 m), which has been logged in the quarry wall, the exceptional quality of the exposure permitted unusual high-resolution observation of the mm- to dm-thick marly layers which are found at the top of many limestone beds. In the upper part of the section the thinnest marly levels are observed as mm-thick recessive partings between limestone beds while the thickest levels probably corresponds to poorly exposed and densely vegetated parts of the slope. The first part of interval A (0–7m) consists mainly of an alternation of chara-ostracodal mudstones-wackestones, bio-peloidal packstones-grainstones with nubecularids and mili-ostracodal wackestones. Between 7 and 15 m from the base of the section the most frequent lithofacies consists of algal wackestones-packstones with *S. dinarica*, alternating with bio-peloidal packstone-grainstones. A prominent bed of requienid floatstone is present at 11 m from the base of the section. The "Orbitolina level" occurs at 15 m from the base of our section. It is composed by two beds. The lower bed is a 120cm thick bioturbated marly limestone crowded with flat low-conical orbitolinids. The argillaceous component decreases upward. The upper bed, which is just 15 cm thick, is separated by the lower bed by a wavy erosional surface and consists of a packstone/grainstone crowded with flat low-conical orbitolinids and codiacean algae (*Boueina hochstetteri moncharmontiae*). Below the wavy base of the "Orbitolina level" the underlying bed is penetrated down to about 1m by a dense network of dissolution cavities filled by orbitolinid packstone (fig. 6).

The "Orbitolina level" is overlain by 70 cm of bio-peloidal packstones-grainstones. The remaining part of interval A is dominated by chara-ostracodal mudstones-wackestones alternating with cm- to dm- thick levels of greenish marls. The thickest marly levels contain nodules of chara-ostracodal mudstones.

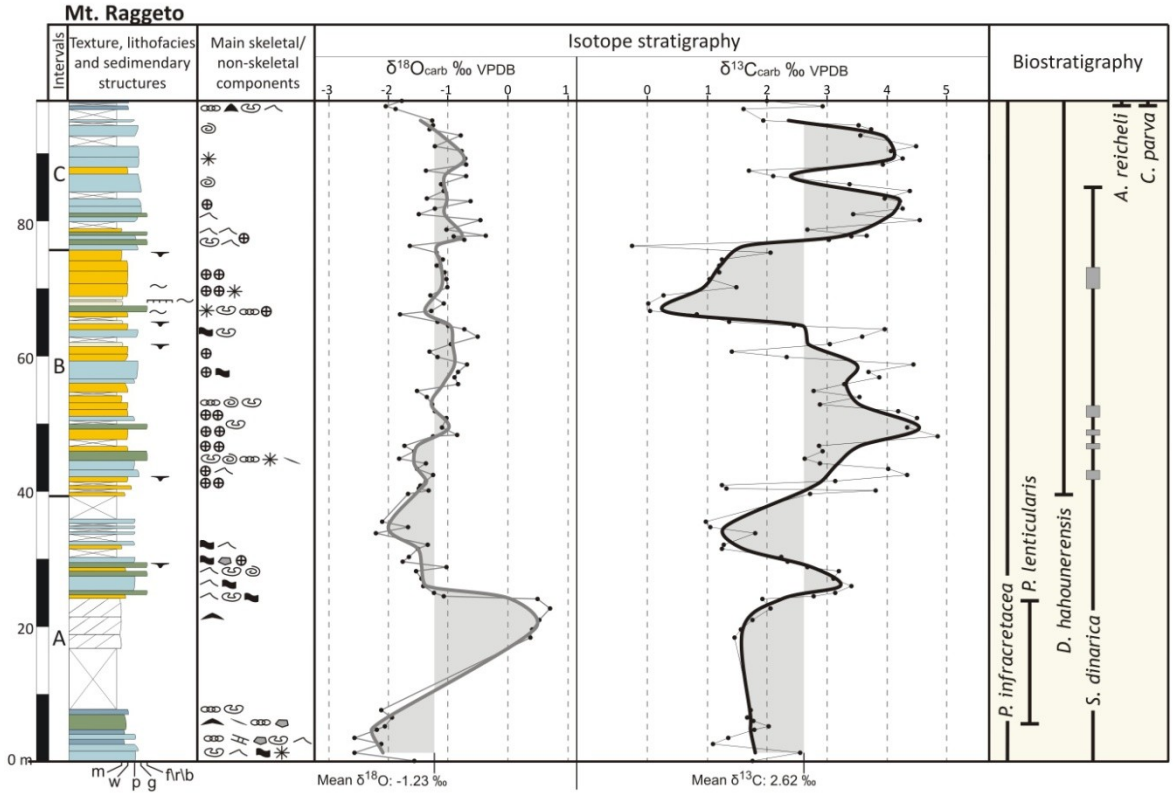


**Figure 9** - Mt. Raggeto section: lithological–sedimentological log, isotope stratigraphy and biostratigraphy. The thick curves represent the 3-point moving averages of O- (grey) and C-isotope ratios (black). See fig. 8 for a key to colours, patterns and symbols.

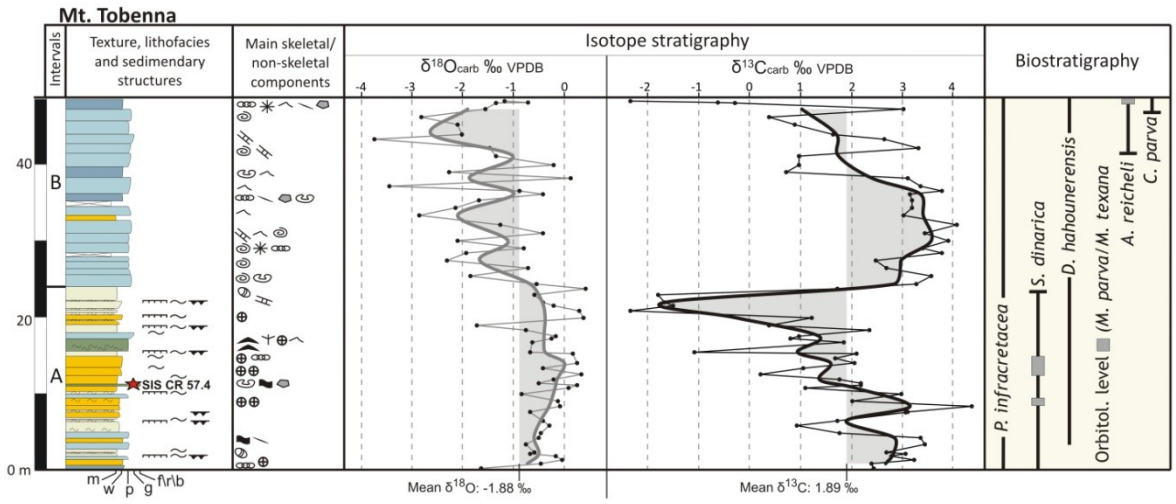


**Figure 10** - Mt. Tobenna section: lithological–sedimentological log, isotope stratigraphy and biostratigraphy. The thick curves represent the 3-point moving averages of O- (grey) and C-isotope ratios (black). See fig. 8 for a key to colours, patterns and symbols.

Interval B (24–48.5 m) was logged on the mountain slope immediately west of quarry edge. It is dominated by bio-peloidal packstones-grainstones with abundant benthic foraminifers, with a few beds of mili-ostracodal mudstones-wackestones. *Lithocodium*/*Bacinella* nodules are a frequent component between 26 and 36 m from the base of the section. The section ends with a bed of foraminiferal packstone crowded with *A. reicheli*.

The following biostratigraphic events have been recognized in the Mt. Tobenna section (fig. 10):

–*P. infracretacea* occurs from the base to the top of the section.

–*S. dinarica* is found from the base of the section to 24 m; an interval of maximum abundance is observed between 9 and 14.6 m from the base of the section.

–*D. hahounerensis* occurs from 3.3 m to the top of the section.

–The "Orbitolina level" is at 15.5−17.2 from the base of the section. It is crowded with the flat low-conical shells of *M. parva* and *M. texana*. The codiacean alga *B. hochstetteri moncharmontiae* is particularly abundant in the packstone/grainstone at the top of the level.

–The FO of *A. reicheli* is at 41.1 m where primitive specimens are first observed. The *A. reicheli* level, containing a rich association of typical specimens of this species, is found at 48.1 m from the base of the section

–The FO of *C. parva* is at 46.2 m.

*Mt. Motola*

This section was logged on the southern slope of Mt. Motola (40°21'53"N, 15°25'42"E), about 65 Km southeast of Salerno (fig. 2). It is 150.3 m thick and has been subdivided into four intervals (fig. 11). Interval A (0−75 m) consists mainly of bio-peloidal packstones-grainstones, mili-ostr-algal mudstones-wackestones and microbial/fenestral mudstones. Two levels of for-algal packstone and requienid-gastropod floatstone occur in the uppermost part. The first 20 m are dominated by peritidal m-thick SU cycles. Subaerial exposure surfaces at the top of the cycles are marked by discontinuous levels of greenish/yellowish marls, infiltrating downwards into microkarstic cavities. Subtidal facies become predominant upwards, marking the onset of a deepening trend, but subaerial exposure surfaces are still present at the top of some cycles. Interval B (75−98 m) is dominated by subtidal facies. It consists mainly of *Palorbitolina* wackestones with sponge spicules and echinoderm fragments, alternating with requienid-gastropod floatstones. Cm- to dm-thick beds of *Lithocodium/Bacinella* bindstone are present at the base of this interval. A m-thick bed of packstone crowded with nubecularid foraminifers occurs at the top. This interval terminates with a prominent subaerial exposure surface, marked by microkarstic cavities with greenish marly infilling.

At the base of interval C (98−126 m) there are about three meters of very poorly exposed section. Centimetric discontinuous marly levels are hardly visible under a thick vegetation and soil cover. The following beds are made of *S. dinarica* packstones alternating with 10 to 50 cm-thick levels of chara-ostracod and mili-ostr-algal mudstone-wackestone, capped by subaerial exposure surfaces. From 107 to 122 m, interval C consists mainly of very thick amalgamated beds (up to 6 m-thick) of bio-peloidal packstone-grainstone, with a few decimetric intercalations of gastropod-requienid floatstone. The uppermost part of the interval (122−126 m) is made of dm to m-thick beds of bio-peloidal packstone-grainstone alternating with microbial/fenestral mudstones capped by thin seams of marls, which infiltrates downward into microkarstic cavities. Interval D (126−150.3 m) is mainly made of bio-peloidal packstones-grainstones and mili-ostracodal mudstones-wackestones. Microbial/fenestral mudstones capped by subaerial exposure surfaces are present in the uppermost part of the section.

The following biostratigraphic events have been documented in the Mt Motola section (fig. 11):

–The FO of *P. infracretacea* is at 23 m; the range of this species extends beyond the top of this section.

–The FO of *S. dinarica* is at 27.6 m; the acme is at 103.5–104 m, the LO is at 109.6 m.

–The range of *P. lenticularis* spans from 79.2 to 89.7 m.

–The FO and LO of *V. murgensis* are placed at 84 and 89.7 m respectively.

–*D. hahounerensis* occurs from 85.4 to 137.3 m.

–The range of *A. reicheli* spans from 123 to 126.4 m; the maximum abundance ("*A. reicheli* level") is observed at 125.1 to 126.4 m.

–The FO of *C. parva* is at 137.3 m.

The "Orbitolina level" is missing in this section. Bio-lithostratigraphic correlation suggests that it is lost in the gap associated with the prominent subaerial exposure surface at the boundary between intervals B and C.

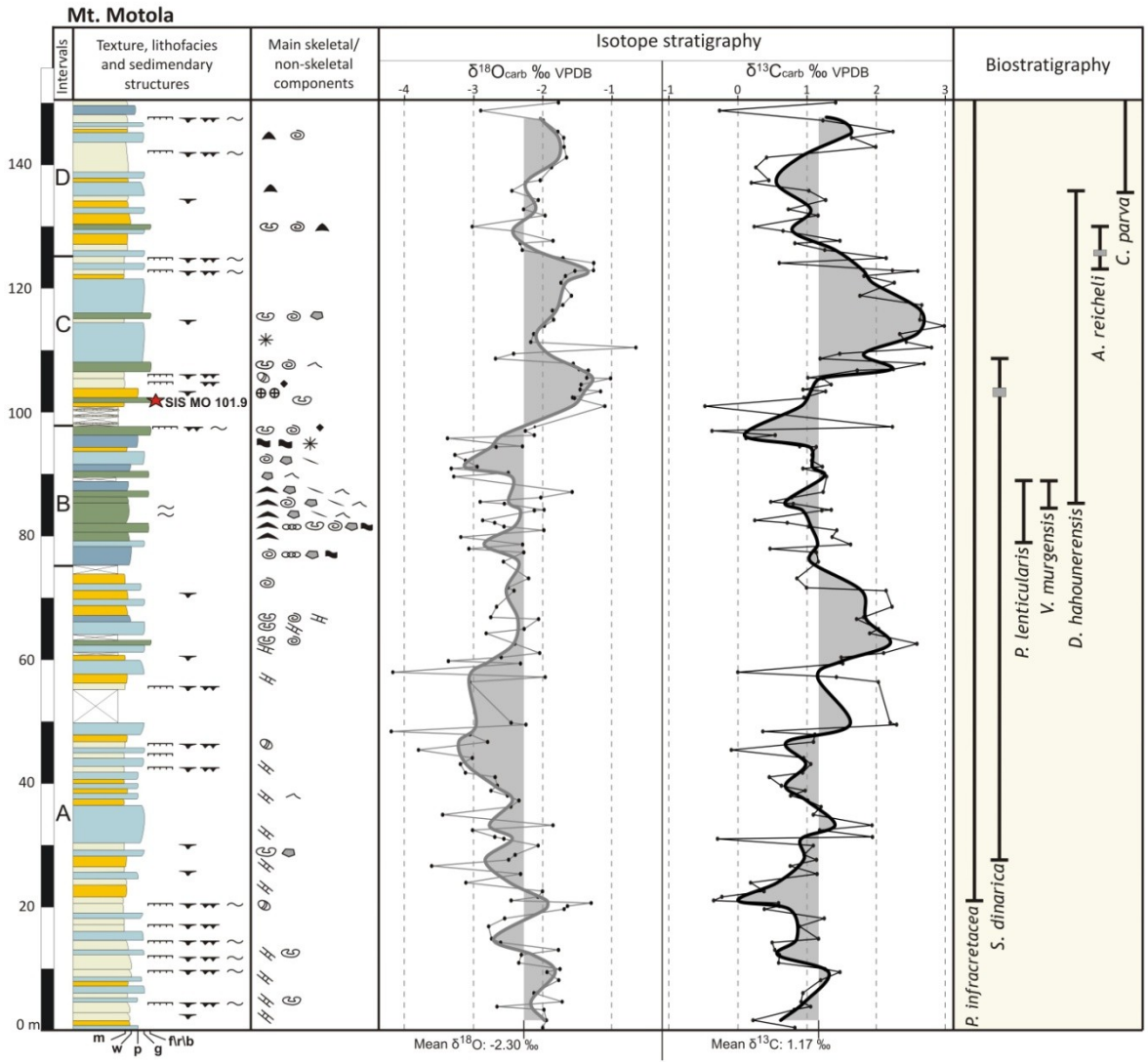


**Figure 11** - Mt. Motola section: lithological–sedimentological log, isotope stratigraphy and biostratigraphy. The thick curves represent the 3-point moving averages of O- (grey) and C-isotope ratios (black). See fig. 8 for a key to colours, patterns and symbols.

*Mt. Coccovello*

This 135.2 m-thick composite section was logged on the southern slope of Mt. Coccovello (40°02'38"N, 15°42'32"E), about 3 Km north of Maratea (fig. 2). It has been subdivided into four intervals (A-D) based on the major changes of lithofacies associations and on the occurrence of some prominent subaerial exposure surfaces (fig. 12). Interval A

(0−67.2 m) is dominated by intertidal microbial/fenestral mudstones alternating with mili-ostr-algal mudstones-wackestones and bio-peloidal packstones-grainstones. The latter become more frequent in the upper part of the interval, highlighting the onset of a deepening trend. Subaerial exposure surfaces are frequent at the base and from 22 to 42 m.

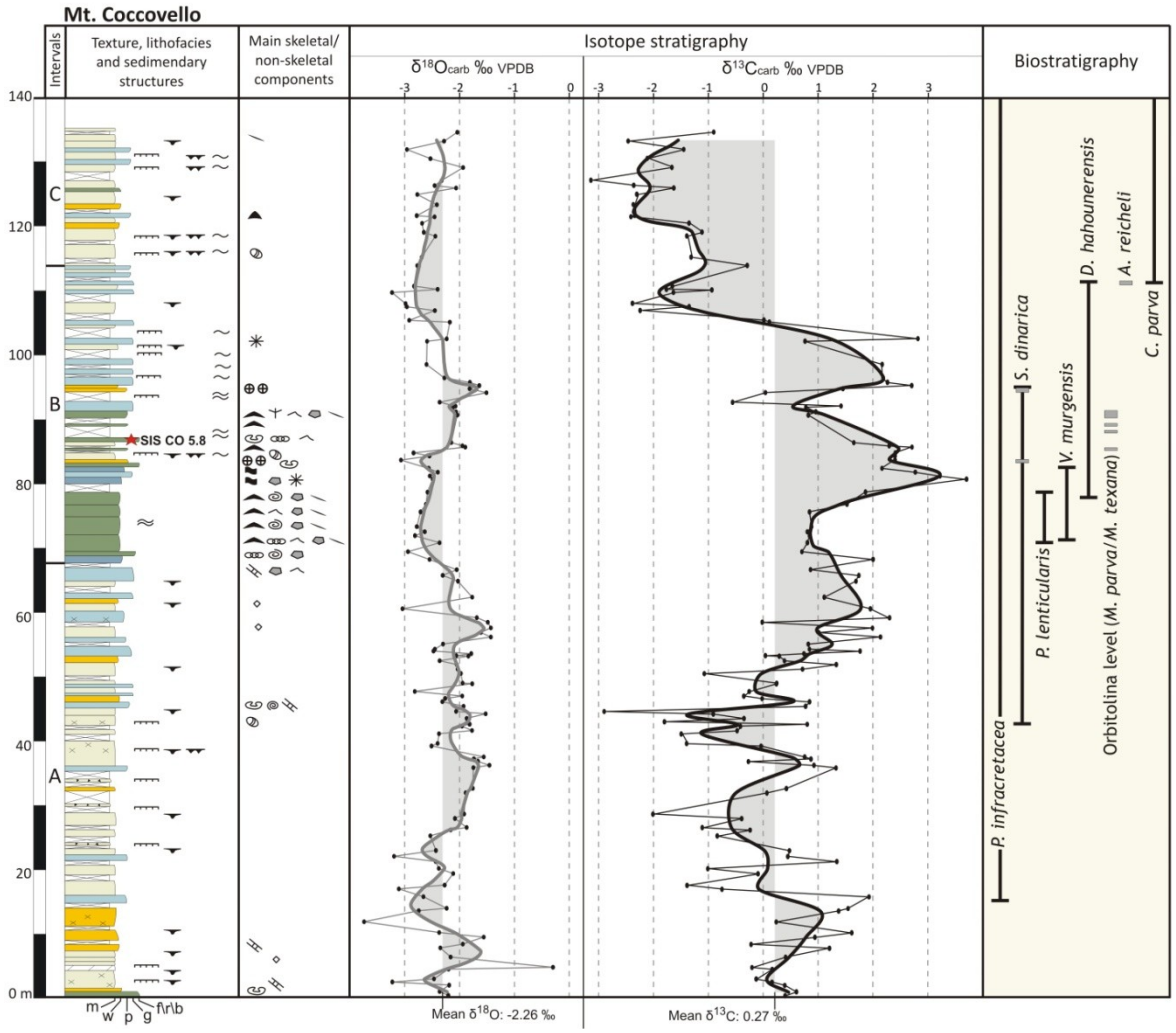


**Figure 12** - Mt. Coccovello section: lithological–sedimentological log, isotope stratigraphy and biostratigraphy. The thick curves represent the 3-point moving averages of O- (grey) and C-isotope ratios (black). See fig. 8 for a key to colours, patterns and symbols.

The lower part of interval B, from 67.2 to 79.1 m, consists mainly of *Palorbitolina* wackestones. About 2 m of *Lithocodium/Bacinella* bindstone occur in the lowermost part of the interval (from 69 to 71 m). The upper part (from 80 to 85 m) is made of dm-thick beds of for-algal wackestone-packstone, crowded with nubecularid foraminifers, overlain by a bed of *S. dinarica* packstone. The interval terminates with a bed of microbial/fenestral mudstone, capped by a subaerial exposure surface. Interval C (85−120 m) starts with a thin marly level crowded with flat low-conical orbitolinids, followed by a distinctive requienid floatstone. The orbitolinid marls penetrate downwards into a network of microkarstic cavities. From 87 to 91 m the section is characterized by very poor exposure, with discontinuous cm-thick orbitolinid marls cropping out from a dense vegetation and soil cover. A bed of orbitolinid-codiacean packstone terminates this poorly exposed portion. The next segment (from 92 to 119 m) consists mainly of bio-peloidal packstones-grainstones alternating with microbial/fenestral mudstones. The uppermost five meters of interval C are almost entirely made of chara-ostracod mudstones and fenestral mudstones,

capped by subaerial exposure surfaces. Interval D (119−135.2 m) is mainly made of an alternation of bio-peloidal packstones-grainstones and microbial/fenestral mudstones, with a few beds of mili-ostracodal mudstone-wackestone. A couple of prominent subaerial exposure surfaces occur in the upper part of this interval.

The following biostratigraphic events were recognized in the Mt. Coccovello section (fig. 10):

−*P. infracretacea* first occurs at 15.6 m and is present up to the top of the section.

−The FO of *S. dinarica* is at 42.3 m; its first acme is at 84.3 m, the second acme is at 94.5 m.

−*P. lenticularis* is present from 70.8 to 79.1 m.

−The FO and LO of *V. murgensis* are placed at 70.8 and 82.4 m respectively.

−*D. hahounerensis* occurs from 78.7 to 87 m.

−The base of the "Orbitolina level" is a 5 to 10 cm-thick discontinuous marly layer which occurs at 85.0 m above a prominent subaerial exposure surface and infiltrates downward into microkarstic cavities. This level contains *M. parva* and *M. texana*. Other cm-thick discontinuous marly levels with the same microfauna occur across a 5 m thick interval of poor exposure. The typical packstone with *Mesorbitolina* and the codiacean alga *B. hochstetteri moncharmontiae*, which elsewhere represents the top of the "Orbitolina level", occurs at 91.2 m.

−The *A. reicheli* level corresponds to a 20 cm-thick layer at 110.8 m.

### *5.4.4 Carbon and strontium isotope stratigraphy*

*Mt. Croce*

One hundred and fifty samples were analyzed for the Mt. Croce section (fig. 8). The $\delta^{13}C$ values range between -1.43‰ and +4.18‰, with an average value of +1.68‰.The lower part of the $\delta^{13}C$ curve shows a rising trend with superimposed higher frequency fluctuations. Carbon isotope ratios increase from slightly negative values at the base of the section to a maximum of +2.1‰ at 39.1 m, about 6 m below the base of the "Palorbitolina limestones". After a 1‰ decrease, the $\delta^{13}C$ curve makes a plateau at about +1‰, which corresponds almost entirely to the "Palorbitolina limestones". This plateau is followed by a marked positive excursion which starts 4 m below the top of the "Palorbitolina limestones", peaks at about + 3‰ and then decreases to pre-excursion values of +1‰ at 76.5 m, just above the "Orbitolina level". From there it starts a new very broad positive excursion that peaks at about +4‰ 10 m above the second acme of *S. dinarica*, and returns at pre-excursion values 1 m above the *A. reicheli* level. The last part of the $\delta^{13}C$ curve is characterized by values fluctuating between +1 and +2‰.

Three fragments of requienid shells from a floatstone at 57.4 m from the base of the section, 3 m below the top of the "Palorbitolina limestones", have been analysed for SIS. Their $^{87}Sr/^{86}Sr$ mean value gives a numerical age of 124.1 Ma (tab. 2).

*Mt. Raggeto*

Ninety-two samples, among which five dolomites, were analyzed for the Mt. Raggeto section. The $\delta^{13}C$ values range between -0.2‰ and +4.8‰, with an average value of +2.62‰ (fig. 9). In the first part of the curve (0–22m), corresponding to the "Palorbitolina limestones" and to the thick dolomitic interval, there is a plateau at about +1.6‰, with superimposed high- frequency fluctuations between +1 and +2‰. Then, there is a sharp positive excursion of about 1.5-2‰, which peaks at +3.41‰ at 25.9 m from the base of the section. This is followed by a very broad positive excursion, which occupies all the central part of the logged section, reaching peak values of nearly +5‰ at about 50 m

from the base of the section, at a level corresponding to the first interval of maximum abundance of *S. dinarica*. A stepped decline, with superimposed high-frequency fluctuations, leads to a minimum value of about 0‰ at 67 m from the base of the section, just below the second interval of maximum abundance of *S. dinarica*. The $\delta^{13}C$ curve ends with another positive excursion showing two positive peaks at about +4‰, separated by a relative minimum of about +2‰ at 87m from the base of the section. The last few meters of the sections are marked by a steep decrease to values of about +1.6‰.

*Mt. Tobenna*

Sixty-five samples were analyzed for the Mt. Tobenna section. The $\delta^{13}C$ values range between -2.4‰ and +4.4‰, with an average of +1.89‰ (fig. 10). The first 10m of the curve are characterized by wildly fluctuating values with two closely spaced positive excursions peaking at +3.5‰ and at +4.4‰. Then there is a prolonged decreasing trend, with superimposed high-frequency fluctuations, reaching a minimum value of -2.3‰ a few meters above the "Orbitolina level", in correspondence of a cluster of dm-thick greenish marly levels indicating prolonged subaerial exposure. From this minimum there is a very sharp rise to a value of +3.5‰ at 25.4 m from the base of the section, just above the last occurrence of *S. dinarica*. After a positive plateau, defined by $\delta^{13}C$ values oscillating mainly between +3 and +4‰, there is a decreasing trend with superimposed high-frequency fluctuations. Very depleted values of -2.4‰ are reached at the end of the section, in correspondence of the *A. reicheli* level.

Three fragments of requienid shells from a floatstone occurring 5.8m below the base of the "Orbitolina level" have been analysed for SIS. After discarding as altered one shell, because of its low Sr concentration (<550 ppm), the $^{87}Sr/^{86}Sr$ mean value of the two well preserved shells gives a numerical age of 119.86 Ma (tab. 2).

*Mt. Motola*

One hundred and thirty-seven samples were analyzed for the Mt. Motola section (fig. 11). The $\delta^{13}C$ values range between -0.48‰ and +2.98‰, with an average value of +1.17‰.The first part of the smoothed $\delta^{13}C$ curve shows an overall rising trend, reaching a peak of about +2.2‰ at 62.6 m, about 16.6 m below the base of the “Palorbitolina limestones”. From this peak, $\delta^{13}C$ values decrease and then make a plateau, roughly corresponding to the “Palorbitolina limestones”, defined by values fluctuating around +1‰. After a very sharp decrease to 0‰, there is a broad positive excursion, peaking at about +2.8‰ some 11 m above the acme of *S. dinarica* and returning at values of about +1‰ 4 m above the *A. reicheli* level. The $\delta^{13}C$ curve terminates with a rising trend to a peak of about +1.6‰.

Four fragments of requienid shells, contained in a floatstone occurring immediately below the acme of *S. dinarica* (at 101.9 m from the base of the section), have been analysed for SIS. Their $^{87}Sr/^{86}Sr$ mean value gives a numerical age of 119.12 Ma (tab. 2).

*Mt. Coccovello*

One hundred and twenty-nine samples were analyzed for the Mt. Coccovello section (fig. 12). The $\delta^{13}C$ values range between -3.12‰ and +3.71‰, with an average value of +0.27‰.The first part of the $\delta^{13}C$ smoothed curve shows an overall decreasing trend, from +0.3‰ at the base to -1.3‰ at 44 m, with superimposed higher frequency fluctuations. Then there is a rising trend, peaking at about +1.8‰ 8 m below the base of the “Palorbitolina limestones”. From this peak, $\delta^{13}C$ values decrease to about +1‰ and stay around this value for most of the interval corresponding to the “Palorbitolina limestones”. Then there is a prominent positive excursion, peaking at +3.2‰ some 2 m above the top of

the "Palorbitolina limestones" and declining to a minimum of +0.6‰ 0.5 m above the top of the "Orbitolina level".

After a sharp positive shift to about +2.1‰, there is a very marked decrease to a minimum of -1.9‰, roughly corresponding to the *A. reicheli* level. The $\delta^{13}C$ curve terminates with a rebound to -1‰, followed by a new decrease to -2.2‰.

Three fragments of requienid shells from a floatstone at 86.4 m from the base of the section, 1 m above the first level of marls with *Mesorbitolina*, have been analysed for SIS. Their $^{87}Sr/^{86}Sr$ mean value gives a numerical age of 122.87 Ma (tab. 2).

Table 2 - Elemental concentration, Sr-isotope ratio and SIS age

| Section | Sample no. | Sr | Mg | Fe | Mn | $^{87}Sr/^{86}Sr$ | ±2 s.e. ($*10^{-6}$) | Age [Ma] | | |
|---|---|---|---|---|---|---|---|---|---|---|
| | | [ppm] | | | | | | Min | Mean | Max |
| **Motola** | MO 101.9A | 1232 | 2351 | 19.1 | 6.3 | 0.707313 | | | | |
| | MO 101.9B | 899 | 1053 | 26.6 | 1.4 | 0.707323 | | | | |
| | MO 101.9D | 949 | 1007 | 28.9 | 1.6 | 0.707309 | | | | |
| | MO 101.9E | 933 | 987 | 23.4 | 0.5 | 0.707308 | | | | |
| | | | | | **average** | **0.707313** | 7 | 118.4 | **119.1** | 119.9 |
| **Tobenna** | TB 2.5A* | 544 | 2732 | 181 | 19.2 | 0.707335 | | | | |
| | TB 2.5B | 832 | 1906 | 85.4 | 9.6 | 0.707327 | | | | |
| | TB 2.5C | 956 | 2052 | 81.7 | 8.5 | 0.707319 | | | | |
| | | | | | **average** | **0.707323** | 7 | 119.1 | **119.9** | 120.7 |
| **Coccovello** | CO 5.8 A | 1012 | 1172 | <0.5 | 2.3 | 0.707375 | | | | |
| | CO 5.8 C | 929 | 1036 | 32.7 | 3.2 | 0.707362 | | | | |
| | CO 5.8 B | 848 | 1008 | 66.5 | 7.4 | 0.707382 | | | | |
| | | | | | **average** | **0.707373** | 12 | 122.1 | **122.9** | 123.5 |
| **Croce** | CR 57.4 A | 1148 | 1920 | 94.4 | 2.4 | 0.707388 | | | | |
| | CR 57.4 B | 1289 | 1702 | 4.0 | 0.8 | 0.707429 | | | | |
| | CR 57.4 C | 1411 | 1967 | 110.5 | 0.0 | 0.707393 | | | | |
| | | | | | **average** | **0.707403** | 26 | 122.9 | **124.1** | 125.2 |

Numerical age from McArthur et al. (2001, look-up table version 4: 08/04) calculated by combining the statistical uncertainty of the mean of the isotopic values with the uncertainty of the seawater curve. *: diagenetically altered sample.

## *5.5 Discussion*

### *5.5.1 Reliability of the $\delta^{13}C$ record*

During the last two decades C-isotope stratigraphy has been successfully applied to high resolution dating and correlation of Cretaceous carbonate platforms (Wagner, 1990; Jenkyns, 1995; Ferreri et al., 1997; Masse et al., 1999; D'Argenio et al., 2004; Wissler et al., 2004; Parente et al. 2007; Burla et al., 2008; Vahrenkamp, 2010; Huck et al., 2011; Millán et al., 2011). On the other hand, it is well known that, besides post-depositional diagenetic alteration (Dickson and Coleman, 1980; Allan and Matthews, 1982; Lohmann, 1988; Marshall, 1992), biological fractionation and local palaeoceanographic conditions may cause the carbon isotope signal of platform carbonates to deviate from the open ocean

global signal (Weber and Woodhead, 1969; Patterson and Walter, 1994; see Immenhauser et al., 2008, for a recent review). A recent study concluded that, in Kimmeridgian shallow water carbonates of the Jura Mountains, the general trend of $\delta^{13}C$ values faithfully record the long-term global variations of the open ocean while higher order fluctuations "might result from variations in local environmental conditions on the shallow platform" (Colombié et al., 2011).

Therefore, before attempting a correlation with the reference curves of pelagic and hemipelagic successions, we tried to assess if the stable isotope record of the studied successions is significantly biased by diagenesis and/or by local environmental conditions.

Below subaerial exposure surfaces $\delta^{13}C$ values are commonly depleted, implying the influence of soil-derived $CO_2$, while $\delta^{18}O$ values may be enriched because of the preferential removal of $^{16}O$ in the pore waters through evaporation (Allan and Matthews, 1982; Joachimski, 1994).

Diagenesis in the vadose zone is generally characterized by depleted $\delta^{18}O$ values and highly variable $\delta^{13}C$. Strong covariation between $\delta^{13}C$ and $\delta^{18}O$ is taken as proof of diagenetic alteration of the stable isotope signal under the influx of meteoric water in the mixing zone (Allan and Matthews, 1982), or as a trend of progressively decreasing alteration within the freshwater phreatic zone (Swart, 2011).

The scatter plots of carbon and oxygen isotope ratios (fig. 13) show that the covariance between $\delta^{13}C$ and $\delta^{18}O$ values is very low to moderate for the five studied sections ($r = 0.01–0.46$). However, some lithofacies associations show higher correlation coefficients (tab. 3) that could be partly the result of mixing-zone diagenesis or of alteration within the freshwater phreatic zone. Some very negative $\delta^{13}C$ values, especially at Mt. Coccovello and Mt. Tobenna, are associated with subaerial exposure surfaces. Evaporation during exposure is probably also responsible for $\delta^{18}O$ values >0‰ in the first part of the Mt. Tobenna section. Conversely, some very depleted $\delta^{18}O$ values, especially at Mt. Motola and in the upper part of the Mt. Tobenna section, are seemingly due to vadose diagenesis.

Summing up, the effects of diagenesis are certainly seen in our isotopic records. They are probably responsible for some high-frequency fluctuations, defined by one or a few data points, but they are not so pervasive as to distort completely the pristine marine signal. The scatter plots of carbon and oxygen isotope ratios show also that there is no clear separation between the data points of the different lithofacies associations (fig. 13). This suggests that variations in $\delta^{13}C$ are not the result of facies changes. The bias of local palaeoenvironmental conditions could have been partly counteracted by the fact that we did not use bulk samples but strived to sample the micritic matrix also in the grainy facies. On the other hand, the lack of a strict relationship between facies type and $\delta^{13}C$ has been observed also in the recent sediments of the Great Bahama Bank (Swart et al., 2009).

With the exception of Mt. Coccovello, the $\delta^{13}C$ and $\delta^{18}O$ mean values of the studied sections fall within the range of Barremian–Aptian seawater (taken from the "low-latitude" biotic calcite record of Prokoph et al., 2008) (fig. 14, tab. 4). Apart from Mt. Raggeto, whose samples plot almost entirely in the field of pristine Barremian-Aptian calcite, a tail of more depleted values is observed in all the other sections and especially for the Mt. Tobenna and Mt. Coccovello sections (fig. 13). This pattern conforms to the facies distribution, indicating that Mt. Raggeto is the most open marine among the studied sections, followed by Mt. Croce. The other sections show more restricted facies and were located in a more inner platform position. A similar pattern of more negative values in the most restricted sections has been observed also in the Cenomanian–Turonian platform carbonates of the ACP (Parente et al., 2007).

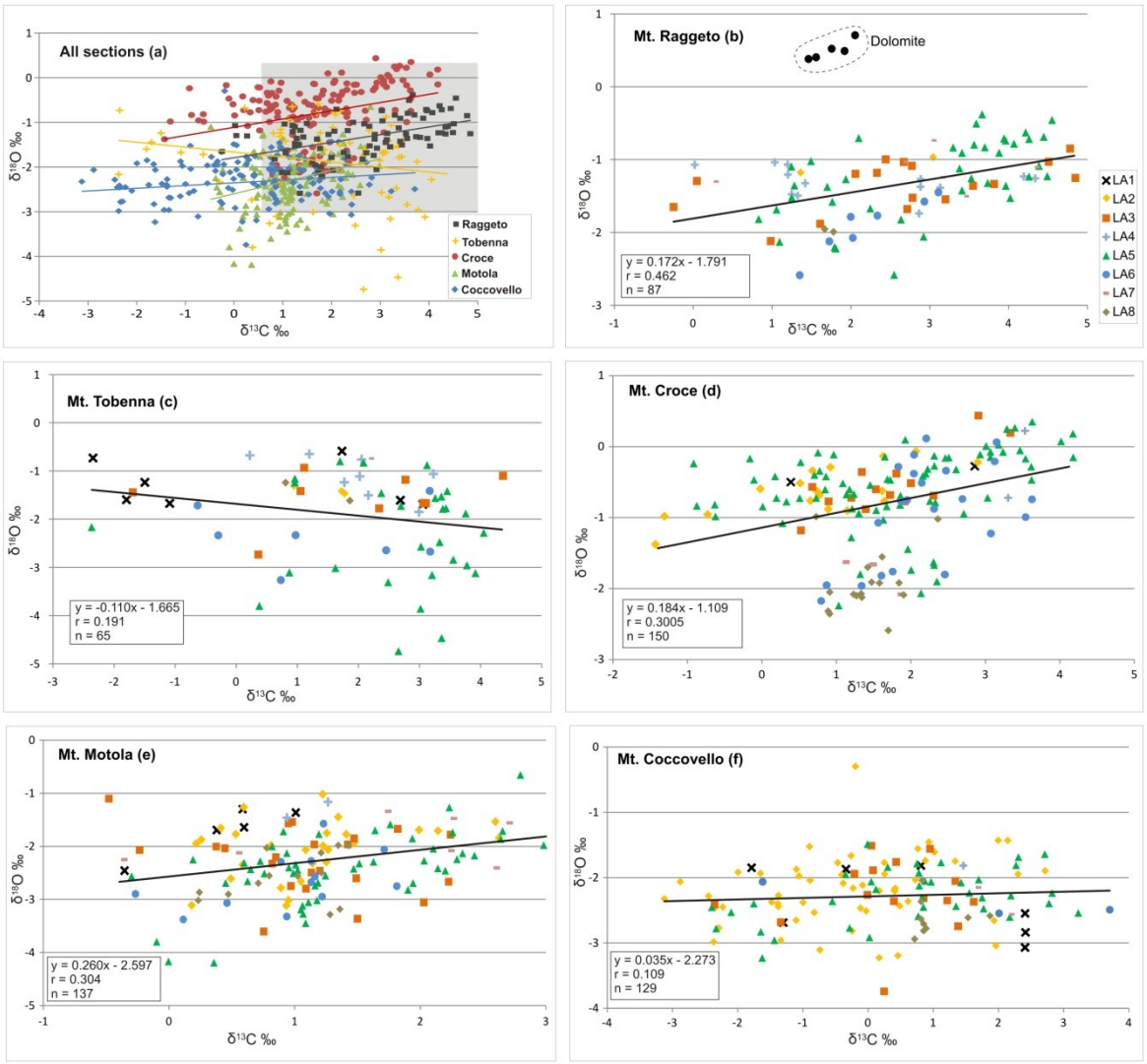


**Figure 13** - Cross-plots of $\delta^{13}C$ vs. $\delta^{18}O$ for the whole dataset (a) and for each studied section (b-f). The all-lithofacies dataset (a) shows very low to moderate covariance (r = 0.01-0.46). Supratidal and intertidal lithofacies associations show higher covariance of stable isotope ratios (diagrams b–c; see also tab. 2. On the other hand, there is no clear relation between lithofacies and isotopic value. The shaded rectangle in diagram (a) indicates the range of well-preserved biotic calcite of shallow marine tropical-subtropical carbonates (from Prokoph et al., 2008).

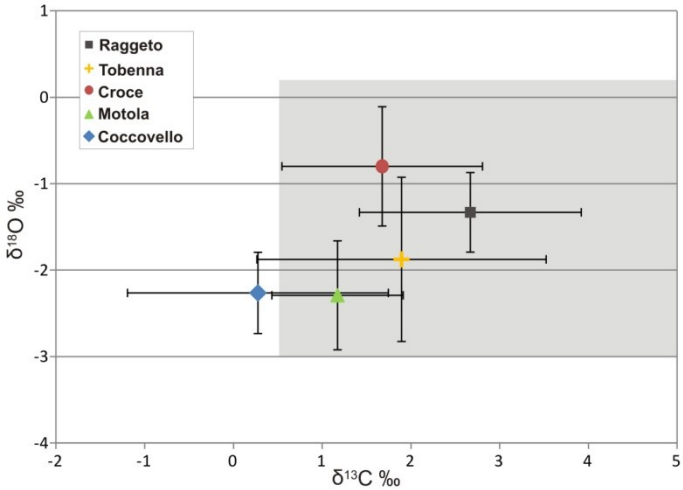


**Figure 14** - Plot of the mean ± standard deviation of carbon and oxygen isotope ratios for each studied section. With the exception of Mt. Coccovello, the $\delta^{13}C$ and $\delta^{18}O$ mean values of the studied sections fall

within the range of Barremian–Aptian seawater, represented by the "low-latitude" biotic calcite record of Prokoph et al. (2008).

Table 3 - Statistical results for C and O isotopes covariation in the studied sections

| Section | LA | n | r | a | b |
|---|---|---|---|---|---|
| Raggeto | LA1 | 0 | * | * | * |
| | LA2 | 2 | * | * | * |
| | LA3 | 17 | 0.51 | 0.12 | -1.66 |
| | LA4 | 13 | 0.30 | -0.04 | -1.20 |
| | LA5 | 40 | 0.57 | 0.26 | -2.02 |
| | LA6 | 7 | 0.93 | 0.56 | -3.16 |
| | LA7 | 6 | 0.15 | 0.02 | -1.23 |
| | LA8 | 2 | * | * | * |
| | **ALL** | **87** | **0.46** | **0.17** | **-1.80** |
| Tobenna | LA1 | 7 | 0.19 | -0.04 | -1.29 |
| | LA2 | 3 | * | * | * |
| | LA3 | 9 | 0.24 | 0.07 | -1.67 |
| | LA4 | 8 | 0.65 | -0.28 | -0.54 |
| | LA5 | 28 | 0.06 | -0.05 | -2.22 |
| | LA6 | 7 | 0.01 | 0.00 | -2.34 |
| | LA7 | 1 | * | * | * |
| | LA8 | 2 | * | * | * |
| | **ALL** | **65** | **0.19** | **-0.11** | **-1.66** |
| Croce | LA1 | 2 | * | * | * |
| | LA2 | 17 | 0.74 | 0.22 | 0.8 |
| | LA3 | 14 | 0.78 | 0.41 | -1.22 |
| | LA4 | 2 | * | * | * |
| | LA5 | 73 | 0.31 | 0.14 | -0.83 |
| | LA6 | 22 | 0.52 | 0.48 | -1.97 |
| | LA7 | 3 | * | * | * |
| | LA8 | 17 | 0.21 | 0.22 | -2.24 |
| | **ALL** | **150** | **0.30** | **0.18** | **-1.11** |
| Motola | LA1 | 5 | 0.93 | 0.86 | -2.07 |
| | LA2 | 27 | 0.33 | 0.28 | -2.36 |
| | LA3 | 22 | 0.29 | -0.26 | -1.98 |
| | LA4 | 2 | * | * | * |
| | LA5 | 49 | 0.6 | 0.5 | -3.11 |
| | LA6 | 12 | 0.5 | 0.44 | -3.07 |
| | LA7 | 7 | 0.35 | 0.13 | -2.1 |
| | LA8 | 13 | 0.34 | 0.36 | -2.93 |
| | **ALL** | **137** | **0.30** | **0.26** | **-2.6** |
| Coccovello | LA1 | 7 | 0.59 | -0.17 | -2.27 |
| | LA2 | 54 | 0.25 | 0.1 | -2.15 |
| | LA3 | 15 | 0.08 | 0.04 | -2.28 |
| | LA4 | 1 | * | * | * |
| | LA5 | 38 | 0.43 | 0.11 | -2.35 |
| | LA6 | 3 | * | * | * |
| | LA7 | 2 | * | * | * |
| | LA8 | 9 | 0.05 | 0.03 | -2.64 |
| | **ALL** | **129** | **0.01** | **0.03** | **-2.27** |

LA = lithofacies association; n = number of observations; r = Pearson correlation coefficient; a = slope of the regression line; b = intercept of the regression line; * = not calculated when n<5.

The smoothed $\delta^{13}C$ curves of figures 8 to 12 show that, besides the higher order fluctuations at metric to sub-metric scale, defined by only one or a few points, there are some isotopic trends and excursions which are defined by many data points and extend across intervals that are tens of meters thick. These major features of the $\delta^{13}C$ curves are

statistically significant because, at least in the Mt. Raggeto, Mt. Croce and Mt. Motola sections, they represent deviations from the mean value that are 2-3 times the standard deviation. Moreover, they persist across changes of lithofacies association, suggesting that they are not caused by local changes of palaeoenvironmental conditions. Finally, as discussed in the next paragraph, the major trends and excursions can be correlated between the five studied sections, suggesting that the forcing was, if not global, at least regional.

Table 4 - Mean and Standard deviation for carbon and oxygen isotope ratios of the studied sections.

| Section | MEAN ±STDEV | |
|---|---|---|
| | $\delta^{13}C$ ‰ | $\delta^{18}O$ ‰ |
| **Raggeto** | 2.67 ±1.25 | -1.33 ±0.46 |
| **Tobenna** | 1.89 ±1.63 | -1.87 ±0.95 |
| **Croce** | 1.67 ±1.13 | -0.79 ±0.69 |
| **Motola** | 1.17 ±0.74 | -2.29 ±0.63 |
| **Coccovello** | 0.27 ±1.47 | -2.26 ±0.47 |

### *5.5.2 The problem of gaps in the carbon isotope stratigraphy of carbonate platforms*

The stratigraphic archive has been described as containing more gaps than record (Ager, 1993). This is particularly true of shallow water carbonate platforms whose record is typically characterized by shallowing-upward cycles truncated by subaerial exposure surfaces. Shallowing-up sequences can be created by progradation or migration of sedimentary systems (e.g., Ginsburg, 1971; Pratt and James, 1986) but in many cases they are best interpreted as formed during one cycle of sea-level change (Strasser, 1991; Strasser et al., 1999). After emersion, a certain lag time elapses before prolific benthic carbonate production catches up (Tipper, 1997). As a result, shallowing upward cycles are expected to be asymmetric, with a thin transgressive deposit (including a lag) and a thicker highstand deposit (Strasser et al., 1999). High frequency cyclicity is generally superimposed on longer term cycles of sea-level changes. In simple "fully allocyclic" models, amplitude and duration of sea-level changes, together with subsidence rate, govern the thickness of elementary cycles, the duration of gaps and the distribution of "missed beats" in the different parts of the longer term cycle (Sadler, 1994). Thinner cycles and longer gaps, corresponding to missing elementary cycles, are expected during large scale lowstands. Conversely, thickest beds and shortest gaps are expected during large scale maximum flooding (Strasser et al., 1999). More complex distribution of gaps is obtained if stochastic models of carbonate production, transport, and deposition are applied (Burgess and Wright, 2003).

The presence of gaps can severely hamper the interpretation of the carbon isotope curves of carbonate platform sections. If elementary cycles represent precession cycles, any feature in the target $\delta^{13}C$ curve of the deep-water reference sections which lasts less than 20 kyr will have few, if any, chances of being recorded, due to the pervasive distribution of gaps at this timescale. Missed beats will conceal even longer traits of the target curve, especially during long term lowstands, expressed in the rock record as higher order sequence boundary zones (Strasser et al., 2000).

A Milankovitch cyclicity has been inferred for the shallow water Barremian–Aptian carbonates of the ACP (D'Argenio et al., 2004 and references therein). A 20 kyr duration, corresponding to the precession cycle, has been inferred for the elementary cycles. Higher order cycles, expressed as bundles and superbundles of elementary cycles, have been

interpreted as controlled respectively by the 100 kyr and 400 kyr eccentricity cycle. Based on high resolution cyclostratigraphic correlation with the Serra Sbregavitelli section, showing the most open marine record, many missed beats were identified in the other sections at the cycle, bundle and superbundle scale. The longest inferred gaps are of about 500 kyr in the Mt. Raggeto section and up to 1 Myr in the Mt. Tobenna-Mt. Faito composite section (see figure 8 in D'Argenio et al., 2004). Such very long gaps may potentially hide also the major features of the reference $\delta^{13}C$ curve, considering that a duration of about 1.2 Myr has been estimated for the rising limb (stages C4–C6) of the positive CIE associated with the "Selli event" (Li et al., 2008; Malinverno et al., 2010).

### *5.5.3 Platform-to-basin chemostratigraphic correlation*

Assuming that the carbon isotope record of the five studied sections was not shaped by local palaeoenvironmental changes and diagenetic overprint, we attempted a chemostratigraphic correlation with the reference carbon isotope curve of the Cismon Apticore in the southern Alps (Menegatti et al., 1998; Erba et al., 1999) and with the composite curve of Herrle et al. (2004) from the Vocontian Basin of south-eastern France. For the nomenclature of the isotopic segments we refer to Wissler et al. (2003) for the Barremian–Early Aptian interval (B3–B8/A1–A3) and to Menegatti et al. (1998) for the isotopic excursion of the Selli event (C3–C7) (fig. 15).

A correlation between the carbon isotope curves of the studied sections is possible by using as tie points the last occurrence of *P. lenticularis*, the two acmes of *S. dinarica*, the "Orbitolina level" and the *A. reicheli* level. At Mt. Raggeto there are three positive $\delta^{13}C$ excursions at values > +3-4‰ between the "Palorbitolina limestones" and the FO of *A. reicheli*. The first excursion is rather short (it takes less than 10 m) and peaks a few meters above the last occurrence of *P. lenticularis*. A positive excursion of similar shape and amplitude, occurring in the same stratigraphic position, is observed also at Mt. Croce and at Mt. Coccovello. At Mt. Motola this positive excursion is seemingly truncated by a small gap, because there is only a minor positive peak at about +1‰, nearly corresponding with the LO of *P. lenticularis*. The Mt. Tobenna section starts above the LO of *P. lenticularis* and this first excursion is probably represented only by the small peak at +3‰ occurring at the base of the section.

We correlate the first positive excursion of the Mt. Raggeto curve with the A1-A2 segments of Wissler et al. (2003). This correlation is supported by the SIS numerical age of 124.1±1.1 Ma, corresponding to the *D. oglanlensis* ammonite zone, of the requienid level occurring 3 m below the LO of *P. lenticularis* at Mt. Croce. This is in agreement with the correlation of the Mt. Raggeto curve of Wissler et al. (2004) and is further supported by their magnetostratigraphic data, placing the M0 within superbundle R14, which corresponds to the top of the "Palorbitolina limestones" (Amodio et al., 2003). Accordingly, the distinctive negative trend preceding this positive excursion in the Mt. Croce, Mt. Motola and Mt. Coccovello sections can be correlated to the B7–B8 segments of Wissler et al. (2003). Chemostratigraphic correlation becomes less compelling for the lower part of these sections, mainly because of the lack of independent tie-points and because of the small amplitude of isotopic excursions in the reference curves (< 1‰). Nevertheless, a tentative correlation is supplied in figure 15, which suggests that the lowermost part of the Mt. Motola and Mt. Coccovello sections might extend into the Lower Barremian.

The second positive excursion of the Mt. Raggeto curve is much broader (nearly 30-40 m). It starts some 10 m above the LO of *P. lenticularis*, peaks at +4.9‰ at a level corresponding to the first acme of *S. dinarica*, and finishes with values close to 0‰ a few m below the second acme of *S. dinarica*. This second positive excursion is completely missing at Mt. Motola. In the other sections the rising limb and the peak interval

(corresponding to values above +4‰) are largely missing, while the decreasing limb is at least partly recorded in the Mt. Tobenna and Mt. Coccovello section, less in the Mt. Croce section. In these three sections the "Orbitolina level" occurs in what is left of the decreasing limb of this positive excursion. In agreement with Wissler et al. (2004; see also Ferreri et al., 1997) we correlate this second positive excursion with the positive CIE associated with the "Selli event". This correlation is also supported by the SIS ages of 119.9 Ma for a requienid bed 5.8 m below the "Orbitolina level" at Mt. Tobenna and of 119.2 Ma for a level immediately below the second acme of *S. dinarica* at Mt. Motola (fig. 15 and tab. 2). On the contrary, this correlation is at odds with the SIS age of 122.9 Ma obtained for a requienid level occurring 1 m above the first marls with *Mesorbitolina* at Mt. Coccovello (fig. 15 and tab. 2).

The third positive excursion of the Mt. Raggeto curve starts a few meters below the second acme of *S. dinarica*, peaks at about 4.5‰ and decreases to values <0‰ at the top of the section, close to the FO of *A. reicheli*. This positive excursion is well expressed in all the other sections but at Mt. Coccovello, where its rising limb and peak interval are truncated by a gap, whose occurrence is supported also by the truncated range of *S. dinarica* just above its second acme (fig. 15). The correlation of this excursion with the reference curve is more problematic. It could correspond to the broad positive excursion spanning the *P. melchioris*, *N. nolani* and the lower part of the *H. jacobi* ammonite zones in the composite $\delta^{13}C$ curve of the Vocontian basin (Herrle et al., 2004; Föllmi et al., 2006). Alternatively, it could embrace also the positive excursion spanning the Aptian-Albian boundary.

The chemostratigraphic correlation proposed above differs from the one we proposed in previous works, when the more complete Mt. Raggeto section was not yet included in our database (Di Lucia and Parente, 2008; Di Lucia, 2009). In particular, since we missed the most prominent positive excursion, which is fully recorded only at Mt. Raggeto, we misidentified the next positive excursion (the one starting above the "Orbitolina level") as the Selli event excursion. Our mistake stemmed from the impossibility of estimating correctly the duration of gaps, which are below biostratigraphic resolution, without making reference to a more complete section and with very few independent points of chronostratigraphic calibration (like SIS data or well dated biostratigraphic markers). This highlights once more the difficulty of applying carbon isotope stratigraphy in inherently incomplete and poorly dated shallow water carbonate platform sections.

### *5.5.4 Biostratigraphic criteria for the Selli event in central Tethyan carbonate platforms*

Chemostratigraphic correlation with the well dated carbon isotope curves of the Cismon core and of the Vocontian composite section allows individuating in the carbonate platform successions of the southern Apennines the segments corresponding to the OAE1a and to propose a set of biostratigraphic criteria to individuate the stratigraphic interval equivalent to the OAE1a in the carbonate platforms of the central and southern Tethys. These criteria will be particularly useful when carbon isotope stratigraphy is not available or when chemostratigraphic correlation is biased by low resolution or by the overprint of local palaeoceanographic processes and/or of early meteoric diagenesis. A survey of the recent literature shows that this is often the case in shallow water carbonate sections. For instance, some recently published carbon isotope curves from the Barremian–Aptian of the Adriatic-Dinaric carbonate platform show no evidence of the broad positive excursion associated with the Selli event and of the preceding negative shift (Tešović et al., 2011). In another case study, the OAE1a positive CIE is not present in the carbon isotope record of bulk/micritic matrix samples, while it is faithfully reproduced by the biotic calcite of rudist shells (Huck et al., 2010).

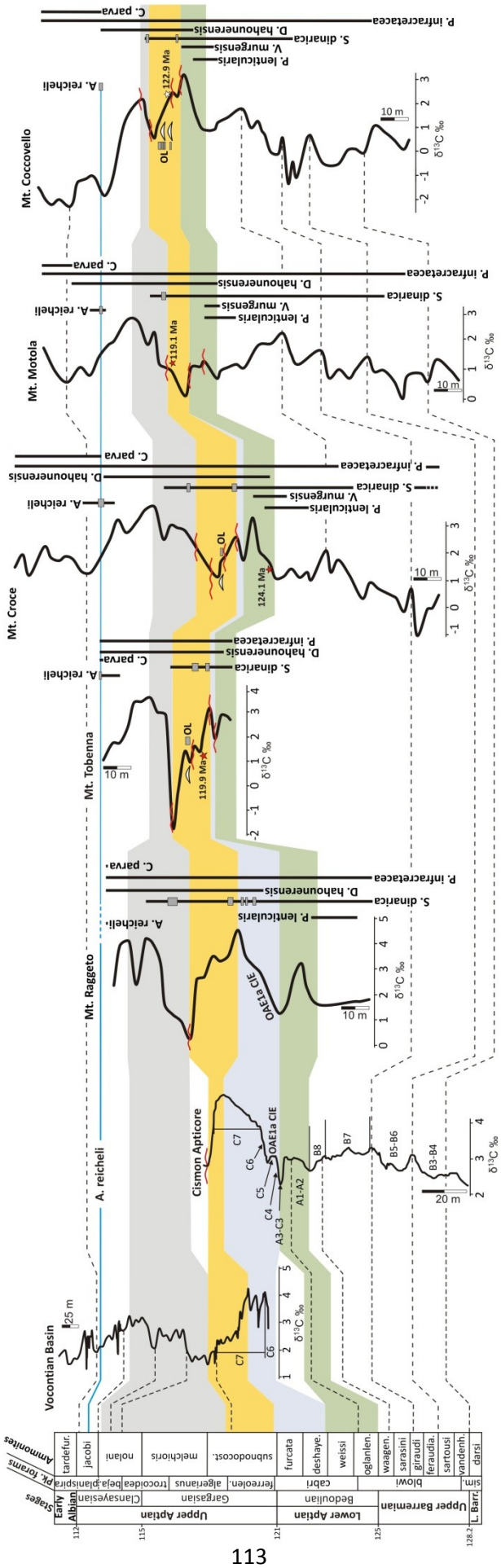
Mt. Coccovello
Mt. Motola
Mt. Croce
Mt. Tobenna
Mt. Raggeto
Vocontian Basin
A. reicheli
Cismon Apticore
OAE1a CIE
OL
122.9 Ma
119.1 Ma
124.1 Ma
119.9 Ma
10 m
20 m
25 m
δ13C ‰
C. parva
P. infracretacea
D. hahounerensis
S. dinarica
V. murgensis
P. lenticularis
A. reicheli
C5
C6
C7
A1-A2
A3-C3
B8
B7
B5-B6
B3-B4
Stages
Ammonites
Pk. foram.
Early Albian
Upper Aptian
Lower Aptian
Upper Barremian
L. Barr.
tardefur.
jacobi
nolani
melchioris
subnodocost.
furcata
deshaye.
weissi
oglanlen.
waagen.
sarasini
giraudi
feraudia.
sartousi
vandenh.
darsi
sim.
blowi
cabri
ferreolen.
algerianus
trocoidea
bejaiaensis
Gargasian
Clansayesian
Bedoulian

**Figure 15 (previous page)** - Chemostratigraphic correlation of the five sections of the Apenninic Carbonate Platform with the reference section of the Cismon Apticore (Belluno Basin, northern Italy) (Erba et al., 1999) and with the composite hemipelagic curve of south-eastern France (Herrle e al., 2004; Föllmi et al., 2006). This correlation uses as independent tie-points a Gargasian age for the "Orbitolina level"(see text) and the numerical ages of three levels dated by strontium isotope stratigraphy (filled red stars). The nomenclature of chemostratigraphic segments is from Wissler et al. (2003; B3–B8/A1–A3) and from Menegatti et al. (1998; C3–C7). The ammonite and planktonic foraminiferal biozones and their calibration to the Geological Time Scale are from Gradstein et al. (2004). The red stars indicate the SIS samples; the white star at Mt. Coccovello corresponds to a SIS age that is at odds with carbon isotope stratigraphy (diagenetically altered sample).

Based on the chemostratigraphic correlation of figure 15, the segment of decreasing $\delta^{13}C$ values leading to the C3 negative peak, which is taken as the onset of the Selli event, starts a few meters above the LO of *P. lenticularis* and *V. murgensis*. The C4-C6 segments, corresponding to the interval of enhanced accumulation of organic matter in deep-water sections, ends just below the first acme of *S. dinarica*, which roughly corresponds to the C7 segment of peak $\delta^{13}C$ values. The whole CIE associated with the OAE1a is bracketed in the ACP between the LO of *V. murgensis* and the "Orbitolina level".

These criteria are particularly useful because they are based on biostratigraphic events that are widely employed in the most popular biostratigraphic schemes of central and southern Tethyan carbonate platforms (Velić, 2007; Chiocchini et al., 2008). In particular, the acme of *S. dinarica* is easily picked in the field and is widely recognized in central Tethyan carbonate platforms (Carras et al., 2006 and references therein; Velić, 2007). The "Orbitolina level", containing *M. parva* and *M. texana*, has long been used as a bio-lithostratigraphic marker in the geological maps of southern Apennines.

### *5.5.5 Chronostratigraphic calibration of carbonate platform biostratigraphy*

The biozonations of the Lower Cretaceous carbonate platforms of the central Tethys (Apenninic, Adriatic and Gavrovo-Tripolitza platforms) are mainly based on calcareous algae and larger benthic foraminifera. The chronostratigraphic calibration of these schemes has always posed serious problems because ammonites, and calcareous plankton and nannoplankton, which are the pillars of Cretaceous chronostratigraphy, are notably absent from carbonate platform successions.

The problem of chronostratigraphic calibration has been explicitly acknowledged by some authors (De Castro, 1991; Chiocchini et al., 2008). Others (Bachmann and Hirsch, 2006; Velić, 2007) have anchored their biostratigraphic schemes to the chronostratigraphic ages of orbitolinid larger foraminifera, which have been established mainly in Northern Tethyan carbonate platforms.

We highlight several shortcomings in this indirect correlation:

–The precise isochrony of FOs and LOs of orbitolinid species between the northern and central-southern carbonate platforms has been never tested against independent evidence.

–Orbitolinids are generally found in discrete intervals and sometimes are totally lacking in inner platform facies. Namely, the flat low-conical species are generally found in marly or calcareous marly levels, which seemingly represent transgressive to maximum flooding intervals (Vilas et al., 1995; Immenhauser et al., 1999; Jones et al., 2004). The local range of these taxa could be related more to the occurrence of the appropriate facies, controlled by local to regional sea-level history, than to evolutionary processes of speciation and extinction.

–The chronostratigraphic calibration of orbitolinid biostratigraphy is still the matter of intense scientific debate, even in the areas where it has been first proposed, like the

Urgonian Platform of the northern Tethyan margin (Arnaud et al., 1998; Clavel et al., 2007; Föllmi, 2008; Conrad et al., 2011; Godét et al., 2011; Huck et al., 2011).

For all these reasons, we advocate the supremacy of chemostratigraphic correlation, used in this paper, to establishing the chronostratigraphic calibration of carbonate platform biostratigraphy.

The high-resolution chemostratigraphic correlation with the well-dated reference sections of the Cismon Apticore and of the Vocontian basin of south-eastern France is here used to establishing the chronostratigraphic age of the biostratigraphic events recognized in the carbonate platform successions of the southern Apennines (fig. 15). We refer to the lowest FO and to the highest LO, assuming that the small differences between the ranges observed in the three studied sections are the result of the lack of appropriate facies, of small gaps or of other sampling biases.

−The FO of *P. infracretacea* correlates with the lowermost Upper Barremian (*H. sartousi* ammonite zone). This species persists until the top of the five studied sections.

−The range of *P. lenticularis* spans from the uppermost Barremian (*P. waagenoides* zone) to the lowermost Aptian (upper part of the *D. oglanlensis* zone). In the studied sections the levels rich of *P. lenticularis* (LA8, "Palorbitolina limestones") mark a transgressive interval corresponding to the B8-A1 segments of the carbon isotope curves. Therefore, chemostratigraphy supports a correlation of the "Palorbitolina limestones" of southern Apennines with the "Couches inférieures à Orbitolines" of the French Vercors and with the "Lower Orbitolina Beds" of the northern Tethyan Helvetic platform (Arnaud et al., 1998; Clavel et al., 2002; Föllmi et al., 2007; Föllmi and Gainon, 2008).

−The range of *V. murgensis* straddles the Barremian-Aptian boundary (FO in the upper part of the *P. waagenoides* zone, LO in the lower part of the *D. weissi* zone).

−The FO of *D. hahounerensis* is close to the base of the Aptian (*D. oglanlensis* ammonite zone). The LO correlates with the Upper Aptian *H. jacobi* ammonite zone.

−The first acme of *S. dinarica* begins in latest Early Aptian (*D. furcata* zone) and straddles the Bedoulian-Gargasian boundary, terminating in the lower part of the *E. subnodosocostatum* zone. The second acme is roughly correlated with the lowermost part of the *P. melchioris* zone. The LO can be correlated with the upper part of the *N. nolani* ammonite zone.

−The "Orbitolina level" of the southern Apennines, containing an association of *M. parva* and *M. texana*, correlates with the upper part of the *E. subnodosocostatum* zone, confirming the middle Gargasian age proposed by Cherchi et al. (1978). A Gargasian age for the FO of *M. texana*, has been recently restated by Schroeder et al. (2010), and remains one of the tie points for the calibration of the Aptian biostratigraphy of central and southern Tethyan carbonate platforms (Simmons, 1994; Witt and Gökdağ, 1994; Bachmann and Hirsch, 2006; Velić, 2007). However, it is worth noting that in the northern Tethyan Helvetic carbonate platform *M. texana* has been found in the upper Schrattenkalk Fm. (Schroeder in Schenk, 1992; Schroeder et al, 2007), which has been dated by carbon isotope stratigraphy and ammonites as middle Early Aptian, close to the boundary between the *D. weissi* and the *D. deshayesi* zones (Föllmi, 2008; Föllmi and Gainon, 2008). The "Orbitolina level" of the southern Apennines cannot be correlated with the "Couches supérieures à orbitolines" of the French Vercors and the "Upper Orbitolina Beds" of the Helvetic Alps (Linder et al., 2006; Föllmi and Gainon, 2008). Instead, a correlation with the "Niveau Fallot" of the Vocontian Basin (Friedrich et al., 2003), recently proposed by Raspini (2011), is compatible with our chemostratigraphic data.

–The *A. reicheli* level, consisting of a bed rich of fully developed specimens of this alveolinid species, is correlated with the middle part of the *H. jacobi* zone (Upper Aptian). In the Mt. Motola, Mt. Tobenna and Mt. Croce section this level is preceded by some meters of limestones with a few small primitive specimens of *A. reicheli*.

–The FO of *C. parva* is correlated with the middle part of the *H. jacobi* zone, in the Upper Aptian.

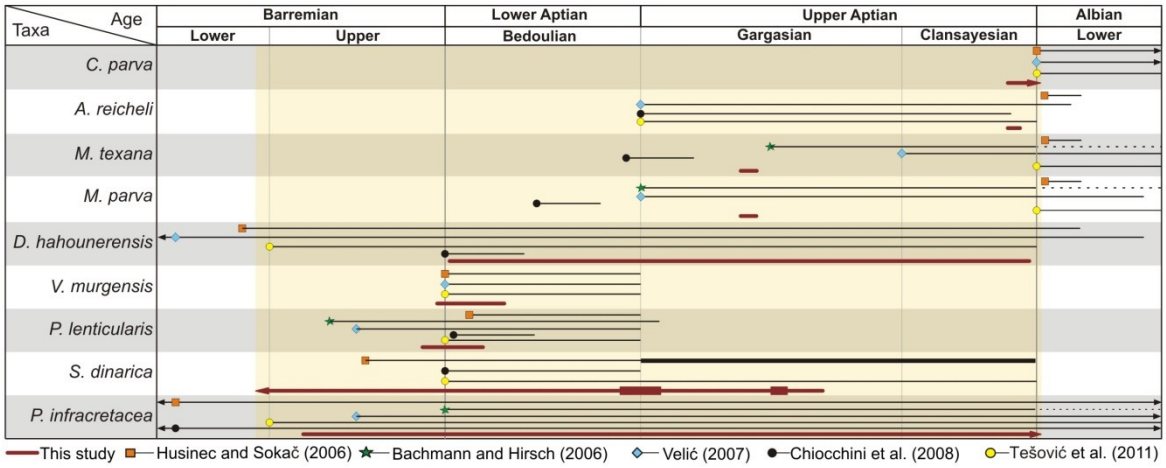


**Figure 16** - Chronostratigraphic calibration of the Apenninic Carbonate Platform biostratigraphy. The calibration is based on the chemostratigraphic correlation with well-dated basinal sections (see figure 15). The chronostratigraphic calibration of the same biostratigraphic events, proposed by previous works on the Apenninic and other central and southern Tethyan carbonate platforms, is given for comparison. The shaded field indicates the chronostratigraphic interval covered by the sections studied in this paper.

In the scheme of figure 16, the chronostratigraphic ranges supported by our chemostratigraphic correlation are compared with the ranges given for the same species in other biostratigraphic schemes of central and southern Tethyan carbonate platforms (Bachmann and Hirsch, 2006; Husinec and Sokač, 2006; Velić, 2007; Chiocchini et al., 2008; Tešović et al., 2011).

Some discrepancies emerge, which might be at least partly due to a slight diachrony of the biostratigraphic events between different carbonate platforms. However, it must be re-emphasized that the chronostratigraphic calibration proposed in this paper is the first direct calibration based on isotope stratigraphy. For all the other biostratigraphic schemes cited above, the chronostratigraphic calibration is largely based on the ages proposed for orbitolinids in the carbonate platforms of the Northern Tethyan margin. This indirect chronostratigraphic calibration might be biased for several reasons, as discussed above.

## *5.6 Conclusions*

The geological archive of the resilient central and southern Tethyan carbonate platforms contains valuable information on the response of tropical and subtropical neritic ecosystems to the palaeoenvironmental perturbations associated with the massive injection of $CO_2$ into the Atmosphere–Ocean system during the early Aptian OAE1a. The first step to unlock this archive is the precise chronostratigraphic dating and correlation of shallow water carbonate successions with deep-water successions, which represent the reference record of palaeoceanographic events. In this paper we fulfill this task by integrating high-resolution carbon isotope stratigraphy and biostratigraphy, with additional support by strontium isotope stratigraphy on a limited set of samples. Chemostratigraphic correlation of five sections of the Apenninic Carbonate Platform of southern Italy with the Cismon

Apticore and the composite section of the Vocontian Basin permits the chronostratigraphic calibration of carbonate platform biostratigraphy across the Barremian–Aptian interval.

The main result derived from this calibration is the definition of biostratigraphic criteria to individuate, in the carbonate platforms of the central and southern Tethys, the stratigraphic interval equivalent to the OAE1a. The interval of decreasing $\delta^{13}C$ values preceding the C3 negative peak, which marks the onset of the Selli event, starts a few meters above the LO of *P. lenticularis* and just above the LO of *V. murgensis*. The C4-C6 segments, which correspond in deep-water sections to the interval of black shales deposition, ends just below the first acme of *S. dinarica*. The second acme of this species roughly corresponds to the C7 segment of peak $\delta^{13}C$ values. The "Orbitolina level" marks the return the pre-excursion values at the end of the broad positive CIE associated with the OAE1a.

Another valuable result is the definition of a biostratigraphic criterion to spike the Barremian–Aptian boundary in central-southern Tethyan carbonate platforms. According to our calibration, the boundary is very closely approximated by the first occurrence of *V. murgensis* and *D. hahounerensis*.

In all the biostratigraphic schemes published so far for the ACP and other central and southern Tethyan platforms, the chronostratigraphic calibration was anchored to the ages established for selected taxa of orbitolinid foraminifera in the carbonate platform of the Northern Tethyan margin. We propose the first chronostratigraphic calibration constrained by carbon and strontium isotope stratigraphy. Chemostratigraphy is being successfully applied to Cretaceous carbonate platforms. Its integration with biostratigraphy hold the promise of producing standard biozonations, based on larger foraminifera and calcareous algae, perfectly tied to the chronostratigraphic scale. This would open the possibility of fully exploiting the valuable archive of palaeoenvironmental changes preserved by Cretaceous carbonate platforms.

## *5.7 References*


Ager D.V. (1993). The Nature of the Stratigraphical Record, 3rd ed. xiv+151 pp., John Wiley & Sons, 1993.

Allan J.R. and Matthews R.K. (1982). Isotope signature associated with early meteoric diagenesis. Sedimentology 29, 797–897.

Amodio S., Buonocunto F.P., D'Argenio B., Ferreri V. and Gorla L. (2003). Cyclostratigraphy of Cretaceous shallow water carbonates. Case histories from central and southern Italy, AAPG Search and Discovery Article, #90017.

Arnaud H., Arnaud-Vanneau A., Blanc-Alétru M.-C., Adatte T., Argot M., Delanoy G., Thieuloy J.-P., Vermeulen J., Virgone A., Virlouvet B. and Wermeille S. (1998). Répartition stratigraphique des orbitolinidés de la plate-forme urgonienne subalpine et jurassiene (SE de la France), Géologie Alpine 74, 3–89.

Arthur M.A., Brumsack H.-J., Jenkyns H.C. and Schlanger S.O. (1990). Stratigraphy, geochemistry, and paleoceanography of organic carbon-rich Cretaceous sequences, in: Ginsburg, N. and Baudoin, B. (Eds.): Cretaceous Resources, Events and Rhythms. Kluwer, Dordrecht, 75–119..

Bachmann M. and Hirsch F. (2006). Lower Cretaceous carbonate platform of the eastern Levant (Galilee and the Golan Heights): stratigraphy and second-order sea-level change, Cret. Res. 27, 487–512.

Bonardi G., D'Argenio B. and Perrone V. (1988). Carta Geologica dell'Appennino meridionale. SELCA, Firenze.

Bosellini A. (2002). Dinosaurs "re-write" the geodynamics of the eastern Mediterranean and the paleogeography of the Apulia Platform. Earth Sci. Rev. 59, 211–234.

Buonocunto F.P. (1998). Litostratigrafia di alta risoluzione nel Cretacico di piattaforma Carbonatica dell'Appennino Campano. Ph.D. Thesis, Università Federico II, Napoli, 184 p.

Burgess P. M. and Wright V.P. (2003). Numerical forward modelling of carbonate platform dynamics: An evolution of complexity and completeness in carbonate strata. J. Sed. Res. 73, 637–652.

Burla S., Heimhofer U., Hochuli P.A., Weissert H. and Skelton P. (2008). Changes in sedimentary patterns of coastal and deep sea successions from the North Atlantic (Portugal) linked to Early Cretaceous environmental change. Palaeogeography, Palaeoclimatology, Palaeoecology 257, 38–57.

Carannante G., Graziano R., Ruberti D. and Simone L. (1997). Upper Cretaceous temperate-type open shelves from northern (Sardinia) and southern (Apennines-Apulia) Mesozoic Tethyan margins. In: James, N.P. and Clarke, J. (Eds.), Cool-water carbonates, SEPM Spec. P., 56, 309–325, 1997.

Carras N., Conrad M.A. and Radoičić R. (2006). Salpingoporella, a common genus of Mesozoic Dasycladales (calcareous green algae). . 25, 457–51.

Cherchi A., De Castro P. and Schroeder R. (1978). Sull'etá dei livelli a Orbitolinidi della Campania e delle Murge Baresi (Italia meridionale). Boll. Soc. Nat., Napoli, 87, 363–385.

Chiocchini M., Farinacci A., Mancinelli A., Molinari V.and Potetti M. (1994). Biostratigrafia a foraminiferi, dasicladali e calpionelle delle successioni carbonatiche mesozoiche dell'Appennino centrale (Italia). Studi Geologici Camerti, Volume Speciale, 1994, "Biostratigrafia dell'Italia centrale", 9–129.

Chiocchini M., Chiocchini R.A. Didaskalou P. and Potetti M. (2008). Microbiostratigrafia del Triassico superiore, Giurassico e Cretacico in facies di piattaforma carbonatica del Lazio centro-meridionale e Abruzzo: revisione finale. Mem. Descr. Carta Geol. d' It., 5–170.

Clavel B., Schroeder R., Charollais J., Busnardo R., Martin Closas C., Decrouez D., Sauvagnat J. and Cherchi A. (2002). Les "Couches inférieures à orbitolines" (Chaînes subalpines septentrionales): mythe ou réalité?. Revue de Paléobiologie, Genève, 21, 865–871.

Clavel B., Charollais J., Conrad M., Jan du Chêne R., Busnardo R., Gardin S., Erba E., Schroeder R., Cherchi A., Decrouez, D., Granier B., Sauvagnat J. and Weidmann M. (2007). Dating and progradation of the Urgonian limestone from the Swiss Jura to southeast France. Zeitschrift der Deutschen Gesellschaft für Geowissenschaften, 158, 4, 1025–1062.

Colombié C., Lécuyer C. and Strasser A. (2011). Carbon- and oxygen-isotope records of palaeoenvironmental and carbonate production changes in shallow-marine carbonates (Kimmeridgian, Swiss Jura). Geol. Mag. 148 (1), 133–153.

Conrad M., Clavel B., Granier B., Charollais J., Busnardo R., Erba E., Gardin S., Jan du Chêne R., Decrouez D., Cherchi A., Schroeder R., Sauvagnat J. and Weidmann M. (2011). "Stratigraphic, sedimentological and palaeoenvironmental constraints on the rise of the Urgonian platform in the western Swiss Jura" by A. Godet et al. (2010) Sedimentology 57, 1088–1125: Discussion, Sedimentology, doi: 10.1111/j.1365-3091.2011.01277.x, 2011.

D'Argenio B., De Castro P., Emiliani C. and Simone L. (1975). Bahamian and Apenninic limestones of identical lithofacies and age. AAPG Bull. 59, 524–533.

D'Argenio B. and Alvarez W. (1980). Stratigraphic evidence for crustal thickness changes on the southern Tethyan margin during the Alpine cycle. GSA Bull., 91, 12, 681–689.

D´Argenio B., Ferreri V., Ardillo F and Buonocunto F.P. (1993). Microstratigrafia e stratigrafia sequenziale. Studi sui depositi di piattaforma carbonatica. Cretacico del Monte Maggiore (Appennino Meridionale). Boll. Soc. Geol. Ital. 112, 739–749.

D'Argenio B., Ferreri V., Iorio M., Raspini A. and Tarling D.H. (1999a). Diagenesis and remanence acquisition in the Cretaceous carbonates of Monte Raggeto, Southern Italy, in Tarling, D.H. and Turner, P., (Eds): Palaeomagnetism and Diagenesis in Sediments: Geol. Soc. Lond., Spec. P. 151, 147–156.

D'Argenio B., Ferreri V., Raspini A., Amodio S. and Buonocunto F.P.(1999b). Cyclostratigraphy of a carbonate platform as a tool for high-precision correlation. Tectonophysics, 315, 357–385.

D'Argenio B., Ferreri V., Weissert H., Amodio S., Buonocunto F.P. and Wissler L. (2004). A multidisciplinary approach to global correlation and geochronology: the Cretaceous shallow water carbonates of southern Apennines, Italy. In: D'Argenio, B., Fischer, A.G., Premoli Silva I., Weissert, H. and Ferreri, V. (Eds.): Cyclostratigraphy: Approaches and Case Histories, SEPM Spec. P., 81, 103–122.

Davey S.D. and Jenkyns H.C. (1999). Carbon-isotope stratigraphy of shallow water limestones and implications for the timing of Late Cretaceous sea-level rise and anoxic events (Cenomanian–Turonian of the peri-Adriatic carbonate platform, Croatia). Eclogae Geol. Helv. 92, 163–170.

De Castro P. (1963). Nuove osservazioni sul livello ad Orbitoline in Campania. Boll. Soc. Nat. Napoli, 71, 103–135.

De Castro P. (1991). Mesozoic, in: Barattolo, F., De Castro, P. and Parente, M. (eds.): 5th International Symposium on Fossil Algae. Field Trip Guide-Book, Giannini, Napoli, 21–38.

Dickson J.A.D. and Coleman M.L. (1980). Changes in carbon and oxygen isotope composition during limestone diagenesis. Sedimentology 27, 107–118.

Di Lucia M. (2009). Il record dei cambiamenti globali nelle piattaforme del Cretacico medio dell´Appennino meridionale. PhD thesis, Università Federico II, Napoli, http://www.fedoa.unina.it/3342/.

Di Lucia M. and Parente M. (2008). Carbon-isotope stratigraphy of upper Barremian-lower Albian shallow water carbonates of southern Apennines (Italy): high-resolution correlation with deep-water reference sections. Rendiconti Online Soc. Geol. It. 2, 65–70.

Erba E., Channell J.E.T., Claps M., Jones C., Larson R.L., Opdyke B.N., Silva I.P., Riva A., Salvini G. and Torricelli S. (1999). Integrated stratigraphy of the Cismon APTICORE (Southern Alps, Italy): a "reference section" for the Barremian–Aptian interval at low latitudes. J. Foramin. Res. 29, 371–391.

Erba E., Bottini C., Weissert H.J. and Keller C.E. (2010). Calcareous Nannoplankton Response to Surface-Water Acidification around Oceanic Anoxic Event 1a. Science. 329, 428–432.

Ferreri V., Weissert H., D'Argenio B. and Buonocunto F.P. (1997). Carbon-isotope stratigraphy: a tool for basin to carbonate platform correlation. Terra Nova 9, 57–61.

Föllmi K.B. (2008). A synchronous, middle Early Aptian age for the demise of the Helvetic Urgonian platform related to the unfolding oceanic anoxic event 1a («Selli event»). Revue de Paléobiologie, Genève, 27, 2, 461–468.

Föllmi K.B., Godet A., Bodin S. and Linder P. (2006). Interactions between environmental change and shallow water carbonate buildup along the northern Tethyan margin and their impact on the Early Cretaceous carbon isotope record. Paleoceanography, 21, 4211–4216.

Föllmi K.B., Bodin S., Godet A., Linder P. and van de Schootbrugge B. (2007). Unlocking paleo-environmental information from early Cretaceous shelf sediments in the Helvetic Alps: stratigraphy is the key!.Swiss J. Geosci. 100, 349–369.

Föllmi K.B. and Gainon F. (2008). Demise of the northern Tethyan Urgonian carbonate platform and subsequent transition towards pelagic conditions: the sedimentary record of the Col de la Plaine Morte area, central Switzerland. Sediment. Geol. 205, 142–159.

Friedrich O., Reichelt K., Herrle J. O., Lehmann J., Pross J. and Hemleben C. (2003). Formation of the Late Aptian Niveau Fallot black shales in the Vocontian Basin (SE France): evidence from foraminifera, palynomorphs, and stable isotopes. Mar. Micropaleontol. 49, 65–85.

Frijia G., Parente M. and Iannace A. (2005). Thermal maturity of the Southern Apenninic Platform Unit (Southern Italy): constraints from Rock-Eval Pyrolysis $T_{max}$ data. Atti Ticinensi di Scienze della Terra, serie speciale, 10, 95–98.

Frijia G. and Parente M. (2008). Strontium isotope stratigraphy in the upper Cenomanian shallow water carbonates of southern Apennines: Short-term perturbations of marine $^{87}Sr/^{86}Sr$ during the oceanic anoxic event 2. Palaeogeography, Palaeoclimatology, Palaeoecology 261, 15–29.

Ginsburg R.N. (1971). Landward movement of carbonate mud: new model for regressive cycles in carbonates. Bull. Am. Assoc. Pet. Geol. 55, 340.

Godet A., Föllmi K.B., Bodin S., De Kaenel E., Matera V., Adatte T., Arnaud-Vanneau A., Arnaurd H. and Vermeulen J. (2011). A Late Barremian age for the onset of Urgonian-type facies in the Swiss Jura Mountains. Reply to the discussion by Conrad et al. on "Stratigraphic, sedimentological and palaeoenvironmental constraints on the rise of the Urgonian Platform in the western Swiss Jura'' by Godet et al. (2010), Sedimentology, 57, 1088–1125. Sedimentology, doi:10.1111/j.1365-3091.2011.01276.x, 2011.

Gradstein F.M., Ogg J.G. and Smith A.G. (2004). (Eds.): A Geologic Time Scale 2004. Cambridge University Press, 589 pp.

Hallock P. (2001). Coral reefs, carbonate sediment, nutrients, and global change, in: Stanley, G.D. (Ed.): Ancient reef ecosystems: their evolution, paleoecology and importance in earth history, New York: Kluwer Academic/Plenum Publishers, 388–427.

Herrle J. O., Kößler P., Friedrich O., Erlenkeuser H. and Hemleben C. (2004). High-resolution carbon isotope records of the Aptian to lower Albian from SE France and the Mazagan Plateau (DSDP Site 545), A stratigraphic tool for paleoceanographic and paleobiologic reconstruction. Earth Planet. Sci. Lett. 218, 149–161.

Hillgärtner H., van Buchem F.S.P., Gaumet F., Razin P., Pittet B., Grötsch J. and Droste H.J. (2003). The Early Cretaceous carbonate margin of the eastern Arabian platform (northern Oman): Sedimentology, sequence stratigraphy and environmental change. J. Sed. Res. 73, 756–773.

Huck S., Rameil N., Korbar T., Heimhofer U., Wieczorek T.D. and Immenhauser A. (2010). Latitudinally different responses of Tethyan shoal-water carbonate systems to the Early Aptian oceanic anoxic event (OAE 1a). Sedimentology 57, 1585–1614.

Huck S., Heimhofer U., Rameil N., Bodin S. and Immenhauser, A. (2011). Strontium and carbon-isotope chronostratigraphy of Barremian-Aptian shoal-water carbonates: Northern Tethyan platform drowning predates OAE 1a. Earth Planet. Sc. Lett., doi: 10.1016/j.epsl.2011.02.031.

Husinec A. and Sokač B. (2006). Early Cretaceous benthic associations (foraminifera and calcareous algae) of a shallow tropical-water platform environment (Mljet Island, southern Croatia). Cret. Res. 27, 418–441.

Immenhauser A., Schlager W., Burns S.J., Scott R.W., Geel T., Lehmann J., van der Gaast S. and Bolder-Schrijver L.J.A. (1999). Late Aptian to Late Albian sea level fluctuations constrained by geochemical and biological evidence (Nahr Umr Formation, Oman). J. Sed. Res. 69, 434–446.

Immenhauser A., Hillgärtner H. and van Bentum E. (2005). Microbial–foraminiferal episodes in the Early Aptian of the southern Tethyan margin: ecological significance and possible relation to oceanic anoxic event 1a. Sedimentology 52, 77–99.

Immenhauser A., Holmden C. and Patterson W.P. (2008). Interpreting the Carbon-Isotope Record of Ancient Shallow Epeiric Seas: Lessons from the Recent. In: Pratt, B.R. and Holmden, C., (Eds.): Dynamics of Epeiric Seas: Geological Association of Canada Special Publication, 48, 135–174.

Jenkyns H.C. (1995). Carbon-isotope stratigraphy and paleoceanographic significance of the Lower Cretaceous shallow water carbonates of Resolution Guyot, mid-Pacific Mountains, in: Winterer, E.L., Sager, W.W., Firth, J.V. and Sinton, J.M. (Eds.): Proceedings of the Ocean Drilling Program, Scientific Results, 143, Ocean Drilling Program, College Station, TX, 99–104..

Joachimsky M. (2004). Subaerial exposure and deposition of shallowing upward sequences: evidence from stable isotopes of Purbeckian peritidal carbonates (basal Cretaceous), Swiss and French Jura Mountains. Sedimentology 41**,** 805–824.

Jones B., Simmons M. and Whittaker J. (2004). Chronostratigraphic and paleoenvironmental significance of agglutinated and associated larger benthonic foraminifera from the Lower to ‘‘Middle’’ Cretaceous of the Middle east. In: Proceeding of the Sixth International Workshop on Agglutinated Foraminifera, M. Bubik, M. and Kaminski, M.A. (Eds), Grzybowski Found. Spec. Publ., 8, 229–235.

Larson R.L. and Erba E. (1999). Onset of the mid-Cretaceous greenhouse in the Barremian-Aptian: Igneous events and the biological, sedimentary, and geochemical responses. Paleoceanography 14, 663–678.

.P., Osleger D.A., Arthur M.A., Bice D.M., Herbert T.D., Erba E. and Premoli Silva I. (2008). Toward an orbital chronology for the early Aptian Oceanic Anoxic Event (OAE1a, ~120 Ma). EPSL 271, 88–100..

Linder P., Gigandet J., Hüsser J.L., Gainon F. and Föllmi K.B. (2006). The early Aptian Grünten Member: description of a new lithostratigraphic unit of the Helvetic Garschella Formation. Eclogae Geol. Helv. 99, 327–341.

Lohmann K.C. (1988). Geochemical patterns of meteoric diagenetic systems and their application to studies of paleokarst. In: James, N.P. and Choquette, P.W., (Eds.): Paleokarst. Springer, Berlin, 58–80.

Malinverno A., Erba E. and Herbert T.D. (2010). Orbital tuning as an inverse problem: Chronology of the early Aptian oceanic anoxic event 1a (Selli Level) in the Cismon APTICORE. Paleoceanography 25, PA2203, doi: 10.1029/2009PA001769.

Marshall J.D. (1992). Climatic and oceanographic isotopic signals from the carbonate rock record and their preservation. Geol. Mag. 129, 143–160.

Masse J.P., El Albani A. and Erlenkeuser H. (1999). Stratigraphie isotopique ($\delta^{13}C$) de l’Aptien inférieur de Provence (SE France): Application aux corrélations plate-forme/bassin. Eclogae Geol. Helv. 92, 259–263.

McArthur J.M., Howarth R.J. and Bailey T.R. (2001). Strontium Isotope Stratigraphy: LOWESS Version 3: best fit to the marine Sr-Isotope Curve for 0–509 Ma and accompanying look-up table for deriving numerical age. J. Geol. 109, 155–170..

Méhay S., Keller C.E., Bernasconi S.M., Weissert H., Erba E., Bottini C. and Hochuli P.A. (2009). A volcanic $CO_2$ pulse triggered the Cretaceous Oceanic Anoxic Event 1a and a biocalcification crisis. Geology 37, 819–822.

Menegatti A.P., Weissert H., Brown R.S., Tyson R.V., Farrimond P., Strasser A. and Caron M. (1998). High-resolution $\delta^{13}C$ stratigraphy through the early Aptian "Livello Selli" of the Alpine Tethys. Paleoceanography 13, 530–545.

Millán M.I., Weissert H.J., Owen H., Fernández-Mendiola P.A. and Garcia-Mondéjar J. (2011). The Madotz Urgonian platform (Aralar, northern Spain): Paleoecological changes in response to Early Aptian global environmental events. Palaeogeography, Palaeoclimatology, Palaeoecology, doi: 10.1016/j.palaeo.2011.10.005.

Parente M., Frijia G. and Di Lucia M. (2007). Carbon-isotope stratigraphy of Cenomanian– Turonian platform carbonates from southern Apennines (Italy): a chemostratigraphic approach to the problem of correlation between shallow water and deep-water successions. J. Geol. Soc. Lond. 164, 609–620.

Patterson W.P. and Walter L.M. (1994). Depletion of $\delta^{13}C$ in seawater $CO_2$ on modern carbonate platforms: significance for the carbon isotopic record of carbonates. Geology 22, 885–888..

Pittet B., van Buchem F.S.P., Hillgärtner H., Razin P., Grötsch J. and Droste H.J. (2002). Ecological succession, palaeoenvironmental change, and depositional sequences of Barremian - Aptian shallow water carbonates in northern Oman. Sedimentology 49, 555–581.

Pratt B.R. and James N.P. (1986). The St George Group (Lower Ordovician) of western Newfoundland: tidal flat island model for carbonate sedimentation in shallow epeiric seas. Sedimentology 33, 313–343.

Prokoph A., Shields G.A. and Veizer J. (2008). Compilation and time-series analysis of a marine carbonate $\delta^{18}O$, $\delta^{13}C$, $^{87}Sr/^{86}Sr$ and $\delta^{34}S$ database through Earth history. Earth Sci. Rev. 87, 113–133.

Raspini A. (1998). Microfacies analysis of shallow water carbonates and evidence of hierarchically organized cycles. Aptian of Monte Tobenna, Southern Apennines, Italy. Cret. Res. 19, 197–223.

Raspini A. (2001). Stacking pattern of cyclic carbonate platform strata: Lower Cretaceous of southern Apennines, Italy. J. Geol. Soc. Lond. 158, 353–366.

Raspini A. (2011). Shallow water carbonate platforms (Late Aptian, Southern Apennines) in the context of supraregional to global changes. Solid Earth Discuss. 3, 901–942, 2011, www.solid-earth-discuss.net/3/901/2011/ doi:10.5194/sed-3-901-2011.

Sadler P.M. (1994). The expected duration of upward-shallowing peritidal carbonate cycles and their terminal hiatuses. Geol. Soc. Am. Bull. 106,791–802..

Sartoni S. and Crescenti U. (1962). Ricerche biostratigrafiche nel Mesozoico dell'Appennino meridionale. Giornale di Geologia 29, 161–293.

Schenk, K. (1992). Die Drusberg- und Schrattenkalk-Formation (Unterkreide) im Helvetikum des Berner Oberlandes. Unpublished PhD Thesis, University of Berne.

Schroeder R., Schenk K., Cherchi A. and Schwizer B. (2007). Sur la présence de grands foraminifères d'âge aptien supérieur dans l'Urgonien de la Nappe du Wildhorn (Suisse centrale). Note préliminaire. Revue de Paléobiologie 26, 665–669.

Schroeder R., van Buchem F.S.P., Cherchi A., Baghbani D., Vincent B., Immenhauser A. and Granier B. (2010). Revised orbitolinid biostratigraphic zonation for the Barremian – Aptian of the eastern Arabian Plate and implications for regional stratigraphic correlations. GeoArabia Special Publication, 4, 1, 49–96.

Simmons M.D. (1994). Micropalaeontological biozonation of the Kahmah Group (Early Cretaceous), Central Oman Mountains. In: Simmons, M.D. (Ed.): Micropalaeontology and Hydrocarbon Exploration in the Middle East. Chapman and Hall, London, 177–219.

Skelton P.W. and Gili E. (2011). Rudists and carbonate platforms in the Aptian: a case study on biotic interactions with ocean chemistry and climate. Sedimentology, doi: 10.1111/j.1365-3091.2011.01292.x, 2011.

Strasser A. (1991). Lagoonal–peritidal sequences in carbonate environments: autocyclic and allocyclic processes. In: Einsele, G., Ricken, W. and Seilacher, A. (Eds.): Cycles and Events in Stratigraphy, Springer, Berlin, 709–721.

Strasser A., Pittet B., Hillgärtner H. and Pasquier J.-B. (1999). Depositional sequences in shallow carbonate-dominated sedimentary systems: concepts for a high-resolution analysis. Sed. Geol. 128, 201–221.

Strasser A., Hillgärtner H., Hug W. and Pittet B. (2000). Third-order depositional sequences reflecting Milankovitch cyclicity. Terra Nova 12, 303–311..

Strasser A., Védrine S. and Stienne N. (2011). Rate and synchronicity of environmental changes on a shallow carbonate platform (Late Oxfordian, Swiss Jura Mountains). Sedimentology, doi: 10.1111/j.1365-3091.2011.01236.x.

Swart P.K. (2011). Is there really a mixing-zone stable carbon and oxygen isotope signal? Abstracts, 28th IAS Meeting of Sedimentology 2011, Zaragoza, Spain.

Swart P.K., Reijmer J.J.G. and Otto R. (2009). A re-evaluation of facies on Great Bahama Bank II: variations in the $\delta^{13}C$, $\delta^{18}O$ and mineralogy of surface sediments. Int. Assoc. Sedimentol. Spec. Publ., 41, 47–59.

Tešović B.C., Glumac B. and Bucković D. (2011). Integrated biostratigraphy and carbon isotope stratigraphy of the Lower Cretaceous (Barremian to Albian) Adriatic-Dinaridic carbonate platform deposits in Istria, Croatia. Cret. Res. 32, 301–324.

Tejada, M.L.G., Suzuki, K., Kuroda, J., Coccioni, R., Mahoney, J.J., Ohkouchi, N., Sakamoto, T. and Tatsumi, Y.: Ontong Java Plateau eruption as a trigger for the early Aptian oceanic anoxic event, Geology, 37, 855–858, 2009.

Tipper J.C. (1997). Modeling carbonate platform sedimentation – Lag comes naturally. Geology 25, 495–498.

Vahrenkamp V.C. (2010). Chemostratigraphy of the Lower Cretaceous Shu'aiba Formation: A $\delta^{13}C$ reference profile for the Aptian Stage from the southern Neo-Tethys Ocean. GeoArabia Spec. P., 4, 1, 107–137.

Velić I. (2007). Stratigraphy and palaeobiogeography of Mesozoic benthic foraminifera of the Karst Dinarides (SE Europa). Geologia Croatica 60 (1), 1–113.

Vilas L., Masse J.P. and Arias C. (1995). Orbitolina episodes in carbonate platform evolution: the early Aptian model from SE Spain. Palaeogeography, Palaeoclimatology, Palaeoecology 119, 35–45.

Wagner P.D. (1990). Geochemical stratigraphy and porosity controls in Cretaceous carbonates near the Oman Mountains. In: Robertson, A.H.F., Searle, M.P. & and Ries, A.C. (Eds): The Geology and Tectonics of the Oman Region, Geol. Soc. Spec. Publ., 49, 127–137.

Weber J.N. and Woodhead P.M.J. (1969). Factors affecting the carbon and oxygen isotopic composition of marine carbonate sediments-II. Heron Island, Great Barrier Reef, Australia. Geochim. Cosmochim. Ac. 33, 19–38.

Weissert H. and Erba E. (2004). Volcanism, $CO_2$ and paleoclimate: a Late Jurassic-Early Cretaceous oxygen isotope record. J. Geol. Soc. Lond. 161, 695–702.

Wissler L., Funk H. and Weissert H. (2003). Response of Early Cretaceous carbonate platforms to changes in atmospheric carbon dioxide levels, Palaeogeogr. Palaeocl., 200, 187–205, 2003.

Wissler L., Weissert H., Buonocunto F.P., Ferreri V. and D'Argenio B. (2004). Calibration of the Early Cretaceous time scale: a combined chemostratigraphic and cyclostratigraphic approach to the Barremian-Aptian interval Campania Apennines and southern Alps (Italy). In: D'Argenio, B. et al. (Eds): Cyclostratigraphy, approaches and case histories, SEPM Spec. P., 81, 123–134, 2004.

Witt W. and Gökdağ H. (1994). Orbitolinid biostratigraphy of the Shu'aiba Formation (Aptian), Oman - implications for reservoir development, in: Simmons, M.D. (Ed.): Micropalaeontology and Hydrocarbon Exploration in the Middle East. Chapman and Hall, London, 241–271.

# CHAPTER 6 – CONCLUSIONS AND PERSPECTIVES

The main aim of the present doctoral thesis was to investigate the response of the Apenninic Carbonate Platform to the early Toarcian (T-OAE) and the early Aptian (OAE1a) oceanic anoxic events. To fulfill this task, a detailed study of two Lower Jurassic and two Lower Cretaceus sections was carried out. In the absence of black shales and of a reliable biostratigraphic criterion, carbon isotope stratigraphy was used to identify the segments corresponding to the OAEs. As a by-product, this led to unprecedented high-resolution dating of the studied sections with the first chemostratigraphically constrained calibration of their biostratigraphy.

Concerning the T-OAE, phosphorus content and clay minerals of Mercato San Severino and Monte Sorgenza sections were successfully used to discriminate the relative role of ocean acidification *vs* enhanced nutrient flux on the carbonate factory, and to compare the response of the ACP with that of other carbonate platforms for which increased nutrient levels have been implied as the main cause of crisis or drowning.

For the early Aptian OAE1a, the integration of the study of Monte Raggeto and Monte Tobenna sections with the data of a previous doctoral thesis (Di Lucia, 2009) allowed to define the biostratigraphic criteria to individuate, in the carbonate platforms of the central and southern Tethys, the stratigraphic interval equivalent to the OAE1a.

The main results can be summarized as follows:

*early Toarcian OAE*

- In the ACP, the Lithiotis/Palaeodasycladus carbonate factory was wiped out at the onset of early Toarcian negative carbon isotope excursion, seemingly marking the definitive extinction of these massive biocalcifiers. The extinction of carbonate platform biocalcifiers is coeval with the biocalcification crisis of calcareous nannoplankton. The coincidence with the negative CIE, interpreted as the result of the massive injection of $CO_2$ into the atmosphere-ocean system, is consistent with a scenario of ocean acidification at the onset of the T-OAE. This suggests that the demise of the Lithiotis/Paleodasycladus carbonate factory was caused by ocean acidification. Moreover, clay minerals and P content across the early Toarcian OAE show no evidence of enhanced weathering in the ACP, excluding any role of the enhanced nutrient levels on the demise of the massive biocalfiers.
- In the ACP, and in other resilient platforms of the Tethyan ocean, the disappearance of biocalcifiers coincide with a shift to chemical precipitation in the form of massive oolitic limestones. Similar to what observed for the Permian-Triassic boundary crisis, chemical precipitation took over on carbonate platforms as soon as ocean alkalinity recovered.
- Clay-minerals and P content of the Apenninic Carbonate Platform recorded increased weathering across the Pliensbachian-Toarcian boundary. Unlike many carbonate platforms of the Peri-Tethyan domain, which responded to the shift of nutrient levels by either drowning or shifting to heterotrophic carbonate production, the ACP continued growing in shallow water with no significant shift in the composition of the carbonate factory.
- Lower subsidence rate, compared to other Peritethyan carbonate platforms, was most probably a significant factor explaining the resilience of the ACP to Early Toarcian palaeoenvironmental perturbations.

*early Aptian OAE*

- The interval of decreasing $\delta^{13}C$ values values preceding the C3 negative peak, which marks the onset of the Selli event, starts just above the LO of *V. murgensis*. The C4-C6 segments, which correspond in deep-water sections to the interval of black shales deposition, ends just below the first acme of *S. dinarica*. The latter roughly corresponds to the C7 segment of peak $\delta^{13}C$ values. The "Orbitolina level" marks the return the pre-excursion values at the end of the broad positive CIE associated with the OAE1a.
- The Barremian–Aptian boundary in central-southern Tethyan carbonate platforms is very closely approximated by the first occurrence of *V. murgensis* and *D. hahounerensis*.

To better understand the response of the Apenninic Carbonate Platform to the global changes during the Early Toarcian, different integrative studies could be carried out.

Information on the type and thermal maturity of the bulk organic matter can be obtained by Rock-Eval pyrolysis which provide TOC (Total Organic Carbon, wt%), HI (Hydrogen Index, mg HC/g TOC), OI (Oxygen Index, mg $CO_2$/g TOC) and Tmax (°C). In particular, the crossplots of HI/OI values will give indication about the origin of the organic matter (continental *vs* marine). This could help explaining why the first prominent negative CIE, which in this thesis has been associated to the Pliensbachian-Toarcian stage boundary, is present in the $\delta^{13}C_{org}$ record but absent in the $\delta^{13}C_{carb}$ one. In fact a variation in the relative contribution of continental *vs* marine organic matter across the boundary stage cannot be excluded.

Calcium-isotope ratio ($\delta^{40/44}Ca$) analyses could better constrain the scenario of ocean acidification at the onset of the early Toarcian OAE. Calcium isotopes are useful in identifying and quantifying changes in geochemical cycles during OAEs and other severe carbon-cycle perturbation episodes, because the calcium-isotope ratio of seawater changes in response to large flux imbalances. Secular variation in the calcium isotope composition of marine sediments provide a tool for distinguishing among several extinction scenarios and thereby constraining the causes of mass extinction. This tool has been successfully used in the study of the end-Permian mass extinction (Payne et al., PNAS 2010) and for the early Aptian (OAE1) and the Cenomanian-Turonian boundary (OAE2) events (Blättler et al., EPSL 2011).

For the early Aptian, the study of total P concentration and of clay mineral assemblages could help to investigate changes of continental weathering across the OAE1a. Moreover a more exaustive biostratigraphic study could further improve the bio-chemostratigraphic scheme proposed for the Barremian-Aptian interval in this thesis.

# APPENDIX

## *Carbon and oxygen isotopes of Mercato San Severino section*

| h (m) | $\delta^{18}O_{carb}$ (‰) | $\delta^{13}C_{carb}$ (‰) | $\delta^{13}C_{org}$ (‰) |
|---|---|---|---|
| 0.2 | -1.75 | 2.42 | |
| 0.8 | -2.21 | 1.93 | |
| 1.2 | -2.49 | 2.69 | |
| 1.9 | -1.66 | 2.88 | |
| 2.5 | -2.47 | 2.59 | |
| 2.9 | -2.18 | 2.99 | |
| 3.3 | -1.18 | 2.66 | |
| 4 | -2.53 | 3.05 | |
| 4.7 | -1.76 | 3.06 | |
| 5.2 | -2.32 | 2.84 | |
| 5.6 | -1.90 | 2.86 | |
| 6.5 | -1.90 | 3.07 | |
| 6.7 | -1.62 | 2.94 | |
| 7.4 | -2.52 | 1.71 | |
| 8.1 | -2.23 | 3.03 | |
| 8.5 | -2.33 | 2.77 | |
| 8.6 | -1.47 | 2.33 | |
| 10.2 | -2.20 | 2.16 | |
| 10.5 | -1.94 | 2.56 | |
| 11 | -1.87 | 2.25 | |
| 11.6 | -1.17 | 2.87 | |
| 12.1 | -1.87 | 2.57 | |
| 12.6 | -1.43 | 2.83 | |
| 13.3 | -2.01 | 2.84 | |
| 14.1 | -2.44 | 2.63 | |
| 14.8 | -1.76 | 3.01 | |
| 15.8 | -1.85 | 2.26 | |
| 16.3 | -1.70 | 2.22 | |
| 16.8 | -1.23 | 2.76 | |
| 17.4 | -1.28 | 2.89 | |
| 18.1 | -1.11 | 2.89 | |
| 18.9 | -1.80 | 2.81 | |
| 19.7 | -1.55 | 2.38 | |
| 20.4 | -1.85 | 2.23 | |
| 20.8 | -2.78 | 1.53 | |
| 21.5 | -1.22 | 2.95 | |
| 21.9 | -1.20 | 2.90 | |
| 22.6 | -2.01 | 2.84 | |
| 23 | -1.44 | 2.93 | |
| 23.7 | -1.81 | 2.60 | |
| 25.3 | -2.36 | 1.71 | |
| 25.9 | -2.59 | 1.86 | |
| 26.4 | -1.76 | 2.57 | |
| 27.3 | -2.11 | 2.47 | |
| 28 | -1.80 | 2.13 | |
| 28.5 | -1.67 | 2.20 | |
| 29.4 | -1.40 | 2.37 | |
| 29.8 | -1.78 | 1.56 | |

| h (m) | $\delta^{18}O_{carb}$ (‰) | $\delta^{13}C_{carb}$ (‰) | $\delta^{13}C_{org}$ (‰) |
|---|---|---|---|
| 30.6 | -1.32 | 2.64 | |
| 31.1 | -2.09 | 2.72 | |
| 31.7 | -1.11 | 2.13 | |
| 32.5 | -1.77 | 2.53 | |
| 33.2 | -1.36 | 2.30 | |
| 34.1 | -0.98 | 2.57 | |
| 34.7 | -2.18 | 0.60 | |
| 35.5 | -1.77 | 2.33 | |
| 36.2 | -1.89 | 2.02 | |
| 36.9 | -2.47 | 2.41 | |
| 37.7 | -1.83 | 2.61 | |
| 38.7 | -1.80 | 2.80 | |
| 39.5 | -1.11 | 2.78 | |
| 40.2 | -1.39 | 2.64 | |
| 40.7 | -1.62 | 1.69 | |
| 41.4 | -2.16 | 2.60 | |
| 42.1 | -1.75 | 2.11 | |
| 42.7 | -2.11 | 1.91 | |
| 42.9 | -2.14 | 2.25 | |
| 43.7 | -2.12 | 2.70 | |
| 44.1 | -1.81 | 2.70 | -25.20 |
| 44.6 | -1.36 | 2.32 | |
| 44.9 | -1.96 | 1.78 | |
| 45.4 | -1.47 | 2.31 | |
| 46.4 | -1.93 | 2.59 | |
| 46.7 | -1.90 | 2.24 | |
| 47.6 | -2.16 | 1.95 | |
| 48.4 | -1.76 | 2.05 | |
| 48.7 | -2.03 | 1.98 | -23.73 |
| 49.2 | -1.75 | 3.19 | |
| 49.8 | -1.73 | 2.20 | |
| 50.3 | -1.59 | 2.51 | |
| 50.8 | -1.72 | 1.52 | |
| 51.1 | -1.76 | 2.17 | |
| 51.8 | -1.75 | 2.27 | |
| 52.5 | -1.76 | 2.80 | -25.18 |
| 52.8 | -1.87 | 2.33 | |
| 53.6 | -1.70 | 2.71 | |
| 54 | -1.25 | 2.62 | |
| 55 | -2.08 | 1.92 | |
| 55.5 | -1.72 | 2.39 | |
| 56.3 | -1.92 | 2.49 | |
| 56.7 | -1.60 | 3.09 | -25.12 |
| 57.1 | -2.58 | 2.36 | |
| 57.3 | -1.34 | 1.84 | |
| 58.4 | -1.49 | 2.31 | |
| 59.3 | -2.16 | 2.24 | |
| 60 | -3.35 | 1.93 | |

| h (m) | $\delta^{18}O_{carb}$ (‰) | $\delta^{13}C_{carb}$ (‰) | $\delta^{13}C_{org}$ (‰) |
|---|---|---|---|
| 60.3 | -2.92 | 1.78 | |
| 60.6 | -2.76 | 2.13 | |
| 61.4 | -2.01 | 2.04 | -25.49 |
| 62.5 | -1.88 | 2.58 | |
| 63 | -1.51 | 1.20 | |
| 63.5 | -1.34 | 2.17 | |
| 64.1 | -2.29 | 2.35 | |
| 64.7 | -2.10 | 0.93 | |
| 65.3 | -2.36 | 1.20 | -24.09 |
| 66 | -1.83 | 2.83 | |
| 66.9 | -2.27 | 1.91 | |
| 67.9 | -1.86 | 2.43 | |
| 68 | -1.85 | 2.61 | |
| 68.3 | -2.69 | 1.26 | |
| 69.1 | -2.27 | 2.08 | |
| 69.7 | -1.72 | 2.40 | |
| 70.3 | -1.58 | 2.44 | -25.20 |
| 70.9 | -1.70 | 2.85 | |
| 71.5 | -2.18 | 2.58 | |
| 72.3 | -1.31 | 2.09 | |
| 72.7 | -2.67 | 2.79 | |
| 73.4 | -2.12 | 2.24 | |
| 74.1 | -2.27 | 2.31 | |
| 74.3 | -2.46 | 1.90 | |
| 75 | -1.93 | 2.18 | -25.82 |
| 75.5 | -2.53 | 1.86 | |
| 76.7 | -1.80 | 2.50 | |
| 77 | -2.77 | 2.32 | |
| 78 | -2.21 | 2.65 | |
| 78.4 | -1.76 | 2.60 | |
| 78.6 | -1.80 | 2.71 | |
| 79.4 | -1.76 | 2.63 | -24.38 |
| 79.8 | -2.24 | 2.17 | |
| 80.5 | -2.23 | 1.33 | |
| 80.7 | -1.86 | 2.14 | |
| 81 | -1.60 | 2.79 | |
| 81.6 | -1.52 | 2.48 | |
| 82 | -1.33 | 2.75 | |
| 82.5 | -1.85 | 2.79 | |
| 83.1 | -1.36 | 2.52 | |
| 83.4 | -1.39 | 2.78 | -25.41 |
| 84 | -1.78 | 2.50 | |
| 84.8 | -1.98 | 2.58 | |
| 85.3 | -1.87 | 1.98 | |
| 85.8 | -2.32 | 2.03 | |
| 86.4 | -1.64 | 2.34 | |
| 87.5 | -2.76 | 0.60 | |
| 87.8 | -1.59 | 1.88 | |

| h (m) | $\delta^{18}O_{carb}$ (‰) | $\delta^{13}C_{carb}$ (‰) | $\delta^{13}C_{org}$ (‰) |
|---|---|---|---|
| 87.5 | -2.76 | 0.60 | |
| 87.8 | -1.59 | 1.88 | |
| 88.3 | -2.20 | 1.86 | -24.07 |
| 89 | -2.30 | 3.06 | |
| 90 | -2.03 | 3.22 | |
| 91.3 | -1.38 | 2.65 | |
| 91.7 | -1.27 | 2.45 | |
| 92.3 | -1.28 | 2.28 | |
| 93 | -1.60 | 2.83 | |
| 93.9 | -1.64 | 2.65 | |
| 94.8 | -1.74 | 2.81 | |
| 95.3 | -1.73 | 1.79 | |
| 96.2 | -2.14 | 1.85 | |
| 95.3 | -1.73 | 1.79 | |
| 96.2 | -2.14 | 1.85 | |
| 97.3 | -2.10 | 2.70 | |
| 97.5 | -2.37 | 2.12 | -25.28 |
| 98.3 | -1.85 | 2.38 | |
| 99.4 | -1.48 | 2.60 | |
| 100.4 | -1.70 | 2.77 | |
| 100.7 | -1.70 | 2.53 | |
| 101.3 | -1.47 | 2.52 | |
| 102.5 | -1.84 | 1.64 | |
| 103.6 | -1.91 | 1.60 | -25.28 |
| 103.8 | -1.93 | 2.60 | |
| 104.3 | -2.03 | 1.44 | |
| 104.9 | -2.50 | 0.16 | |
| 105.2 | -2.72 | 3.37 | |
| 105.8 | -2.16 | 2.36 | |
| 106.7 | -1.61 | 1.32 | -23.54 |
| 107.1 | -2.21 | 2.07 | |
| 107.5 | -1.99 | 2.10 | -26.71 |
| 108.3 | -2.27 | 2.07 | |
| 109 | -2.13 | 2.39 | -26.58 |
| 110 | -2.19 | 2.59 | -27.09 |
| 110.5 | -1.87 | 2.70 | |
| 111.1 | -1.97 | 2.72 | |
| 111.9 | -2.02 | 2.91 | -25.69 |
| 112.3 | -1.39 | 2.84 | |
| 112.7 | -1.61 | 2.96 | -25.40 |
| 113.3 | -1.58 | 2.60 | -25.65 |
| 114 | -2.15 | 2.95 | |
| 114.6 | -2.39 | 3.50 | -24.79 |
| 115.6 | -1.93 | 2.38 | |
| 115.9 | -2.00 | 1.45 | -23.53 |
| 116.1 | -1.97 | 1.50 | |
| 116.4 | -2.45 | 1.61 | |
| 116.5 | -2.03 | 3.14 | -24.81 |

| h (m) | $\delta^{18}O_{carb}$ (‰) | $\delta^{13}C_{carb}$ (‰) | $\delta^{13}C_{org}$ (‰) |
|---|---|---|---|
| 117 | -2.33 | 3.16 | |
| 117.7 | -2.23 | 3.73 | -24.61 |
| 118.1 | -2.22 | 3.54 | |
| 118.6 | -1.83 | 4.22 | -24.94 |
| 119.6 | -2.05 | 3.07 | |
| 120.2 | -1.90 | 3.44 | -24.95 |
| 121.1 | -1.78 | 3.56 | -24.58 |
| 122.4 | -2.01 | 3.35 | |
| 122.5 | -1.92 | 3.39 | |
| 122.9 | -1.55 | 3.07 | -24.99 |
| 123.5 | -1.68 | 3.33 | -24.22 |
| 124.1 | -1.84 | 3.16 | -25.10 |
| 124.5 | -1.87 | 2.89 | |
| 125.2 | -2.13 | 3.39 | -24.41 |
| 125.6 | -2.15 | 3.12 | |
| 125.8 | -2.07 | 2.38 | |
| 126.1 | -2.22 | 2.26 | -26.50 |
| 126.2 | -2.39 | 2.29 | |
| 126.5 | -2.64 | 2.41 | |
| 126.6 | -2.68 | 2.39 | |
| 127.1 | -2.81 | 1.61 | -27.84 |
| 127.7 | -2.51 | 1.58 | |
| 128 | -2.93 | 1.57 | -28.12 |
| 128.6 | -3.79 | 2.67 | -27.55 |
| 128.7 | -2.82 | 0.95 | |
| 129.8 | -3.06 | 2.64 | |
| 130.5 | -2.54 | 2.40 | -27.99 |
| 131.2 | -2.43 | 2.69 | -28.24 |
| 132.1 | -2.96 | 3.23 | -27.41 |
| 132.8 | -2.28 | 3.40 | |
| 133.3 | -2.33 | 2.55 | -27.66 |
| 133.8 | -2.46 | 2.71 | |
| 134.3 | -2.38 | 2.64 | -26.47 |
| 134.8 | -2.53 | 2.71 | |
| 135.2 | -2.48 | 2.87 | -26.91 |
| 135.8 | -2.47 | 3.07 | |
| 136.3 | -2.52 | 3.15 | |
| 136.7 | -2.95 | 3.63 | |
| 137.4 | -2.66 | 3.69 | -25.73 |
| 138 | -2.63 | 3.47 | |
| 138.6 | -2.49 | 3.42 | -26.09 |
| 139.7 | -2.57 | 3.48 | |
| 139.9 | -1.90 | 3.68 | -24.80 |
| 140.7 | -2.46 | 3.42 | -26.64 |
| 141.5 | -2.20 | 2.88 | -26.80 |
| 142.5 | -2.56 | 3.34 | -26.98 |
| 143.9 | -3.40 | 2.86 | -26.79 |
| 144 | -6.30 | 2.60 | |

| h (m) | $\delta^{18}O_{carb}$ (‰) | $\delta^{13}C_{carb}$ (‰) | $\delta^{13}C_{org}$ (‰) |
|---|---|---|---|
| 144.7 | -3.06 | 3.18 | -26.98 |
| 145.4 | -2.74 | 3.44 | |
| 146.7 | -3.44 | 2.84 | |
| 148.7 | -2.49 | 2.64 | |
| 150.3 | -2.50 | 2.65 | |
| 152.1 | -2.50 | 2.84 | |
| 154.5 | -2.61 | 2.75 | |
| 156.6 | -2.46 | 2.63 | |
| 158.9 | -2.36 | 2.67 | |
| 160.4 | -2.31 | 2.69 | |
| 162.1 | -2.40 | 2.58 | |
| 163.7 | -2.48 | 2.50 | |
| 154.5 | -2.61 | 2.75 | |
| 156.6 | -2.46 | 2.63 | |
| 158.9 | -2.36 | 2.67 | |
| 160.4 | -2.31 | 2.69 | |
| 162.1 | -2.40 | 2.58 | |
| 163.7 | -2.48 | 2.50 | |

## *Carbon and oxygen isotopes of Monte Sorgenza section*

| **h** (m) | $\delta^{18}O_{carb}$ (‰) | $\delta^{13}C_{carb}$ (‰) | $\delta^{13}C_{org}$ (‰) |
|---|---|---|---|
| 120.5 | -1.92 | 1.39 | -24.75 |
| 121.5 | -2.61 | 1.77 | |
| 122.4 | -1.92 | 1.04 | -24.15 |
| 123.7 | -2.49 | 1.04 | |
| 125 | -2.21 | 1.28 | -23.72 |
| 126 | -2.18 | 1.13 | |
| 126.8 | -2.80 | -0.71 | -25.20 |
| 130 | -1.70 | 0.69 | -24.89 |
| 131.4 | -1.13 | 1.59 | -22.75 |
| 132.6 | -1.62 | 1.14 | -24.35 |
| 133.7 | -1.30 | 1.24 | -23.90 |
| 134.6 | -1.39 | 1.59 | |
| 134.9 | -1.48 | 1.68 | -25.58 |
| 135.6 | -1.21 | 1.92 | -25.64 |
| 136.8 | -1.47 | 1.73 | -27.23 |
| 138.2 | -1.51 | 2.01 | -25.34 |
| 139.4 | -1.20 | 2.41 | -25.11 |
| 140.3 | -1.84 | 1.96 | |
| 141.1 | -1.49 | 1.88 | -25.29 |
| 141.4 | -1.62 | 1.47 | |
| 141.8 | -0.97 | 2.45 | |
| 142.6 | -1.05 | 2.52 | -25.24 |
| 143.1 | -1.42 | 2.11 | |
| 143.8 | -2.00 | 2.51 | -25.49 |
| 144.9 | -1.60 | 2.10 | -24.46 |
| 145.7 | -1.00 | 2.83 | -24.38 |
| 146.5 | -1.26 | 2.81 | -24.15 |
| 147.5 | -1.34 | 2.86 | -23.86 |
| 148.2 | -1.78 | 2.63 | -24.60 |
| 149.4 | -1.59 | 3.27 | -24.23 |
| 149.9 | -1.39 | 3.22 | -23.61 |
| 151 | -1.77 | 2.82 | -23.57 |
| 151.4 | -1.83 | 3.15 | -24.37 |
| 152.4 | -2.16 | 2.02 | -23.75 |
| 153 | -2.82 | 0.29 | -23.92 |
| 153.9 | -2.23 | 2.29 | -25.07 |
| 154.6 | -2.01 | 1.26 | -29.15 |
| 155.5 | -2.54 | 1.04 | -29.38 |
| 156.5 | -1.80 | 1.64 | |
| 157.7 | -1.55 | 2.17 | |
| 158.5 | -2.15 | 1.94 | -28.03 |
| 159.8 | -2.07 | 2.41 | -27.70 |
| 160.7 | -1.83 | 2.51 | -27.15 |
| 161.2 | -1.17 | 2.74 | -25.33 |
| 163.1 | -1.00 | 2.60 | -25.46 |

***P content and clay-mineral assemblages of Mercato San Severino section***

| **h** (m) | **P** (ppm) | **mica** (%) | **I/S** (%) | **chlorite** (%) | **kaolinite** (%) |
|---|---|---|---|---|---|
| 0 | 14 | 71 | 14 | 9 | 6 |
| 4.6 | 26 | 71 | 14 | 9 | 5 |
| 8.4 | 27 | 78 | 13 | 5 | 4 |
| 12.6 | 25 | 54 | 11 | 17 | 18 |
| 17.3 | 14 | 75 | 15 | 4 | 6 |
| 21.2 | 27 | 63 | 14 | 23 | 0 |
| 26.2 | 13 | 67 | 25 | 5 | 2 |
| 26.5 | | 63 | 14 | 23 | 0 |
| 30.9 | 15 | 76 | 5 | 12 | 7 |
| 35.3 | 26 | 51 | 28 | 13 | 7 |
| 37.6 | | 69 | 21 | 10 | 0 |
| 39.3 | 23 | 87 | 13 | 0 | 0 |
| 42.6 | | 40 | 32 | 14 | 14 |
| 44.2 | 19 | 72 | 14 | 7 | 6 |
| 48.9 | 18 | 73 | 15 | 8 | 3 |
| 52.3 | | 58 | 33 | 6 | 3 |
| 53.4 | 12 | 67 | 13 | 8 | 11 |
| 59.5 | 22 | 65 | 25 | 0 | 11 |
| 60.8 | 20 | 53 | 17 | 20 | 10 |
| 62.6 | 22 | 54 | 27 | 18 | 1 |
| 62.7 | | 55 | 32 | 8 | 5 |
| 63 | 35 | 58 | 15 | 16 | 11 |
| 63.4 | 20 | 58 | 22 | 15 | 6 |
| 64.2 | 25 | 56 | 25 | 11 | 9 |
| 64.9 | 20 | 76 | 4 | 14 | 6 |
| 65.9 | 18 | 66 | 6 | 16 | 12 |
| 66.4 | 24 | 45 | 15 | 15 | 26 |
| 67 | 18 | 44 | 19 | 16 | 21 |
| 67.8 | 20 | 79 | 8 | 8 | 5 |
| 68.2 | 28 | 37 | 18 | 15 | 29 |
| 68.6 | 19 | 57 | 9 | 16 | 17 |
| 69.2 | 19 | 51 | 17 | 13 | 19 |
| 69.9 | 30 | 47 | 40 | 7 | 7 |
| 70.5 | 20 | 64 | 3 | 16 | 17 |
| 71.5 | 24 | 44 | 18 | 15 | 24 |
| 71.8 | 34 | 37 | 19 | 18 | 25 |
| 72 | 50 | 48 | 23 | 10 | 19 |
| 72.1 | | 39 | 17 | 19 | 24 |
| 72.2 | | 45 | 29 | 15 | 11 |
| 72.3 | 38 | 51 | 13 | 16 | 19 |
| 72.4 | 16 | 49 | 7 | 13 | 30 |
| 72.9 | 37 | 40 | 20 | 15 | 26 |
| 73.2 | 34 | 36 | 7 | 18 | 39 |
| 73.6 | 26 | 43 | 24 | 11 | 22 |
| 74 | 30 | 37 | 20 | 16 | 26 |
| 74.5 | 18 | 47 | 5 | 12 | 35 |
| 75.5 | 32 | 43 | 8 | 19 | 30 |
| 76.1 | 14 | 51 | 13 | 13 | 23 |

| **h** (m) | **P** (ppm) | **mica** (%) | **I/S** (%) | **chlorite** (%) | **kaolinite** (%) |
|---|---|---|---|---|---|
| 77 | 14 | 66 | 4 | 9 | 21 |
| 78.3 | 22 | 58 | 6 | 13 | 24 |
| 78.8 | 14 | 63 | 11 | 9 | 17 |
| 79.4 | 20 | 65 | 10 | 9 | 16 |
| 80 | 8 | 73 | 5 | 8 | 14 |
| 80.4 | 15 | 74 | 6 | 11 | 9 |
| 81.1 | 21 | 52 | 16 | 14 | 18 |
| 81.7 | 12 | | | | |
| 82 | 10 | 61 | 13 | 18 | 8 |
| 82.3 | 12 | 41 | 36 | 10 | 13 |
| 83 | 28 | | | | |
| 83.6 | 10 | | | | |
| 83.9 | 8 | 66 | 22 | 5 | 7 |
| 84.5 | 6 | | | | |
| 85.7 | 8 | 56 | 15 | 9 | 21 |
| 86.4 | 6 | 70 | 6 | 8 | 15 |
| 87.1 | 6 | 68 | 11 | 11 | 10 |
| 88 | 6 | | | | |
| 88.7 | 6 | 63 | 23 | 5 | 9 |
| 89.2 | 8 | 83 | 17 | 0 | 0 |
| 90.2 | 8 | | | | |
| 91.1 | 8 | 76 | 24 | 0 | 0 |
| 92.2 | 8 | 78 | 8 | 6 | 8 |
| 93.3 | 8 | 89 | 11 | 0 | 0 |
| 94.5 | 8 | 59 | 12 | 16 | 13 |
| 95.8 | 18 | 53 | 9 | 22 | 16 |
| 96.6 | 10 | | | | |
| 97.4 | 12 | 66 | 34 | 0 | 0 |
| 98.4 | 12 | | | | |
| 99.8 | 10 | 70 | 30 | 0 | 0 |

***P content and clay-mineral assemblages of Mercato San Severino section***

| **h** (m) | **P** (ppm) | **mica** (%) | **I/S** (%) | **chlorite** (%) | **kaolinite** (%) |
|---|---|---|---|---|---|
| 0 | | 51 | 21 | 14 | 14 |
| 3.4 | | 67 | 10 | 19 | 3 |
| 7.8 | | | | | |
| 11.9 | | 72 | 21 | 4 | 3 |
| 15.8 | | 48 | 26 | 19 | 7 |
| 19.7 | | 57 | 11 | 18 | 13 |
| 23.8 | | 56 | 16 | 19 | 9 |
| 30.1 | 26 | | | | |
| 31.1 | 23 | | | | |
| 32 | 29 | 70 | 9 | 12 | 9 |
| 33.3 | 24 | | | | |
| 34.6 | 26 | | | | |
| 35.6 | 25 | | | | |
| 36.4 | 23 | | | | |
| 39.6 | 27 | 51 | 10 | 0 | 39 |
| 41 | 29 | | | | |
| 42.2 | 31 | 64 | 4 | 12 | 20 |
| 43.3 | 28 | | | | |
| 44.2 | 33 | | | | |
| 44.5 | 28 | 36 | 10 | 9 | 45 |
| 45.2 | 22 | | | | |
| 46.4 | 25 | 32 | 14 | 15 | 39 |
| 47.8 | 24 | | | | |
| 49 | 26 | 41 | 2 | 12 | 45 |
| 49.9 | 33 | | | | |
| 50.7 | 34 | 27 | 6 | 12 | 55 |
| 51 | 34 | | | | |
| 51.4 | 34 | | | | |
| 52.2 | 27 | 37 | 13 | 16 | 34 |
| 52.7 | 27 | | | | |
| 53.4 | 28 | 35 | 3 | 11 | 51 |
| 54.5 | 32 | 36 | 10 | 11 | 42 |
| 55.3 | 25 | 29 | 9 | 17 | 44 |
| 56.1 | 26 | 33 | 16 | 12 | 38 |
| 57.1 | 25 | 30 | 15 | 11 | 44 |
| 57.8 | 27 | | | | |
| 59 | 28 | | | | |
| 59.5 | 28 | | | | |
| 60.6 | 32 | 39 | 3 | 13 | 45 |
| 61 | 23 | | | | |
| 62 | 30 | 50 | 19 | 7 | 24 |
| 62.6 | 29 | | | | |
| 63.5 | 8 | 48 | 22 | 8 | 22 |
| 64.2 | 11 | | | | |
| 65.1 | 14 | 74 | 26 | 0 | 0 |

| **h** (m) | **P** (ppm) | **mica** (%) | **I/S** (%) | **chlorite** (%) | **kaolinite** (%) |
|---|---|---|---|---|---|
| 66.1 | 11 | | | | |
| 67.3 | 18 | | | | |
| 68.1 | 16 | 56 | 23 | 11 | 10 |
| 69.4 | 16 | | | | |
| 70.3 | 16 | 52 | 22 | 16 | 10 |

## *Carbon and oxygen isotopes of Monte Raggeto section*

| h (m) | $\delta^{18}O$ (‰) | $\delta^{13}C$ (‰) |
|---|---|---|
| 0.1 | 1.76 | -1.58 |
| 1.3 | 2.55 | -2.58 |
| 2.6 | 1.09 | -2.13 |
| 3.5 | 1.35 | -2.59 |
| 4.7 | 1.79 | -2.20 |
| 5.2 | 2.02 | -2.07 |
| 6.0 | 1.78 | -1.99 |
| 6.5 | 1.67 | -1.95 |
| 7.6 | 1.73 | -2.12 |
| 18.3 | 1.46 | 0.38 |
| 19.5 | 1.56 | 0.40 |
| 20.9 | 1.76 | 0.52 |
| 22.6 | 2.05 | 0.71 |
| 24.0 | 1.92 | 0.49 |
| 24.4 | 2.77 | -1.09 |
| 24.9 | 3.14 | -1.24 |
| 25.9 | 3.41 | -1.42 |
| 27.0 | 3.11 | -1.45 |
| 28.1 | 3.20 | -1.55 |
| 28.7 | 2.67 | -1.03 |
| 29.5 | 2.34 | -1.77 |
| 30.2 | 2.25 | -1.67 |
| 31.4 | 1.25 | -1.52 |
| 32.0 | 1.28 | -1.36 |
| 33.6 | 1.81 | -2.22 |
| 34.5 | 1.06 | -1.68 |
| 35.3 | 0.98 | -2.12 |
| 35.8 | 2.71 | -1.68 |
| 39.9 | 3.82 | -1.33 |
| 40.2 | 1.33 | -1.49 |
| 40.7 | 1.25 | -1.47 |
| 41.3 | 3.13 | -1.39 |
| 42.2 | 4.34 | -1.26 |
| 43.1 | 4.02 | -1.53 |
| 43.9 | 2.88 | -1.37 |
| 44.6 | 2.64 | -1.82 |
| 45.7 | 2.93 | -1.58 |
| 46.5 | 2.86 | -1.74 |
| 47.9 | 4.85 | -1.25 |
| 48.1 | 4.78 | -0.85 |
| 49.2 | 4.34 | -1.10 |
| 50.6 | 4.51 | -1.03 |
| 51.6 | 4.19 | -1.23 |
| 52.6 | 2.89 | -1.27 |
| 53.7 | 3.55 | -1.36 |
| 54.6 | 2.78 | -1.52 |

| h (m) | $\delta^{18}O$ (‰) | $\delta^{13}C$ (‰) |
|---|---|---|
| 55.6 | 3.30 | -0.83 |
| 56.6 | 3.88 | -0.91 |
| 57.4 | 3.70 | -0.83 |
| 58.5 | 4.45 | -0.69 |
| 59.6 | 2.33 | -1.18 |
| 60.4 | 1.42 | -1.33 |
| 61.5 | 3.04 | -0.96 |
| 62.6 | 3.59 | -0.51 |
| 63.7 | 3.96 | -0.74 |
| 64.2 | 2.44 | -1.00 |
| 64.8 | 1.36 | -1.18 |
| 65.8 | 0.83 | -1.82 |
| 66.3 | 0.05 | -1.29 |
| 67.4 | 0.02 | -1.07 |
| 68.6 | 0.27 | -1.30 |
| 69.8 | 1.49 | -1.02 |
| 71.0 | 1.03 | -1.04 |
| 72.0 | 1.20 | -1.07 |
| 73.0 | 1.20 | -1.21 |
| 73.9 | 1.25 | -1.10 |
| 74.9 | 2.06 | -1.20 |
| 75.9 | -0.25 | -1.65 |
| 76.8 | 3.03 | -0.74 |
| 77.3 | 3.41 | -0.91 |
| 77.4 | 3.66 | -0.38 |
| 78.3 | 2.67 | -1.03 |
| 79.7 | 4.55 | -0.46 |
| 80.6 | 3.44 | -1.50 |
| 81.4 | 4.26 | -1.23 |
| 82.5 | 4.22 | -0.63 |
| 82.9 | 3.96 | -1.36 |
| 84.0 | 4.39 | -1.09 |
| 85.0 | 3.38 | -1.12 |
| 86.2 | 2.10 | -0.70 |
| 87.0 | 1.70 | -1.37 |
| 87.9 | 3.94 | -0.71 |
| 88.8 | 4.26 | -0.72 |
| 89.9 | 4.07 | -0.78 |
| 90.6 | 4.49 | -1.23 |
| 92.2 | 3.56 | -0.80 |
| 93.1 | 3.74 | -1.32 |
| 93.7 | 3.53 | -1.26 |
| 94.4 | 1.94 | -1.27 |
| 96.1 | 1.61 | -1.88 |
| 96.5 | 2.92 | -2.06 |
| 97.3 | 2.00 | -1.79 |

## *Carbon and oxygen isotopes of Monte Tobenna section*

| h (m) | $\delta^{18}O$ (‰) | $\delta^{13}C$ (‰) |
|---|---|---|
| 0.2 | 2.45 | -2.64 |
| 0.8 | 2.37 | -1.46 |
| 1.3 | 3.23 | -1.06 |
| 1.8 | 2.77 | -1.18 |
| 2.1 | 3.05 | -1.69 |
| 2.3 | 2.69 | -1.61 |
| 3.3 | 3.43 | -1.77 |
| 4.2 | 3.36 | -1.53 |
| 4.8 | 1.77 | -1.47 |
| 5.8 | 0.94 | -1.31 |
| 6.4 | 1.73 | -1.42 |
| 7.5 | 3.06 | -1.66 |
| 7.6 | 3.11 | -1.67 |
| 8.3 | 4.37 | -1.10 |
| 9.0 | 2.02 | -1.11 |
| 9.9 | 2.99 | -1.85 |
| 10.7 | 1.11 | -0.93 |
| 11.1 | 2.18 | -0.74 |
| 11.3 | 2.16 | -1.50 |
| 11.8 | 1.77 | -1.23 |
| 12.5 | 0.22 | -0.68 |
| 13.3 | 1.05 | -1.42 |
| 14.0 | 2.05 | -0.76 |
| 14.6 | 1.70 | -0.80 |
| 15.2 | 2.08 | -0.83 |
| 15.4 | -1.09 | -1.67 |
| 16.7 | 1.86 | -1.62 |
| 17.2 | 0.81 | -1.24 |
| 17.5 | 0.96 | -1.16 |
| 18.3 | 2.34 | -1.78 |
| 18.9 | 0.36 | -2.73 |
| 19.9 | 1.20 | -0.65 |
| 20.8 | -2.35 | -0.73 |
| 21.5 | -1.50 | -1.24 |
| 21.9 | -1.69 | -1.44 |
| 22.9 | -1.80 | -1.60 |
| 23.7 | 1.73 | -0.59 |
| 24.3 | 3.26 | -1.56 |
| 25.4 | 3.55 | -2.84 |
| 26.4 | 2.70 | -1.72 |
| 27.4 | 2.49 | -3.31 |
| 28.4 | 3.78 | -2.96 |
| 29.0 | 3.38 | -1.78 |
| 30.0 | 3.92 | -3.12 |
| 31.0 | 3.45 | -1.42 |
| 32.1 | 4.05 | -2.28 |

| h (m) | $\delta^{18}O$ (‰) | $\delta^{13}C$ (‰) |
|---|---|---|
| 33.3 | 3.02 | -3.86 |
| 34.3 | 3.20 | -3.16 |
| 35.3 | 3.17 | -2.67 |
| 36.1 | 3.17 | -1.41 |
| 36.5 | 3.76 | -1.88 |
| 37.1 | 3.36 | -4.47 |
| 38.2 | 3.12 | -0.88 |
| 39.0 | 0.73 | -3.26 |
| 39.9 | 0.96 | -1.24 |
| 41.1 | 0.97 | -2.33 |
| 42.1 | 3.33 | -2.48 |
| 43.3 | 2.65 | -4.74 |
| 43.9 | 1.62 | -3.01 |
| 45.2 | 0.87 | -3.10 |
| 46.2 | 0.38 | -3.80 |
| 47.2 | 3.02 | -2.57 |
| 48.0 | -0.30 | -2.34 |
| 48.1 | -0.63 | -1.71 |
| 48.3 | -2.37 | -2.16 |